LA-8807-MS

Informal Report

MASTER

Multisource Data Set Integration and Characterization of Uranium Mineralization for the Montrose Quadrangle, Colorado

UNITED STATES DEPARTMENT OF ENERGY

Grand Junction Office, Colorado

University of California

LOS ALAMOS SCIENTIFIC LABORATORY
Post Office Box 1663 Los Alamos, New Mexico 87545

DISTRIBUTION OF THIS DOCUMENT IS UNLIMITED

LA-8807-MS
Informal Report

UC-51
Issued: April 1981

DISCLAIMER

Multisource Data Set Integration and Characterization of Uranium Mineralization for the Montrose Quadrangle, Colorado

By

Stephen L. Bolivar
Susan H. Balog
Katherine Campbell
L. Erik Fugelso
Thomas A. Weaver
George W. Wecksung

Submitted to
Bendix Field Engineering Corporation
P.O. Box 1569
Grand Junction, CO 81501

UNITED STATES DEPARTMENT OF ENERGY

Grand Junction Office, Colorado

CONTENTS

LIST OF ILLUSTRATIONS

Plate No.

LIST OF TABLES

Table No.

ACKNOWLEDGMENT

Financial support from Bendix Field Engineering Corporation is acknowledged. Completion of the program would have been impossible without unselfish effort by all involved. Many thanks to Donald Janney (Image Processing) for guidance, to Tom Bement and Carlotta McInteer for aid in statistical analysis, and to David Broxton, who supplied several of the figures, tables, and part of the geologic summary in Chapter II. Special acknowledgment is also due many personnel of the Los Alamos Geosciences Division: this includes John Tubb and Anthony Garcia and their associates, who provided graphics and visual aids, and Nancy Eckhoff and Nancy Bazzell, who typed the manuscript. Aaron Waters (Los Alamos) and Lou Fleischhauer (Bendix) edited the manuscript and provided valuable comments and constructive revisions. Final responsibility for errors, of course, rests with the authors.

ABSTRACT

Several data-classification schemes were developed by the Los Alamos National Laboratory to detect potential uranium mineralization in the Montrose 1° x 2° quadrangle, Colorado. A first step was to develop and refine the techniques necessary to digitize, integrate, and register various large geological, geochemical, and geophysical data sets, including Landsat 2 imagery, for the Montrose quadrangle, Colorado, using a grid resolution of 1 km. All data sets for the Montrose quadrangle were registered to the Universal Transverse Mercator projection. The data sets include hydrogeochemical and stream sediment analyses for 23 elements, uranium-to-thorium ratios, airborne geophysical survey data, the locations of 90 uranium occurrences, a geologic map (scale 1:250 000), and Landsat 2 (bands 4 through 7) imagery. Geochemical samples were collected from 3965 locations in the 19 200 km^2 quadrangle; aerial data were collected on flight lines flown with 3-5 km spacings. These data sets were smoothed by universal kriging and interpolated to a 179 x 119 rectangular grid (each grid block is 1 km^2). A mylar transparency of the geologic map was prepared and digitized. Locations for the known uranium occurrences were also digitized. The Landsat 2 imagery was digitally manipulated and rubber-sheet transformed to quadrangle boundaries and bands 4 through 7 were resampled to both a 1-km and 100-m resolution.

All possible combinations of three, for all data sets, were examined for general geologic correlations by utilizing a color microfilm output. Subsets of data were further examined for selected test areas. Two classification schemes for uranium mineralization, based on selected test areas in both the Cochetopa and Marshall Pass uranium districts, are presented. Areas favorable for uranium mineralization, based on these schemes, were identified and are discussed.

The methodology developed in this study is a rapid and efficient method of resource evaluation on a reconnaissance scale. Also, this methodology can easily be adapted to other types of geologic interpretation, such as environmental impact analysis or strategic mineral evaluations.

INTRODUCTION

Background Information

Pirkel et al (1979) integrated and analyzed airborne radiometric data for the Lubbock and Plainview, Texas, 1° x 2° quadrangles. They identified areas favorable to uranium deposition and also possible paleochannels. Wecksung and Fugelso (1980) made a preliminary integration of Landsat imagery, uranium hydrogeochemical and stream sediment data, and a geology map for the Talkeetna 1° x 3° quadrangle, Alaska. This revealed correlations between high uranium concentrations, geologic formations, and certain physiographic features. If several data sets, including Landsat imagery, airborne geophysical data, and hydrogeochemical and stream sediment data are integrated into one large data set, a wealth of information can be extracted. Consequently, a data integration/remote sensing (DIRS) project was established by the authors of this report; the major emphasis is toward integrating data sets that may be helpful in identifying areas of uranium mineralization possibly favorable for economic development in the Montrose 1° x 2° quadrangle, Colorado.

The DIRS project was also initiated to interpret the huge quantity of data generated by the Los Alamos work on the National Uranium Resource Evaluation (NURE) program. The major objective of the NURE program was assessment of the nuclear fuel resources in the conterminous US and Alaska (US Department of Energy, 1979). The program included a nationwide airborne geophysical reconnaissance, a nationwide hydrogeochemical and stream sediment reconnaissance, subsurface geologic investigations, and topical geologic studies. We were involved with the collection, chemical analysis, and open filing of resulting data from a geochemical reconnaissance of water and stream- or lake-sediment samples for a total of more than 220 000 locations in New Mexico, Colorado, Wyoming, Montana, and Alaska. Over half of these sediment samples have been analyzed for uranium and more than 40 other elements of economic, national security, and geologic importance. Other Department of Energy laboratories were responsible for the geochemical reconnaissance in other parts of the US (Bolivar, 1980a). Los Alamos statisticians are also involved in data reduction of the enormous quantity of raw data from the NURE airborne geophysical surveys.

Prior to the DIRS program, large data sets generally were examined independently, and a significant amount of information available was seldom incorporated into final evaluations. There simply is too much data to assimilate by customary techniques. The great volume of data for a regional area, e.g., a 1° x 2° quadrangle, seems almost a deterrant to analysis. With DIRS, all available information is used, and cross-correlated to extract new information not available from the individual data sets (e.g., Lankston and Lankston, 1979; Termain et al, 1980; Wecksung and Fugelso, 1980).

Since the inception of the DIRS project in May 1980, our staff has worked on two pilot projects: data-integration development for the Talkeetna, Alaska, 1° x 3° quadrangle, and uranium-deposit characterization for the Montrose, Colorado, 1° x 2° quadrangle. For the Talkeetna study, procedures were developed for digitizing many kinds of information--maps, data tables, graphs, and text. Computer programs were written that efficiently pack these digital data into a "super data set" for rapid computer processing, including overlay and display techniques by computer-graphics, cross-correlating the various data sets statistically, and finally identifying geographical areas of interest.

The Montrose 1° x 2° quadrangle, Colorado, was selected for a more detailed attempt at characterizing uranium mineralization, and also as a continuation of the above efforts to a more sophisticated level. The Montrose quadrangle provides a variety of known uranium prospects and two major, yet distinct, uranium districts. Moreover, a quadrangle report is available that utilizes sophisticated statistics in interpreting the original NURE hydrogeochemical and stream sediment data (Beyth et al, 1980b). Also, a geochemical study for part of this quadrangle (Maassen, 1980), and the NURE aerial radiometric report have already been published (geoMetrics, 1979b). The rapid progress in study of the Montrose quadrangle owes much to prior development of programs and procedures for the Talkeetna pilot study.

Results of these pilot studies are both promising and surprising. The quantity of subtle and unforseen information extracted, is unexpectedly large. Geochemical dispersion haloes can be contoured and mapped, previously unknown geologic structures are outlined, and areas of potential uranium mineralization are identified. Field verification of the new interpretations will follow.

Objective and Procedures

The short-term objective of this project is to characterize known uranium occurrences in the Montrose 1° x 2° quadrangle and to find other areas in the quadrangle with similar characteristics. It has been accomplished by integrating, in the computer, available NURE geochemical reconnaissance data, geologic map information (rock type and geologic structure), uranium-mineral-occurrence data, radiometric and magnetic data from the NURE nationwide airborne geophysical survey, and Landsat imagery.

In order to efficiently integrate large volumes of data, it is necessary to get the various data sets into spatially comparable formats. Therefore, after data sets are obtained, they are digitized and geometrically registered to the Universal Transverse Mercator (UTM) projection. The UTM coordinate system is a rectangular equal area projection and the coordinate boundaries chosen are slightly larger than the Montrose quadrangle boundaries. For the Montrose quadrangle a 1-km grid resolution was selected. Point data (such as NURE data) are statistically smoothed and interpolated to the rectangular grid. Data available on a finer grid, such as Landsat imagery and geologic information, are subsampled to 1 km UTM grid.

Once the data sets are integrated and spatially registered, they can be examined statistically for relationship between data sets and individual variables and also for significant patterns derived from the data.

Individual data sets can be analytically and visually overlain. Small test areas containing known uranium occurrences, predominantly from the Cochetopa and Marshall Pass uranium districts, were extracted and examined. A preliminary classification for each district, based on characteristics of the known occurrences in each district, was then generated and iteratively refined. Finally, this classification will be tested for the entire Montrose quadrangle to determine if similar uranium occurrences can be found.

Report Format

This report is divided into seven units: (1) problems and objectives, (2) brief summary of the geology and mineral occurrences, Montrose quadrangle, (3) the data sets, description, and procedures used to register each, (4) discussion of the analytical techniques and statistical routines used, and examples of the resulting preliminary classification, (5) how the data sets can be used and refined with an image processing facility, and (6) future problems and potential directions that the program could take. In Unit 7, conclusions summarize significant accomplishments from the study.

Appendix A contains a coded list of the digitized uranium occurrences for the Montrose quadrangle. Appendix B consists of linear gray-level maps for the 23 geochemical elements, U/Th ratios, four airborne geophysical data sets, and four Landsat bands. Appendix C contains basic statistics (by entire quadrangle and by physiographic/geochemical province) and Appendix D contains cumulative frequency plots of the raw geochemical data. Appendix E brings together statistical association by variable information for each host-rock type of uranium deposit. Appendix F consists of the correlation coefficients for the quadrangle as a whole and by physiographic/geochemical province. Lastly, Appendix G contains the raw data for factor analysis for the quadrangle as a whole.

Plate I is a transparency that includes known uranium occurrences (according to Nelson-Moore et al, 1978); this transparency can be overlain for comparison with any other representation of the Montrose quadrangle. Tick marks indicating UTM corners are included on most figures.

GEOLOGY AND MINERAL DEPOSITS OF THE MONTROSE QUADRANGLE, COLORADO

General Information

The Montrose 1° x 2° quadrangle, Colorado, is bounded by 38° and 39° north latitude and 106° and 108° west longitudes. The climate is typical for the Rocky Mountains. Annual precipitation ranges from 600 mm in the mountains and heavily forested regions to less than 250 mm in the lower elevations (NOAA, 1976 and 1977). About one-half of the annual precipitation results from thermally induced summer thundershowers.

The vegetation in both the western half of the quadrangle and in intermontane basins consists principally of sagebrush and native grasses. Forests of aspen, pine, and spruce characterize the mountainous areas. Paved highways and unimproved dirt roads provide access to all but the most rugged mountain areas. Montrose is the largest town (population about 5000).

Physiographic Setting

The Montrose quadrangle comprises about 19 200 km^2 in southwestern Colorado. It includes sections of the Southern Rocky Mountain and Colorado Plateau physiographic provinces (Fig. 1). The West Elk Mountains, San Juan Mountains, and Sawatch Range are the dominant drainage divides within the quadrangle (Fig. 2).

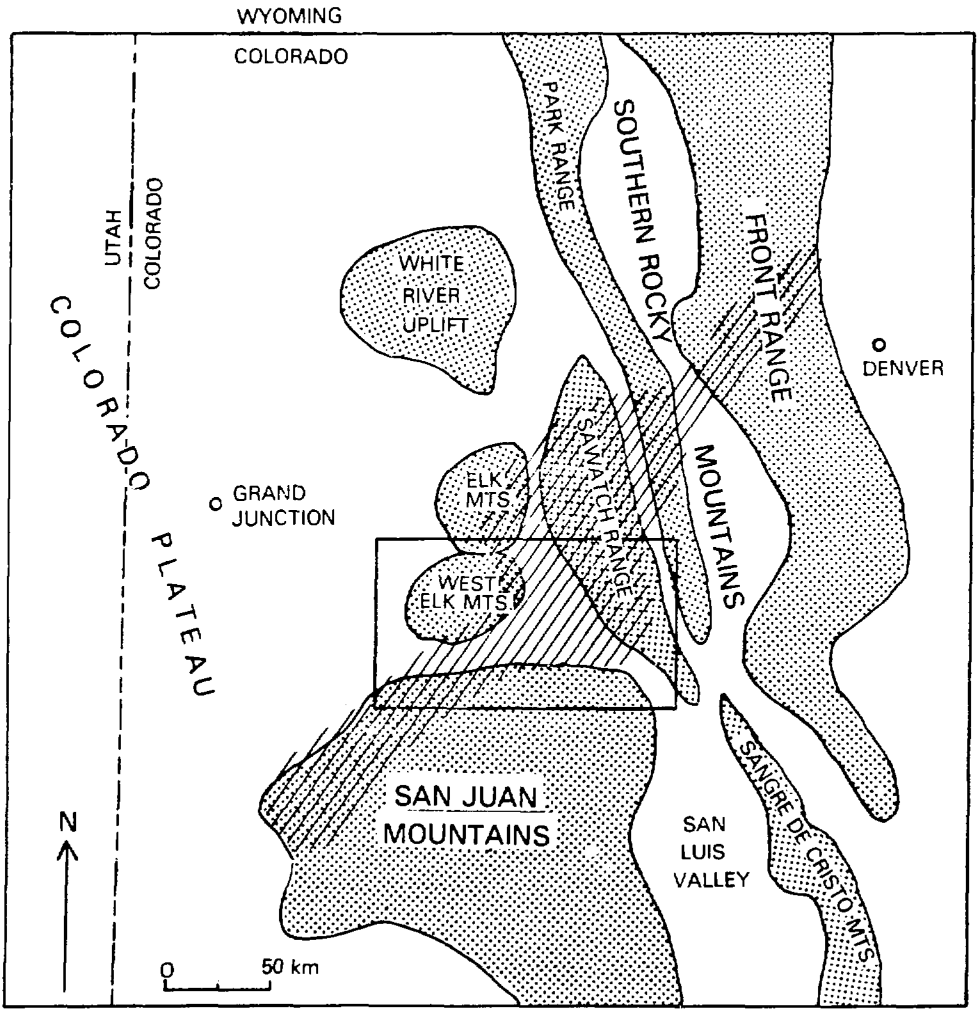

Fig. 1. Major geographic features in south-central Colorado (modified from Tweto, 1968; Colorado mineral belt is striped; inset is study area)

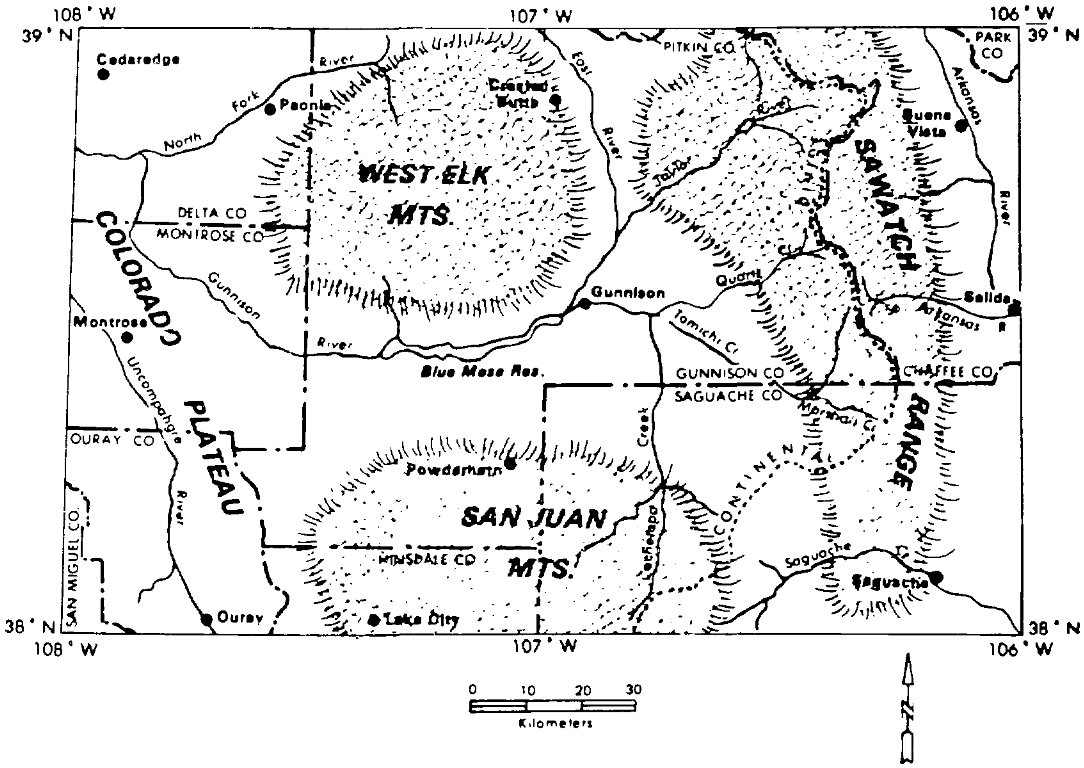

Fig. 2. Location and drainage map for the Montrose quadrangle, Colorado.

The highest elevations occur in the northeast corner; where Mount Harvard (4393 m) and Mount Antero (4349 m) are the two highest peaks. Deepest drainages in the mountainous regions vary from 2100 m to 2499 m. Between the mountain regions are irregular ridges and intermontane basins (USGS, 1956).

Elevations on the Colorado Plateau vary from 2700 m to 3150 m on mesa tops to a low of 1500 m above sea level in the northwest corner of the quadrangle. Most major stream channels range from 1700 to 2100 m above sea level. The Plateau is characterized by flat-topped mesas, rolling hills, and dissected plateaus. It includes some badland topography. The Montrose quadrangle encompasses parts of two major drainage basins separated by the Continental Divide (Fig. 2). The Arkansas River drainage is east whereas the Gunnison River drains west. The Gunnison River and its tributaries, the North Fork and the Uncompahgre Rivers, drain most of the quadrangle area.

Major Rock Types

A wide variety of igneous, metamorphic, and sedimentary rocks, representing most major geologic periods crop out in the Montrose quadrangle. A generalized geologic map, Fig. 3, shows the distribution of major rock units. Lithology and regional geology of this region has been described in detail by many investigators (e.g., Weimer and Haun, 1960; Haun and Kent, 1965; Epis, 1968; Tweto, 1968 and 1975; Mallory, 1972; Tweto et al, 1976a). Only a brief summary (most of it modified from Broxton et al, 1979) is given here.

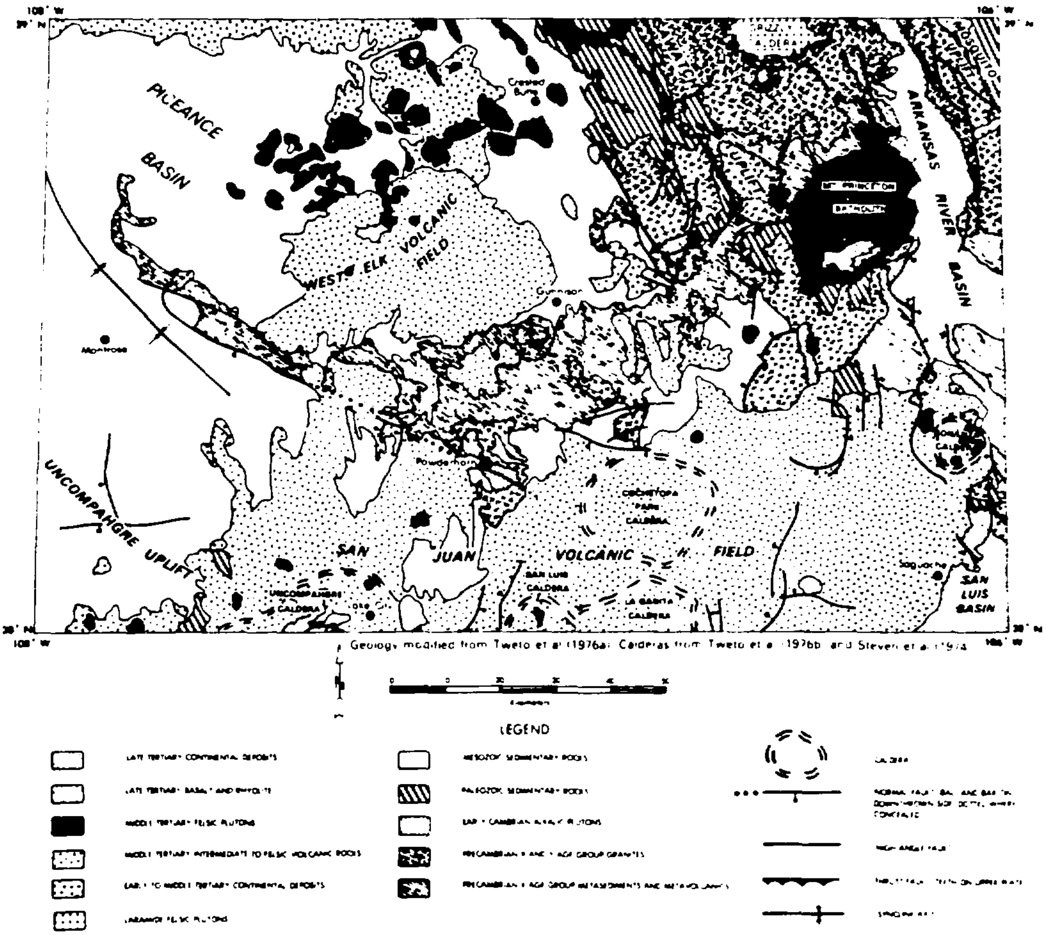

Fig. 3. Generalized geologic map of the Montrose quadrangle, Colorado.

The oldest rocks consist of Precambrian X granites (age >1700 m.y.b.p.), quartzites, metarhyolites, greenstones, metagreywackes, gneisses, and schists exposed in the Sawatch Range and along the Gunnison River. The metasedimentary and metavolcanic rocks have undergone regional metamorphism, and are intruded by 1700-m.y.-old granitic batholiths. The plutons are generally syntectonic, foliated, and of granodioritic composition. Contemporaneous intrusions of granitic and alkalic-rich mafic plutons of Precambrian Y age (~1400 m.y.b.p.) are found in the central part of the quadrangle. These plutons are generally post-tectonic, unfoliated, and of quartz monzonite to granite composition (King, 1976). Near Powderhorn, the Precambrian rocks are intruded by the Iron Hill carbonatite complex, an early Cambrian, alkalic pluton associated with thorium mineralization (Armbrustmacher, 1979; Armbrustmacher and Brownfield, 1979). About 20 per cent of the quadrangle is underlain by Precambrian metamorphic and igneous rocks.

Paleozoic rocks, mostly of marine origin, are sparse in distribution. Cambrian through Mississippian marine sandstones, shale, and limestones unconformably overlie crystalline basement rocks in the northeastern and southwestern parts of the quadrangle. Early Paleozoic units are thin in these areas as a result of erosion during a late Paleozoic-early Mesozoic uplift of the Uncompahgre Highland. Pennsylvanian and Permian arkosic redbeds in the north central and southwest parts of the quadrangle and along margins of the Sawatch Range are thicker, for they represent synorogenic clastic sediments shed into basins flanking the uplift.

Triassic and Jurassic fluvial and lacustrine sediments are relatively thin because of regional uplift during this time. These sediments were deposited over much of the eroded Precambrian core of the Uncompahgre Highland as well as over the flanking basin deposits. By Cretaceous time, transgressive/regressive seas covered the entire region, resulting in deposition of marine shales and sandstones interfingering with nonmarine sandstones, carbonaceous shales, and variegated mudstones. In the quadrangle, Triassic rocks occur only in the southwest corner, Jurassic rocks overlie Precambrian rocks in the central area, and fairly thick Cretaceous deposits are found predominantly in the western half. The Jurassic and Cretaceous rocks combined cover about 25 per cent of the quadrangle.

With the onset of the Laramide orogeny in late Cretaceous time, the northwest-trending Sawatch Anticline and Uncompahgre Plateau were uplifted, resulting in widespread erosion of older rock units and deposition of orogenic clastic sediments in basins adjacent to the uplifts. Erosional remnants of these Laramide orogenic sediments (e.g., Ohio Creek and Wasatch formations) are preserved only in the northwest part and in scattered areas in the eastern part of the quadrangle. These Tertiary sedimentary rocks are relatively rare. The Sawatch Anticline and the Uncompahgre Plateau, a rejuvenated portion of the late Paleozoic Uncompahgre Highland, are reactivated basement blocks characterized by large vertical displacements during the Cretaceous through the early Tertiary.

Intermediate to felsic volcanism and plutonism (recorded in sediments of the Wasatch formation) accompanied the Laramide deformation. The intrusive rocks range in age from Late Cretaceous to Miocene. Most of this Laramide volcanism and plutonism was localized along northeast-trending Precambrian shear zones and is associated with the earliest stages of mineralization in the Colorado Mineral Belt (Warner, 1978). The most abundant intrusive rocks are Oligocene quartz monzonites found primarily north of the West Elk volcanic field, but extending to the Sawatch Range, and the Mount Princeton batholith (on the eastern side of the Sawatch Range). These felsic intrusives include epizonal stocks, laccoliths, dikes, and sills.

Two dominant areas of volcanism affected the Montrose quadrangle, one centered in the West Elk volcanic field, and the other in the San Juan volcanic field (Lipman et al, 1978). These Tertiary volcanic rocks (mostly Oligocene) cover about 35 per cent of the quadrangle (Fig. 3). The northern third of the San Juan volcanic field, which underlies the southern third of the Montrose quadrangle, is a deeply dissected Oligocene volcanic plateau. This plateau exposes a lower sequence of predominantly andesite flows and breccias that are overlain by a sequence of silicic ash-flow-tuff sheets capped in some places by Miocene basalt flows (Lipman et al, 1978). Several caldera complexes, stocks, plugs, sills, and dikes represent deeply eroded volcanic centers and epizonal plutons that acted as sources for the volcanic rocks (Fig. 3). Just north of the Gunnison River, the lower sequence of lavas and breccias of the San Juan volcanic field coalesces with volcanic deposits of similar age and composition derived from the West Elk Mountains. The West Elk volcanics cover a 32-km diameter area in the center of the quadrangle and consist of a thick sequence of volcaniclastic debris overlain by ash flow tuffs. Several Oligocene ash-flow tuffs also occur within the Sawatch Range.

Epeirogenic uplift, bimodal basalt-rhyolite volcanism, and block faulting characterize late Tertiary deformation in the Montrose quadrangle. The Rio Grande rift zone developed at this time (Miocene). The Arkansas River Basin lies in a down-faulted graben superimposed on the crest of the Laramide Sawatch Anticline. The faults, which probably follow Precambrian structural trends define the northernmost segment of the Rio Grande Rift. Late Tertiary orogenic sediments, represented by the Santa Fe and Dry Union formations, partly fill the Arkansas River Graben. Several normal faults border the rift along its eastern boundary (Fig. 3)

Structure

Most of the major structures are delineated in Fig. 3. The quadrangle includes all or part of the Gunnison, Uncompahgre, Sawatch, and Mosquito Uplifts as well as parts of the Piceance Basin and Rio Grande Rift (Arkansas River Basin or Arkansas River Graben). The West Elk and the San Juan volcanic fields partially cover several of the structural features.

Most of these features have been described in the previous section with the exception of the Gunnison Uplift (not shown in Fig. 3). This uplift is bounded by the Black Canyon of the Gunnison River to the north. It generally coincides with Precambrian basement rocks. This uplift forms a convex arc in the center of the quadrangle; the southern boundary of the uplift is covered by the San Juan volcanic field.

The majority of the structural features in the Montrose quadrangle trend north-northwest. These structures and their associated faults probably follow Precambrian lineaments (Tweto, 1975) along which recurrent movement occurred in the late Paleozoic, Laramide, and late Tertiary.

Most mapped faults are found in the eastern-northeastern parts of the quadrangle and are probably associated with structural development of the Sawatch and other uplifts during the Laramide orogeny. Most such faults are also high angle with significant displacements (Tweto, 1975).

Several normal faults along the boundary of the Arkansas River Basin (Miocene) are probably associated with the Rio Grande Rift zone. Other normal faults are associated with the caldera collapse and late-Tertiary uplift of the San Juan Mountains. The most striking caldera complex, easily visible on Landsat imagery, is Cochetopa Dome, about 7 km southwest of Gunnison. This Oligocene intrusive is surrounded by a series of arcuate faults.

Radioactive Mineral Occurrences

There are approximately 90 separate known locations where uranium mineralization has been identified or where anomalous radioactivity occurs in the Montrose quadrangle (Fig. 4). The mineralization at these occurrences appears to be fracture and/or stratigraphically controlled. Mineralization is also commonly associated with shear zones, fault breccias, fractures, and vein fillings.

Over half of the known uranium occurrences in the quadrangle are found in three major uranium districts: the Cochetopa, Marshall Pass, and Powderhorn districts (Fig. 4). In fact, nearly 600 000 tons of uranium ore containing between 0.11 and 1.17 per cent U_3O_8 have been produced from the Montrose quadrangle (compiled from Nelson-Moore et al, 1978). Most of this production is from mines in the Cochetopa and Marshall Pass districts. These mining districts and other uranium occurrences in the quadrangle are briefly described in Table I and their locations are shown in Fig. 4. More detailed descriptions of the individual uranium occurrences are summarized in Finch (1967), Olson (1976), and Nelson-Moore et al (1978).

The Cochetopa district is located about 25 km southeast of Gunnison, and mineralization occurs in an 11-km diameter region. In this district, uranium mineralization is localized along fault breccias of the Los Ochos fault where Morrison sandstones and shales are faulted against Precambrian X age granites and schists. The principal ore bodies are associated with intensely altered areas in the fault breccia and in adjacent wall rocks, although mineralization can occur in quartz-calcite-barite veins and shear zones that cut Precambrian schists (geoMetrics, 1979b). Although no mines are active in this area at the present time, 486 000 tons of ore yielding 1 351 000 lb of U_3O_8 have been produced, mainly from the Los Ochos and T-2 mines (Nelson-Moore et al, 1978).

The Marshall Pass district is located near the Continental Divide about 25 km southwest of Salida, actually 5 km west of Marshall Pass itself. The deposits occur in a region 8 km in diameter (Fig. 4). Both structurally controlled and stratigraphically controlled deposits are found, e.g., some deposits occur in regolith overlying Precambrian crystalline rocks and one major mine, the Little Indian No. 36, is in a 2-m thick carbonaceous layer of Ordovician Harding sandstone (geoMetrics, 1979b). However, most uranium deposits in the Marshall Pass district are concentrated along or near the Chester fault. The Chester fault displaces Precambrian X granites and schists

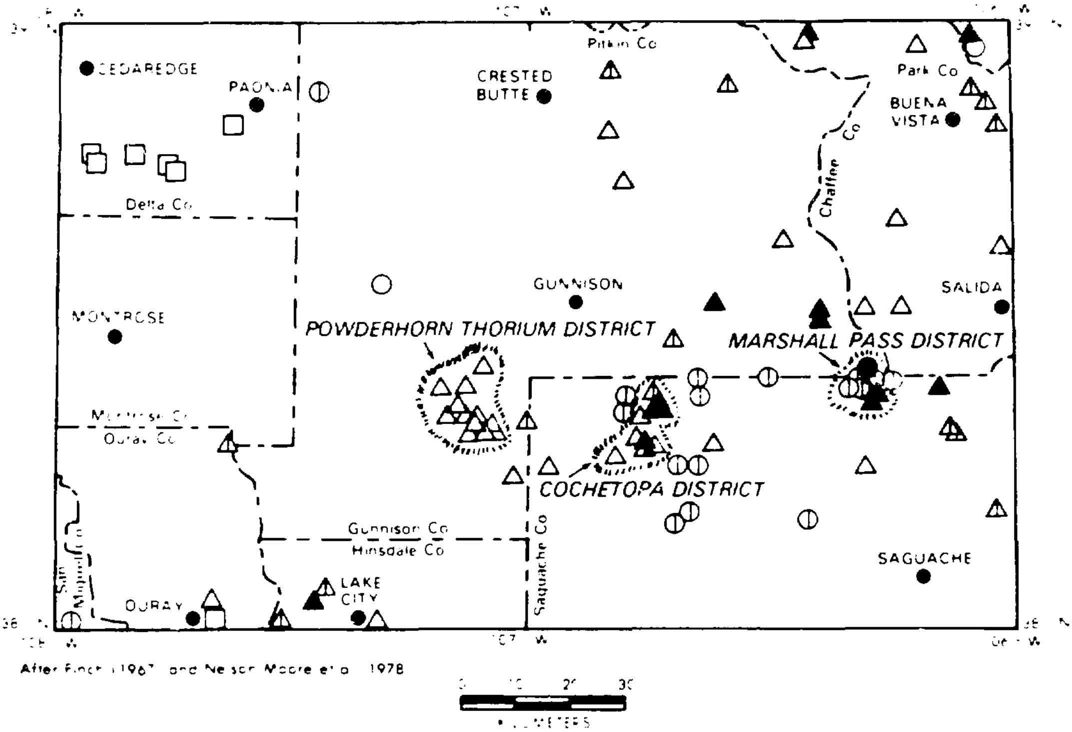

LEGEND

NOTE A brief description of each major district or area is included in Table II
One symbol may represent several occurrences or claims

△ Vein, pegmatite, breccia zone, and related types, uranium mineralization strongly suspected (usually because of abnormal radioactivity) but not megascopically visible

⚠ Vein, pegmatite, breccia zone, and related types, uranium mineralization documented, but no past production.

▲ Vein, pegmatite, breccia zone, and related types, uranium ore production documented

○ Peneconcordant occurrence with uranium mineralization strongly suspected (usually because of abnormal radioactivity) but not megascopically visible

⦶ Peneconcordant occurrence; uranium mineralization documented, but no past production

● Peneconcordant occurrence, uranium ore production documented

□ Spring deposit with abnormal radioactivity

Fig. 4. Uranium occurrences in the Montrose quadrangle, Colorado.

TABLE I

MAJOR URANIUM AND THORIUM DISTRICTS IN THE MONTROSE QUADRANGLE, COLORADO
(Locations of specific occurrences are shown in Fig. 4)

County	District or Area	Description	References
Delta	Gunnison River Area	The five occurrences in this area are radioactive spring deposits that are found in the Dakota sandstone. One is associated with a fault. No uranium mineralization is visible, abnormal radium contents have been reported.	Cadigan et al, 1976.
San Miguel Ouray Hinsdale	Southwest Montrose Quadrangle	Only 18 tons of ore of average grade 0.20% U_3O_8 are reported from these three counties (Nelson-Moore et al, 1978). Most uranium occurrences are in veins in Tertiary volcanics; one radioactive spring deposit is known. Uranium mineralization is associated with rhyolite-latite intrusives and breccia zones. The dominant uranium minerals are uranophane and pitchblende. In San Miguel county tabular ore bodies are found in the Entrada sandstone. Average ore grade is 0.05% U_3O_8 and is closely associated with vanadium. One such occurrence is reported in the extreme southwest corner of the Montrose quadrangle.	Burbank, 1940; Burbank and Pierson, 1953; Larsen and Cross, 1956; US AEC, 1966d; Fischer et al, 1968.
North Gunnison Chaffee Park	Northeast Montrose Quadrangle	About 200 tons of ore, with average grades of 0.12 to 0.22% U_3O_8, have been taken from deposits in this area (Nelson-Moore et al, 1978). Most uranium occurrences are vein types found in pegmatites in Precambrian granitic rocks; some are associated with veins, dikes, and fault breccias of Tertiary intrusives, a few are found along Paleozoic quartzite-Precambrian granite fault contacts. Deposits are usually small in size. Uranium mineralization is associated with faults, fractures, alteration zones, carbonaceous trash (especially in fault zones), and base-metal mineralization. Autunite, columbite, pitchblende, brannerite, and monazite are the dominant uranium minerals. These types of occurrences are not restricted to these three counties, but are found throughout the Montrose quadrangle.	Guillotte, 1945; Adams, 1953; Heinrich, 1958; Baillie, 1962; US AEC, 1966b; US AEC, 1966c; Gallagher et al, 1977.
Gunnison	Powderhorn Thorium District	Most of the thorium occurrences in this district consist of radioactive anomalies in veins. These veins are found in Precambrian granite, schist, and gneiss. Deposits consist of thorite, minor amounts of uranium, quartz, barite, hematite, and sulfides.	Larsen, 1942; Olson and Wallace, 1956; US AEC, 1966a; Murphy et al, 1978; Nelson-Moore et al, 1978.
Saguache	Cochetopa District	Production totals for this district to 1971 are about 486 000 tons of ore containing 0.11 to 0.20% U_3O_8 (Nelson-Moore et al, 1978). Uranium mineralization generally occurs in fault breccia or shear zones between the Morrison formation (or to a lesser extent the Dakota sandstone) and Precambrian rocks, or in veins cutting Precambrian rocks. Uranium mineralization may also be associated with malachite, azurite, or other base-metal mineralization. The Morrison formation is comprised predominantly of sandstone and mudstone, whereas the Precambrian rocks are generally granite or schist. Primary uranium-bearing minerals include pitchblende, uranophane, autunite, torbernite, and zippeite.	Derzay, 1956; Malan and Ranspot, 1959; Eckel, 1961; US AEC, 1966c; Finch, 1967; Olson, 1976
Saguache	Periphery of Cochetopa District	Around the periphery and southeast of the Cochetopa district, several uranium occurrences are reported in the Miocene Potosi Volcanic Series, or in Cretaceous rocks which are overlain by these volcanics.	Malan and Ranspot, 1959; Nelson-Moore et al, 1978.
Saguache Gunnison	Marshall Pass District	Over 105 000 tons of ore ranging from 0.25 to 1.17% U_3O_8 have been produced from this district. All occurrences in this area are related to the Chester fault or Indian Creek anticline. Principal host rocks include the Ordovician Harding quartzite and Pennsylvanian Belden shale, which are in fault contact with Precambrian rocks. The Harding quartzite is a porous silty sandstone, whereas the Precambrian rocks include highly fractured granites, schists, and pegmatites. Uranium mineralization is associated with iron-stained, fossiliferous, and carbonaceous zones. Sulfides may or may not be present. Primary uranium minerals include pitchblende, uraninite, and uranophane with minor amounts of gummite, autunite, and zippeite. Several occurrences, not within this district but with similar types of uranium mineralization, are found to the southeast.	Malan and Ranspot, 1959; Ranspot and Spengler, 1957; Nelson-Moore et al, 1978.

against Paleozoic sedimentary formations. Uranium mineralization, including pitchblende, uranophane, and autunite (Gross, 1965), is mainly confined to the Paleozoic rocks, among them the Ordovician Harding quartzite, Devonian Chaffee formation, Mississippian Leadville limestone, and Pennsylvanian Belden formation. Over 105 000 tons of ore containing between 0.25 and 1.17 per cent U_3O_8 have been produced from this district with most of the production coming from the Pitch Mine, an underground mine which is currently being reopened as an open-pit operation (Nelson-Moore et al, 1978).

The Powderhorn district is located in the southcentral part of the Montrose quadrangle. Many occurrences in this area show only abnormal radioactivity, although several do contain both uranium and thorium mineralization (Olson and Wallace, 1956). Thorium, principally in the form of pyrochlore, is concentrated in veins and shear zones on the margins of the Iron Hill Complex, an early Cambrian alkalic intrusion made up of pyroxenite, uncompahgrite, ijolite, nepheline syenite, and carbonatite. Country rocks are predominantly Precambrian crystalline units. Thorium levels are too low to be of economic interest under present market conditions unless the thorium is extracted as a by-product of potential niobium, rare earth, and uranium deposits within the alkalic complex.

About one-half of the known uranium occurrences in Fig. 4 are not found in the three major districts but instead occur scattered throughout the area, particularly in the northeast and eastern portions of the quadrangle. Some of these occurrences are similar to deposits described, many are associated with Precambrian pegmatites or veins, and a few are associated with Tertiary volcanics and intrusives (Table I).

Data presented by Phair and Gottfried (1964) indicate that rocks of the Front Range (Fig. 1) are predominantly thorium rich and define a geochemical thorium province. Furthermore, the portion of the Front Range transected by the Colorado Mineral Belt was considered a metallogenic uranium province because of the large number of mineable uranium deposits located near the trend of the mineral belt. Because of similarities in Precambrian bedrock geology, the presence of workable uranium deposits, and the projection of the Colorado Mineral Belt through the area, portions of the Montrose quadrangle might be extensions of Front Range thorium and uranium provinces described by Phair and Gottfried. Tweto (1968) suggested that northwest-trending faults intersecting northeast-trending veins are principal habitats for uranium mineralization, particularly on the fringes or outside of the Colorado Mineral Belt. Nash (1980) has suggested similar potential for uranium mineralization along major Laramide uplifts.

Base- and Precious-Metal Occurrences

Although the emphasis of this report is on uranium mineralization, the data from this study can also be used to evaluate other potential economic mineral deposits and strategic mineral resources. Therefore, we have included a brief description of known economic deposits in the Montrose quadrangle (modified from Beyth et al, 1980b).

Most of the known base- and precious-metal mineralization within the Southern Rocky Mountains occurs along the Colorado Mineral Belt, a northeast-trending zone of major metal deposits associated with Laramide and middle Tertiary plutons aligned along reactivated Precambrian shear zones (Warner, 1978). This belt traverses the Montrose quadrangle diagonally, extending from the Mosquito Range in the northeast, through the Sawatch-Gunnison crystalline terrane, to the Uncompahgre and Lake City calderas in the southwestern part of the quadrangle.

The major base- and precious-metal mining districts in the Montrose quadrangle are briefly described in Table II and their locations are shown in Fig. 5. In addition, the Colorado resources map published by the USGS (1971) shows the locations and types of many smaller mineral deposits. An extensive catalog of mineral occurrences and mines in the Montrose quadrangle was compiled by Truebe (1974).

There are two main periods of mineralization within the Colorado Mineral Belt (Burbank and Luedke, 1968; Tweto, 1968; Simmons and Hedge, 1978): the older period is related to emplacement of late Cretaceous--early Tertiary (Laramide) plutons, and the younger to widespread middle Tertiary extrusive and intrusive activity. The principal types of deposits formed at these two times are disseminated or stockwork molybdenum deposits associated with Tertiary plutons, precious- and base-metal veins in Tertiary volcanic rocks, and base-metal veins and replacement deposits in Paleozoic sedimentary rocks (Tweto, 1968). Mineralization is structurally controlled in many cases, being localized at the intersection of northwest- and east-trending structural lines with the Colorado Mineral Belt and along ring fractures associated with caldera systems (Tweto, 1968).

TABLE II

MAJOR BASE-METAL MINING DISTRICTS IN THE MONTROSE QUADRANGLE, COLORADO

Mining District	Principal Commodity	Description	References
Uncompahgre (Ouray)	Silver, gold, lead, copper, zinc	Fissure veins and bedded replacement deposits in the Dolores and Morrison formations, Leadville limestone, Dakota quartzite, and Molas formation, associated with quartz monzonite intrusives.	Burbank (1947), Vanderwilt (1947), King and Allsman (1950), Koschmann and Bergendahl (1968).
Lake City	Silver lead, gold, copper, zinc.	NE and NW trending fissure veins in andesite, rhyolite, and Eocene monzonite porphyry intrusives.	Irving and Bancroft (1911), Vanderwilt (1947), Burbank and Luedke (1968).
Ruby (Irwin, Keystone, Forest Queen, and Mt. Emmons)	Molybdenum.	Stockwork deposits associated with intermediate to felsic porphyry intrusive.	Vanderwilt (1947).
	Silver, zinc, lead copper.	Veins in the Wasatch formation and Paleocene Ohio Creek formation.	
Gold Brick-Quarry Creek (Ohio City, Gold Hill, and Cumberland Pass)	Silver, gold, lead.	N5°W trending veins in Precambrian granite and schist, replacement deposits in Fremont dolomite, Leadville limestone, and limestone beds in the Belden shale.	Crawford and Worcester (1916); Vanderwilt (1947), Hanley et al (1950), Staatz and Trites (1955), Belser (1956); Dings and Robinson (1957).
	Molybdenum, tungsten.	E-W and NE trending quartz veins in Precambrian quartz monzonite and Cambrian quartzite.	
	Lepidolite, beryl, feldspar, columbite-tantalite.	NE and N-S trending pegmatite dikes in Precambrian schists, quartzite, metadiorite, and gneiss.	
Tincup	Silver, gold, lead.	Bedded replacement deposits in Leadville limestone associated with quartz diorite and quartz monzonite intrusives, N-S trending quartz veins along faults, and placer deposits.	Hill (1909); Vanderwilt (1947); Dings and Robinson (1957); Parker (1974).
Chalk Creek (Alpine, Romley, St. Elmo)	Gold, silver, lead, copper, zinc.	N-S to NE trending quartz veins in Tertiary quartz monzonite intrusive.	Vanderwilt (1947); Dings and Robinson (1957).
Tomichi (White Pine)	Lead, zinc, silver, copper, gold.	Replacement and contact deposits, fissure veins in Manitou dolomite and Leadville limestone, associated with quartz monzonite and granite porphyry intrusive.	Hill (1909), Crawford (1913); Vanderwilt (1947), Dings and Robinson (1957).
Monarch	Silver, gold, lead, zinc, copper.	Replacement deposits in limestones and dolomites of the Manitou formation, Leadville limestone, and Fremont formation, NE-trending veins in Tertiary quartz monzonite instrusive.	Crawford (1909, 1913), Vanderwilt (1947), Dings and Robinson (1957), Heyl (1964).
Brown's Canyon	Fluorspar.	NW trending fissure veins along faults in Precambrian granite and gneiss, and Tertiary rhyolite porphyry.	Van Alstine (1947), Brady (1975).
Bonanza King (Kerber Creek)	Silver, lead, zinc, copper, gold.	NE and N-S trending quartz veins in Tertiary andesite, latite, rhyolite, diorite, monzonite, and granite porphyry.	Burbank (1932, 1947), Vanderwilt (1947), Koschmann and Bergendahl (1968), USGS and Colorado Mining Industrial Development Board (1968).

* Modified from Mardirosian (1976), locations shown in Fig. 5.

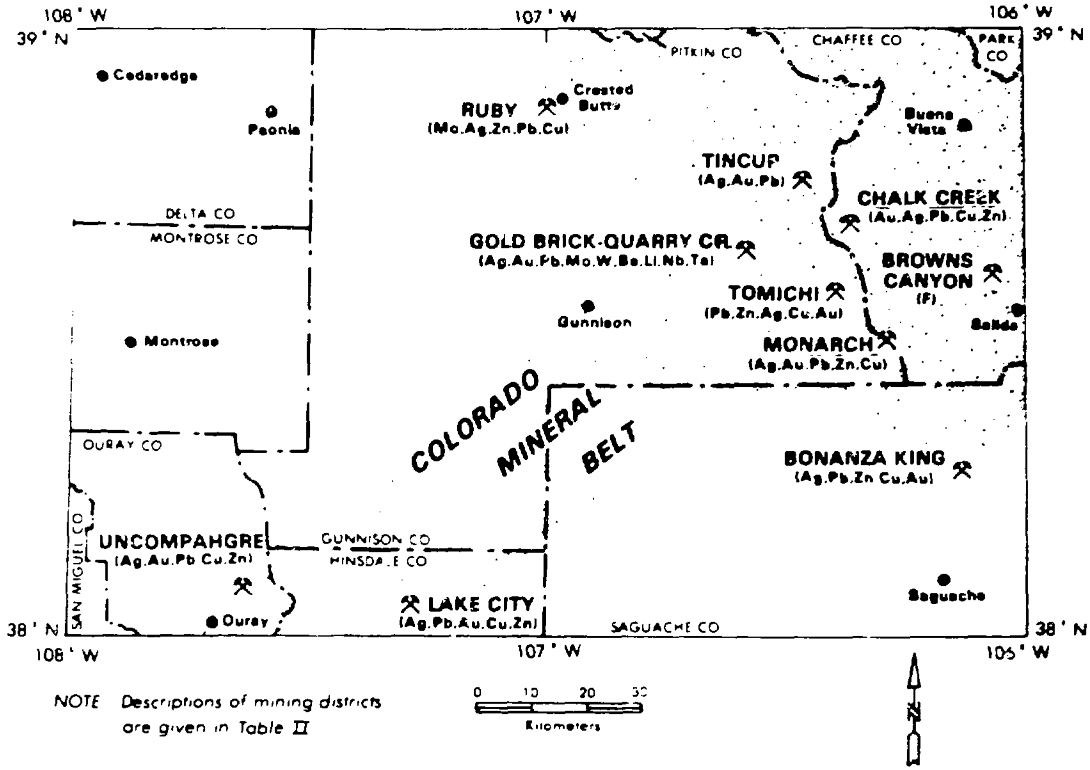

Fig. 5. Major base-metal mining districts in the Montrose quadrangle, Colorado.

DATA SET DESCRIPTION, DIGITIZATION, AND REGISTRATION

Introduction

This unit describes the nature and sources of data used, including NURE airborne geophysical data, NURE hydrogeochemical and stream sediment analyses, geologic information, and Landsat imagery. Although each data set is independent, a common factor is that every set covers approximately the same geographic area. Furthermore, each data set has its own built-in resolution; the hydrogeochemical data are from irregularly spaced sample points, whereas airborne geophysical data are from densely sampled flight lines spaced several kilometers apart. Landsat imagery has a much finer resolution of approximately 60 m.

Data integration requires resampling each data set to a common grid. Due to the diversity in the original sampling grids, integration is generally a tedious exercise. Extensive use is made of rubber sheet transformation (Landsat imagery), interpolation schemes (NURE data), and data reformatting. Ideally, the finished product gives computer access to all data sets simultaneously for any desired location.

For the Montrose quadrangle, the reference grid selected has a grid spacing of one kilometer, exactly coinciding with the UTM grid for this part of Colorado. The 1-km spacing is also the smallest reasonable choice for concordance with the kriging interpolation schemes used for airborne and the geochemical data. Because the corners of the Montrose 1° x 2° quadrangle do not form a perfect rectangle on the UTM projection, the smallest rectangle that can be defined on the sample grid that will cover the entire quadrangle was selected. This results in an index set of 119 rows and 179 columns to cover the 1° x 2° sheet--a total of 21 301 grid cells. All data sets are keyed to grid cell locations rather than latitude and longitude.

Description of Data Sets

Geochemical Data. Our geochemical data sets are compiled from two separate studies done as part of the US Department of Energy's NURE program (Bolivar, 1980a). As part of this program (Bolivar, 1980b), the Los Alamos National Laboratory conducted a hydrogeochemical and stream sediment reconnaissance for uranium in the Montrose quadrangle, Colorado, during which 1365 water and 1857 sediment samples were collected from 1877 locations (Broxton et al, 1979). Water samples come from streams, springs, and wells and were analyzed for uranium by fluorometry. Sediment samples were taken from streams and springs and were analyzed for uranium by delayed-neutron counting, for 31 additional elements by neutron activation analysis, for 9 elements by energy dispersive x-ray fluorescence, and for 2 elements by arc-source emission spectrography. Standard sampling procedures as defined by Sharp and Aamodt (1978) were used in the field. Sample densities were nominally one sample location per 10 km^2 (Fig. 6A). All samples were collected during July 1976 and July and August of 1977. A sample location overlay (scale 1:250 000) can be found as Plate I of Broxton et al (1979).

In the summer of 1979, Los Alamos conducted a detailed follow-up hydrogeochemical and stream sediment survey in a portion of the Montrose quadrangle. A total of 2088 stream sediment samples were collected at a nominal density of one sample location per km^2 (note: 1034 water samples

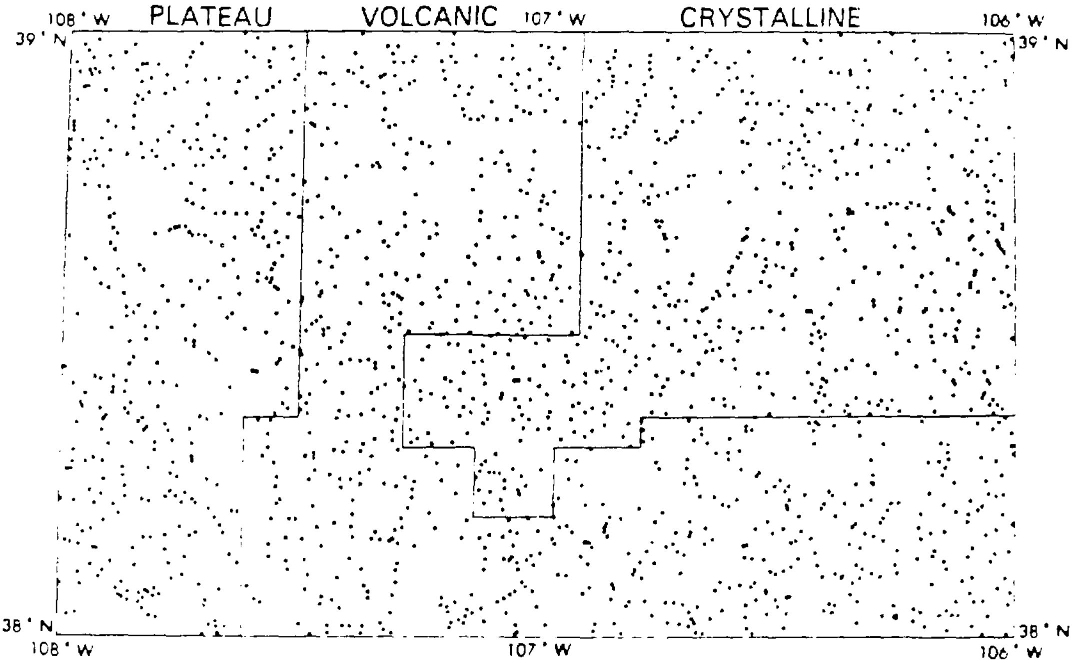

Fig. 6A. Sample locations for the Montrose quadrangle (Broxton et al, 1979).

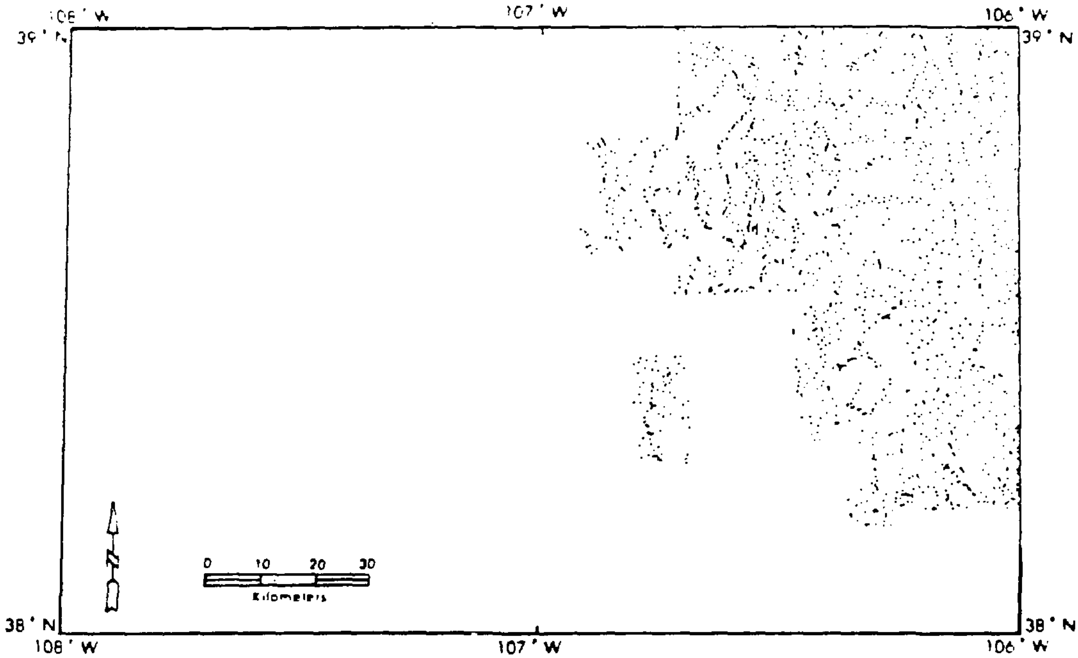

Fig. 6B. Sample locations for the Montrose special study (Maassen, 1980).

Fig. 6. Geochemical sample locations and major physiographic/geochemical provinces for the Montrose quadrangle, Colorado.

were also collected). Samples were analyzed for uranium and for 45 other elements (Maassen, 1980). The majority of samples are from, or near, the Sawatch Range (Fig. 6B).

By combining these two data bases, we obtain a geochemical data base with 3965 sample locations (some locations are for sediment samples only, some are for water samples only, however most are for both a water and sediment sample). We then selected 24 elements we believed would be most beneficial as an aid in identifying uranium mineralization. The report of Beyth et al (1980b) examines the data of Broxton et al (1979) by using multivariate statistical analyses. Beyth's results helped to identify those elements that would be most favorable for our work. We also tried to select elements that had a minimal number of values below our analytical detection limit (Bolivar, 1980b). Also included are the elements arsenic, zirconium, and selenium, which the Department of Energy required for the followup study (Maassen, 1980). Table III is a list of elements selected. The U/Th ratios (not shown in Table III) comprise a separate data set.

The element selenium was selected as one of the 24 elements; however, because all but 18 of the analyses are below the detection limit, correlations between Se and other elements must be viewed with caution.

Furthermore, because the Sawatch special study involved collection of 2088 additional samples, the sample populations are biased for the northeast corner of the quadrangle (Fig. 6). This corner is also crossed by the Colorado Mineral Belt (Fig. 5); consequently many base-metals are enriched in this area and several other elements have concentrations an order of magnitude or more above their normal crustal abundances. In order to compensate for this bias and because regional background concentrations for elements analyzed in geochemical surveys can be expected to vary as a function of topography, hydrology, and especially geology, the Montrose quadrangle was subdivided into three major physiographic/geochemical provinces: the Sawatch-Gunnison crystalline terrane, the San Juan-West Elk volcanic field, and the Western Plateau area. The Sawatch-Gunnison crystalline terrane is underlain principally by Precambrian igneous and metamorphic rocks and, to a lesser extent, by Paleozoic sedimentary formations and Tertiary plutonic rocks. The San Juan-West Elk volcanic province is underlain by mid-Tertiary intermediate to felsic volcanic rocks, whereas the Western Plateau is underlain by gently dipping Mesozoic sedimentary formations. The province boundaries selected and

TABLE III

DETECTION LIMITS AND ANALYTICAL METHODS FOR SELECTED ELEMENTS
(from Bolivar, 1980b)

Element	Symbol	Minimum Detection Limit (in ppm)[a]	Method of Analysis[b]
Aluminum	Al	200	NAA
Arsenic	As	5	XRF
Barium	Ba	400	NAA
Calcium	Ca	5000	NAA
Cerium	Ce	10	NAA
Cobalt	Co	2	NAA
Chromium	Cr	20	NAA
Copper	Cu	10	XRF
Dysprosium	Dy	2	NAA
Iron	Fe	2000	NAA
Hafnium	Hf	1	NAA
Potassium	K	3000	NAA
Lithium	Li	1	ES
Manganese	Mn	10	NAA
Lead	Pb	5	XRF
Scandium	Sc	0.1	NAA
Selenium	Se	5	XRF
Thorium	Th	0.8	NAA
Titanium	Ti	200	NAA
Vanadium	V	5	NAA
Zirconium	Zr	5	XRF
Zinc	Zn	30	NAA
Uranium (in sediment)	Us	0.01	DNC
Uranium (in water)[c]	Uw	0.02 (in ppb)	F

[a] Because of elemental interference, detection limits will shift as a function of sediment composition.

[b] NAA = neutron activation analysis, XRF = x-ray fluorescence, ES = arc-source emission spectroscopy, DNC = delayed neutron counting, F = fluorometry.

[c] All water samples with uranium concentrations >40 ppb are reanalyzed by DNC.

the respective number of geochemical sample locations for both waters and sediments are shown in Fig. 6.

The elemental concentration analyses represent point data at irregularly spaced sample locations; therefore, it is necessary to get this data into a spatially comparable format with the other data sets. This was done by "universal kriging" on a moving window interpolated to a regular grid. Universal kriging is a statistical method (Olea, 1974) used to obtain spatially interpolated values from a set of irregularly spaced data points. The standard assumption is that the spatial covariance in small regions is dependent only on the distance between points. If this covariance function were known, an unbiased estimate of the elemental concentration at an unsampled location can be formed, together with an estimate of the variance. In practice, the spatial covariance function (actually, a related function, the variogram) must be estimated as well.

Thus an estimate of the elemental concentration was formed for each grid center on the 1-km grid as a weighted average of nearby samples. The nearest five samples were used, provided there were five within a 5-km radius of the grid point; also, all samples within 500 m were used, even when the total is greater than 5. When there were two or less samples within 5 km of a grid point, no estimate was computed and the grid point was assigned a zero value. The weighting of these samples depended on their distance from the grid point and on the estimated variogram. No provision was made for stream drainages. Because some elemental concentrations can be below detection limits (explained in Table III), such values are down-weighted.

Airborne Radiometric and Aeromagnetic Data. In fall 1978, as part of the NURE program, an airborne radiometric and aeromagnetic survey was made of western Colorado and eastern Utah. Data processing methods, regional geology, and evaluation techniques for this regional survey are summarized in geoMetrics (1979a); geoMetrics (1979b) is a geologic summary and evaluation of the Montrose quadrangle. A summary of the characterization of all uraniferous provinces by aerial spectrometry can be found in Saunders (1979).

Surface gamma radiation is produced primarily by the radioactive decay of potassium-40, thorium-232, and uranium-238. Gamma-ray intensities are measured by an airborne spectrometer from the potassium-40, thallium-208, and bismuth-214 peaks. Because the parent heavy nuclides do not have distinct gamma-ray peaks, daughter thallium and bismuth intensities are read; the daughter products bismuth-214 (for uranium-238) and thallium-208 (for thorium-232) are assumed to be in equilibrium with their parent nuclides (Adams and Gasparini, 1970).

Moving at a standard ground speed of 110 kmph (70 mph), the airborne spectrometer measures gamma radiation from only the top 20-50 cm of ground surface (Gregory and Horwood, 1963). Each data point is an integrated measurement of gamma rays taken normally from a helicopter and accumulated over a fixed period of time, usually one second. For the Montrose quadrangle, one-second samples correspond to a 215-m (700-ft) long by 185-m (600-ft) oval on the ground, i.e., one data point represents about a 40 000 m^2 area (geoMetrics, 1979a). The Montrose quadrangle contains over 200 000 points for each of the aerial radiometric and aeromagnetic bands.

East-west profiles were flown at 4.8-km (3-mile) spacing for the southeast quarter of the Montrose quadrangle and 3.2 km (2 miles) for the rest of the quadrangle. North-south tie lines were flown at 19.2-km (12-mile) spacing. Flight lines were flown at a 122-m (400-ft) mean terrane clearance at an average ground speed of 70 mph (geoMetrics, 1979a).

Digital tapes containing raw spectral data and magnetic data were obtained from geoMetrics via Bendix Field Engineering Corporation, Grand Junction. The data consist of equivalent thorium (eTh), equivalent uranium (eU), percent potassium (K40), and magnetic data for the flight lines. A total of 220 anomalies (according to criteria listed in geoMetrics, 1979a) is shown on the uranium anomaly/interpretation map (Fig. 4, in geoMetrics, 1979b). This map also shows the flight line spacings.

The first step in getting from densely sampled flight lines to the 1-km rectangular grid is to smooth and subsample the noisy aerial radiometric data along flight lines. This is done using an automated kriging procedure, where the parameters of the variogram are estimated locally, depending on the local signal-to-noise ratio. The result is an adaptive filter. In regions where the data are not changing much, relative to the noise, the smoothed estimate is almost an unweighted average of measurements in a relatively long segment of the flight line (about 1.5 km); in a region where the signal is changing rapidly, nearby measurements are much more heavily weighted than more distant ones. These kriged estimates (together with error estimates) were computed every 0.4 km along each flight line, that is, at about one-tenth the density of the original one-second measurements.

From this point, interpolation onto the rectangular grid proceeds much as for the hydrogeochemical data. A variogram is computed and used to form an estimate at each grid center point as a weighted average of the smoothed data (with associated errors). All of the smoothed data within 3.5 km of a given grid center point were used in forming an estimate at that center point; a circle of this radius intersects at least two flight lines, except when centered at a few points in the southeast part of the quadrangle.

The aeromagnetic data were similarly treated, except that along flight lines, as there is very little noise in these data, values at 0.4-km intervals were determined by linear interpolation between the two nearest measurements.

Note that areas of highest concentrations for our geophysical data will not exactly coincide with the locality of the highs shown in Fig. 4 of geoMetrics (1979b). This is the result of the kriging algorithm, which smoothes the data over the specified grid (in this case, 1 km x 1 km).

Known Uranium Occurrences. About 90 uranium occurrences or areas with abnormal radioactivity are known for the Montrose quadrangle (Fig. 4). These occurrences are described in Table I.

In order to combine this information, which is essentially point data, with other data sets, it was necessary to digitize the occurrences and assign each a UTM coordinate. Each known occurrence was assigned a coded number from which one could identify the deposit type in Nelson-Moore et al (1978). Each occurrence was also assigned a grid cell location for the 179 x 119 rectangular grid. This allowed us to examine any one occurrence by simply identifying the coordinates for that grid cell. The occurrences, their coded identification numbers, and their grid cell coordinates are given in Appendix A.

Geologic Map. The geologic map of Tweto et al (1976a), scale 1:250 000, was used as a base map. Tweto's map contains 57 mappable formations. To facilitate interpretation efforts and because many of these units are depositionally similar, the 57 formations of Tweto were grouped into 13 selected geologic "units" (Table IV).

A mylar transparency was then made for this map by assigning each unit (Table IV) a separate mylar color. Care was taken to assign colors that could "easily" be resolved by a computer when the primary colors are examined. The mylar transparency was used in an attempt to assign each unit a consistent color density.

TABLE IV

GEOLOGIC UNITS

Geologic Unit	Formations of Tweto et al, 1976a
Qal	Qa, Qg, Ql, Qgo, Qd, Qdo, QTa (alluvium, glacial, landslide, unconsolidated deposits)
Tsd	Td, Ts (Dry Union and Santa Fe formations--mostly Pliocene and Miocene sediments)
Tig	Tbb, Tbbi (Miocene basaltic intrusives)
Tas	Tbr, Tbrt, Taf, Tial, Tiql, Tos (Oligocene rhyolitic ash flow tuffs, andesitic lavas and breccias, and sedimentary deposits)
Tga	Tmi (Middle Tertiary granitic intrusives)
Tuf	Tpl, Twm (Oligocene andesitic lavas and breccias and densely welded rhyolitic tuff)
Tgm	Tg, Tt, Two, TKtc (includes Green River, Telluride, and Wasatch formations, and Ohio Creek conglomerates)
Tci	TKi, Cam, Yam (granodioritic Laramide intrusives, and Cambrian alkalic and mafic intrusives of limited outcrop)
Kj	Kmv, Kd, Kdb, Jm, Jmi, Jmw, Jmwe, Jme, KJdm, KJdj, KJdw, KJde (includes Mesaverde formation, Dakota sandstone and Jurassic sandstones)
Km	Km (Mancos shale)
Pal	Trd, TrPdc, PPm, Pmb, Pmbe, Ph, MOr, MDr, MCr (mostly Paleozoic sandstones and limestones; includes Maroon, Minturn, Belden, and Hermosa formations. Also includes Leadville limestone and Harding sandstone)
PCg	Xg, Yg, YXu, YXg (Precambrian Y--1400 m.y.b.p.--age and Precambrian X--1700 m.y.b.p.--age granitic rocks)
PCm	Xb, Xfh, Xm, Xq (Precambrian metamorphics and metavolcanics)

The mylar transparency was then photographed onto 70-mm color film. The color film was digitized on a PDS microdensitomer to obtain three 512 x 340 digital arrays corresponding to the green, red, and blue exposures, respectively, on magnetic tape. The three digital arrays were inserted into a COMTAL 8000 digital display unit to form a color image of the geological map. Training sets were then defined for each of the 13 geological units from inspection of the color display. Finally, each grid cell was classified as belonging to one of the geologic units by using a simple minimum distance classifier. Then the classified 512 x 340 array was resampled, using nearest neighbor interpolation, to the 179 x 119 UTM grid (Fig. 7).

Because the contacts between mylar cutouts (each cutout corresponding to contiguous geologic units) do not fit perfectly, most classification errors occur along boundaries between geologic units. This problem was alleviated somewhat by a median filter operating both as a preprocessor and a postprocessor. Final cleanup of the map was accomplished manually on the 179 x 119 array (Fig. 7B).

Landsat Imagery. Landsat imagery consists of electromagnetic radiation collected in four wavelength regions: 0.5 to 0.6 μm (band 4), 0.6 to 0.7 μm (band 5), 0.7 to 0.8 μm (band 6), and 0.8 to 1.1 μm (band 7). The electromagnetic radiation is recorded by a multispectral scanner (MSS), in a satellite, and transmitted to receiving ground stations by microwave. The MSS receives the ground image at a series of detectors where the intensity of the reflectance is changed to a voltage that is in turn converted to digital values (i.e., brightness values). The MSS scans the earth's surface east to west. A 79 m x 79 m satellite image is reformated and the consequent 56 m x 79 m single value image is transmitted to an earth receiving station. This 56 m x 79 m image is called a Landsat pixel. Electromagnetic radiation for each band is averaged over this area. Brightness values, ranging from 0 to 63, are then assigned to each pixel in each of the four bands. However, the brightness value for any one pixel depends on the relationship between the ground features, local background, and scattering and absorption in the atmosphere. For a complete description of the Landsat system, see USGS (1979) and Bailey (1980).

A Landsat 2 tape (October 1978) that includes most of the Montrose 1° x 2° quadrangle was purchased. Landsat 2 data for any given scene is received on a nine-track 1600 bpi tape set that consists of four magnetic tape files.

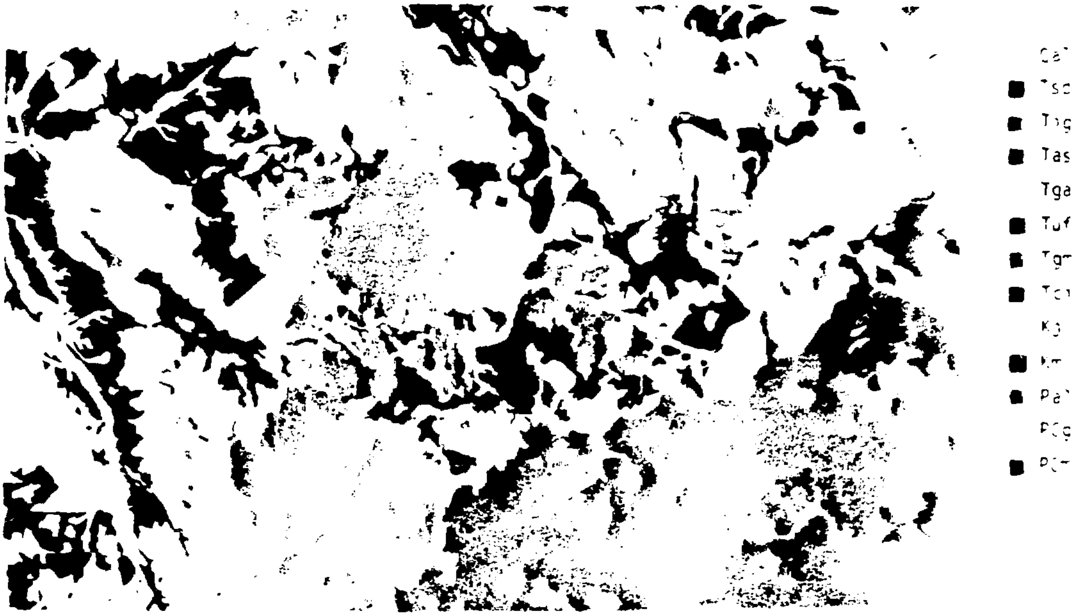

Fig. 7A. Geologic map color transparency (from Tweto et al, 1976a).

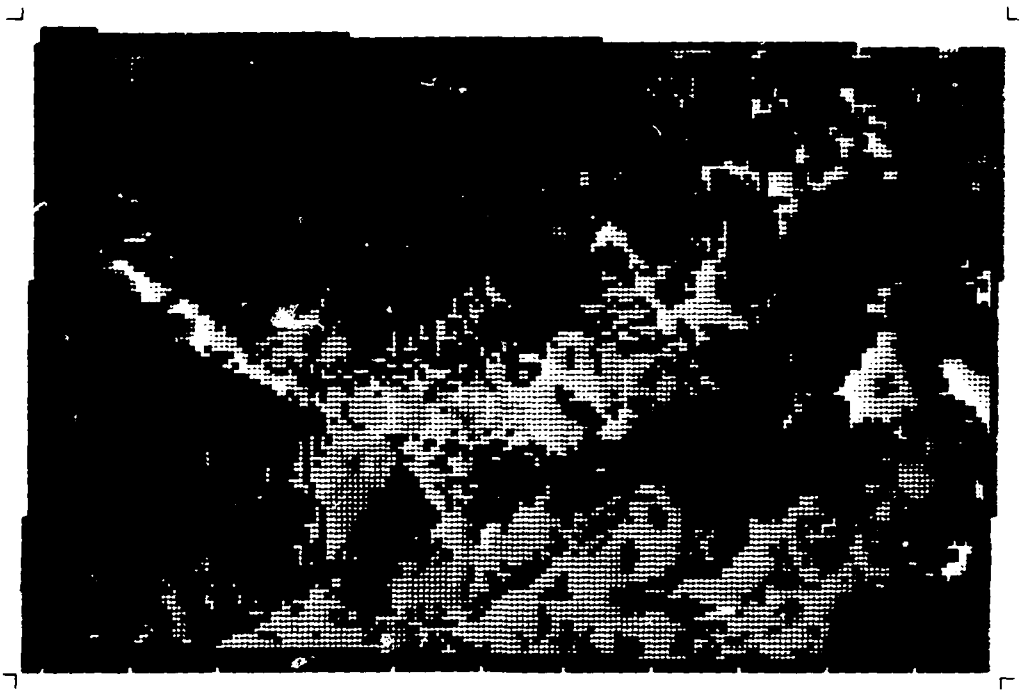

Fig. 7B. Gray level geologic map of the Montrose quadrangle with 1-km grid cell resolution (units described in Table IV).

Fig. 7. Geologic map representations of the Montrose quadrangle, Colorado.

The Landsat 2 imagery is available at a sample interval of 56 m along each scan line with a spacing of 79 m between scan lines (Bailey, 1980); each file holds packed data for the four spectral bands corresponding to 2340 scan lines with 810 pixels per line. Thus, each tape file corresponds to a vertical column, 810 points wide, taken from the scene. The entire scene of 2340 scan lines with 3240 pixels per line is obtained when the files are merged side-by-side.

Because the Landsat image is available on a grid oblique to the UTM grid, it was necessary to resample the Landsat data onto the UTM rectangle. We selected both a 1-km and 100-m resolution for our resampling.

The first step in the processing consists of converting the data in the above format to four files of 2340 lines with 3240 pixels per line, with each file corresponding to a different spectral band.

At this point, three small subimages of size 512 x 512 at full Landsat resolution were selected from different parts of the entire scene. The small images were then displayed and the line and pixel positions of three known landmarks in each image were selected. From knowledge of the latitude and longitude of each of the control points, their coordinates on the UTM projection for the Montrose quadrangle were computed. Thus, by least squares the coefficients in the affine transformation

$$R = a_{11}x + a_{12}y + a_{13}$$

$$C = a_{21}x + a_{22}y + a_{23}$$

were found. Here (x, y) is the coordinate of a grid point on a 1781 x 1181 grid with 100 m spacing, and (R, C) is the row (R), column (C) location of a pixel in the Landsat scene. The a's are the coefficients of the transformation. If R and C were integers, a unique pixel of the Landsat scene would be defined for the UTM grid point (x, y). In general, R and C are not integers, so the nearest pixel to (R, C) is assigned. The above transformation permits rotation, translation, and rubber-sheet stretching of the original Landsat data to fit the specified UTM grid.

In order to form meaningful images for ratios between the various Landsat bands, it is necessary to subtract a constant bias value from each band (Chavez, 1975; Wecksung and Breedlove, 1977). This bias value results from direct scatter of sunlight from the atmosphere into the sensor and it depends mainly on the wavelength of the scattered light. The biases for the individual bands can be estimated by assuming that the raw Landsat data vectors tend to scatter along straight lines that intersect at a common point in spectral space (Chavez, 1975; Wecksung and Breedlove, 1977), whose co-ordinates are just the atmospheric biases. The bias value for Landsat band 7 is known to be very close to zero. Hence, we collected a histogram of data vectors for which the band 7 value was zero (Table V). The peak in the distribution for each band represents the estimate of the atmospheric bias for that band. We observe from Table V that a digital value of 7 never occurred for any band, but this is a peculiarity of Landsat 2 imagery. We can also get the estimates for the correction from Table V. The biases fall off with increasing wave length as predicted by the Rayleigh scattering law.

The end result is two sets of resolution for the Landsat imagery for the Montrose 1° x 2° quadrangle. One set has the resolution of 1 km on the 179 x 119 grid system (Fig. 8A). The other resolution required resampling the Landsat imagery to a grid of 1781 columns and 1181 rows--exactly 10 rows and 10 columns in each of the 179 x 119 grid cells. On this grid, 100 Landsat pixels equal one 1-km grid cell or 100-m resolution for each Landsat pixel (Fig. 8B).

TABLE V

DATA VECTORS AND ATMOSPHERIC CORRECTION VALUES
FOR BANDS 4, 5, 6, AND 7

Digital Number	0	1	2	3	4	5	6	7	8	9
Band 4 frequency	0	0	3	351	3711	4704	6232	0	2811	843
Band 5 frequency	1	80	777	5659	5271	3811	2380	0	583	270
Band 6 frequency	3198	3457	4600	3775	2224	1102	738	0	68	26

	Band 4	Band 5	Band 6	Band 7
Correction value	6	3.4	2	0

Fig. 8A. False-color composite at 1-km grid cell resolution (Bands 4, 5, and 7, log stretched).

Fig. 8B. False-color composite at 100-m grid cell resolution (Bands 4, 5, and 7, log stretched; 512 x 410 pixel area, original data subsampled every fourth pixel).

Fig. 8. Geometrically registered Landsat imagery for the Montrose quadrangle, Colorado. These figures are not to scale with Plate 1.

Landsat imagery usually has a resolution of 56 m (USGS, 1979); however, we felt that our coarse resolution of 1 km was necessary for comparison to all the other data sets at the same resolution. We also felt that our 100 m resolution for our fine grid was also an optimum and logical choice should we require a better resolution than 1 km and that we did not need the 56-m resolution for preliminary work. We used the 100-m grid primarily for preliminary examinations of Landsat data; the 1-km resolution was used in our classification schemes and statistical routines.

Data Access and Manipulation

Two Los Alamos facilities have proven to be indispensable for the DIRS project. The Central Computing Facility, with its two CRAY-1 and four CDC 7600 computers, provides the requisite computing power to manipulate the data, and the DIADS (digital image analysis and display system) facility gives quick-look capabilities for the merged data sets and provides the means to analyze and classify digital Landsat data.

Another major advantage in data integration at Los Alamos is the Common File System (CFS). The CFS is a large, centralized data storage/retrieval system that provides permanent file space. Files can be stored in whatever format they were in when sent to the CFS. Generally, this system utilizes disk storage of 60-bit words, and present on-line capacity is 1.6 trillion 60-bit words with almost infinite off-line storage. There are several time-sharing systems (e.g., NOS, LTSS, CTSS) that are tied into the CFS. There are also an extensive set of flexible utility routines and programs available.

The classification scheme utilized in this study (explained in the next section) was done by simply creating several files, one for each data set, and placing these files in the CFS. The files could be accessed independently or in groups and various statistical programs could be performed.

In running a program, the computer creates an array of the files selected. For the Montrose quadrangle, the array would be 179 x 119 x N (the number of data sets read in). While reading in any data set, statistical manipulations can be performed. For example, if only data one standard deviation above the mean are required for the data set Cu, then the program would compute the mean value and standard deviation and copy only the concentrations of Cu greater than the mean plus one standard deviation into the array. All other values for the data set Cu would be set to zero. Only the information specified is retained.

PRELIMINARY ANALYTICAL TECHNIQUES AND CLASSIFICATION

Introduction

We initially examined various data set combinations manually. To accomplish this, we obtained map copies, scale 1:250 000, of all data sets and physically overlayed them. An example is shown in Fig. 9. This map represents the concentration data for aluminum that has been kriged and computer contoured. Regions with high concentrations are darkened. If one were to overlay all data sets, the stack would become enormous, and by looking at various one-, two-, or three-set combinations (or actually any number of combinations), the task would become exceptionally time-consuming and tedious.

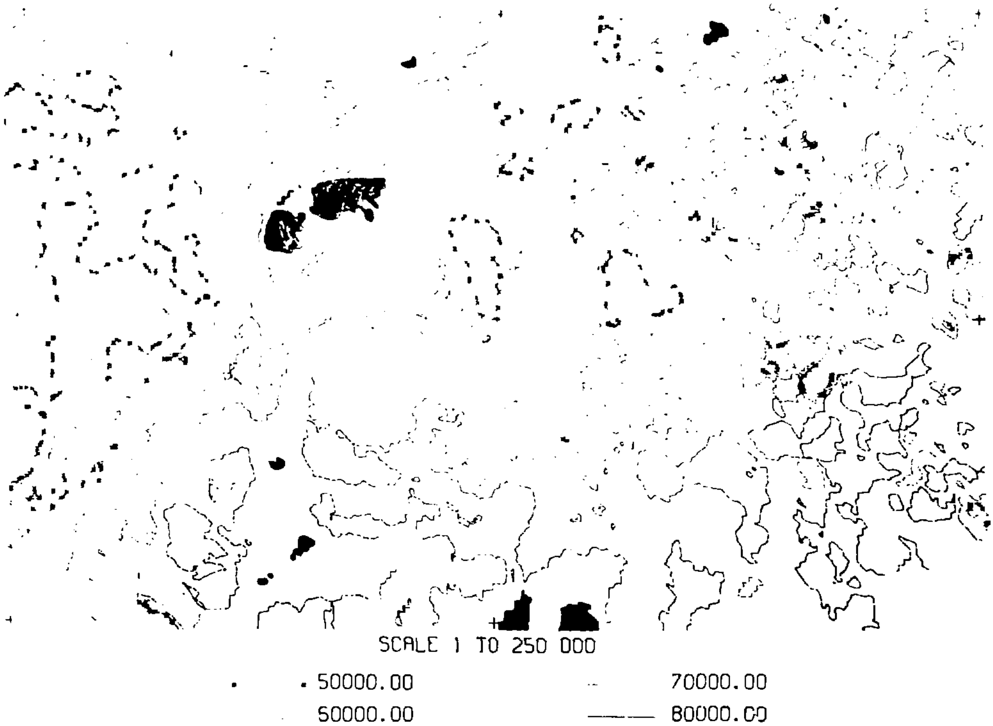

Fig. 9. Computer-generated contour map of Kriged aluminum-in-sediment data for the Montrose quadrangle, Colorado.

However, once a relationship between data sets has been determined, generally by some other method, the map copies at the 1:250 000 scale provide the interpreter with a good scale for more detailed evaluation of regional reconnaissance data.

In order to obtain a faster examination of the relative dispersion for any data set, we utilized a computer routine called DIGIKAM. This provided a three-dimensional view for any data set (Fig. 10). While we were able to recognize regions with high background levels, e.g., in Fig. 10, waters from the Colorado Plateau are enriched in uranium concentrations relative to waters from the West Elk and San Juan volcanic regions, we were unable to make a quantitative evaluation.

We then tried to overlap data sets with our DIADS system. We found that this was very time consuming when trying to form combinations of three; however, the system does allow immediate interactive responses. Consequently, encouraged by the work and procedures of Lowenstein and Howarth (1973), Howarth and Lowenstein (1976), and Webb et al (1978), we decided to instead use the larger computers at Los Alamos. After a routine has been completed (either on a CRAY 1 or CDC 7600 series computer), a file is generated that can be processed on a FR-80 recorder. The output is 35 mm slides that can then be examined conveniently and rapidly. For 23 geochemical data sets (excluding Se) alone, there are 1771 possible combinations of three. However, once on film, all 1771 combinations can be examined in a few hours. This system essentially duplicates DIADS; however, we do not have the luxury of interactive response.

Display Options

It is common practice to overlay two data sets to find correlations; however, a methodology was required by which we could not only examine the enormous quantity of data more efficiently, but also could apply enhancement techniques (e.g., Koch et al, 1979) that make possible a look at higher dimensionality correlations (Howarth and Martin, 1979; Pirkle et al, 1979). So we utilize Colorrocks, a program whereby data sets are displayed three at a time. Colorrocks was developed by Dr. Robert Hausman, a consultant from Pacific Sierra Research Corporation. Relationships between respective data sets can be examined according to the rules of color addition (Table VI). Any required statistical manipulation can be done before display.

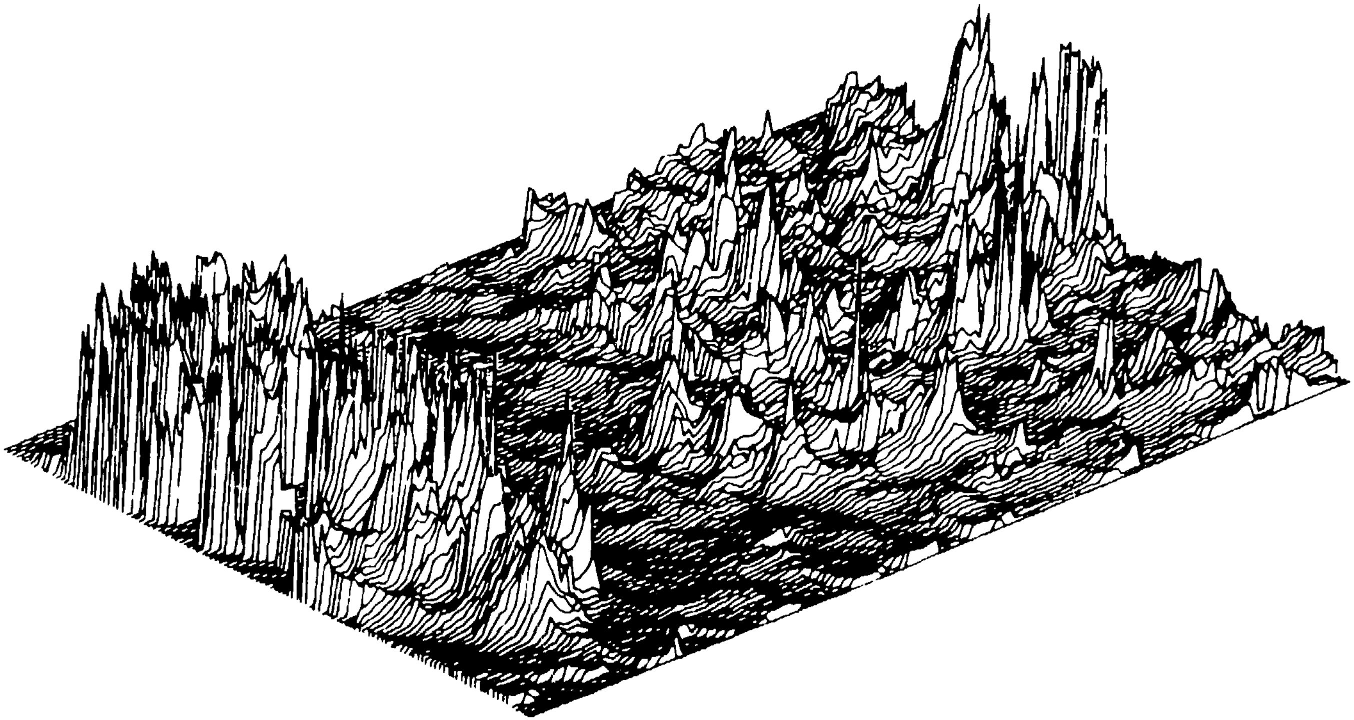

Fig. 10. *A three-dimensional plot for the data set Uw—uranium in waters for the Montrose quadrangle, Colorado; view is from the southwest.*

TABLE VI

COLOR ADDITION CHART

Primary Color	Color Addition
Red	Red + Green = Yellow
Green	Green + Blue = Blue-Green
Blue	Red + Blue = Magenta
	Red + Blue + Green = White

Colorrocks provides several options; examples are shown in Fig. 11. We first looked at linear gray level maps of the kriged data sets that include 23 elements (excluding Se), U/Th ratios, three airborne radiometric bands, one aeromagnetic band, one digitized geologic map, and four Landsat bands (unkriged). Linear gray level maps for these data sets are shown in Appendix B.

In a positive linear gray level map, the data are represented by 256 gray levels (256 equal intervals in the histogram), ranging from white, the lowest value in the data set, to black, the highest value in the data set (e.g., Fig. 11A). The blocky appearance results from the 179 x 119 grid; one block represents 1 km^2.

To aid interpretation, several density slices were made. A density slice allows the interpreter to look at a specific interval of data. If a density slice from one to four standard ($1\sigma - 4\sigma$) deviations above the mean is required, then by convention all values from the lowest to one standard deviation above the mean are assigned a value of 0, i.e., a white color (in a positive print). Values greater than four standard deviations above the mean are assigned black; all other values in the data set are then divided into 254 groups and each group is assigned an increasing intensity of gray. Only the data above the lower cutoff are enhanced, data below this cutoff are ignored. An example is shown in Fig. 11B. This enhancement allows one to look at only the required interval of data. For the Montrose quadrangle, we examined density slices for each data set for 1σ-4σ above the mean, 2σ-4σ above the mean, and 1σ below the mean to 4σ above the mean. An example of a linear gray level map and different density slices for the data set Us (uranium in sediment) are shown in Fig. 11A-C.

This type of enhancement also allows the evaluator to scale the data to any given criteria. In Fig. 11D, the data set Us is scaled to Taylor's (1964) mean crustal abundance for uranium. All values in the Montrose quadrangle that fall below Taylor's crustal abundance appear as white. Note the very good correlation between Fig. 11A and Fig. 11D. If a large part of Fig. 11D appeared as black, then this could suggest that Taylor's (1964) value is erroneous <u>or</u> that the Montrose quadrangle is enriched in Us. However, Taylor's abundances are for whole rocks and our values are for sediments so comparison may or may not be valid.

The next step is to add color and visually integrate the various data sets. In order to simplify the remaining discussion, <u>all color composites that follow are density slices from one to four standard deviations above the mean for the respective data set. The order of color designated to each data set is: red for the first set, green for the second, and blue for the third.</u> Correlations can be recognized by the simple rules of color addition (Table VI). All possible data set combinations of three at a time for the density slice described above have been examined; however, only a few descriptive examples are included in this report.

In Fig. 12, two examples of one to four σ density slices, one for the data sets eU, eTh, K40 (Fig. 12A), and one for eU, Uw, and Us (Fig. 12B) are shown. The information in Fig. 12A is generally that used in interpreting radiometric studies (e.g., geoMetrics, 1979b). In Fig. 12A, some geologic units are extremely well delineated. Compare this figure to Fig. 7 and Table IV. The data set eU (in red) clearly outlines the Cretaceous Mancos (Km) formation and eTh traces the Precambrian granitic rocks (in green). In Fig. 12B, eU correlates with Uw in the western half of the quadrangle (yellow); in the same figure eU correlates well with Us in the eastern half of the quadrangle (magenta), particularly in the vicinity of the Mt. Princeton batholith (Fig. 3).

Utilizing Colorrocks, data sets are then merged with Landsat imagery. This step is a visual aid in determining where the density slice for any particular data set occurs geographically. If desired or if a correspondence is suspected, any data set can be integrated with a particular formation. In Fig. 13, a density slice for the data set Uw (in red), which showed an apparent correlation with the Cretaceous Mancos formation (Km) by inspection of Landsat imagery, was overlain onto Km (in green). The yellow color in

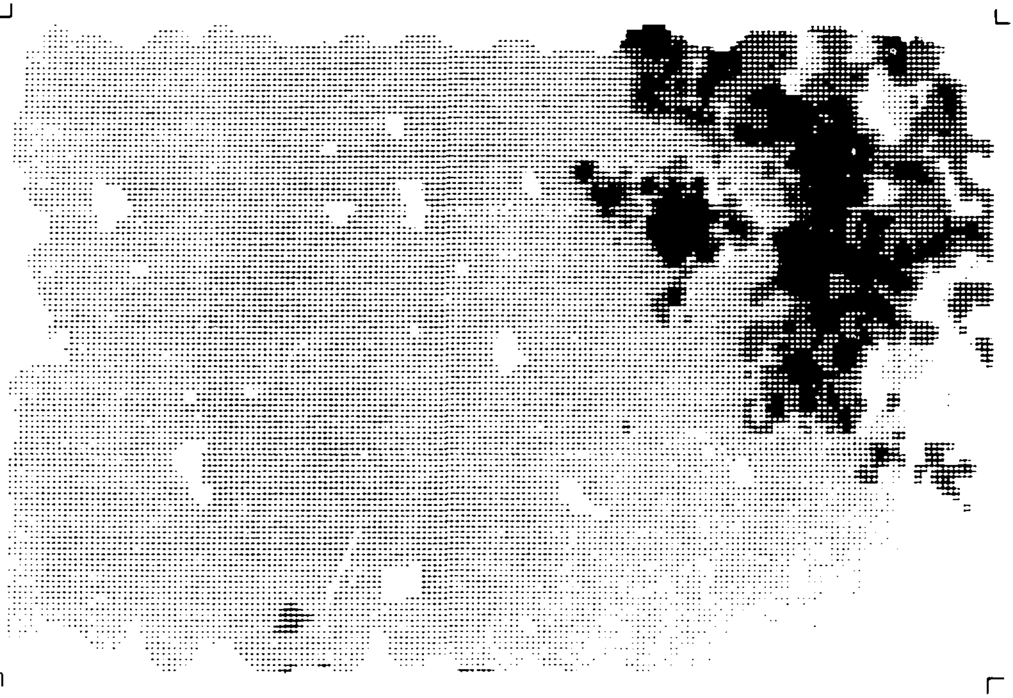

Fig. 11A. *A linear gray level map for Us; 256 gray levels.*

Fig. 11B. *A density slice, 1σ to 4σ above the mean; 256 gray levels.*

Fig. 11. *Gray level representations for the data set Us for the Montrose quadrangle, Colorado. Black represents high values, white represents low values (see text).*

Fig. 11C. A density slice, 2σ to 4σ above the mean; 256 gray levels.

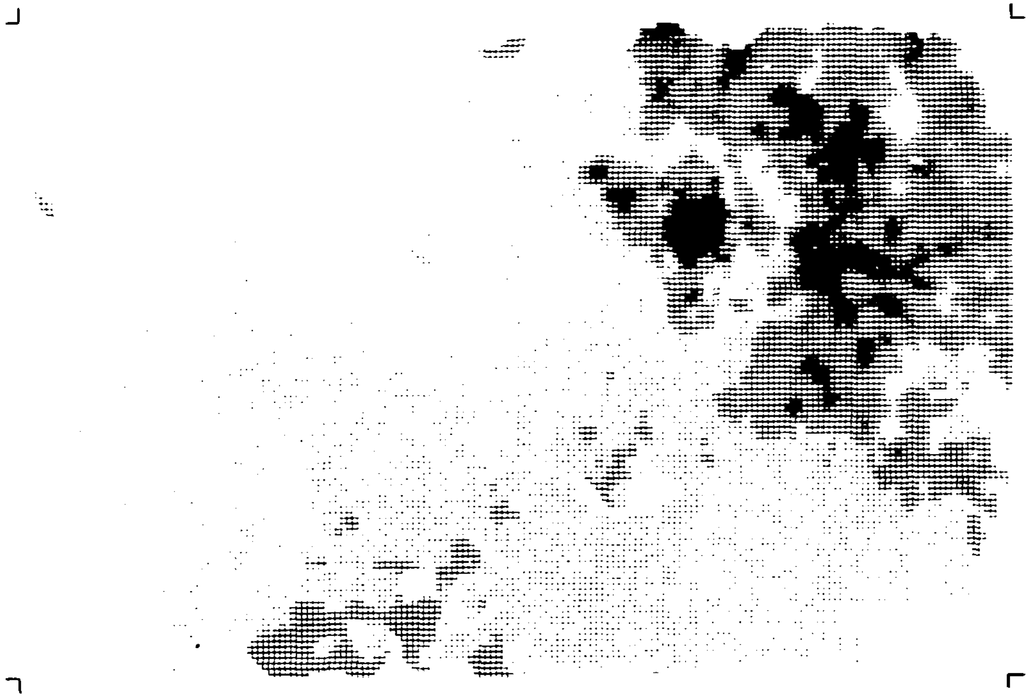

Fig. 11D. A density slice, greater than a crustal abundance value of 2.7 ppm; 256 gray levels.

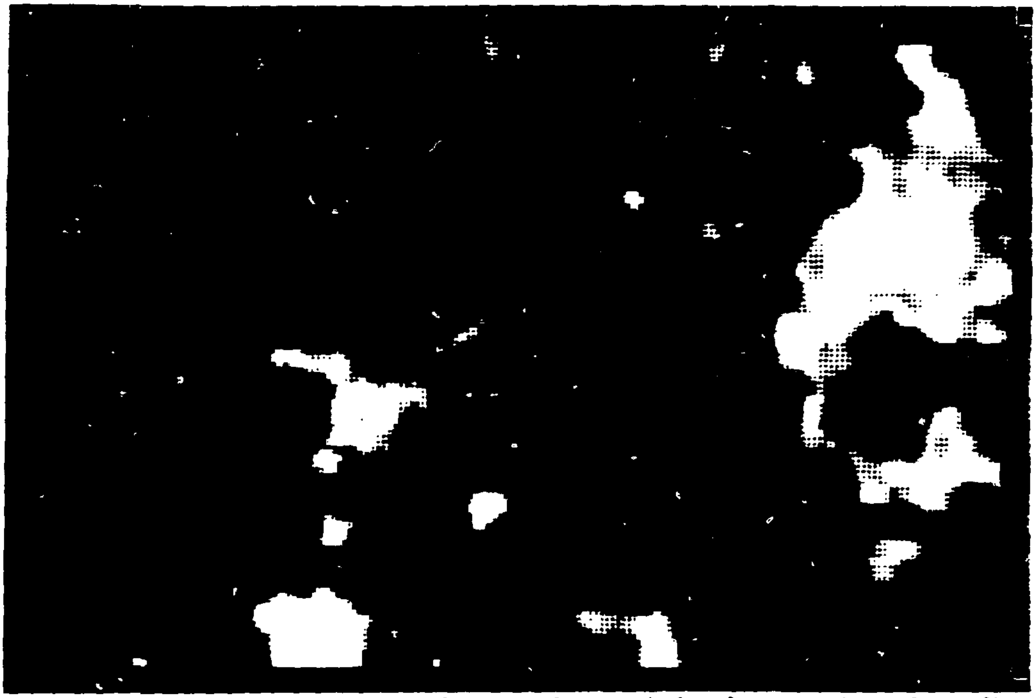

Fig. 12A. *Data sets eU-eTh-K40. These radiometric bands approximately outline Km and Tuf units (Table V).*

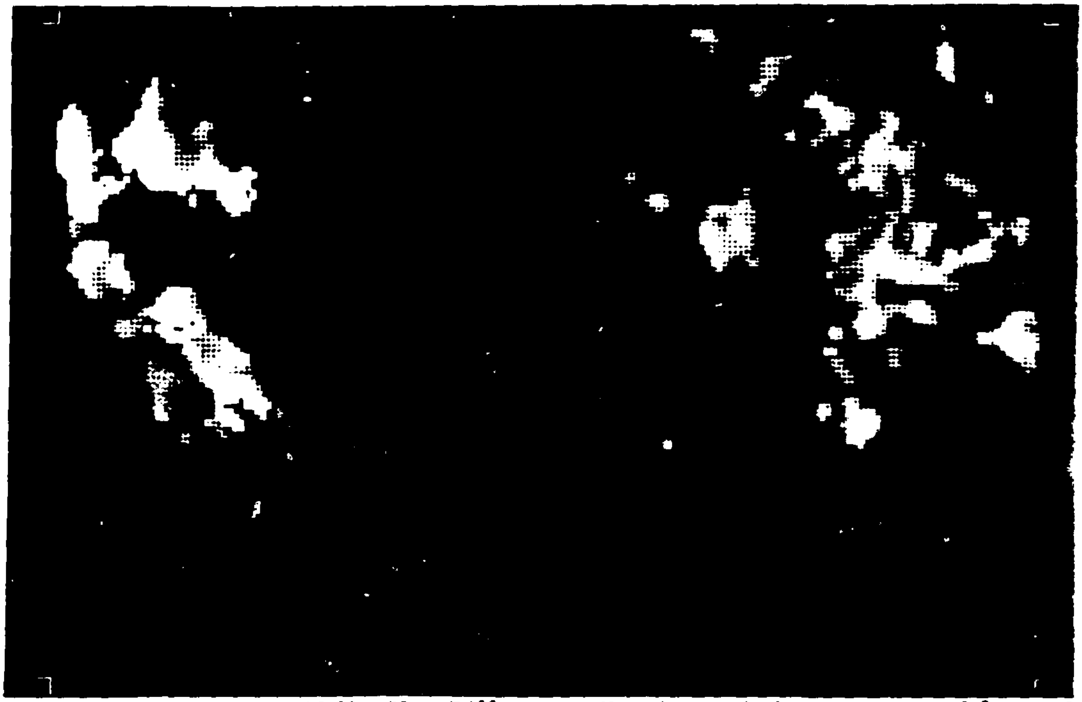

Fig. 12B. *Data sets eU-Uw-Us. Different collection techniques were used for each data set.*

Fig. 12. *Density slices 1σ to 4σ above the mean for various data sets. Color sequence is red-green-blue (Table VI).*

Fig. 13 indicates where there is a high correlation between Uw and Km. The Mancos does contain local calcareous zones (Tweto et al, 1976a). Therefore, this type of correlation is not unexpected because some valence states of uranium are fairly soluble and easily form complexes with carbonate ions (Dall'Aglio, 1971, 1972). The red oval feature in the southeasternmost section of the figure is the Marshall Pass uranium district.

The Colorrocks program for a pilot study on the Talkeetna quadrangle in Alaska (Wecksung and Fugelso, 1980) involved 680 possible combinations (frames) of three for the 17 data sets selected on a grid of 55 x 40. This amount of data took about four hours of CDC 7600 computer time. The output was achieved by using routines from DISSPLA, an independent, proprietary graphics package. For the Montrose quadrangle, with a grid of 179 x 119, only 6 data sets could be run at one time on a CDC 7600; the 23 geochemical data sets alone would require 30 to 35 hours of CDC 7600 computer time. Therefore, the program Colorrocks was modified to run efficiently on the CRAY-1 computer. However, DISSPLA had not yet been implemented on the CRAY and Common Graphics System routines were used instead. All combinations of three for the 23 geochemical data sets (1771 combinations) required only 11 minutes of CRAY computer time.

Accessory Routines

Distribution Routine. In addition to Colorrocks, two accessory routines (also written by Dr. Robert Hausman) were developed. One of these, a Distribution Routine, allows a tally of information for each grid cell. The routine will list the grid cell locations that meet a selected statistical criterion for all data sets.

For example, when examining the 23 geochemical data sets, and considering only the data greater than one standard deviation above the mean for each data set, the Distribution Routine will tally how many elements are one standard deviation or more above the mean for each grid cell. The routine lists elements which meet the selected criteria for each grid cell (an example is shown in Fig. 14).

Sort Routine. A routine was also developed to calculate the percentile value of any data set at any grid cell location. An example is given in Fig. 15.

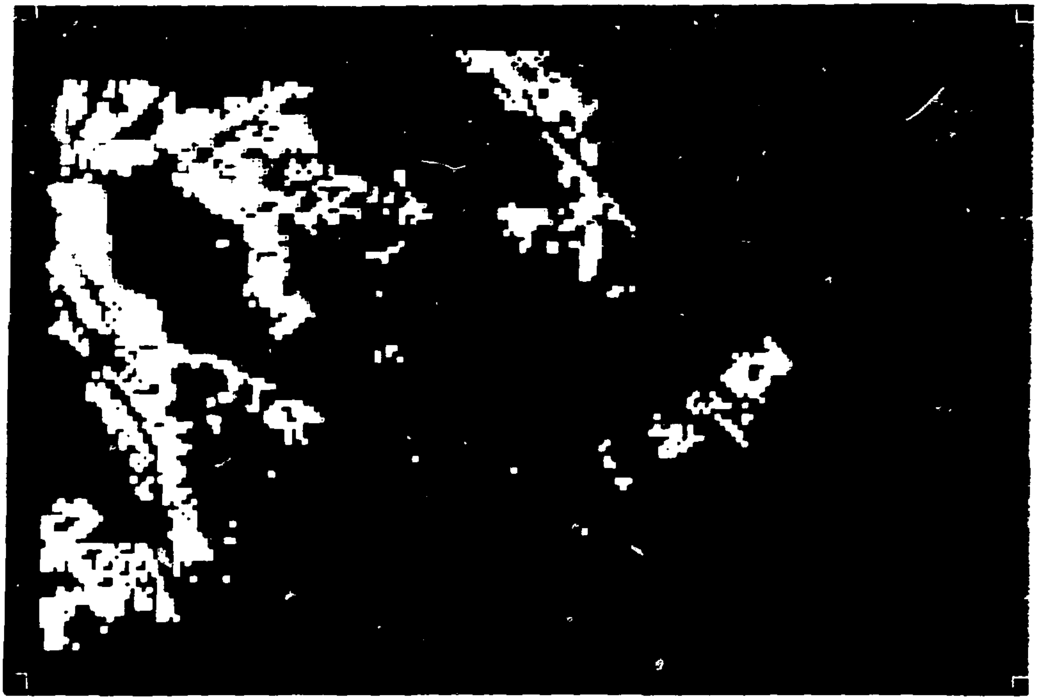

Fig. 13. *A density slice, 1σ to 4σ for the data set Uw (in red) overlain onto the Km unit (in green). Yellow signifies good corelation between the two; see discussion in text.*

		al	as	ba	ca	ce	co	cr	cu	dy	fe	hf	k	li	mn	pb	sc	th	ti	us	uw	v	zn	zr	uth	k40	eth	eu	mag
97	73	*	*	*	*	*	*	*	*	*	*	*	*	*	*	*	*	*	*	*	*	*	*	*	*	*	*		*
98	72	*	*	*	*	*	*	*	*	*	*	*	*	*	*	*	*	*	*	*	*	*	*	*	*	*	*		*
98	73	*	*	*	*	*	*	*	*	*	*	*	*	*	*	*	*	*	*	*	*	*	*	*	*	*	*		*
98	75	*	*	*	*	*	*	*	*	*	*	*	*	*	*	*	*	*	*	*	*	*	*	*	*	*	*		*
99	72	*	*	*	*	*	*	*	*	*	*	*	*	*	*	*	*	*	*	*	*	*	*	*	*	*	*		*
99	73	*	*	*	*	*	*	*	*	*	*	*	*	*	*	*	*	*	*	*	*	*	*	*	*	*	*		*
99	75	*	*	*	*	*	*	*	*	*	*	*	*	*	*	*	*	*	*	*	*	*	*	*	*	*	*		*
101	74	*	*	*	*	*	*	*	*	*	*	*	*	*	*	*	*	*	*	*	*	*	*	*	*	*	*		*
101	75	*	*	*	*	*	*	*	*	*	*	*	*	*	*	*	*	*	*	*	*	*	*	*	*	*	*		*
106	91	*	*	*	*	*	*	*	*	*	*	*	*	*	*	*	*	*	*	*	*	*	*	*	*	*	*		*
110	51	*	*	*	*	*	*	*	*	*	*	*	*	*	*	*	*	*	*	*	*	*	*	*	*	*	*		*
110	52	*	*	*	*	*	*	*	*	*	*	*	*	*	*	*	*	*	*	*	*	*	*	*	*	*	*		*
111	52	*	*	*	*	*	*	*	*	*	*	*	*	*	*	*	*	*	*	*	*	*	*	*	*	*	*		*
111	54	*	*	*	*	*	*	*	*	*	*	*	*	*	*	*	*	*	*	*	*	*	*	*	*	*	*		*
111	55	*	*	*	*	*	*	*	*	*	*	*	*	*	*	*	*	*	*	*	*	*	*	*	*	*	*		*
112	50	*	*	*	*	*	*	*	*	*	*	*	*	*	*	*	*	*		*	*	*	*	*	*	*	*	*	*
112	51	*	*	*	*	*	*	*	*	*	*	*	*	*	*	*	*	*		*	*	*	*	*	*	*	*	*	*
112	52	*	*	*	*	*	*	*	*	*	*	*	*	*	*	*	*	*	*	*	*	*	*	*	*	*	*		*
113	41	*	*	*	*	*	*	*	*	*	*	*	*	*	*	*	*	*	*	*	*	*	*	*	*	*	*	*	
113	53	*	*	*	*	*	*	*	*	*	*	*	*	*	*	*	*	*	*	*	*	*	*	*	*	*	*		*
113	54	*	*	*	*	*	*	*	*	*	*	*	*	*	*	*	*	*	*	*	*	*	*	*	*	*	*		*
114	54	*	*	*	*	*	*	*	*	*	*	*	*	*		*	*	*	*	*	*	*	*	*	*	*	*	*	*
115	74	*	*	*	*	*	*	*	*	*	*	*		*	*	*	*	*	*	*	*	*	*	*	*	*	*		*
125	135	*	*	*	*	*	*	*	*	*	*		*	*	*	*	*	*	*	*	*	*	*	*	*	*	*	*	*
125	106	*	*	*	*	*	*	*	*	*	*		*	*	*	*	*	*	*	*	*	*	*	*	*	*	*	*	*
132	58	*	*	*	*	*	*	*	*	*		*	*	*	*	*	*	*	*	*	*	*	*	*	*	*	*	*	*
133	50	*	*	*	*	*	*	*	*	*	*	*	*	*	*	*		*	*	*	*	*	*	*	*	*	*	*	*
133	52	*	*	*	*	*	*	*	*	*		*	*	*	*	*	*	*	*	*	*	*	*	*	*	*	*	*	*
134	50	*	*	*	*	*	*	*	*	*	*	*	*	*	*	*		*	*	*	*	*	*	*	*	*	*	*	*

Fig. 14. *A slected portion of the Distribution Routine. The grid cell location is given; the data sets fulfilling the given criteria are designated by an *.*

		al	as	ba	ca	ce	co	cr	cu	dy	fe	hf	k	li	mn	pb	sc	th	ti	us	uw	v	zn	zr	k40	eth	eu	mag	geo
166	56	60	3	57	73	32	76	97	77	73	86	24	33	44	83	13	94	4	43	9	59	74	47	8	54	10	4	17	94
166	57	53	10	54	77	44	84	98	72	77	92	25	23	35	92	11	96	10	55	20	51	85	45	6	45	7	2	12	94
166	58	49	20	42	87	73	87	97	79	69	88	9	76	58	92	11	96	4	66	12	63	83	20	5	35	11	13	11	94
166	59	50	31	54	87	47	89	97	77	73	89	19	33	65	87	25	96	14	73	41	86	81	27	12	43	23	39	8	94
166	60	58	31	55	84	35	90	97	80	70	89	22	42	65	84	48	95	11	74	59	89	79	61	12	64	42	64	4	85
166	61	69	29	67	65	81	72	89	81	85	84	80	90	61	71	78	85	91	74	87	88	57	78	44	78	80	79	3	85
166	62	67	26	68	58	85	59	81	70	87	85	89	93	51	68	72	78	87	72	89	88	69	72	55	86	91	84	6	85
166	63	74	23	73	55	88	44	68	64	87	78	90	97	70	61	78	70	91	62	88	90	55	68	57	89	94	87	9	94
166	64	79	20	78	52	91	45	70	61	90	81	91	95	57	57	81	70	92	77	87	82	68	74	70	93	95	88	11	85
166	65	81	22	83	41	90	48	64	64	90	75	90	96	52	72	87	70	92	69	83	73	56	63	69	95	96	87	14	94
166	66	75	24	81	37	91	47	65	57	91	77	91	97	71	81	89	74	92	70	80	67	51	76	72	96	96	85	20	94
166	67	74	37	79	34	91	47	67	57	91	78	92	96	72	83	90	75	92	71	80	66	50	74	67	97	95	82	23	94
166	68	60	55	82	27	85	49	69	53	89	71	89	97	84	59	92	72	90	53	75	67	51	73	65	96	95	80	25	94
166	69	65	68	77	41	86	53	49	73	87	82	90	96	83	79	92	69	91	65	77	77	57	82	64	93	95	79	24	94
166	70	67	72	43	54	89	71	39	77	87	92	91	94	67	62	89	68	95	78	85	88	85	85	71	89	95	78	21	94
166	71	52	75	45	54	94	76	55	74	90	97	93	91	73	61	78	75	97	53	89	89	93	82	75	87	96	81	24	94
166	72	58	62	25	46	95	81	51	79	89	96	93	93	70	65	76	76	98	80	90	80	92	73	67	90	96	87	37	94
166	73	54	65	31	37	96	72	54	79	90	97	93	93	66	59	82	74	99	79	89	73	92	74	78	92	97	91	50	95
166	74	58	51	46	24	91	51	32	33	81	90	90	99	80	79	88	67	96	51	86	52	63	76	69	93	98	94	55	95
166	75	48	49	50	22	92	46	30	54	85	92	91	99	80	84	86	66	95	47	88	44	65	70	74	94	98	97	53	95
166	76	49	62	31	19	95	46	17	33	86	90	91	98	85	96	79	67	97	39	93	45	54	65	72	96	98	99	47	95
166	77	58	44	27	19	95	48	10	50	86	84	90	98	83	90	78	68	97	43	95	57	56	60	73	97	99	99	42	85
166	78	44	81	13	23	96	68	21	70	90	94	92	95	81	86	58	73	99	55	96	65	79	62	72	97	99	99	43	85
166	79	63	89	23	35	95	81	20	88	87	94	88	95	89	75	77	77	98	59	94	75	84	81	70	97	99	98	46	85
166	80	54	86	27	48	94	86	36	92	88	96	88	90	74	61	73	78	99	77	91	80	94	75	63	97	99	97	45	85

Fig. 15. *A selected portion of the Sort Routine. The grid cell location and the cumulative percent value are listed for each data set; e.g., a value of 11 indicates that the respective grid cell has a value coresponding to the 11th percentile on the cumulative frequency curve for that data set.*

The Sort Routine works by ordering all the nonzero grid cell values from lowest to highest for each selected data set. This information is then divided into 100 blocks, each block corresponding to one percent of the nonzero values. Each grid cell in a block is assigned the percentile value (0-99 percent) for that block. For example, assume the data set Cu has 20 000 nonzero values. Actual kriged concentrations range from 9 to 3118 ppm. After all values have been sorted the 200 grids cells with the lowest concentrations are assigned to the 0 percentile block, the next 200 values are assigned to the first percentile block, etc. There is a possible error of up to 1 per cent between the percentile value listed (example shown in Fig. 15) and the true value on the cumulative frequency curve. However, this error is so small that it has no significant effect on our evaluations.

Statistics

Several statistical routines were run on all or portions of the data sets. For the geochemical data, the statistics were gathered on raw data instead of the kriged values. This includes 3965 sample locations for 23 elements. The raw data is the actual value at the sample location. Statistical routines are run on kriged aerial radiometric and aeromagnetic data, and Landsat pixel values (all four bands) subsampled to 100-m or 1-km resolution. No effort was made to quantitatively incorporate this data into the classification routine. However, the data were examined and used in a qualitative manner. Our major purpose in completing these statistical calculations was to show that such routines could be done with minimal difficulty and to develop the algorithms necessary to incorporate this type of methodology into a DIRS program. Once any statistical routine is run, it can simply be added as an additional data set. Most statistical routines were run on the data sets for both the entire quadrangle and for individual provinces. The province boundaries and the respective number of geochemical sample locations for both waters and sediments are shown in Fig. 6.

Basic Statistics. Basic statistics, including parameters such as mean, median, number of samples, and standard deviation, were run on data sets for both the quadrangle and each province using the SPSS statistical package of Nie et al (1975). These data are shown in Appendix C; the data could also be presented in log form (not included). Geochemical samples with elemental concentrations below detection limits (see Table III) were omitted.

Cumulative frequency plots, for the quadrangle as a whole and for each physiographic/geochemical province, for all geochemical data sets are included in Appendix D. These plots provide a valuable aid in selecting threshold values for geochemical data (see discussions by Lepeltier, 1969; and Sinclair, 1976).

Basic statistics can also be run for individual formations. These data (not included) can then be used to identify regional geochemical trends as well as identifying criteria characteristic of any selected formation.

Association by Variable. One way of detecting a relationship between the geochemical and aerial data and the known uranium occurrences is to compare the distribution of the data over the known occurrence sites with the distribution over the whole quadrangle. If the locations of the known occurrences (Fig. 4) appear to be merely a random subset of the points in the whole quadrangle, as far as a given variable, e.g., chromium, is concerned, then there is no indication of association of this variable with uranium mineralization. On the other hand, if a sample appears to come from a significantly different distribution than that for known uranium occurrences, then that variable may be a useful indicator.

Specifically, assume that the quadrangle population is normal (or lognormal) with known mean (the mean of the kriged data for 21 301 grid cells). Let $x_1,\ldots,x_N$ be the kriged values or log values of a given variable at the known occurrence sites, with mean $\bar{x}$ and sample variance s^2. Then if $x_1,\ldots,x_N$ is a random sample from the quadrangle population with mean μ. $\sqrt{N-1}\ (\bar{x}-\mu)/s$ has a Student's t distribution with N-1 degrees of freedom, and the probability that its absolute value is at least as great as the observed value can be computed. If this probability is small, then the sample appears to come from a significantly different population.

We can also compare the sample variance with the quadrangle variance; under the random sample hypothesis, $(N-1)s^2/\sigma^2$ has approximately a chi-square distribution with N-1 degrees of freedom. If s^2 is unexpectedly small (if the above ratio falls in the lower tail of the chi-square distribution), then it appears that the sample values are much more tightly clustered than in general throughout the quadrangle. A variable with a mean significantly different from μ and a small variance could be a particularly good indicator of uranium mineralization.

Table VII summarizes these calculations both for four types of uranium deposits in the Montrose quadrangle and for all uranium deposits. There are only seven deposits of type 3 and five of type 4, so these results may not be too significant; in particular, the type 3 deposits are all together in one corner of the quadrangle. A + (-) in the column indicates a significantly large (small) value of $\bar{x}$ for the variable of that row (significance at the 10 per cent level for a two-sided test or 5 per cent level for a one-sided test), and an "s" indicates that in addition, the sample variance falls in the lower 10 per cent of the anticipated distribution.

The raw data are given in Appendix E, where the "difference" is $\sqrt{N-1}\ \bar{x}-\mu/s$ with the associated probability

$$\Pr\left(\sqrt{N-1}\ \frac{\left|\bar{x}-\mu\right|}{s} \geq \text{difference}\right) ,$$

and the "ratio" is $(N-1)\ s^2/\sigma^2$ with associated probability

$$\Pr\left((N-1)\ \frac{s^2}{\sigma^2} \leq \text{ratio}\right) .$$

"D.F." is the number of degrees of freedom N-1.

Factor Analysis. Encouraged by the results of Beyth et al (1980a, b), factor analysis was run for all data sets using the SPSS statistical package of Nie et al (1975). The major purpose in using factor analysis was data reduction. Factor analysis techniques enable one to cluster the data sets into factors such that the dominant data sets in each factor are highly correlative (Frane and Hill, 1976). This clustering of data sets allows an easier examination of the correlations between data sets.

Each factor is defined by a linear combination of variables. By reducing the dimensionality of all data sets through factor analysis and because little information is lost in the process (Frane and Hill, 1976), the resulting factors hopefully will emphasize underlying relationships among the observable data sets. Because we want to determine correlations between data sets, R-mode factor analysis with varimax orthogonal rotation was performed; this is the recommended procedure of Nie et al (1975) and Joreskog et al (1976).

TABLE VII

ASSOCIATION OF GEOCHEMICAL AND AERIAL VARIABLES WITH KNOWN URANIUM DEPOSITS FOR THE MONTROSE QUADRANGLE, COLORADO

	Deposit Host Rock[a]				
	1	2	3	4	all
Uw	+s	+	+		+s
Us	+s	+s	+s	+	+s
U/Th	+s	+s	+s	+	+s
K40			-s	-s	
eU	+	+	+		+
eTh	+				
Al	+s	-	-		
As					
Ba	+				+
Ca			+	+s	
Ce	+				+s
Co	+	-			
Cr		+	+s	+	+
Cu					+s
Dy	+	+s			+s
Fe	+s			+	+s
Hf	+s	+s	-s		+s
K	+s		-s		+
Li	+s	+s	+s		+s
Mn	+				+
Pb	+s	+s		+	+s
Sc	+s				+
Th	+s		-s	+s	+s
Ti	+	-	-		
V		-			
Zn	+s	+s	+	+	+s
Zr		-s			
magnetics			+s		

[a] Deposit host rock from Nelson-Moore et al (1978).

1 = Igneous, metamorphic; 2 = sandstone; 3 = radioactive springs or ground water, 4 = coal, shale, limestone.

A +s indicates a high positive correlation, a -s indicates a negative correlation.

The correlation coefficients for all data sets for the quadrangle as a whole and for all data sets for each physiographic/geochemical province are included in Appendix F, however, only coefficients greater than 0.50 are plotted. Data sets with correlation coefficients close to 1.0 have the highest correlations.

Some obvious information can be extracted from these coefficients. The elements Ce-Dy-Th, Hf-Zn, and Fe-V are closely correlated for the entire Montrose quadrangle; Ca-Li is most correlative in the Plateau province. The data set Us slightly correlates with Th, whereas Pb-Cu-Zn are highly correlative. These associations would be expected and are supported by the work of Beyth et al (1980b).

A factor matrix (varimax orthogonal rotation with Kaiser normalization) is included in Appendix G. Certain data sets group in particular factors. For example, Landsat forms its own factor isolated from everything else (Factor 2), as does the airborne radiometric data (Factor 4). The geochemical factors are similar to those of Beyth et al (1980b), Ce-Th-Dy group in Factor 3 and Zn-Pb-Cu group in Factor 5. Uranium is associated with resistate and refractory minerals in factor 3, although Us also groups with Cr, Sc, Al, and Dy in factor 8 with a low loading. This suggests uranium in this quadrangle occurs under a variety of geologic conditions, not all of which would be economically feasible to explore.

The factor analysis is preliminary and a much more careful examination of other data with respect to the many options in factor analysis is necessary to obtain fully meaningful results. However, this exercise emphasizes that factor analysis data can be incorporated into a DIRS project.

Classification Schemes for the Cochetopa and Marshall Pass Test Areas

In this section, the procedures and methods used to determine a classification scheme by using test areas from the Cochetopa and Marshall Pass uranium districts are outlined. A preliminary classification scheme was successfully developed for each uranium district.

Some of the statistical data compiled, e.g., factor analysis, have not been incorporated into the quantitative discussions, but were qualitatively considered in selecting criteria for the classification schemes. Furthermore, Landsat imagery were not used in these preliminary classification schemes.

Eventually statistical analyses of these types, as well as subsurface information, will be merged with the data sets for a more complete analysis. Ultimately, a normalized probability that indicates the possibility of mineralization, be it uranium or base metal, will be assigned to each grid cell in the study area, but this effort is beyond the present scope of the DIRS project.

We are looking for regional patterns that may indicate uranium mineralization. These patterns may be independent of any individual high or low value for any given data set. It is the combinations of various data sets that we believe will ultimately help to identify the regional patterns.

For a first approach, potential data sets can be selected by examining the range of values in each data set for those grid cells containing known uranium occurrences. Such data are shown for a selected number of grid cells containing known occurrences in the Cochetopa and Marshall Pass uranium districts in Table VIII. Each occurrence in this table is designated by both grid cell location and code number (from Appendix A). The values in Table VIII represent the kriged data. Classification criteria (i. e., intervals for each data set) were then selected from this table. Criteria for Cochetopa-type uranium mineralization were selected primarily (but not solely) from occurrences 200616, 200619, and 200631. Criteria for Marshall Pass-type mineralization were selected primarily from occurrences 200515, 100621, 400627, and 100618.

The classification scheme utilizes a variation of the Distribution Routine, as explained earlier. Intervals for 28 data sets were selected from Table VIII. Grid cells containing data sets that fulfilled all 28 criteria, 27 of 28, 26 of 28, etc., are thus identified. It was hoped that this procedure might create a halo effect around the test areas and other areas favorable for uranium mineralization.

<u>Cochetopa Uranium District Classification</u>. Two sets of criteria were selected for test areas in the Cochetopa uranium district; based on these criteria, two separate classification schemes were completed, COCH-1 and COCH-2. Only 28 data sets are used (Table IX).

Data set intervals selected for COCH-1 are relatively wide, i.e., the difference between the upper and lower limits for each data set resulted in several areas of potential favorability for uranium mineralization.

TABLE VIII

KRIGED VALUES FOR SELECTED GRID CELLS CONTAINING KNOWN URANIUM OCCURENCES
(Code numbers are explained in Appendix A; cumulative percent in parenthesis.)

Code Number	Grid Cell Location	Al	As	Ba	Ca	Ce	Co	Cr	Cu	Dy
100402	49-10	76802(90)		262.3(33)	19919(14)	76.2(9)	26.01(40)	23.9(32)	31.19(1)	3.22(9)
200616	110-38	54530(71)	14.54(21)	854.7(37)	15651(11)	110.7(13)	12.01(30)	49.3(27)	31.19(1)	5.71(16)
200619	11-43	50348(59)	11.77(17)	623.7(27)	13182(8)	93.7(11)	11.61(29)	56.6(31)	31.19(1)	6.43(18)
200631	113-45	50348(59)	20.77(30)	646.8(28)	22765(16)	85.2(10)	9.23(23)	40.2(22)	31.19(1)	5.71(16)
100506	124-62	49495(58)	17.31(25)	554.4(24)	17074(12)	59.6(7)	12.01(30)	42.0(23)	62.37(2)	6.43(18)
200503	143-59	67435(79)	14.54(21)	739.2(32)	8537(6)	170.4(20)	8.01(20)	29.2(16)	93.56(3)	8.22(23)
200515	151-50	57175(67)	11.08(16)	554.4(24)	18496(13)	110.7(13)	16.41(41)	133.4(73)	31.19(1)	6.43(18)
100621	152-45	71687(84)	9.69(14)	900.9(19)	22765(16)	136.3(16)	12.41(31)	84.1(46)	31.19(1)	11.08(31)
400627	152-47	70829(83)	9.00(13)	831.6(36)	19919(14)	85.2(10)	11.21(28)	89.5(49)	62.37(2)	9.65(27)
100[illegible]	153-45	69976(82)	9.69(14)	877.8(38)	18496(13)	93.7(11)	12.81(32)	89.5(49)	62.37(2)	10.72(30)
100608	164-46	73389(86)	6.92(10)	993.3(43)	14228(10)	119.2(14)	10.41(26)	45.7(25)	31.19(1)	5.36(15)
100649	167-37	63149(74)	19.38(28)	1570.9(68)	4268(3)	187.4(22)	12.01(30)	31.1(17)	842.05(21)	4.65(13)
200801	171-110	58882(69)	--	646.8(28)	21342(15)	110.7(13)	12.01(30)	64.0(35)	31.19(1)	5.36(15)

Code Number	Grid Cell Location	Fe	Hf	K	Li	Mn	Pb	Sc	Th	Ti
100402	49-10	31992(20)	6.55(4)	16716(49)	25.26(16)	1044(16)	10(0)	10.30(32)	11.56(6)	4597(33)
200616	110-38	33592(21)	14.75(9)	18763(55)	36.31(21)	848(13)	10(0)	12.62(39)	11.56(6)	4319(31)
200619	112-43	33592(21)	14.75(9)	18422(54)	44.21(26)	1109(17)	10(0)	11.33(35)	7.71(4)	3622(26)
200631	113-45	27193(17)	9.83(6)	17058(50)	48.94(31)	914(14)	10(0)	9.06(28)	7.71(4)	3065(22)
100506	124-62	22394(14)	8.19(5)	13987(41)	26.84(17)	718(11)	20(1)	12.95(40)	7.71(4)	5015(36)
200503	143-59	23994(15)	18.02(11)	29139(86)	50.52(32)	979(15)	141(7)	8.42(26)	36.61(19)	3343(24)
200515	151-50	60785(38)	6.55(4)	7846(23)	33.15(21)	2284(35)	10(0)	16.83(52)	11.56(6)	6826(49)
100621	152-45	38390(24)	11.47(7)	21492(63)	30.00(19)	1109(17)	20(1)	11.98(37)	17.34(9)	4597(33)
400627	152-47	33592(21)	6.55(4)	20128(59)	36.31(23)	914(14)	10(0)	12.30(38)	9.63(5)	4040(29)
100618	153-45	41590(26)	6.55(4)	17058(50)	36.31(23)	1436(22)	20(1)	13.24(41)	11.56(6)	4179(30)
100608	164-46	36791(23)	13.11(8)	24222(71)	37.89(24)	914(14)	20(1)	10.68(33)	11.56(6)	5154(37)
100649	167-37	54386(34)	9.83(6)	19446(57)	37.89(24)	4307(66)	925(46)	12.30(38)	17.34(9)	4876(35)
200801	171-110	39990(25)	8.19(5)	15693(46)	25.26(16)	783(12)	20(1)	10.03(31)	9.63(5)	4319(31)

Code Number	Grid Cell Location	Us	Uw	V	Zn	Zr	eTh	eU	K40	U/Th
100402	49-10	4.08(2)	0.77(0)	117.19(28)	41.71(1)	24.1(0)	19.5(49)	6.07(67)	2.73(54)	0.40(2)
200616	110-38	6.12(3)	0.77(0)	87.89(21)	41.71(1)	384.8(8)	[illegible](19)	2.60(29)	1.82(36)	0.40(2)
200619	112-43	4.08(2)	2.70(5)	66.96(16)	87.41(2)	384.8(8)	7.2(18)	6.92(77)	1.97(39)	0.40(2)
200631	113-45	10.20(5)	1.54(1)	58.59(14)	87.41(2)	336.7(7)	7.9(20)	7.54(84)	1.62(32)	0.99(5)
100506	124-62	4.08(2)	0.77(0)	87.89(21)	87.41(2)	288.6(6)	6.4(16)	1.89(32)	1.52(30)	0.40(2)
200503	143-59	14.28(7)	0.77(0)	50.22(12)	611.88(14)	412.5(9)	19.9(50)	4.94(55)	3.39(67)	0.20(1)
200515	151-50	18.36(9)	0.77(0)	133.93(32)	87.41(2)	240.5(5)	6.4(16)	3.14(35)	1.52(30)	1.38(7)
100621	152-45	10.20(5)	1.54(1)	92.07(22)	87.41(2)	288.6(6)	11.1(28)	3.50(19)	2.08(41)	0.59(3)
400627	152-47	16.32(8)	3.08(2)	87.89(21)	87.41(2)	240.5(5)	5.6(14)	1.50(19)	1.47(28)	1.58(8)
100618	153-45	16.32(8)	3.08(2)	104.63(25)	131.1(3)	240.5(5)	11.5(29)	1.47(18)	2.13(42)	1.38(7)
100608	164-46	6.12(3)	0.77(0)	96.26(23)	43.71(1)	348.8(8)	13.1(33)	3.14(35)	2.63(52)	0.40(2)
100649	167-37	8.16(4)	0.77(0)	96.26(23)	2884.6(66)	336.7(7)	20.3(51)	4.49(50)	3.09(61)	0.40(2)
200801	171-110	4.08(2)	1.54(1)	104.63(25)	87.41(2)	144.3(3)	12.3(31)	3.05(34)	1.52(30)	0.40(2)

TABLE IX

DATA SET INTERVALS FOR THE COCHETOPA (COCH) AND MARSHALL PASS (MP) CLASSIFICATION SCHEMES*

DATA SET	COCH-1	COCH-2	MP-1	MP-2
Al	45000-75000	50000-70000	55000-80000	65000-80000
As	10-22	10-22	5-20	9-12
Ba	550-1000	600-900	>550	800-1000
Ca	10000-25000	8000-20000	<25000	17000-25000
Ce	<120	75-120	>80	90-150
Co	9-16	9-15	10-20	10-20
Cr	<75	10-60	>0	70-120
Cu	<90	10-75	>0	20-100
Dy	5-7	5-7	<12	6-12
Fe	20000-35000	22000-36000	>30000	30000-70000
Hf	8-16	9-16	5.5-14	5-12
K	12000-20000	15000-20000	14000-25000	7000-23000
Li	25-50	30-50	30-50	25-40
Mn	700-1200	800-1200	>850	800-3000
Pb	<30	1-30	>0	1-50
Sc	9-14	8-13	10-14	11.5-18
Th	>6	>6	>8	>8
Ti	2500-5500	2800-4500	3900-7000	3900-7000
Us	>3	>4	>3	>8
Uw	0-10	>0.1	<5	0.1-5
V	50-150	<90	50-150	85-200
Zn	40-120	<150	>0	50-200
Zr	300-500	250-450	<400	200-325
U/Th	>0.35	>0.35	>0.3	>0.4
K40	1.5-2.1	1.5-2.5	1-3.5	1.4-3.5
eTh	7-9	7-9	>5	>5
eU	>2.5	>2.5	>3	>3
Mag	<-300	<-400	<-300	<-400

*All values in ppm except for Uw, which is in ppb; U/Th, which is a ratio; K40, which is in percent; and Mag, which is in gammas.

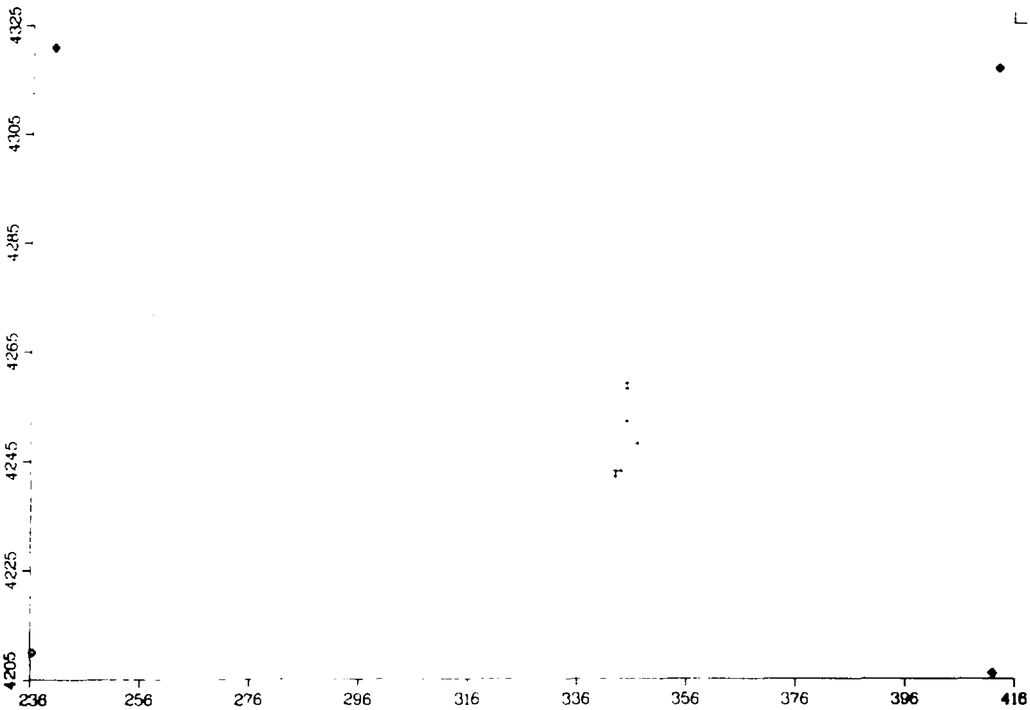

Fig. 16A. Grid cells satisfying 28 criteria.

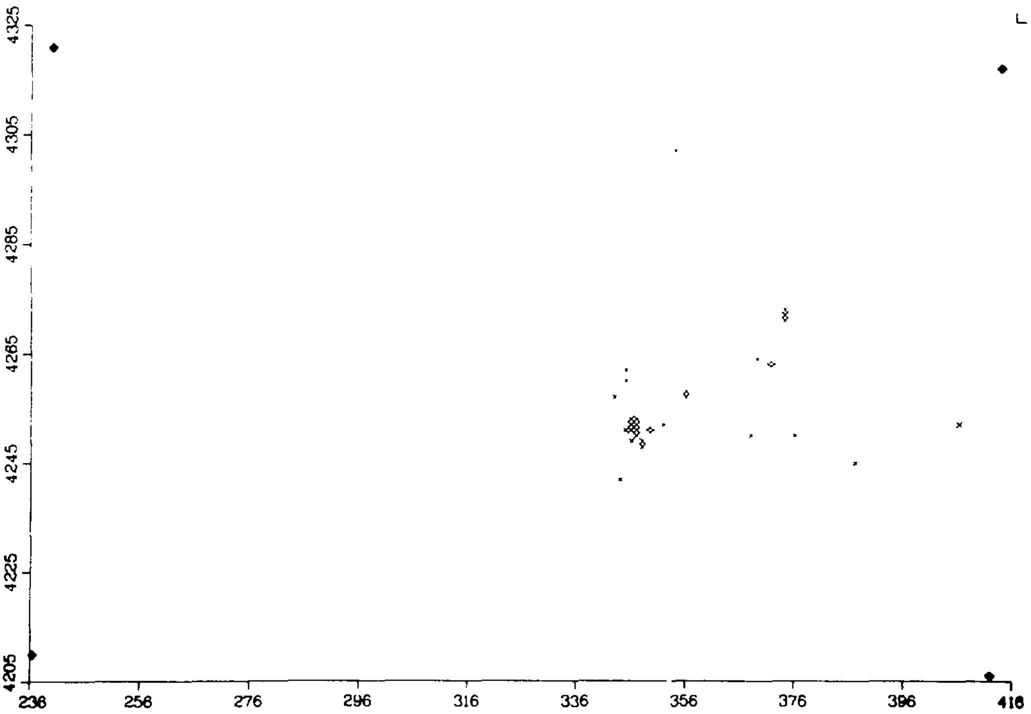

Fig. 16B. Grid cells satisfying 27 of 28 criteria.

Fig. 16. Results for COCH-1 classification scheme. Criteria (i.e., data set intervals) are listed in Table IX.

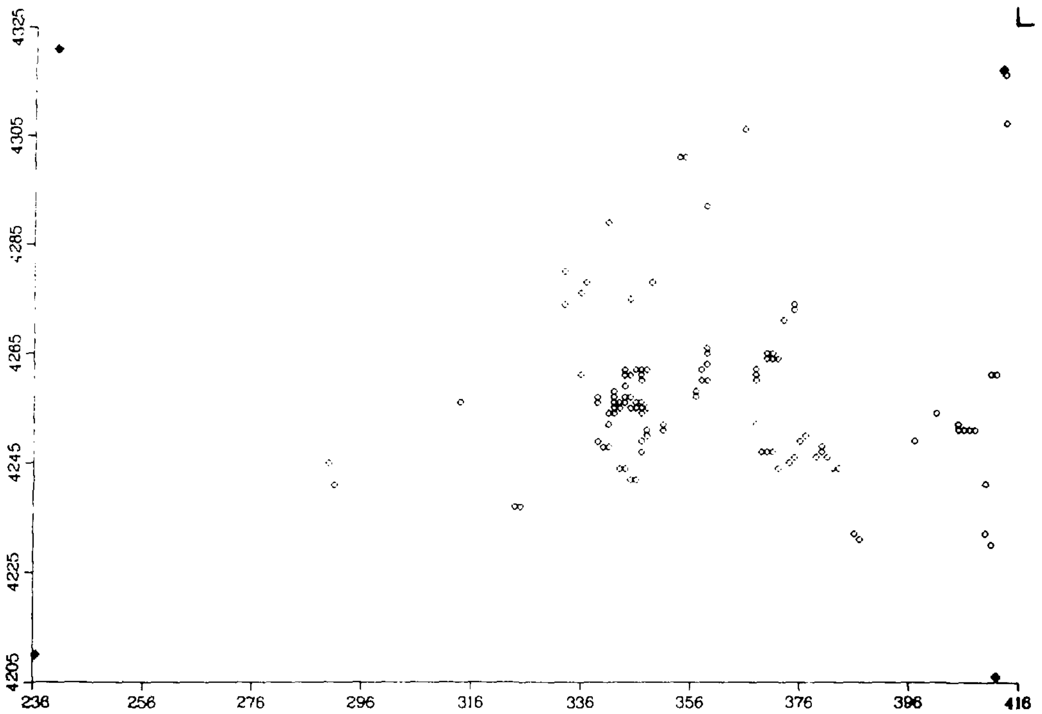

Fig. 16C. *Grid cells satisfying 26 of 28 criteria.*

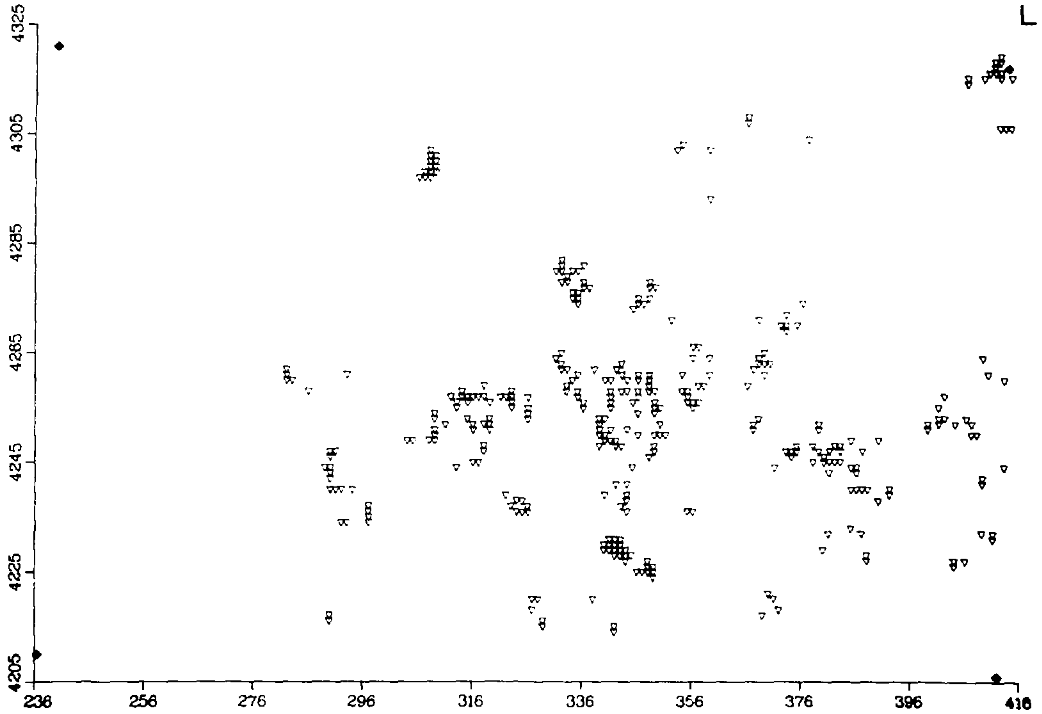

Fig. 16D. *Grid cells satisfying 25 of 28 criteria.*

Figures 16A-D show the grid cells satisfying 28, 27 of 28, 26 of 28, and 25 of the 28 intervals. A color composite for this classification is shown in Fig. 17. Care must be taken to optimize window criteria both to include all training set grid cells and yet be small enough to avoid obtaining the entire quadrangle as an area of favorability. Therefore, a second iteration, whereby the COCH-1 data set intervals were narrowed, particulary with respect to Al, Ba, Ce, Cr, Cu, Ti, and Us, was run. The grid cells satisfying 28 of 28, 27 of 28, 26 or 28, and 25 of 28 of the selected criteria are shown in Fig. 18 and a color composite for this scheme is shown in Fig. 19.

There are nine areas that satisfy 25 or more of the 28 selected intervals for COCH-2 (Fig. 20). Area A contains the Cochetopa mining district, and 46 grid cells cluster in this region. Here, only 3 of the 11 grid cells containing known uranium occurrences were primarily used as test areas, yet 6 (including the three test areas) of the 11 show up as favorable grid cells. All uranium occurrences in this district are surrounded by grid cells of favorability.

Seven cells cluster in Area B, and this is a large number of grid cells relative to all other areas except Area A. Thus, Area B may have good potential for uranium mineralization. Most of these grid cells are from the drainages of Tomichi Creeks (USGS, 1956), just north of the Cochetopa district, and are underlain by either Oligocene ash flow tuffs or Precambrian metamorphic units or on the contact zone between the two (Tweto et al, 1976a). Potential uranium deposits in this area would probably be fault- or vein-controlled (Nelson-Moore et al, 1978).

Area C in Fig. 20 consists of four scattered grid cells. Three of these are underlain by the Mancos formation and would probably not be prime areas of favorability for uranium mineralization. However, the Mancos does contain uranium-rich, coal-bearing units, and these may be influencing the selection of grid cells; radioactive springs have been reported in Cretaceous units in this quadrangle (Cadigan et al, 1976). One grid cell in this cluster is in alluvium but also occurs in an area that drains Precambrian granitic and metamorphic rocks and is near a fault zone. One known occurrence of vein-type mineralization is in this region (Nelson-Moore et al, 1978).

The third most favorable area delineated by this scheme is Area D. Four grid cells occur along the eastern tributaries of Flag Creek (USGS, 1956) and

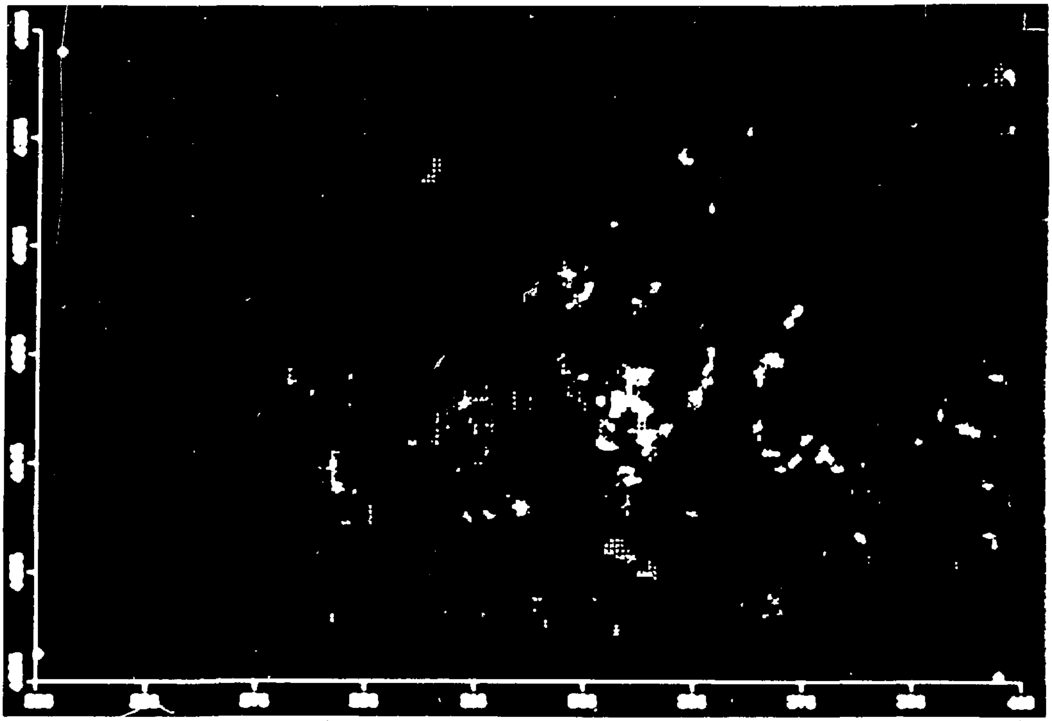

Fig. 17. *Color composite for COCH-1 classification scheme. The grid cells satisfying 28 criteria are in red; the cells satisfying 27 criteria are in magenta; the cells satisfying 26 criteria are in yellow; the cells satisfying 25 criteria are in green; and the cells satisfying 24 criteria are in blue.*

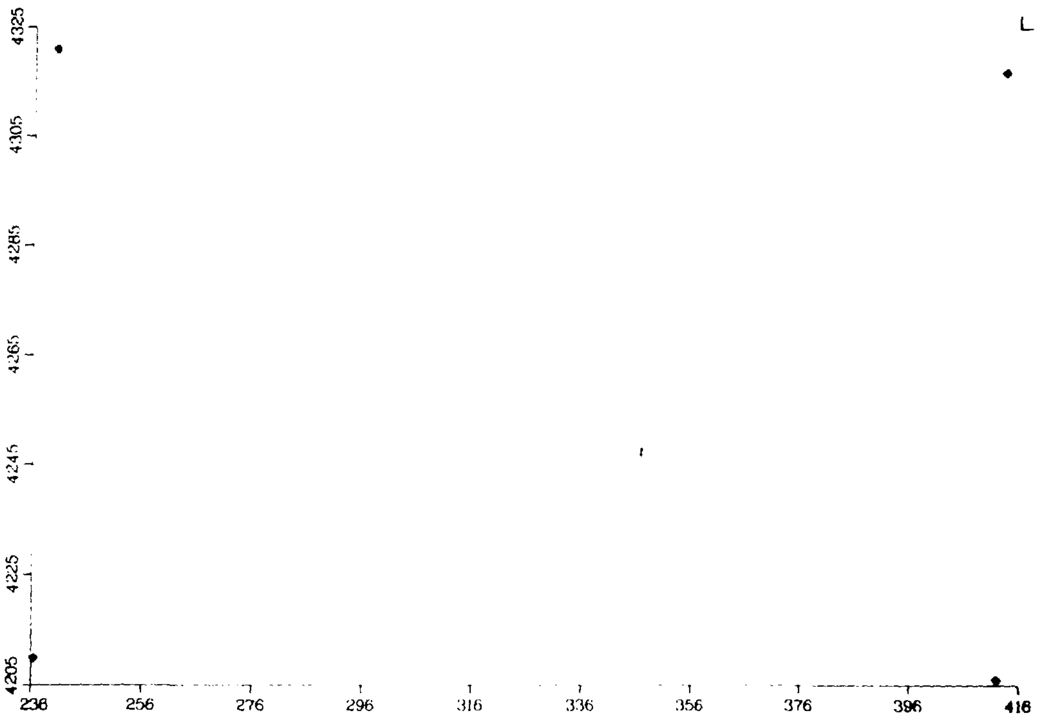

Fig. 18A. Grid cells satisfying 28 criteria.

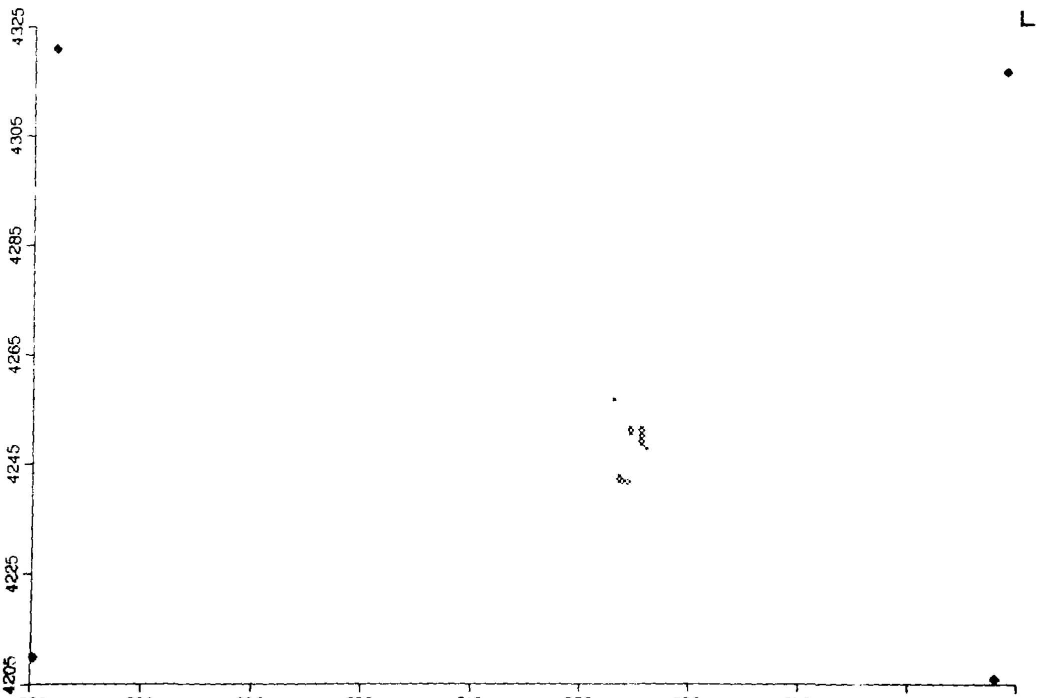

Fig. 18B. Grid cells satisfying 27 criteria.

Fig. 18. Results for COCH-2 classification scheme. Criteria are listed in Table IX.

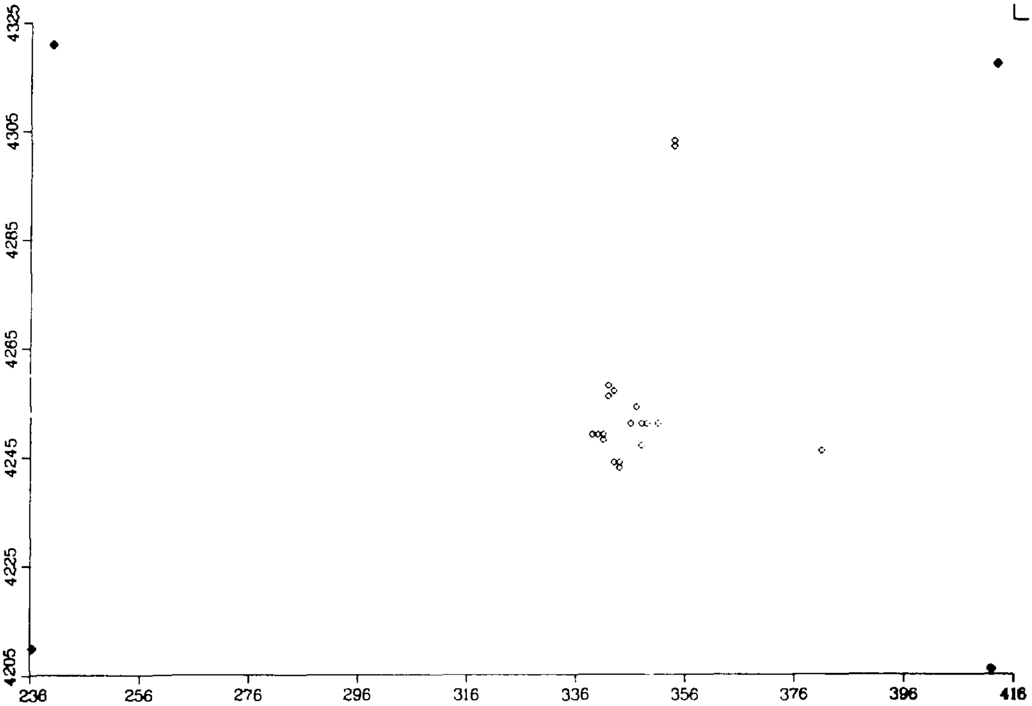

Fig. 18C. Grid cells satisfying 26 criteria.

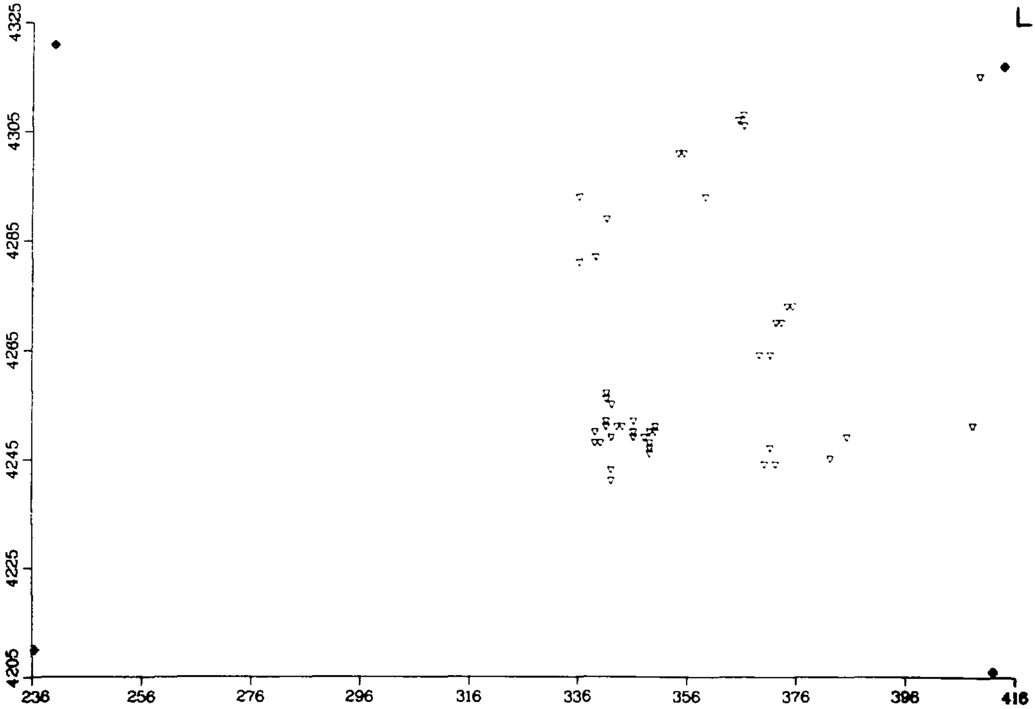

Fig. 18D. Grid cells satisfying 25 criteria.

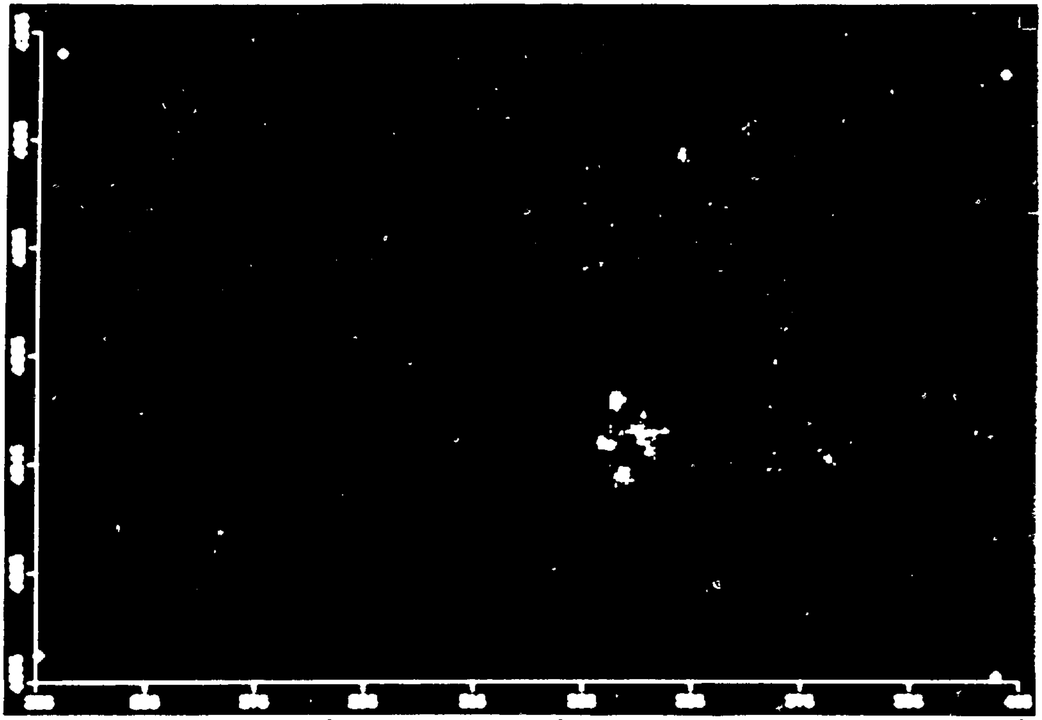

Fig. 19. *Color composite for COCH-2 classification scheme. The grid cells satisfying 28 criteria are in red; the cells satisfying 27 criteria are in magenta; the cells satisfying 26 criteria are in yellow; the cells satisfying 25 criteria are in green; and the cells satisfying 24 criteria are in blue.*

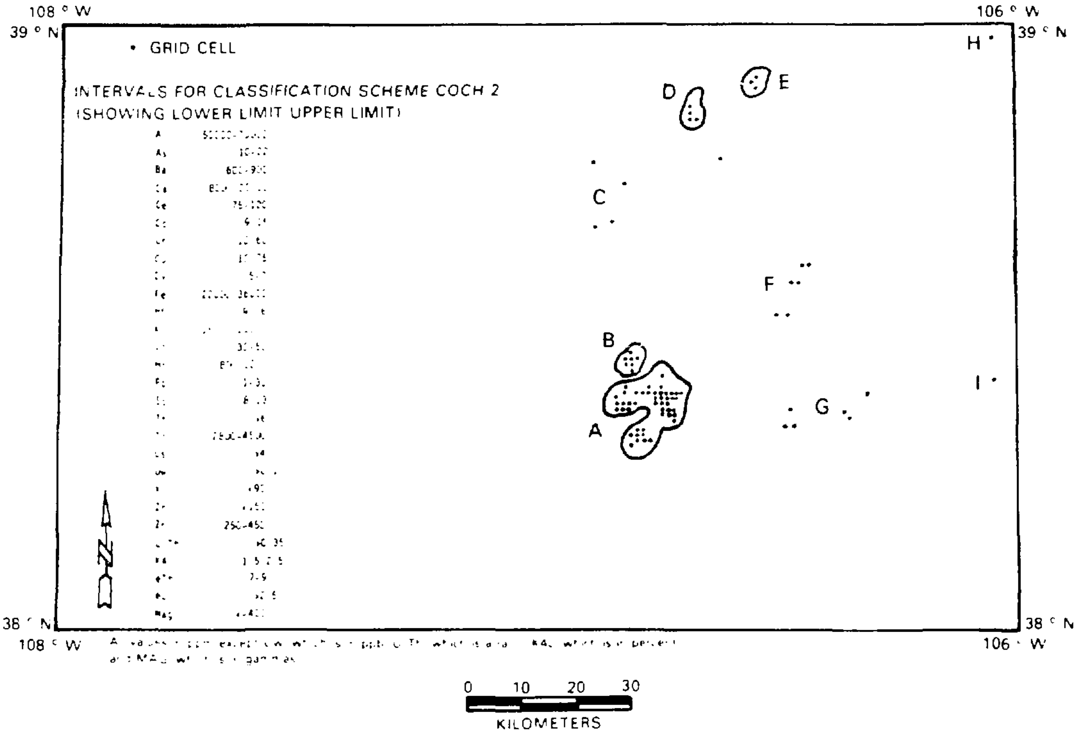

Fig. 20. Schematic diagram for COCH-2 classification scheme. Nine areas of favoribility are delineated based on the criteria in Table IX.

are underlain by Middle Tertiary Oligocene granitic intrusives and Paleozoic formations. Several fault zones are located near this cluster. Paleozoic rocks in fault contact with Precambrian rocks or Tertiary intrusives are favorable for vein- or fault-controlled uranium mineralization in this area. Examples are found in the Marshall Pass district (Malan and Ranspot, 1959; Nelson-Moore et al, 1978).

One grid cell in Area H contains similar geology, and occurs within a few kilometers of two known uranium occurrences (US AEC, 1966b) and, consequently, can be considered as favorable for uranium mineralization.

Area E contains only three grid cells, all of which occur in alluvium that drains Precambrian granitic rocks. Uranium mineralization in this area would probably be in veins or fractures. Area F contains four grid cells also underlain by Precambrian granitic rocks. Two of these cells are also near a fault zone. The other two grid cells border the Mancos formation. In general, any grid cells located in the Precambrian crystalline terrain have some favorability for uranium mineralization and the presence of a fault increases that favorability (Nelson-Moore et al, 1978). This includes the grid cells in Areas D, E, F, H, and I.

The remaining group G contains six grid cells, one of which is located within the Marshall Pass uranium district. The other five grid cells are underlain by, or are in drainages of, Oligocene andesitic lavas and breccias. Although these lavas are not a major host rock for uranium mineralization, they do host several reported uranium occurrences and minor deposits (US AEC, 1966c).

Marshall Pass Uranium District Classification. Two classification schemes, MP-1 and MP-2, were run for Marshall Pass test areas. The criteria selected are listed in Table IX and the results are displayed in Figs. 21 and 22. Twenty-eight data sets were selected for these runs.

For MP-1 there is no selected upper limit for the base-metal data sets because several known uranium occurrences in the Marshall Pass district are associated with base-metal mineralization (US AEC, 1966a). However, the subsequent wide window resulted in a large number of grid cells satisfying the selected intervals (Fig. 21). This method of classification does have its merits, because a large number of known uranium occurrences in the Powderhorn, Cochetopa, and Marshall Pass districts were included in the grid cells identified as satisfying the selected criteria. In addition, the Bonanza mining district and Mt. Princeton batholith were delineated. For MP-2 the data set intervals (Table IX) were narrowed for almost every data set and the result (Fig. 22) contains only 33 grid cells satisfying 25 or more of the criteria. The Marshall Pass area is clearly delineated and also one area northwest of this district, which consists of five grid cells. These cells are underlain by the Mancos formation and may represent only coal-rich zones here. However, the grid cells also occur along fault zones and along the contact between the Mancos and Precambrian granitic rocks. This type of environment is favorable for Marshall Pass-type uranium mineralization (Nelson-Moore et al, 1978). The other seven grid cells are scattered throughout the quadrangle and their significance will not be discussed.

ALTERNATIVE DATA PROCESSING AND ANALYTICAL TECHNIQUES

Introduction

A methodology to integrate large numbers of data sets has evolved by extending the basic structure of the Los Alamos Digital Image Enhancement System (LADIES). LADIES is basically a collection of general digital image processing subroutines that share a common data structure. This methodology utilizes our Digital Image Processing Facility and is independent of the procedures outlined in the previous sections. George Wecksung was primarily responsible for this scheme, and he has written this section to describe the current state of this methodology.

Data Packing

Two-dimensional arrays are stored on disk as a sequence of records (lines), each containing a fixed number of 60-bit floating point numbers (grid cells or Landsat pixels). Disk files with a maximum size of 4096 lines with 4096 numbers per line are possible. Moreover, several disk files of such size may exist simultaneously. Although a maximum of 15 disk files (input, output, and intermediate) can be opened simultaneously on the CDC 7600s at Los Alamos, the total disk resources are quickly exhausted if the files are too large. However, we have had successful experience with six files of 3000 x 2000 numbers, all open at the same time.

The data structure has been extended to accommodate 35 (or more) data sets by partitioning the least significant bits of the CDC 7600 computer machine word into seven 8-bit bytes. The top four bits are left untouched to preserve the floating point structure. As a result of this packing of the 60-bit machine word, each disk file can now hold seven 8-bit data sets. We can also select either the 1-km (179 x 119) or 100-m (1781 x 1181) Landsat resolution. For the Montrose quadrangle, we typically worked with five disk files, each with 1781 x 1181 grid cells--a capacity of 35 data sets.

There are several advantages to the above packing scheme, the most obvious being the capability of dealing with more than 15 data sets, a current limitation of LADIES. The 8-bit byte can contain the dynamic range of any of the input data sets. For example, a Landsat band requires at most seven bits and the geological map only four bits. If any data set should require more

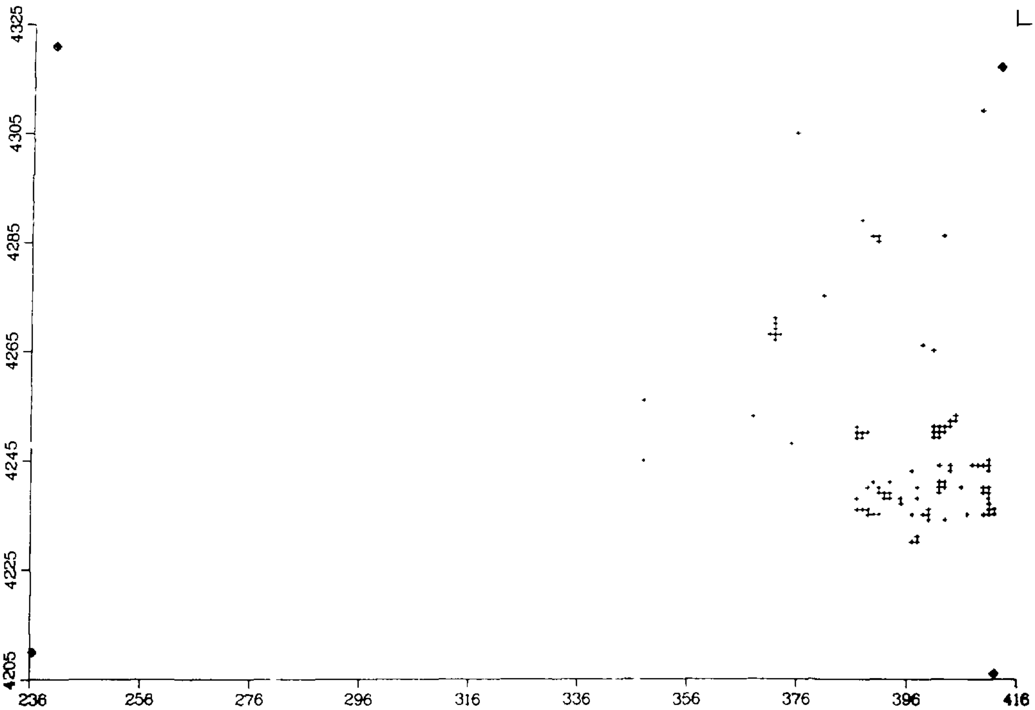

Fig. 21A. Grid cells satisfying 28 criteria.

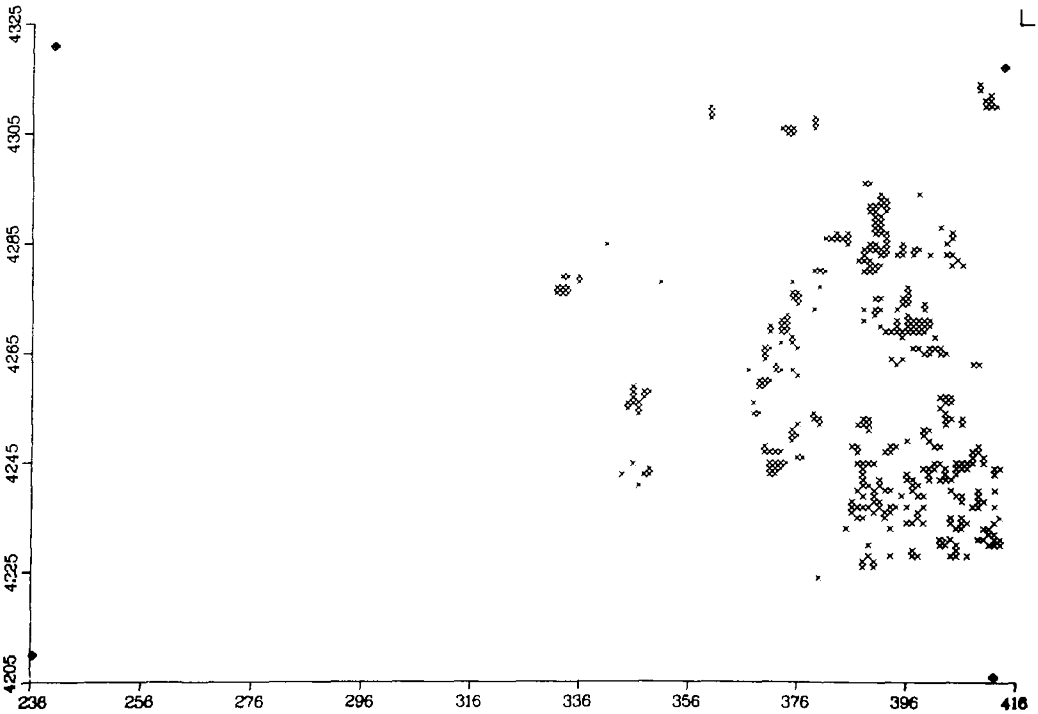

Fig. 21B. Grid cells satisfying 27 criteria.

Fig. 21. Results for MP-1 classification scheme. Criteria are listed in Table IX.

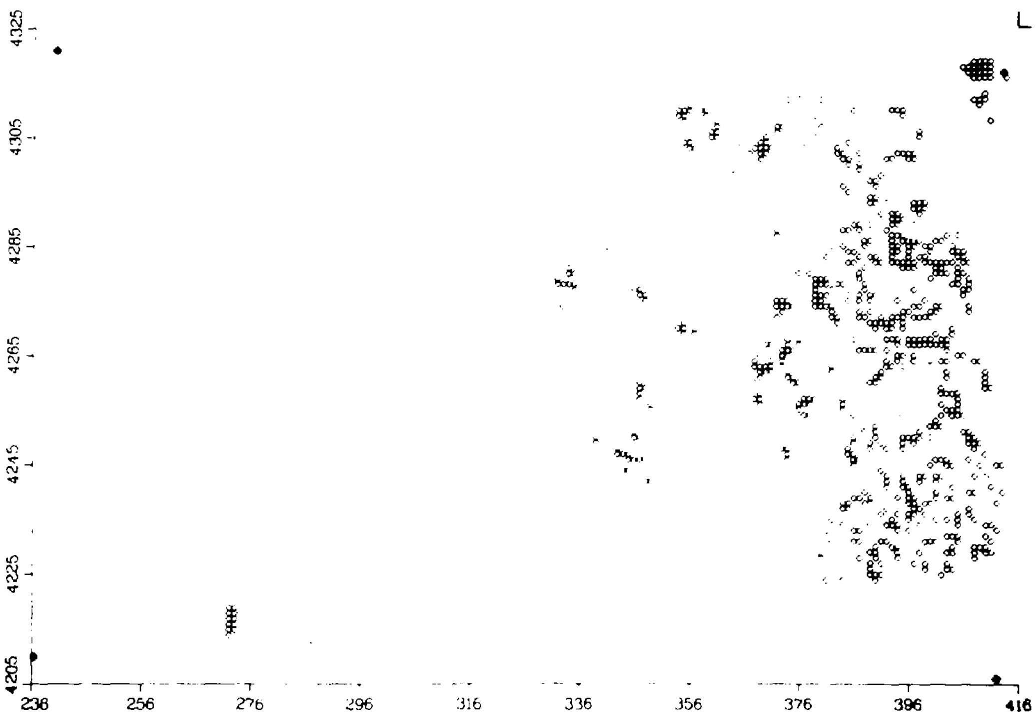

Fig. 21C. Grid cells satisfying 26 criteria.

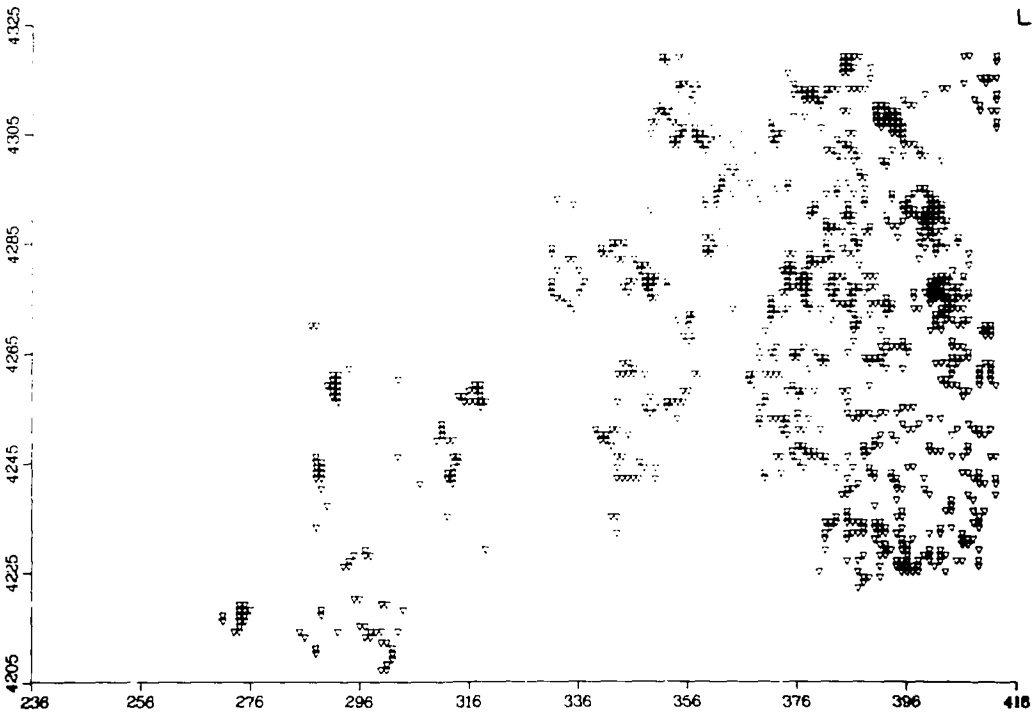

Fig. 21D. Grid cells satisfying 25 criteria.

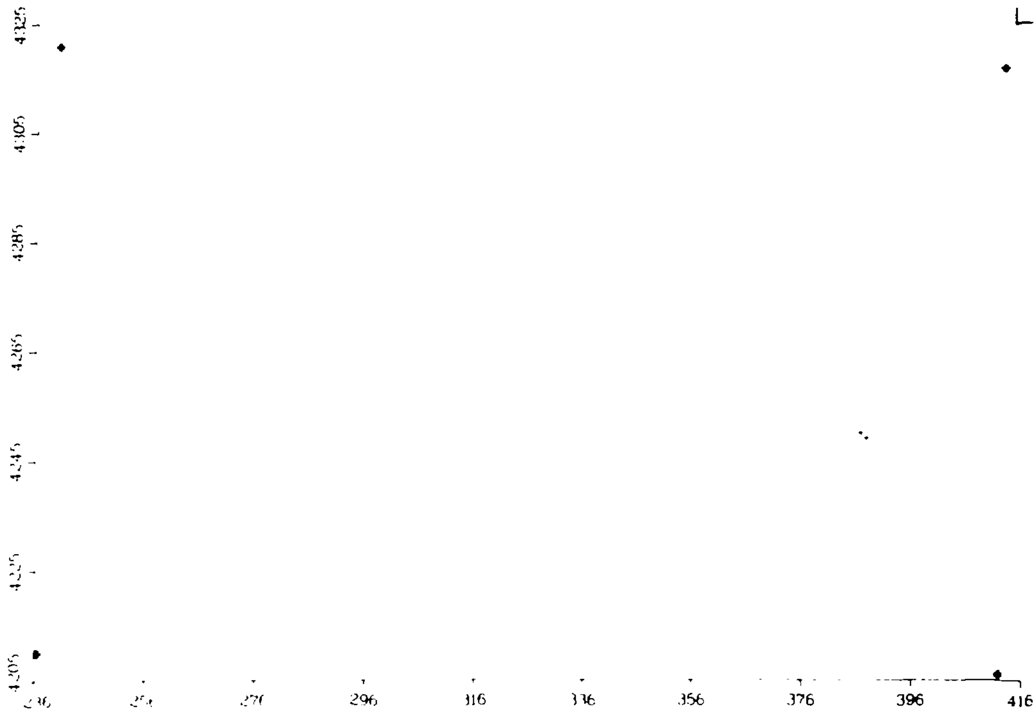

Fig. 22A. Grid cells satisfying 28 criteria.

Fig. 22B. Grid cells satisfying 27 criteria.

Fig. 22. Results for MP-2 classification scheme. Criteria are listed in Table IX.

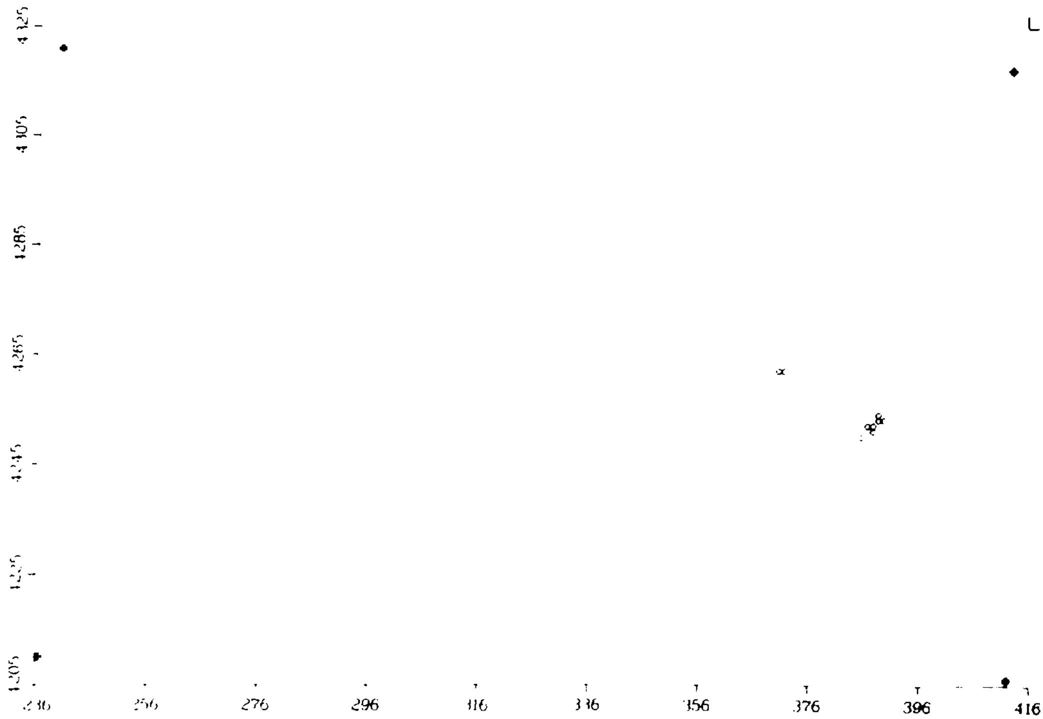

Fig. 22C. Grid cells satisfying 26 criteria.

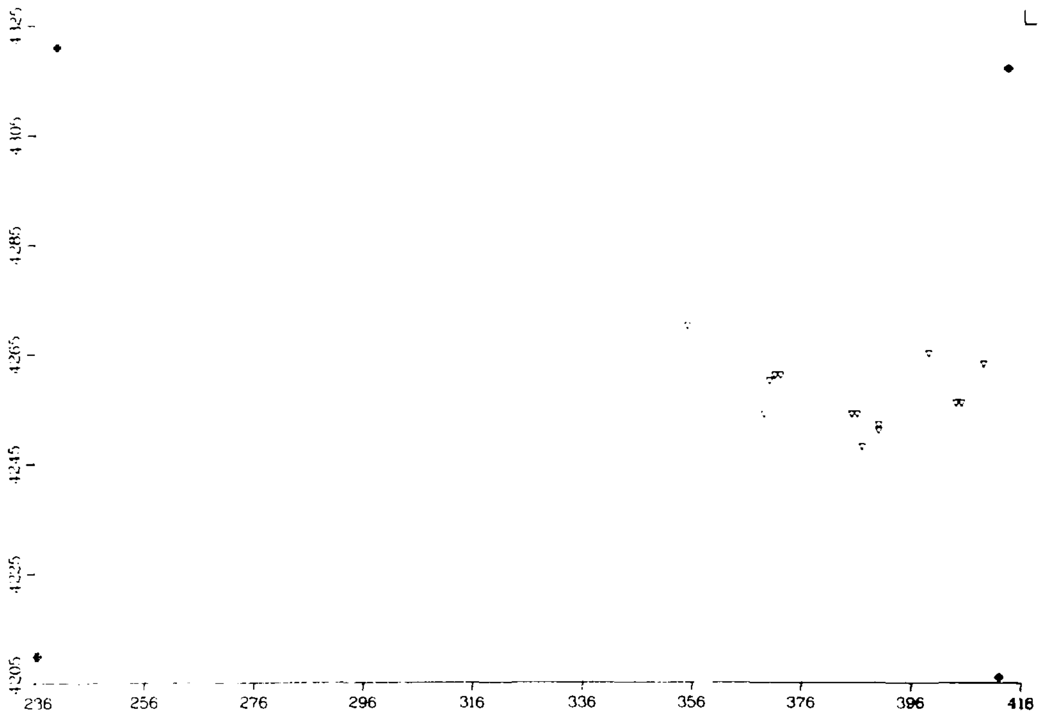

Fig. 22D. Grid cells satisfying 25 criteria.

than eight bits, it can always be treated as a genuine floating point disk file. However, any data set that we display pictorally can have eight bits at most. Many of the data-editing routines in LADIES can be applied directly to integrated data sets because no unpacking is required. For example, we can extract a smaller subsample from within the domain of the original data base. Moreover, packed Landsat 1 or 2 data can be geometrically rectified using the rubber sheet subroutine with no more difficulty than if it were a single floating-point disk file. Lastly, by packing related data sets in the same machine word, we achieve efficiency by inputting only those disk files required.

Covariance Matrix

One reason for wanting true data integration, i.e., simultaneous access to all registered data sets, is to compute the full covariance matrix for all variables. For each ground resolution element, we form the product $x_i x_j$ of the values of the i^{th} and j^{th} data sets for all possible i and j and then average over the domain of the data sets. For example, for 35 data sets, the resulting 35 x 35 matrix has 630 independent components. Given the mean vector and covariance matrix of the integrated data sets, we then calculate the parameters very quickly and cost effectively for a large variety of linear statistical models, as discussed below. Our code is structured to allow great flexibility in accumulating a sample covariance matrix. We can select any subcollection of the data sets and choose as a variable the data set value or its logarithm or any function of the data value. Also, the statistics can be gathered for any particular subset of the geologic units as determined from the digitized geological map.

Basic Statistical Models

Given a covariance matrix collected over some subdomain of data sets, we can calculate the parameters of several important linear statistical models: multiple regression, canonical correlations, and principal components.

In multiple regression, we address the question of how well a linear combination for some of the data sets can predict the value for some other data set. For example, what linear combination $\sum_i a_i x_i$ of Landsat bands $x_1, \ldots, x_4$ can best estimate y, one of the geochemical sets. From the covariances between $x_1, \ldots, x_4$, and y, we can calculate the weights $a_1, \ldots, a_4$, the correlation coefficient ρ between y and $\sum_i a_i x_i$ and the mean square error of the fit.

In canonical correlation, given two different classes $x_1, \ldots, x_p$ and $y_1, \ldots, y_q$ of data sets, we want to find what linear combinations $\sum_i a_i x_i$ and $\sum_i b_i y_i$ of variables from the two classes, respectively, produce a maximum correlation ρ. For example, we might ask what linear combination of the Landsat bands and what linear combination of the NURE geophysical data have maximum correlation. We then find the weights $a_1, \ldots, a_p$ and $b_1, \ldots, b_q$ and the correlation coefficient ρ in terms of S_{11}, S_{22}, the covariance matrices of the x's and the y's and S_{12}, the cross-covariance matrix between the x's and the y's.

In principal components we ask which linear combination of a preselected subset of the data set variables has the largest variance or scatter. Then, if the above linear combination is known, we ask what linear combination of variables that is uncorrelated with the first linear combination has the greatest variance. This process continues until the dimensionality of the data space is exhausted. The solution to the above problem corresponds to selecting a new basis for the data vectors and is found by performing a diagonalization of the covariance matrix of the variables.

Data Processing

Data processing operations on the integrated data sets mainly consist of editing functions, forming new data sets as linear combinations of old ones, density slicing, and stretching. Other important operations include formation of ratio images and bivariate histograms.

The most important editing functions performed on the integrated data set is to resample it to a coarser grid or extract a small subsection at full resolution. This permits either a local analysis at full resolution or a quadrangle-scale analysis with a minimum number of data points.

Regression images, canonical correlation images, and principal component images are formed by taking linear combinations of the original data sets. The basic data processing equation for all of these cases is the same--

$$y = Ax + b \quad ,$$

where x is an n-vector of variables taken from an arbitrary subset of the original data sets, A is an $m \times n$ transformation matrix and b is a bias m-vector, both of which depend on the type of analysis being performed. The y is an output m-vector in which each component is a linear combination of the input variables.

Because we often want to display the components of the y vector as digital images or at least save them in the packed data format, it is necessary to scale the y components to 8 bits (integers between 0 and 255). The scale factors are selected from data set statistics and then absorbed into the transformation matrix A and the bias vector b.

Bivariate Histograms. When the above scaling is carried out, it is easy to construct a bivariate histogram for any pair of components of the output vector y. For a given grid cell location, we have a pair of numbers in the range 0-255 corresponding to the pair of y-components that we wish to plot. This pair of numbers defines a cell in a 256 x 256 histogram array that we increment by 1. After collecting points in the histograms for all pixel or grid cell locations, we can display the histogram as a 256 x 256 image and look for relations between the two output images in the form of linear or low-order curves.

We often like to know what points in the data domain are contributing to what points in the histogram domain. We can examine this to some degree by constructing a color-coded map for the histogram. The map consists of a second 256 x 256 image in color. For each cell in the 256 x 256 histogram, the corresponding cell in the color map is assigned the "color" of the point that contributes to the histogram cell. Here we assume that all points that contribute to a histogram cell have the same color. The color of a point may be defined in a variety of ways. For example, we might choose the Landsat false color corresponding to that point. Another choice is to choose the psuedo-color from the geological map for the classification of the point.

SUGGESTIONS FOR FUTURE WORK

Introduction

In four months time we have developed preliminary classification schemes for uranium mineralization in the Montrose quadrangle, Colorado. By extending and refining the methodology used in an earlier work on the Talkeetna quadrangle, Alaska (Wecksung and Fugelso, 1980), we have prompted the fast progress for this study. We have increased our spatial resolution by a factor of nine, from 9 km^2 for the Talkeetna quadrangle to 1 km^2 for the Montrose quadrangle. During this study, all map information, data already in digital form, and analytical results have been converted into a digitized form that could be easily integrated into one large data set. The methodology has evolved such that essentially any form of data can be converted into a digitized form and subsequently integrated with other data.

During this study other data interpretation schemes were examined (Nichol et al, 1969; Lowenstein and Howarth, 1973; Howarth and Lowenstein, 1976; Earle, 1978; Webb et al, 1978; Garret et al, 1979; Howarth and Earle, 1979; Howarth and Martin, 1979; Webb and Howarth, 1979; Koch et al, 1979). Several technological refinements were identified. The results presented herein represent only a first step toward a DIRS program to rapidly identify and classify potential areas for mineral resources. Discussed below are some steps and refinements leading to a comprehensive DIRS resource evaluation program.

Field Verification

As a result of this study, several areas have been suggested favorable for uranium mineralization. The results, however, desperately need field verification to determine if they are regions truly favorable for uranium development, or only false leads. Therefore, we suggest a field follow-up program as a test of this study. Geographic areas (grid cells) of favorability, based on the classification schemes, would be examined in the field. These areas would be investigated for actual uranium mineralization, host rocks, and structural features favorable for uranium mineralization. Field verification could be done by BFEC or USGS personnel working jointly with Los Alamos National Laboratory representatives.

Refine Classification Scheme

Even though it is obvious in this report that both subtle and precise information can be extracted from the integrated data sets, the exact relationships between individual data sets, their influence upon other data sets, and the contribution each makes to a classification scheme has not yet been examined. The purpose of this report was only to develop the methodology necessary to take data sets in various forms and integrate them into one large data set. Now that data sets have been selected and integrated for the Montrose quadrangle, further analysis routines are very cost effective. We suggest that refinement of intra-data-set relationships for uranium mineralization now be emphasized.

For example, we could incorporate the four Landsat bands. Relationships between Landsat imagery and the other sets then can be examined. Statistical information, such as factor analysis, cluster analysis, or discriminant analysis, is readily incorporated into the classification scheme by simply assigning the respective information as a data set. For example, each factor can be assigned as a data set. A gray representation of factor scores might reveal interesting results. Subsurface geophysical data and well log data could provide a third dimension if this data were also incorporated.

Technology Refinement

Although this report presents a preliminary classification scheme for uranium mineralization of two areas in the Montrose quadrangle, several "bugs" need to be smoothed out as this program develops. One problem involves digitization and classification of the geologic map. Current methodology not only is time consuming, but the digitized map has required precise editing before it was acceptable. About five man-months were spent on preparing the Montrose geologic map.

Because much of this technology is new, there are also several ways to increase the efficiency of the overall program. One way is by rewriting algorithms such that they can do the same amount of work but in a more logical and smaller time frame.

Other Suggestions

It has become apparent during this study that an integrated data set provides a wealth of information no one data set can supply. Consequently, the methodology can be applied to any required classification scheme. Potential uses include strategic mineral resource assessment, nuclear-weapons test identification and verification, natural-hazards analysis, and environmental impact analysis.

SUMMARY OF MAJOR RESULTS

This report describes a DIRS (Data Integration/Remote Sensing) program developed at Los Alamos National Laboratory to integrate various large geological, geochemical, and geophysical data bases with remotely sensed data for the Montrose 1° x 2° quadrangle, Colorado. The primary purpose of the project was to identify in the computer, areas favorable for uranium mineralization in the Montrose quadrangle. Classification schemes described are based on test areas from the Cochetopa and Marshall Pass uranium districts. Several regions that seem to contain some potential for uranium mineralization are identified. However, detailed examination of selected data sets and data set intervals (e.g., the techniques of Beyth et al, 1980a and b) must be coupled with field verification to validate these areas as truly favorable for uranium mineralization. The techniques necessary to digitize, register, and integrate multiple data sets for a 1 km grid resolution are described.

Basic Procedures Followed in Developing Classification Schemes

1. Geochemical data were compiled from 3965 sample locations from Broxton et al (1979) and Maassen (1980). Twenty-two elemental analyses for each sediment location, uranium analyses for waters, and U/Th ratios are included. The elemental concentrations were interpolated to a 1-km rectangular grid by universal kriging.

2. Airborne radiometric and aeromagnetic data were compiled by geoMetrics (1979a and b). Digital tapes contain the raw spectral data and magnetic data. Flight-line data was smoothed and subsampled by an automated kriging procedure depending on the signal-to-noise ratio. These kriged estimates were then interpolated onto the 1-km rectangular grid much as for the hydrogeochemical data.

3. About 90 uranium occurrences (compiled predominantly from Nelson-Moore et al, 1978) were digitized and assigned a UTM coordinate. Each occurrence could then be identified by grid cell in the 1-km rectangular grid.

4. The 57 geologic formations of Tweto et al (1976a) were combined into 13 units (Table V). A mylar transparency, scale 1:250 000, was made, photographed, and digitized. Each grid cell for the 1-km rectangular grid was then classified as belonging to one of the 13 geologic units.

5. A Landsat 2 tape (October 1978) was geometrically corrected and rubber sheet transformed to fit the Montrose 1° x 2° quadrangle. Landsat bands 4 through 7 were resampled to both a 1-km and 100-m resolution.

6. All data sets, in all possible combinations of three, were examined by utilizing the Colorrocks Routine and a color microfilm output. The resultant 35-mm slides were visually examined for potential correlations between respective data sets according to the rules of color addition (Table VI).

7. Subsets of data were examined for selected test areas, for each 1-km grid cell, utilizing the Sort Routine.

8. Various statistical routines (including basic statistics, cumulative frequency, association by variable, and factor analysis) were run for both the entire data set and respective physiographic/geochemical provinces.

9. Two classification schemes were developed for uranium mineralization; one scheme is based on criteria selected from test areas containing known uranium occurrences in the Cochetopa uranium district. The other scheme is based on criteria selected from test areas in the Marshall Pass uranium district.

10. The results of the classification schemes were evaluated.

Major Achievements of this Program

1. Geological, geochemical, and geophysical data, including satellite imagery, in the forms of point data, data already in digital form, map

information, and tabular information were registered to a UTM boundary of the Montrose 1° x 2° quadrangle. All data were digitized and compiled into one data base, and codes were developed to extract data for any area of interest. Since the majority of the algorithms necessary to transform the data into an acceptable format are now available, almost any number of comparable data sets can be quickly and cost effectively prepared for other 1° x 2° quadrangles.

2. Classification schemes for potential uranium mineralization were developed for test areas for both the Cochetopa and Marshall Pass uranium districts. The general classification scheme is adaptable for similar purposes, e.g., one can a classify areas of potential copper mineralization by using known copper deposits as test areas.

3. Subsequent to the development of our classification schemes, we have extended our data structure by repacking the data to accommodate additional data sets. This repacking allows both simultaneous access to all registered data sets and very cost effective manipulation of the integrated data.

4. The methodology developed allows rapid and efficient resource evaluation on a reconnaissance scale. Data integration not only makes obvious information readable, but also enhances subtle relationships in the data that were not anticipated.

REFERENCES CITED

Adams, J. W., 1953, Beryllium deposits of the Mount Antero region, Chaffee County, Colorado, Bull. 982-D, US Geol. Survey, Washington, DC, pp. 95-119.

Adams, J. A. S., and Gasparini, P., 1970, Gamma-ray spectrometry of rocks, Elsevier Publishing Co., New York, NY.

Armbrustmacher, T. J., 1979, Abundance and distribution of thorium in the carbonatite stock at Iron Hill, Powderhorn district, Gunnison County, Colorado, Open-file Report 79-536, US Geol. Survey, Denver, CO, 27 pp.

Armbrustmacher, T. J., and Brownfield, I. K., 1979, The carbonatite stock at Iron Hill, Gunnison County, Colorado--chemical and mineralogical data, Open-file Report 79-537, US Geol. Survey, Denver, CO, 13 pp.

Bailey, G., Brian, 1980, The Landsat satellite system, Sixth Annual Pecora Symposium and Exposition, EROS Data Center, Sioux Falls, SD, pp. 24-26.

Baillie, W. N., 1962, Feldspar occurrences in Colorado, Colorado School of Mines Mineral Industries Bull., v. 5, no. 4, Denver, CO, p.4.

Belser, C., 1956, Tungsten potential in Chaffee, Fremont, Gunnison, Lake, Larimer, Park, and Summit Counties, Colorado, Inf. Circ. 7748, US Bureau Mines, Washington, DC, 31 pp.

Beyth, M., McInteer, C., Broxton, D. E., Bolivar, S. L., and Luke, M. E., 1980a, Multivariate statistical analysis of stream sediments from the Craig NTMS quadrangle, Colorado, Open-file Report GJBX-145(80), US DOE, Grand Junction, CO, 64 pp.

Beyth, M., Broxton, D. E., and McInteer, C., 1980b, Analysis of stream sediment reconnaissance data for mineral resources in the Montrose NTMS quadrangle, Colorado, Los Alamos Scientific Laboratory, Los Alamos, NM (in preparation).

Bolivar, S. L., 1980a, An overview of the National Uranium Resource Evaluation Hydrogeochemical and Stream Sediment Reconnaissance Program, Open-file Report GJBX-220(80), US DOE, Grand Junction, CO, 24 pp.

Bolivar, S. L., 1980b, The Los Alamos Scientific Laboratory approach to hydrogeochemical and stream sediment reconnaissance for uranium in the United States, Los Alamos National Laboratory, Los Alamos, NM (in preparation), pp. 16 and 107.

Brady, B. T., 1975, Map showing fluorspar deposits in Colorado, US Geol. Survey, Mineral Invest. Resources Map MR-70 (1:500 000-scale), prepared in cooperation with the Colorado State Mining and Industrial Development Board and the Colorado State Geol. Survey,(scale, 1:500 000), Denver, CO.

Broxton, D. E., Morris, W. A., and Bolivar, S. L., 1979, Uranium hydrogeochemical and stream sediment reconnaissance of the Montrose NTMS quadrangle, Colorado, including concentrations of forty-three additional elements, Open-file Report GJBX-125(79), US DOE, Grand Junction, CO, 255 pp.

Burbank, W. S., 1932, Geology and ore deposits of the Bonanza mining district, Colorado, with a section on history and production, by C. W. Henderson, Prof. Paper 169, US Geol. Survey, Washington, DC, 166 pp.

Burbank, W. S., 1940, Structural controls of ore deposition in the Uncompahgre district, Ouray County, Colorado, with suggestions for prospecting, Bull. 906-E, US Geol. Survey, Washington, DC, pp. 189-265.

Burbank, W. S., 1947, Summaries of mining districts and mineral deposits, Part II, in Mineral Resources of Colorado, Vanderwilt, J. W., and others, Colorado Mineral Resources Board, Denver, CO, pp. 291-470.

Burbank, W. S., and Luedke, R. G., 1968, Geology and ore deposits of the western San Juan Mountains, Colorado, in Ore Deposits of the United States, 933-1967, Graton-Sales volume, J. D. Ridge (Ed.), Amer. Inst. Min. Eng., New York, pp. 714-733.

Burbank, W. S., and Pierson, C. T., 1953, Preliminary results of radiometric reconnaissance of parts of the northwestern San Juan Mountains, Colorado, Circ. 236, US Geol. Survey, Washington, DC, 11 pp.

Cadigan, R. A., Felmlee, J. K., and Rosholt, J. N., 1976, Radioactive mineral springs in Delta County, Colorado, Open-file Report 76-223, US Geol. Survey, Washington, DC, 39 pp.

Chavez, P. S., Jr., 1975, Atmospheric, solar, and MTF corrections for ERTS digital imagery, Proc. Amer. Soc. Photogrammetry, pp. 69-69a.

Crawford, R. D., 1909, Preliminary report on the geology of Monarch mining district, Chaffee County, Colorado, Bull. 1, Colorado Geol. Survey, Denver, CO, 78 pp.

Crawford, R. D., 1913, Geology and ore deposits of the Monarch and Tomichi districts, Colorado, Bull. 4, Colorado Geol. Survey, Denver, CO, 317 pp.

Crawford, R. D., and Worcester, P. G., 1916, Geology and ore deposits of the Gold Brick district, Colorado, Bull. 10, Colorado Geol. Survey, Denver, CO, 116 pp.

Dall'Aglio, M., 1971, A study of the circulation of uranium in the supergene environment in the Italian Alpine Range, Geoch. Cosmochim. Acta, v. 35, pp. 47-60.

Dall'Aglio, M., 1972, Planning and interpretation criteria in hydrogeochemical prospecting for uranium (with discussion), in S. H. U. Bowie, M. Davis, and D. Ostle (Eds.), Uranium Prospecting Handbook, Institution of Mining and Metallurgy, London, pp. 121-134.

Derzay, R. C., 1956, Geology of the Los Ochos uranium deposit, Saguache County, Colorado, Prof. Paper 300, US Geol. Survey, Washington, DC, pp. 137-141.

Dings, M. G., and Robinson, C. S., 1957, Geology and ore deposits of the Garfield quadrangle, Colorado, Prof. Paper 289, US Geol. Survey, Washington, DC, 110 pp.

Earle, S. A. M., 1978, Spatial presentation of data from regional geochemical stream surveys, Inst. of Min. Metall. Sect. B, 87, pp. B61-B65.

Eckel, E. B., 1961, Minerals of Colorado--A 100-year record, Bull. 1114, US Geol. Survey, Washington, DC, 399 pp.

Epis, R. (Ed.), 1968, Cenozoic volcanism in the southern Rocky Mountains, Colo. School Mines Quart., v. 63, no. 3, Golden, CO, 286 pp.

Finch, W. I., 1967, Geology of epigenetic uranium deposits in sandstone in the United States, Prof. Paper 538, US Geol. Survey, Washington, DC, 121 pp.

Fischer, R. P., Luedke, R. G., and Sheridan, M. J., 1968, Mineral resources of the Uncompahgre primitive area, Colorado, Bull. 1261-C, US Geol. Survey, Washington, DC, 91 pp.

Frane, J. W., and Hill, M., 1976, Factor analysis as a tool for data analysis, Commun. Statist.--Theor. Meth., AS(6), pp. 487-506.

Gallagher, G. L., Edmond, C. L., and D'Andrea, R. F., Jr., 1977, Preliminary evaluation of the uranium favorability in the area northeast of Gunnison, Colorado, GJBX-61(79), US DOE, Grand Junction, CO, 25 pp.

Garrett, R. G., Kane, V. F., and Ziegler, R. K., 1979, Management and analysis of regional geochemical data, 92nd Annual Meeting abstracts and program, Geol. Soc. Am., p. 430.

geoMetrics, 1979a, Aerial gamma ray and magnetic survey Uncompahgre Uplift project, Salina, Utah, Moab, Utah, and Colorado, Montrose and Leadville, Colorado, quadrangles, Open-file Report GJBX-95(79), Final report, vol. I, US DOE, Grand Junction, CO, 57 pp.

geoMetrics, 1979b, Aerial gamma ray and magnetic survey Uncompahgre uplift project, Montrose quadrangle, Colorado, Open-file Report GJBX-95(79), Final report, v. 11, US DOE, Grand Junction, CO, 19 pp. + 164 p. Appendix.

Gregory, A. F., and Horwood, J. L., 1963, A spectrometric study of the attenuation in air of gamma rays from mineral resources, US Atomic Energy Commission Report CEX-60-3, Washington, DC.

Gross, E. B., 1965, A unique occurrence of uranium minerals, Marshall Pass Saguache County, Colorado, Am. Mineralogist, V. 50, pp. 909-923.

Guillotte, G. B., 1945, The geology and ore deposits of the Brown Derby pegmatites, Box Canyon mining district, Gunnison County, Colorado, RMO-45, US AEC, Grand Junction, CO, 22 pp.

Hanley, J. B., Heinrich, E. W., and Page, L. R., 1950, Pegmatite investigations in Colorado, Wyoming, and Utah, 1942-44, Prof. Paper 227, US Geol. Survey, Washington, DC, 125 pp.

Haun, J. D., and Kent, H. C., 1965, Geologic history of Rocky Mountain region, Bull. of Amer. Assoc. of Petrol. Geol., v. 49, no. 11, pp. 1781-1799.

Heinrich, E. W., 1958, Mineralogy and Geology of Radioactive Raw Materials, McGraw-Hill Book Co., NY. 654 pp.

Heyl, A. V., 1964, Oxidized zinc deposits of the United States--Part 3, Colorado, Bull. 1135-C, US Geol. Survey, Washington, DC, pp. C1-C98.

Hill, J. M., 1909, Notes on the economic geology of southeastern Gunnison County, Colorado, in Contributions to Economic Geology, 1908, Bull. 380, US Geol. Survey, Washington, DC, pp. 21-40.

Howarth, R. J., and Earle, S. A. M., 1979, Application of a generalized power transformation in geochemical data, Math. Geol., v. 11, no. 1, pp. 45-62.

Howarth, R. J., and Lowenstein, P. L., 1976, Technical Note, Three-component colour maps from line printer output, Trans. Inst. Min. Metall., v. 85, pp. B234-B237.

Howarth, R. J., and Martin, L., 1979, Computer-based techniques in the compilation, mapping, and interpretation of exploration geochemical data, in P. J. Hood (ed.), Geophysics and geochemistry in the search for metallic ores, Geological Survey of Canada, Economic Geology Report 31, Ottawa, pp. 545-574.

Irving, J. D., and Bancroft, H., 1911, Geology and ore deposits near Lake City, Colorado, Bull. 478, US Geol. Survey, Washington, DC, 128 pp.

Joreskog, K. G., Klovan, J. E., and Reyment, R. A., 1976, Geological Factor Analysis, Elsevier Scientific Publishing Co., Methods in Geomathematics 1, NY, 178 pp.

King, P. B., 1976, Precambrian geology of the United States, US Geol. Survey Prof. Paper 902, Washington, DC, 85 pp.

King, W. H., and Allsman, P. T., 1950, Reconnaissance of metal mining in the San Juan region, Ouray, San Juan, and San Miguel Counties, Colorado, Inf. Circ. 7554, US Bur. Mines, Washington, DC, 109 pp.

Koch, G. S., Howarth, R. J., Carpenter, R. H., and Schuenemeyer, J. H., 1979, Development of data enhancement and display techniques for stream-sediment data collected in the National Uranium Resource Evaluation program of the United States Department of Energy, Open-file Report GJBX-28(80), US DOE, Grand Junction, CO, 223 pp.

Koschmann, A. H., and Bergendahl, M. H., 1968, Principal gold-producing districts of the United States, Prof. Paper 610, US Geol. Survey, Washington, D.C., 283 pp.

Lankston, M. M., and Lankston, R. W., 1979, Integration of NURE and other data sets with emphasis on their utilization in generating exploration models in the Lubbock, TX, 1° x 2° quadrangle, Open-file Report GJBX-135(79), US DOE, Grand Junction, CO, 169 pp. plus appendix.

Larsen, E. S., 1942, Alkalic rocks of Iron Hill, Gunnison County, Colorado, Prof. Paper 197-A, US Geol. Survey, Washington, DC, pp. 1-64.

Larsen, E. S., and Cross, C. W., 1956, Geology and petrology of the San Juan region, southwestern Colorado, Prof. Paper 258, US Geol. Survey, Washington, DC, 303 pp.

Lepeltier, C., 1969, A simplified statistical treatment of geochemical data by graphical representation, Econ. Geol., v. 64, pp. 538-550.

Lipman, P. W., Doe, B. R., Hedge, C. E., and Steven, T. A., 1978, Petrologic evolution of the San Juan volcanic field, southwestern Colorado: Pb and Sr isotope evidence, Geol. Soc. Amer. Bull., v. 89, pp. 59-82.

Lowenstein, P. L., and Howarth, R. J., 1973, Automated colour-mapping of three-component systems and its application to regional geochemical reconnaissance, in Geochemical Exploration 1972, M. J. Jones (Ed.), Inst. of Mining and Metall., London, pp. 297-304.

Maassen, L. W., 1980, Detailed uranium hydrogeochemical and stream sediment reconnaissance data release for the eastern portion of the Montrose NTMS quadrangle, Colorado, including concentrations of forty-five additional elements, Los Alamos Scientific Laboratory, Los Alamos, NM (in preparation).

Malan, R. C., and Ranspot, H. W., 1959, Geology of the uranium deposits in the Cochetopa mining district, Saguache and Gunnison Counties, Colorado, Econ. Geol., v. 54, pp. 1-19.

Mallory, W. M., 1972, Regional synthesis of the Pennsylvanian system, in W. M. Mallory, M. R. Mudge, and W. E. Lumb (Eds.), Geologic atlas of the Rocky Mountain region, Rocky Mt. Assoc. Petrol. Geol., Hirschfeld Press, Denver, CO, pp. 111-127.

Mardirosian, C. A., 1976, Mining districts and mineral deposits of Colorado, 1:1 000 000-scale map, Consulting Geologist, Albuquerque, NM.

Murphy, M., Wollenberg, H., Strisower, B., Bournan, H., Flexser, S., and Carmichael, I., 1978, Uranium in alkaline rocks, Open-file Report GJBX-78(78), US DOE, Grand Junction, CO, pp. 19-52.

Nash, J. T., 1980, Supergene uranium deposits in brecciated zones of Laramide upthrusts--concepts and applications, US Geol. Survey Open-file Report 80-385, Denver, CO, 36 pp.

NOAA (National Oceanic and Atmospheric Administration), 1976, Climatological data, Colorado, V. 80, no. 13, US Dept. of Commerce, Asheville, NC.

NOAA, 1977, Climatological data, Colorado, v. 81, no. 13, US Dept. of Commerce, Asheville, NC.

Nelson-Moore, J. L., Collins, D. B., and Hornbaker, A. L., 1978, Radioactive mineral occurrences of Colorado and bibliography, Bull. 40, Colorado Geol. Survey, Denver, CO, 1054 p.

Nichol, I., Garrett, R. G., and Webb, J. S., 1969, The role of some statistical and mathematical methods in the interpretation of regional geochemical data, Econ. Geol., v. 64, pp. 204-220.

Nie, N. H., Hull, C. H., Jenkins, J. G., Steinbrenner, K., and Bent, D. H., 1975, Statistical Package for the Social Sciences, Second Edition, McGraw-Hill, New York, NY, 675 pp.

Olea, R. A., 1974, Optimal contour mapping using universal kriging, J. Geophy. Res., v. 79, pp. 695-702.

Olson, J. C., 1976, Uranium deposits in the Cochetopa district, Colorado, in relation to the Oligocene erosion surface, US Geol. Survey Open-file Report 76-222, Denver, CO., 13 pp.

Olson, J. C., and Wallace, S. R., 1956, Thorium and rare earth minerals in the Powderhorn district, Gunnison County, Colorado, Bull. 1027-O, US Geol. Survey, Washington, DC, pp. 693-723.

Parker, B. H., 1974, Gold placers of Colorado, Colo. School Mines Quart., v. 69, no. 3, 268 p., and no. 4, Golden, CO, 224 pp.

Phair, G., and Gottfried, D., 1964, The Coloardo Front Range, Colorado, USA as a uranium and thorium province, in J. A. S. Adams, and W. M. Lowder, (Eds.), The Natural Radiation Environment, Univ. of Chicago Press, Chicago, IL, pp. 7-38.

Pirkle, F. L., Campbell, K., Wecksung, G., 1979, Principal components analysis as a tool for interpreting NURE and radiometric survey data, Jour. of Geol., v. 88, pp. 57-67.

Ranspot, H. W., and Spengler, R. G., 1957, Uranium deposits of the Marshall Pass area, Gunnison and Saguache counties, Colorado, DAO--3-TM-42, US AEC, Grand Junction, CO, 36 pp.

Saunders, D. F., 1979, Characterization of uraniferous geochemical provinces by aerial gamma-ray spectrometry, Min. Engineer. (Dec.), pp. 1715-1722.

Sharp, R. R., Jr., and Aamodt, P. L., 1978, Field procedures for the uranium hydrogeochemical and stream sediment reconnaissance as used by the Los Alamos Scientific Laboratory, Open-file Report GJBX-68(78), US DOE, Grand Junction, CO, 64 pp.

Simmons, E. C., and Hedge, C. E., 1978, Minor-element and Sr-isotope geochemistry of Tertiary stocks, Colorado Mineral Belt, Contrib. Mineral. Petrol., v. 67, pp. 379-396.

Sinclair, A. J., 1976, Probability graphs in mineral exploration, Assoc. of Explor. Geochem. Spec. Vol. No. 4, Richmond Printers, British Columbia, Canada, 95 pp.

Staatz, M. H., and Trites, A. F., Jr., 1955, Geology of the Quartz Creek Pegmatite district, Gunnison County, Colorado, Prof. Paper 265, US Geol. Survey, Washington, DC, 111 pp.

Steven, T. A., Lipman, P. W., Hail, W. J., Jr., Barker, F., and Luedke, R. G., compilers, 1974, Geologic map of the Durango quadrangle, southwestern Colorado. Map I-764 (1:250 000 scale), US Geol. Survey, Denver. CO.

Taylor, S. R., 1964, Abundance of chemical elements in the continental crust: a new table, Geochim. Cosmochim. Acta 28, pp. 1273-1285.

Termain, P. A., Donovan, T. J., and Chavez, P. S., Jr., 1980, Integration of geological, geochemical, and geophysical spatial data of the Cement Oil Field, Oklahoma, test site, Sixth Annual Pecora Symposium and Exposition (abstract), EROS Data Center, Sioux Falls, SD, p. 57.

Truebe, H., 1974, Mineral occurrences in the Montrose quadrangle, Consulting Geologist, Crested Butte, CO, 237 pp.

Tweto, O., 1968, Geologic setting and interrelationships of the mineral deposits in the mountain province of Colorado and south central Wyoming, in Ore Deposits of the United States 1933-1967, Graton-Sales Volume, J. D. Ridge (ed.), Amer. Inst. Min. Eng., New York, pp. 551-588.

Tweto, O., 1975, Laramide (Late Cretaceous-early Tertiary) orogeny in the Southern Rocky Mountains, in Cenozoic History of the Southern Rocky Mountains, B. F. Curtis (Ed.), Geol. Soc. Am. Memoir 144, Washington, DC, pp. 1-44.

Tweto, O., Steven, T. A., Hail, W. J., Jr., and Moench, R. H., compilers, 1976a, Preliminary geologic map of the Montrose 1° x 2° quadrangle, southwestern Colorado, Map MF-761 (1:250 000 scale), US Geol. Survey, Denver, CO.

Tweto, O., Moench, R. H., and Reed, J. C., Jr., compilers, 1976b, Preliminary geologic map of the Leadville 1° x 2° quadrangle, northwestern Colorado, Map MF-760 (1:250 000 scale), US Geol. Survey, Denver, CO.

US AEC (Atomic Energy Commission), 1966a, Preliminary reconnaissance reports on reported occurrences of uranium deposits, Gunnison County, Colorado, PB-172 544, US AEC, Grand Junction, CO, 50 pp.

US AEC, 1966b, Preliminary reconnaissance reports on reported occurrences of uranium deposits, Park County, Colorado, PB-172 560, US AEC, Grand Junction, CO, 54 pp.

US AEC, 1966c, Preliminary reconnaissance reports on reported occurrences of uranium deposits, Saguache County, Colorado, PB-172 567, US AEC, Grand Junction, CO, 32 pp.

US AEC, 1966d, Preliminary reconnaissance reports on reported occurrences of uranium deposits, Hinsdale County, Colorado, PB-172 545, US AEC, Grand Junction, CO, 4 pp.

US Department of Energy, 1979, National Uranium Resource Evaluation, Interim Report, June 1979, Open-file Report GJO-111(79), US DOE, Grand Junction, CO, 131 pp.

USGS (US Geologial Survey), 1956 (revised 1962), Montrose, Colorado, topographic map NJ 13-4 (1:250 000 scale), Denver, CO.

USGS, 1971, Reported occurrences of selected minerals in Colorado, 1:500 000-scale map, compiled by the Branch of Mineral Classification Conservation District, Denver, CO.

USGS, 1979, Landsat Data Users Handbook, Revised Edition, Arlington, VA (paged in sections).

USGS and Colorado Mining Industrial Development Board, 1968, Mineral and water resources of Colorado, US 90th Cong., 2d sess., Senate Comm. Interior and Insular Affairs, Comm. Print, Washington, DC, 302 pp.

Van Alstine, R. E., 1947, Fluorspar investigations, in Mineral Resources of Colorado, Vanderwilt, J. W., and others, Colorado Mineral Resources Board, Denver, CO, pp. 457-465.

Vanderwilt, J. W., 1947, Metals, nonmetals, and fuels, Part 1, in Mineral Resources of Colorado, Vanderwilt, J. W., and others, Colorado Mineral Resources Board, Denver, CO, pp. 1-290.

Warner, L. A., 1978, The Colorado lineament: A middle Precambrian wrench fault system, Geol. Soc. of Amer. Bull., v. 89, pp. 161-171.

Webb, J. S., and Howarth, R. J., 1979, Regional geochemical mapping, Sect. B288, Phil. Trans. R. Soc. London, pp. 81-93.

Webb, J. S., Thornton, I., Thompson, M., Howarth, R. J., and Lowenstein, P. L., 1978, The Wolfson Geochemical Atlas of England and Wales, Oxford University Press, Oxford, 72 pp.

Wecksung, G. W., and Breedlove, J. R., Jr., 1977, Some techniques for digital processing, display, and interpretation of ratio images in multispectral remote sensing, Soc. Photo-Optical Instru. Eng., v. 119, pp. 47-54.

Wecksung, G. W., and Fugelso, E., 1980, Exploratory analysis techniques for multisource integrated geological data sets, Sixth Annual Pecora Symposium and Exposition (abstract), EROS Data Center, Sioux Falls, SD, p. 114.

Weimer, R. J., and Haun, J. D., (Eds.), 1960, Guide to the geology of Colorado, Geol. Soc. of America, Rocky Mt. Assoc. of Geol., Colorado Scientific Society, Denver, CO, 303 pp.

APPENDIX A

The following lists the grid cell coordinates for each coded uranium occurrence. The occurrence locations are shown in Fig. 4 and described in Table I. The code is as follows.

The first three digits refer to the host rock as defined by Nelson-Moore et al, 1978. A 100 is an igneous or metamorphic host; a 200 is a sandstone, arkose, conglomerate, siltstone, or lake sediment; a 300 is a spring deposit or ground water occurrence; a 400 designates a coal, shale, or limestone host; 500 is undetermined. The fourth digit identifies the county.

1 = Delta	4 = Hinsdale	7 = Chaffee
2 = San Miguel	5 = Gunnison	8 = Park
3 = Ouray	6 = Saguache	

The fifth and sixth digit are location numbers from Plate 7 of Nelson-Moore et al (1978). The pixel coordinates are given column first (179 maximum) and line second (119 maximum).

Code Number	Grid Cell Column	Grid Cell Line	Code Number	Grid Cell Column	Grid Cell Line
100304	34	39	100609	111	37
100402	49	10	100610	105	35
100403	43	7	100618	153	45
100405	51	11	100620	109	38
100406	60	6	100621	152	45
100502	80	43	100626	166	38
100505	86	32	100630	109	42
100506	124	62	100637	155	48
100508	76	45	100639	116	23
100509	78	43	100640	118	24
100510	78	49	100641	140	23
100511	108	85	100642	116	33
100512	81	40	100646	120	33
100514	80	41	100649	167	37
100516	83	40	100704	162	109
100517	127	103	100705	158	61
100518	78	40	100710	157	77
100519	83	40	100712	176	94
100520	81	52	100713	177	72
100521	105	95	100717	141	112
100523	89	42	100718	141	112
100525	73	48	100720	174	98
100526	75	43	100722	171	101
100525	73	48	200214	4	6
100526	75	43	200501	52	103
100527	63	68	200503	143	59
100601	123	36	200504	143	60
100603	150	32	200515	151	50
100605	111	47	200524	116	56
100608	164	46	200602	148	47

Code Number	Grid Cell Column	Grid Cell Line	Code Number	Grid Cell Column	Grid Cell Line
200606	149	47	300101	18	93
200611	152	48	300102	36	98
200615	174	24	300103	10	93
200616	110	38	300104	11	92
200617	149	48	300105	24	91
200619	112	43	300106	25	90
200623	110	37	300311	31	7
200631	113	45	400312	30	11
200635	120	49	400522	136	74
200636	120	46	400627	152	47
200638	133	49	400708	151	61
200644	107	43	400803	172	109
200645	107	46	500507	105	105
200646	114	44	500651	92	33
200801	171	110			

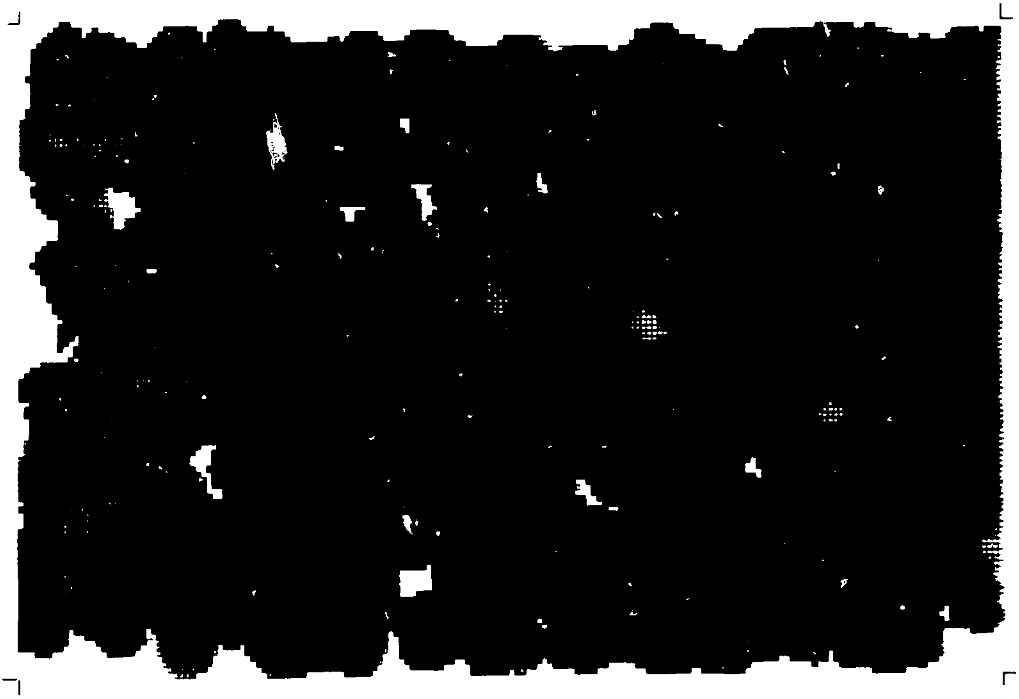

Al Aluminum

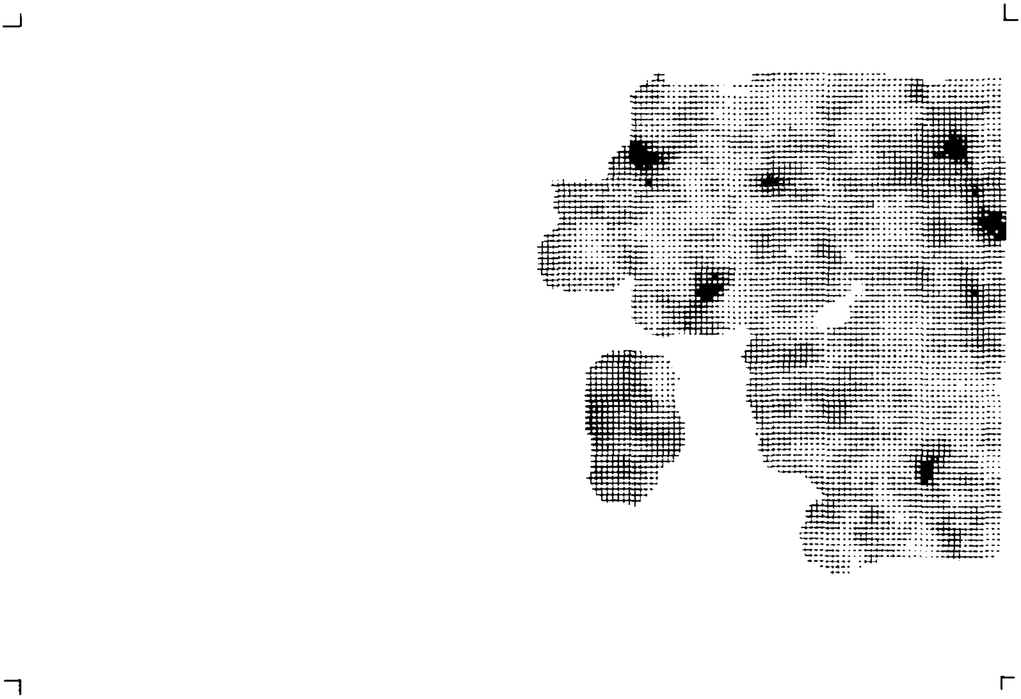

As Arsenic

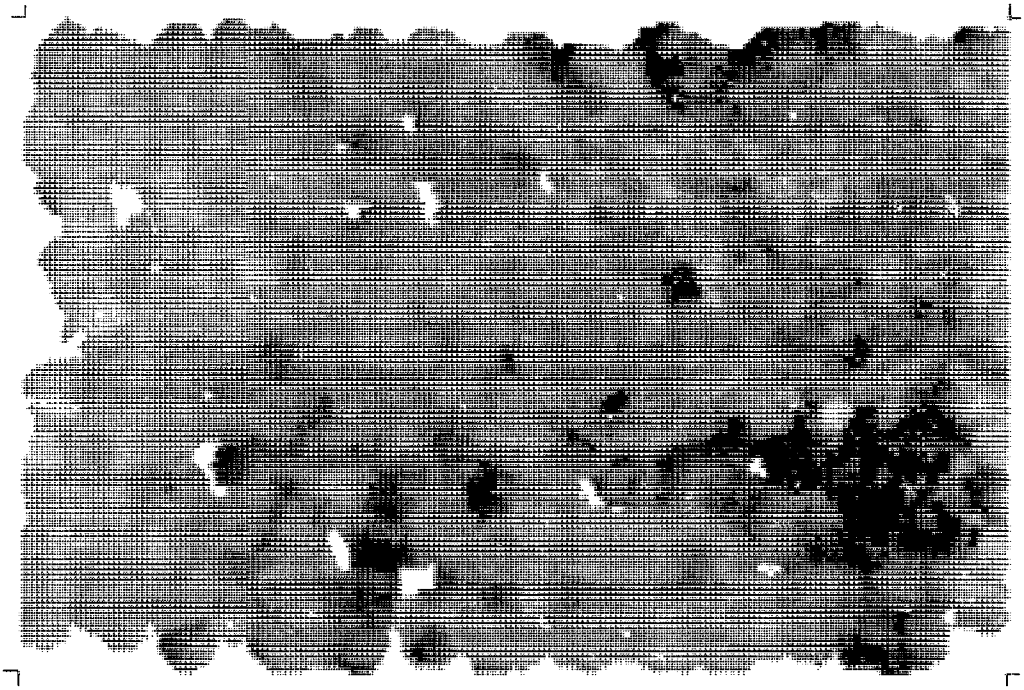

Ba Barium

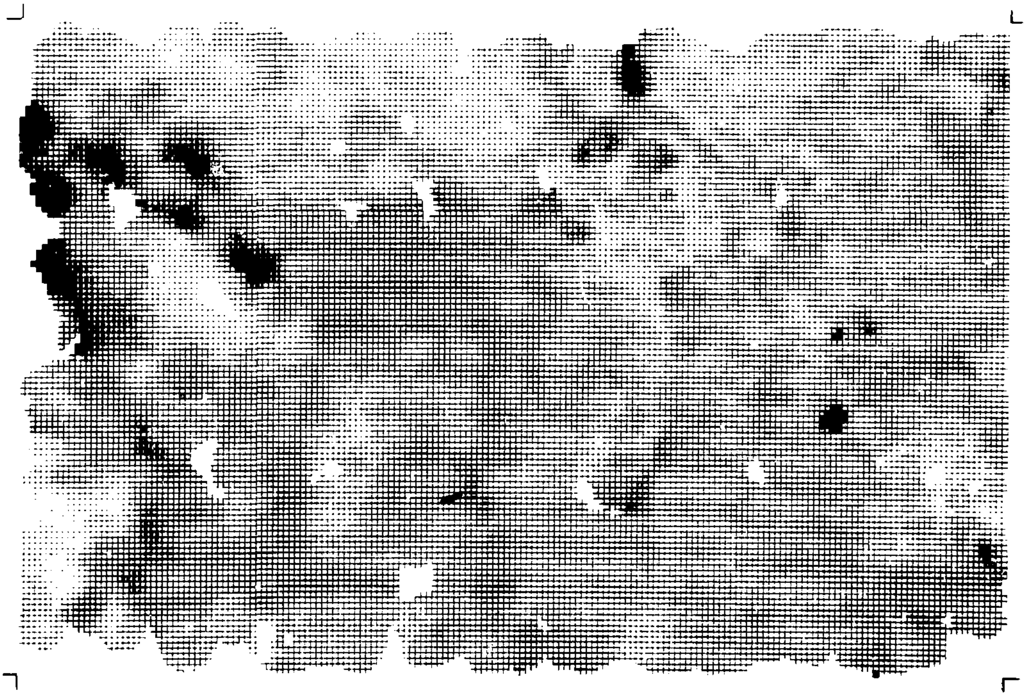

Ca Calcium

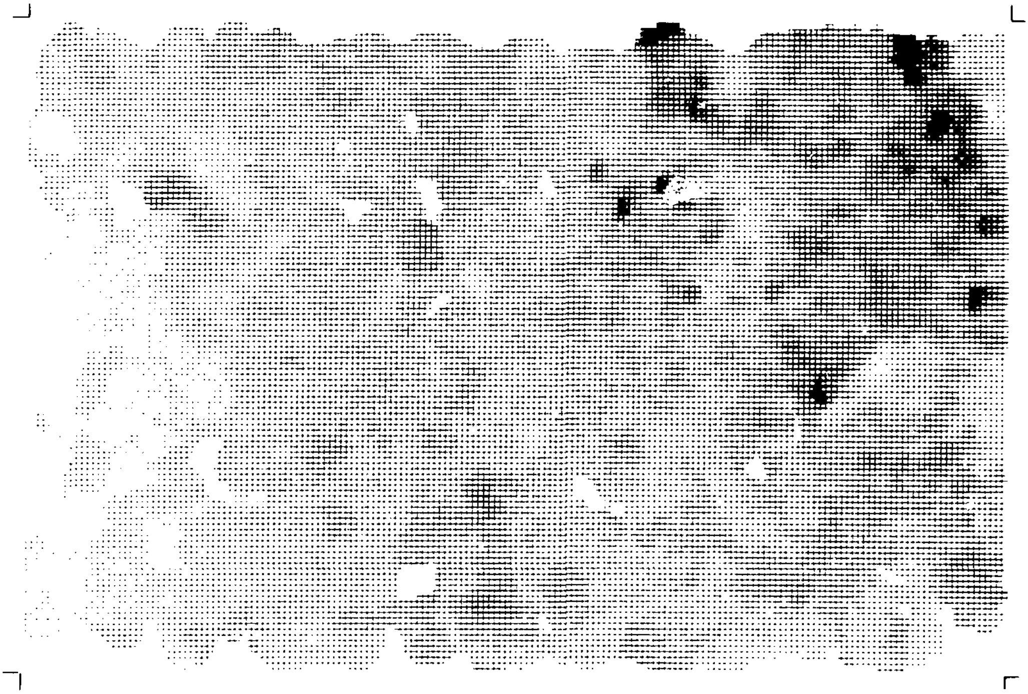

Ce Cerium

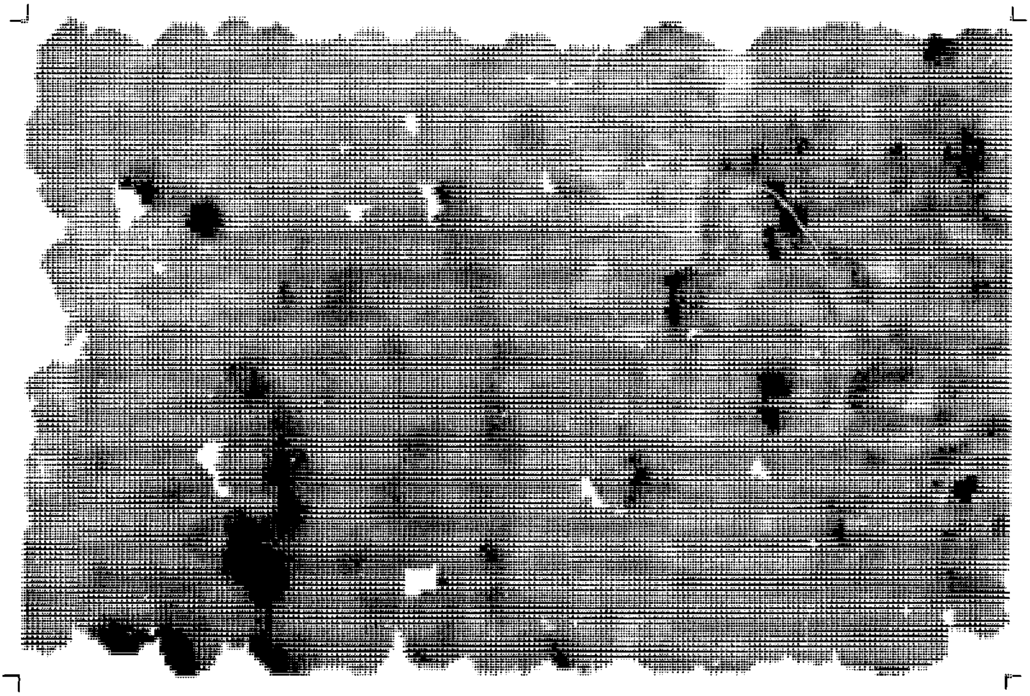

Co Cobalt

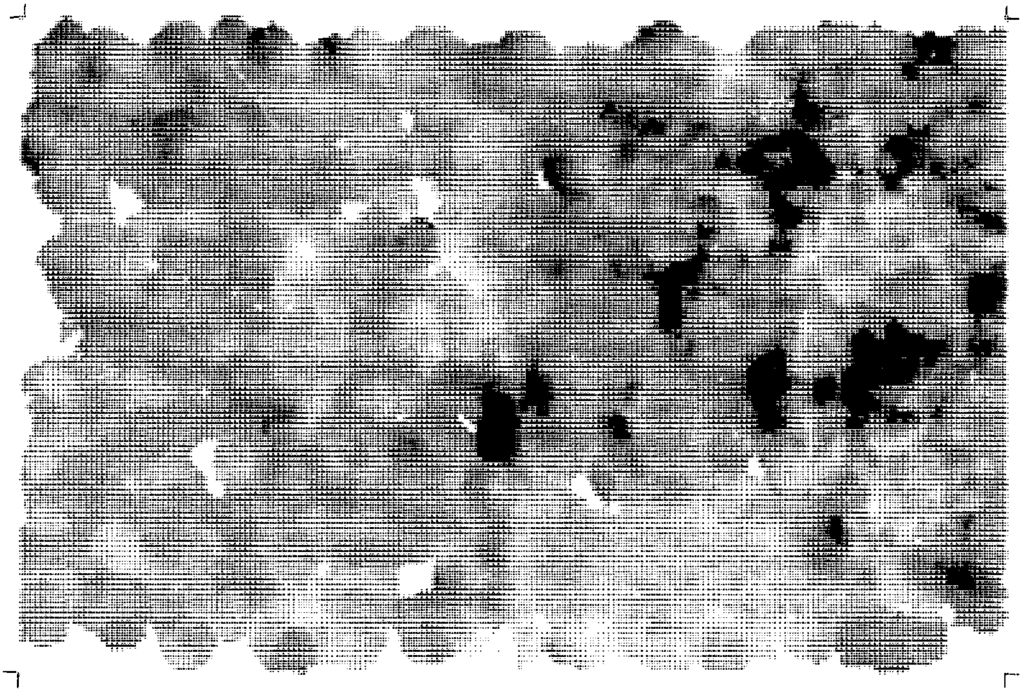

Cr Chromium

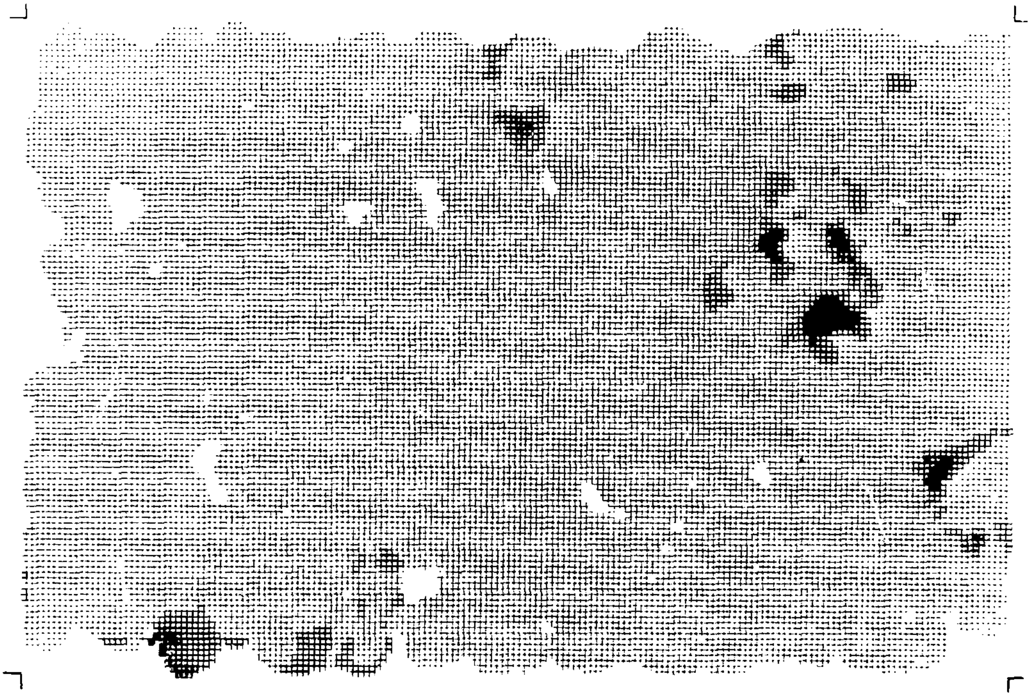

Cu Copper

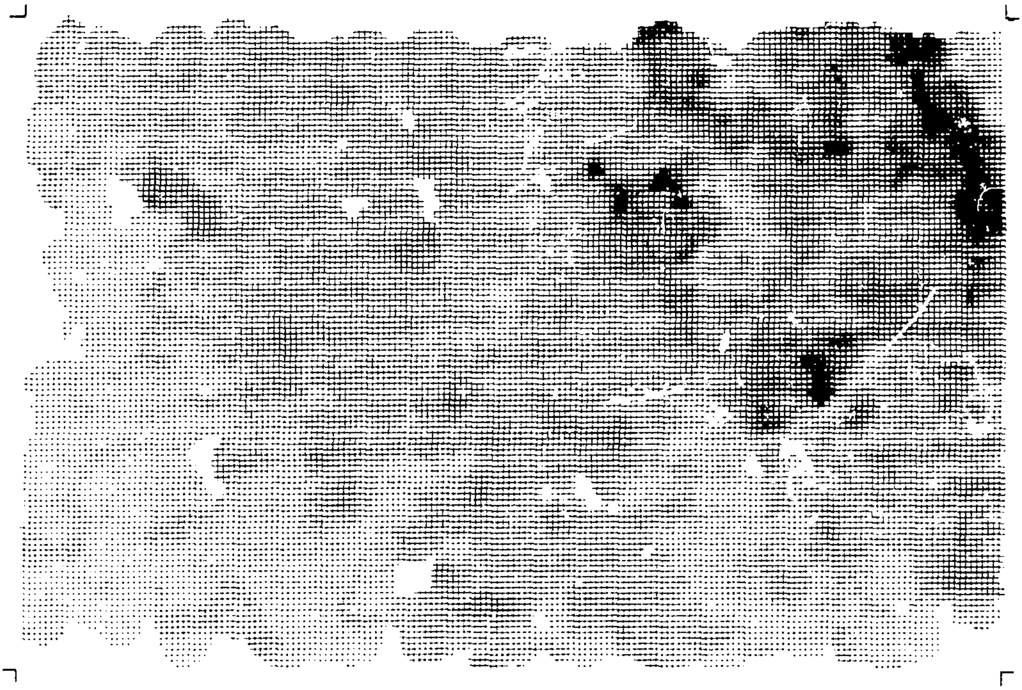

Dy Dysprosium

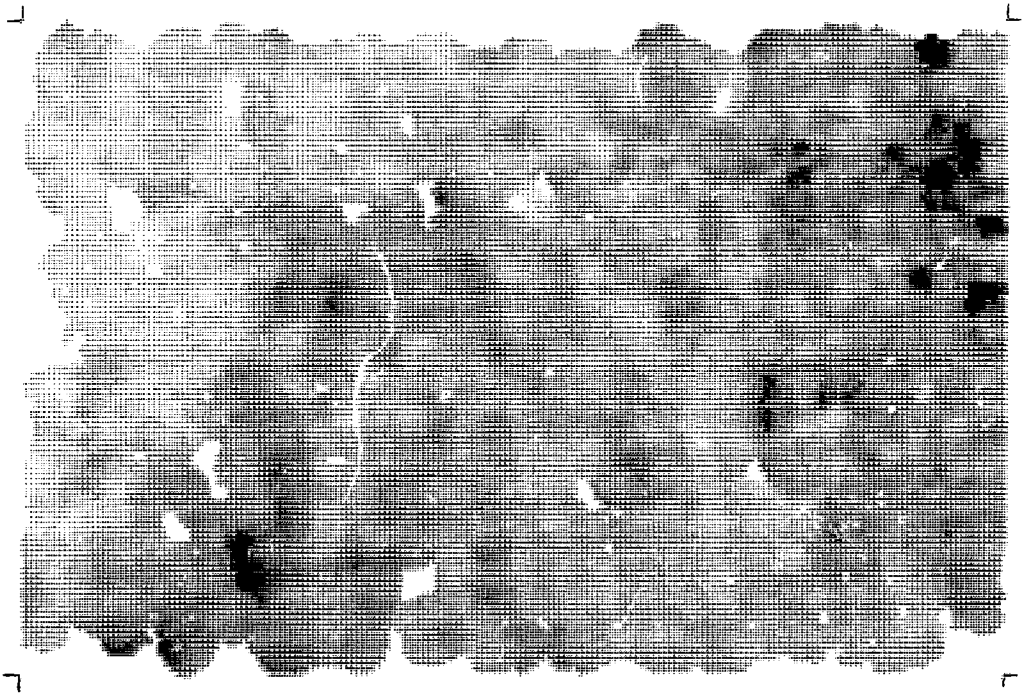

Fe Iron

Hf Hafnium

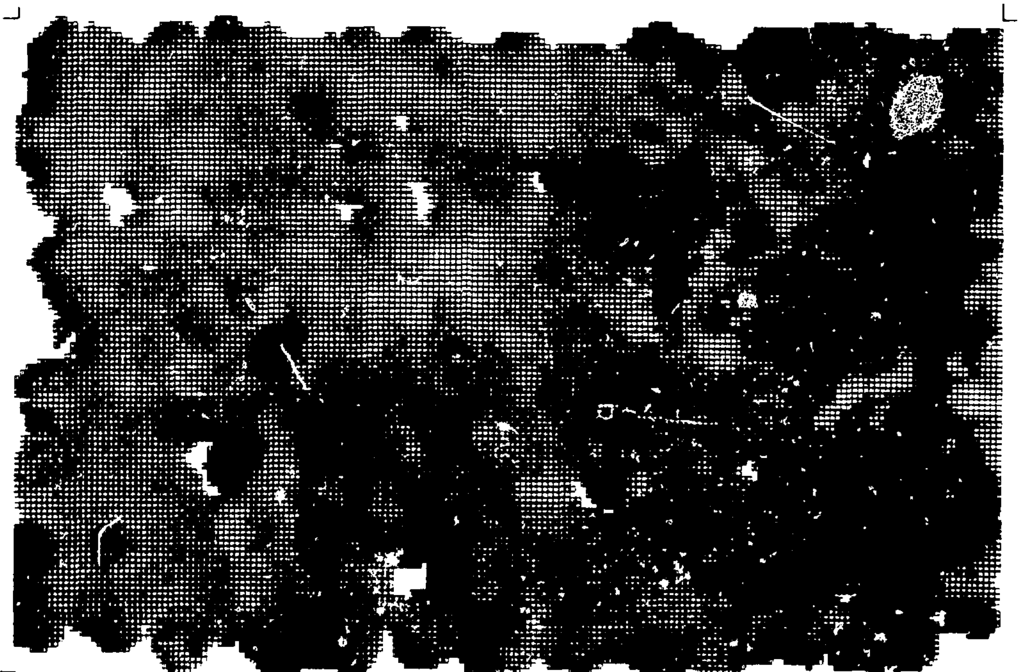

K Potassium

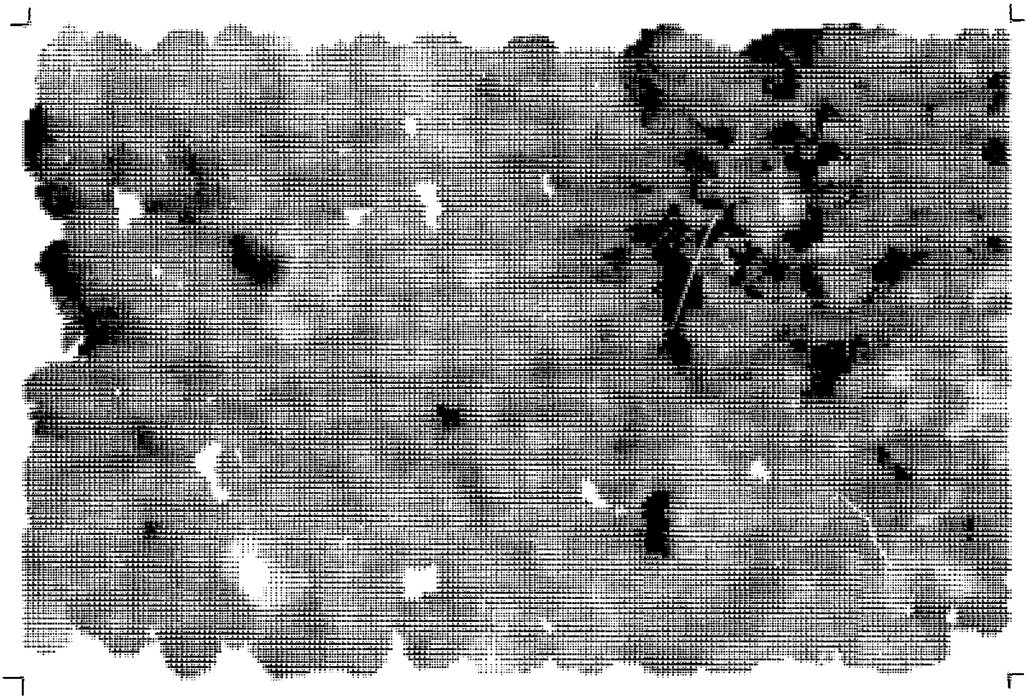

Li Lithium

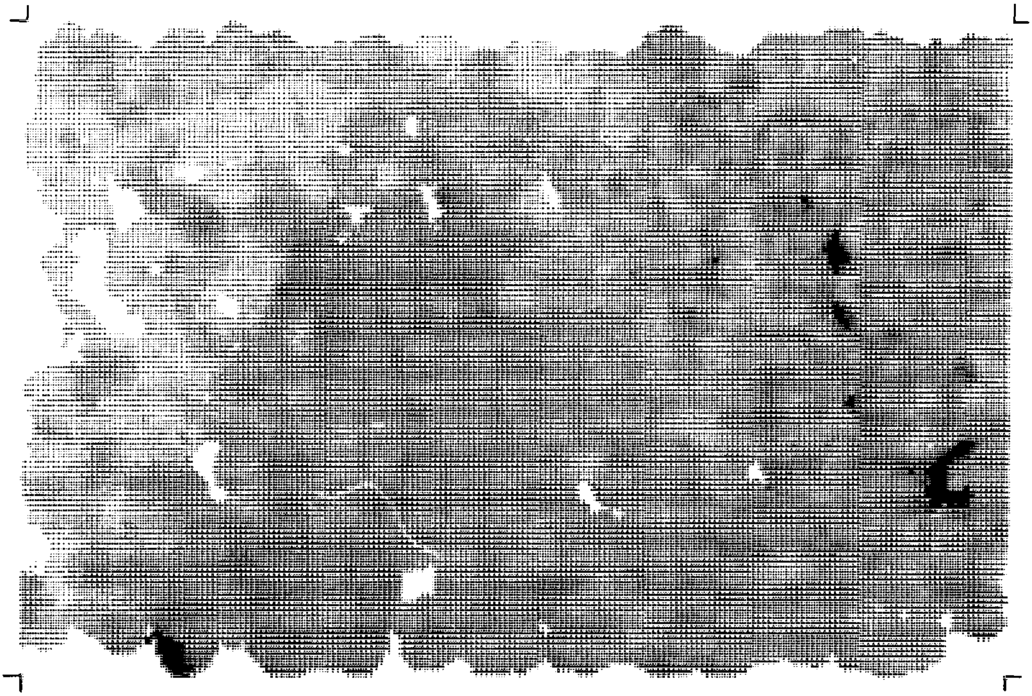

Mn Manganese

Pb Lead

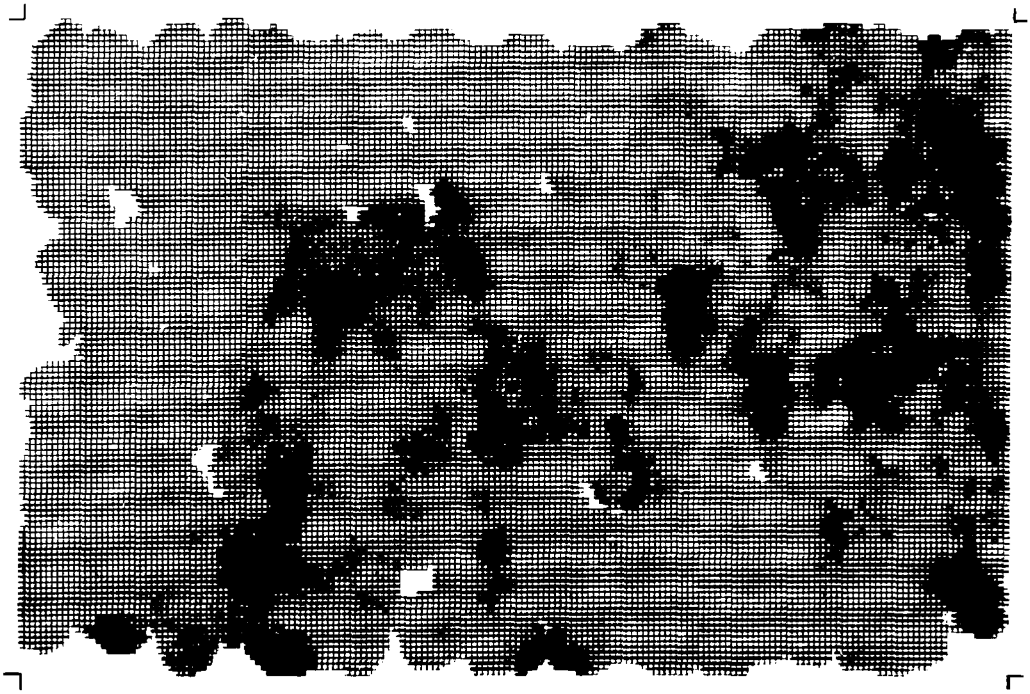

Sc Scandium

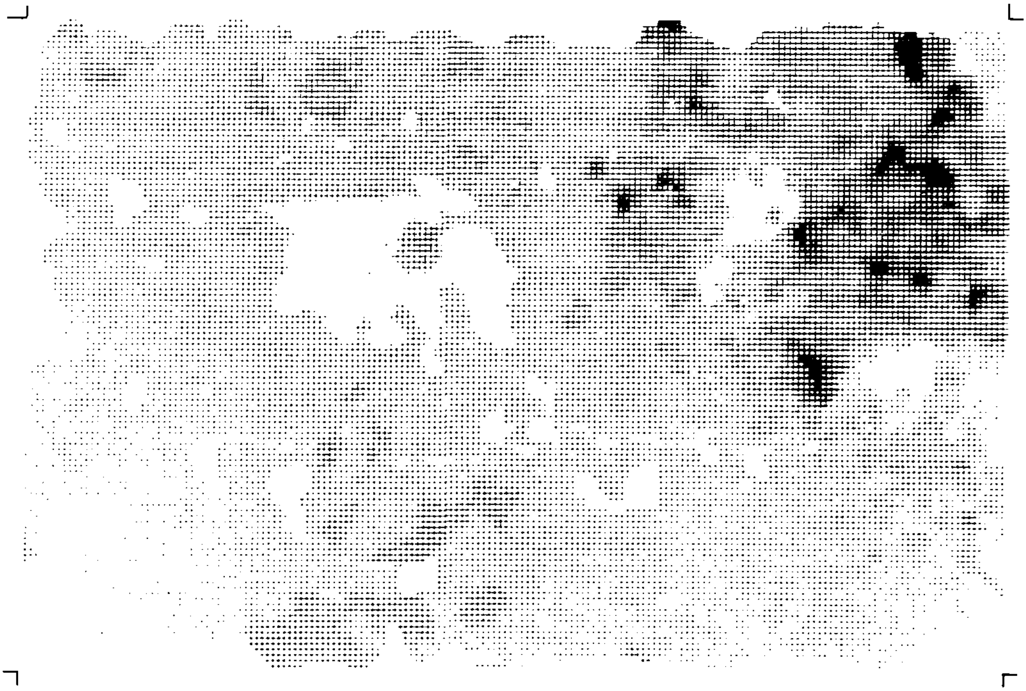

Th Thorium

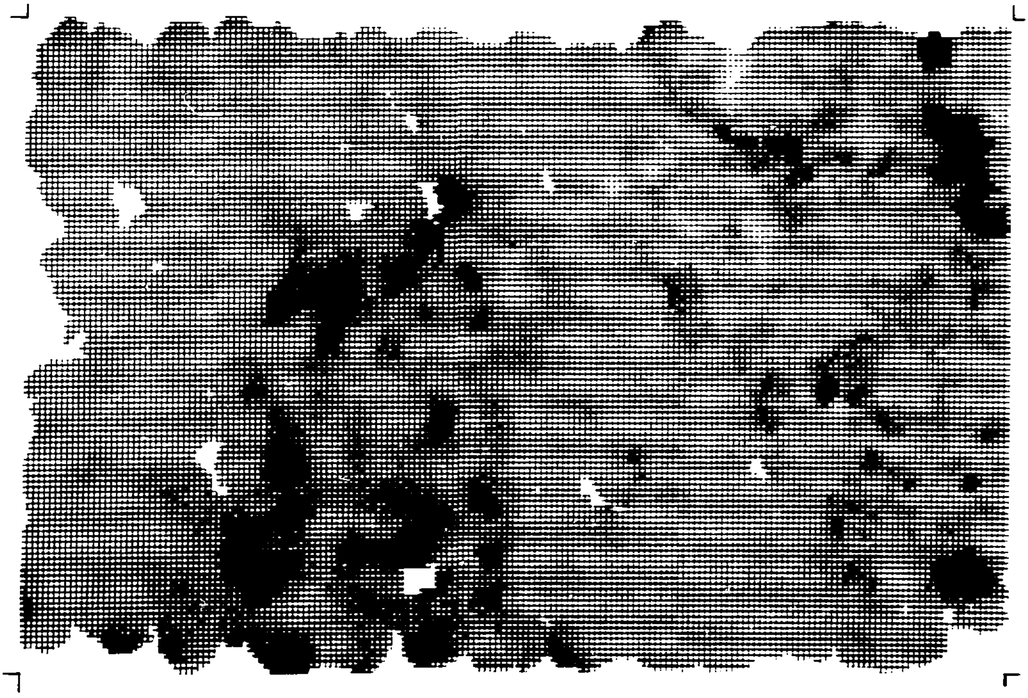

Ti Titanium

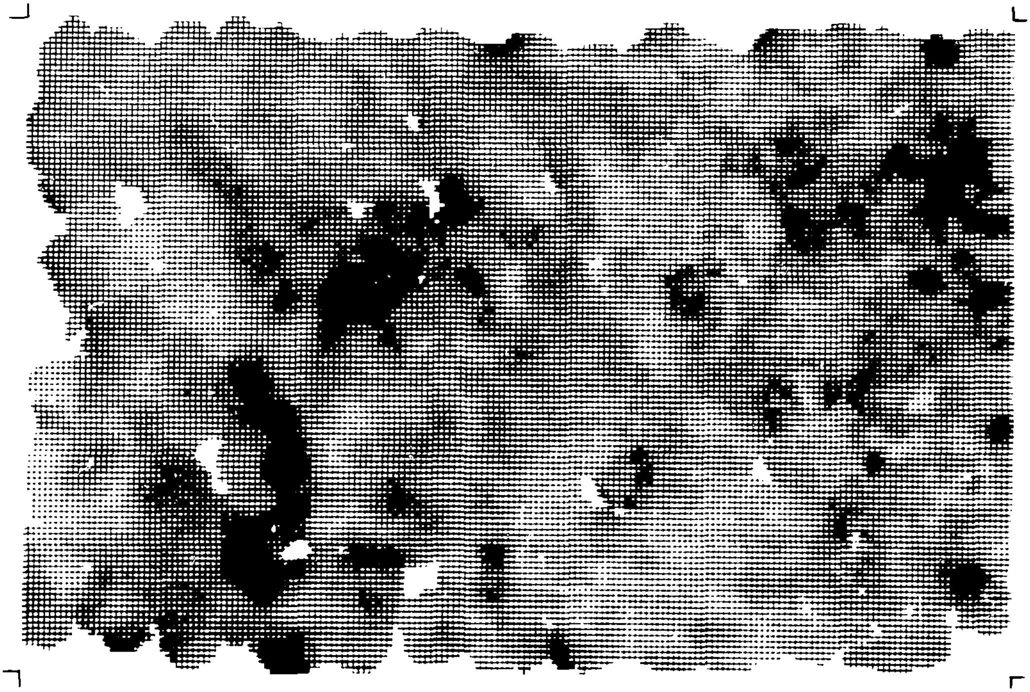

V Vanadium

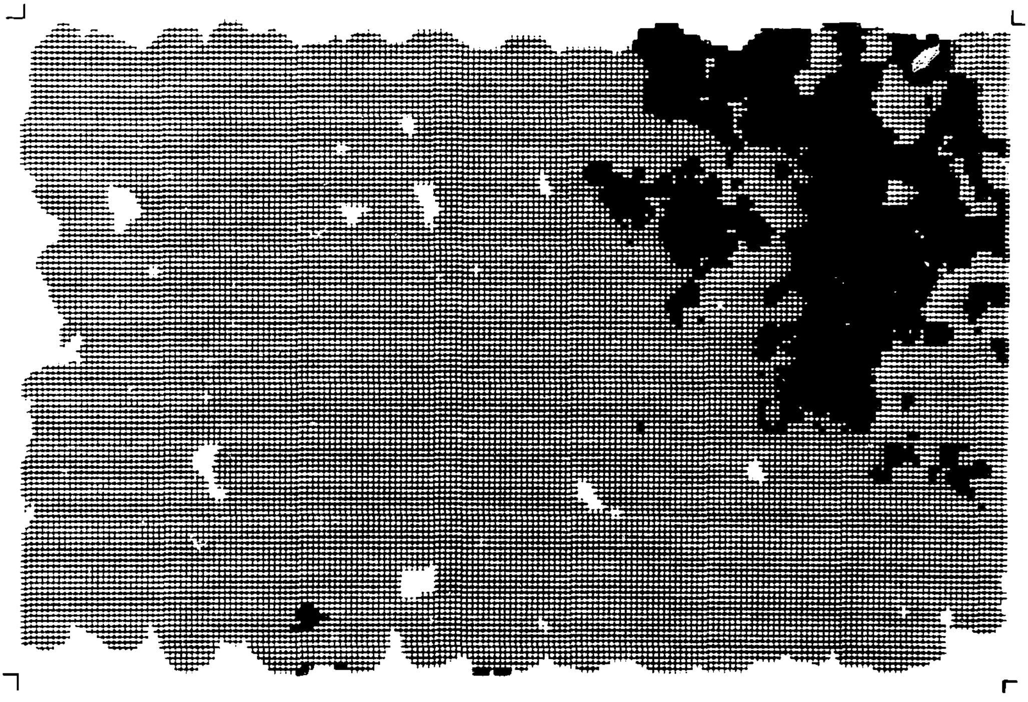

Us Uranium (in sediments)

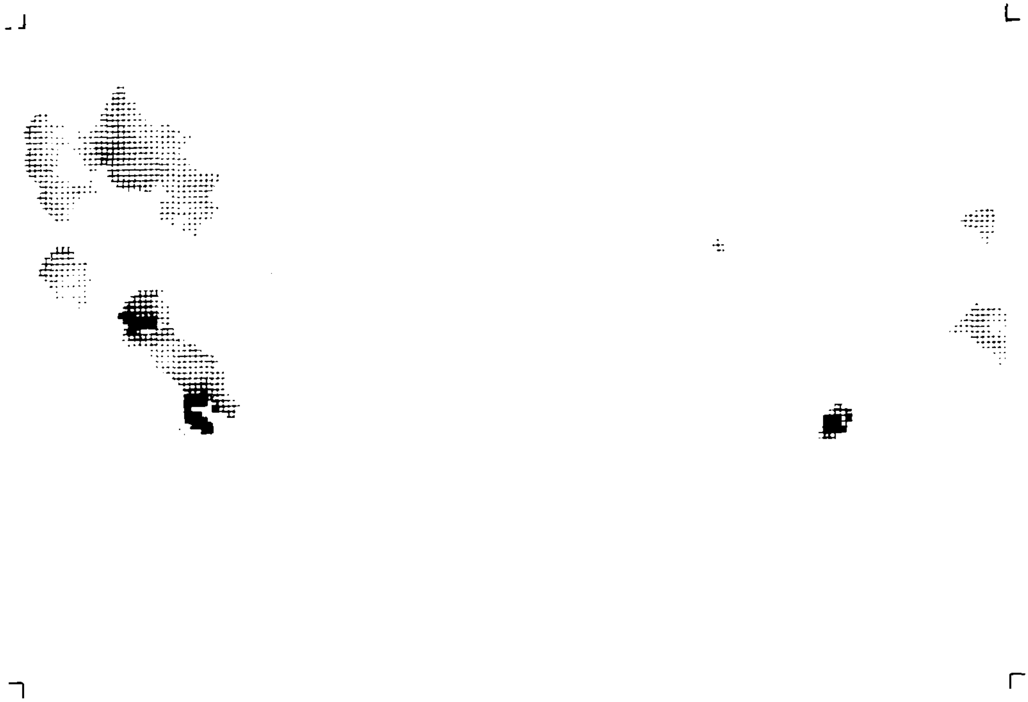

Uw Uranium (in waters)

Zn Zinc

Zr Zirconium

U/Th U/Th ratio

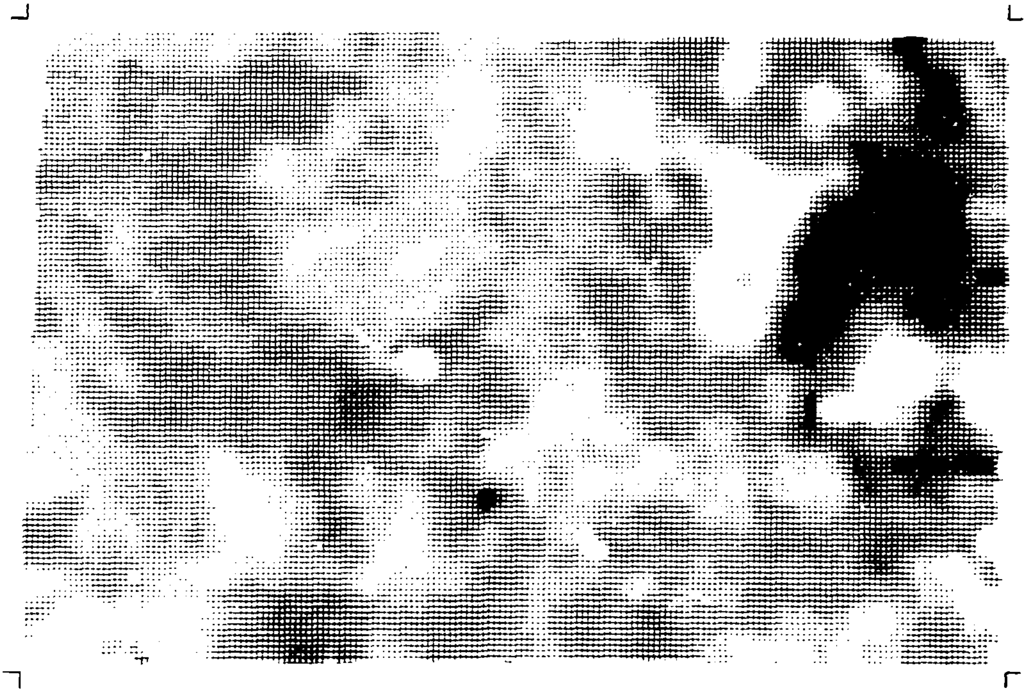

eTh Equivalent Thorium

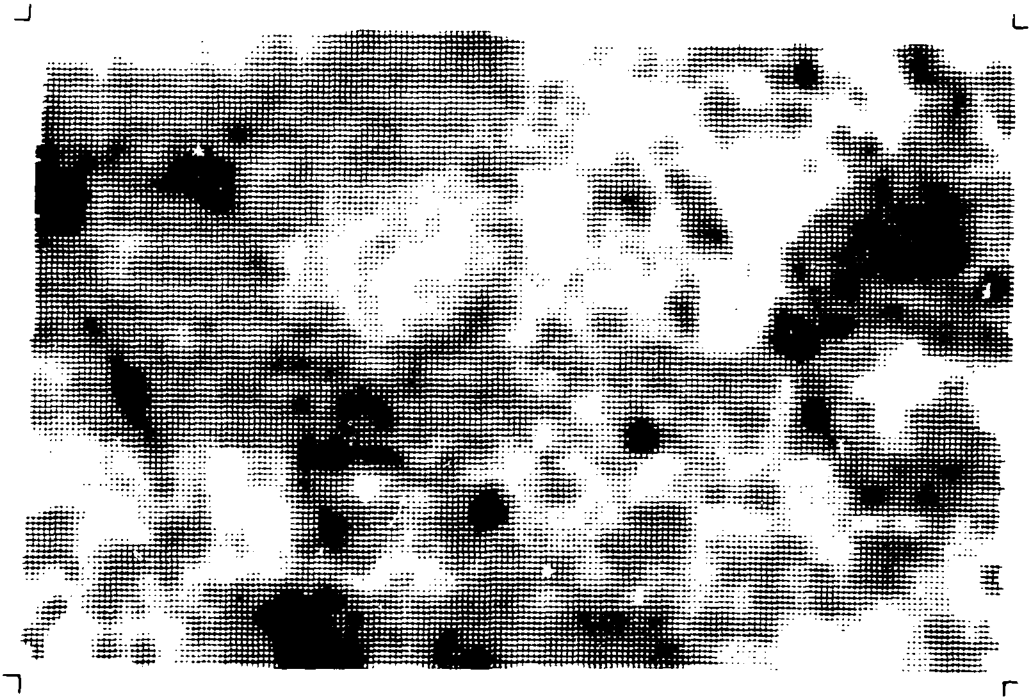

eU Equivalent Uranium

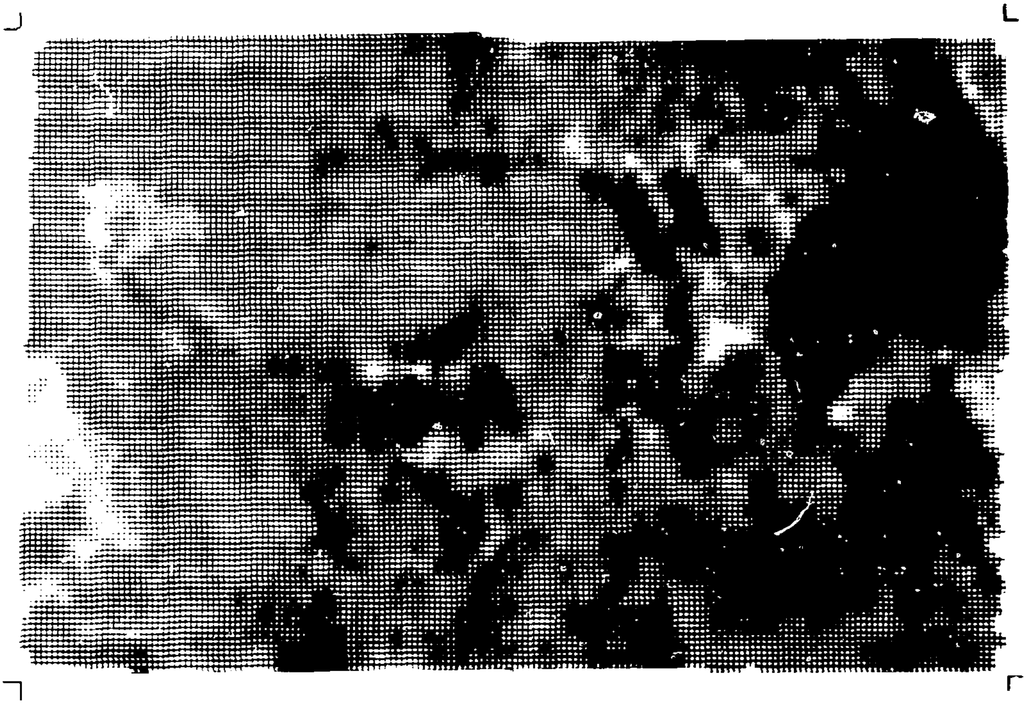

K40 Percent Potassium

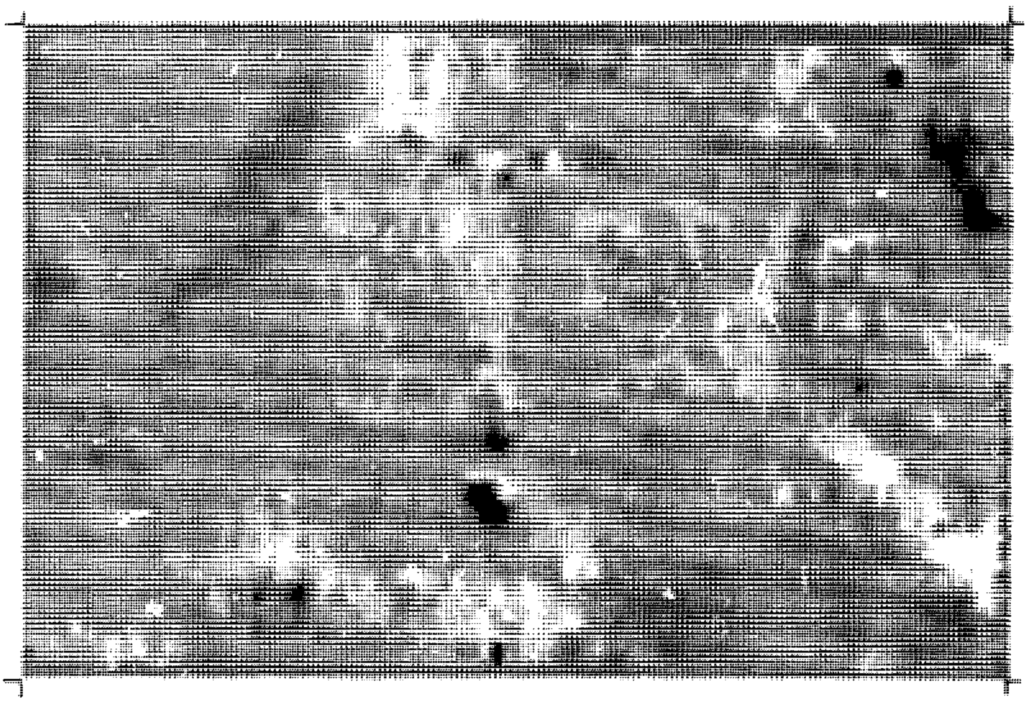

Mag Aeromagnetic

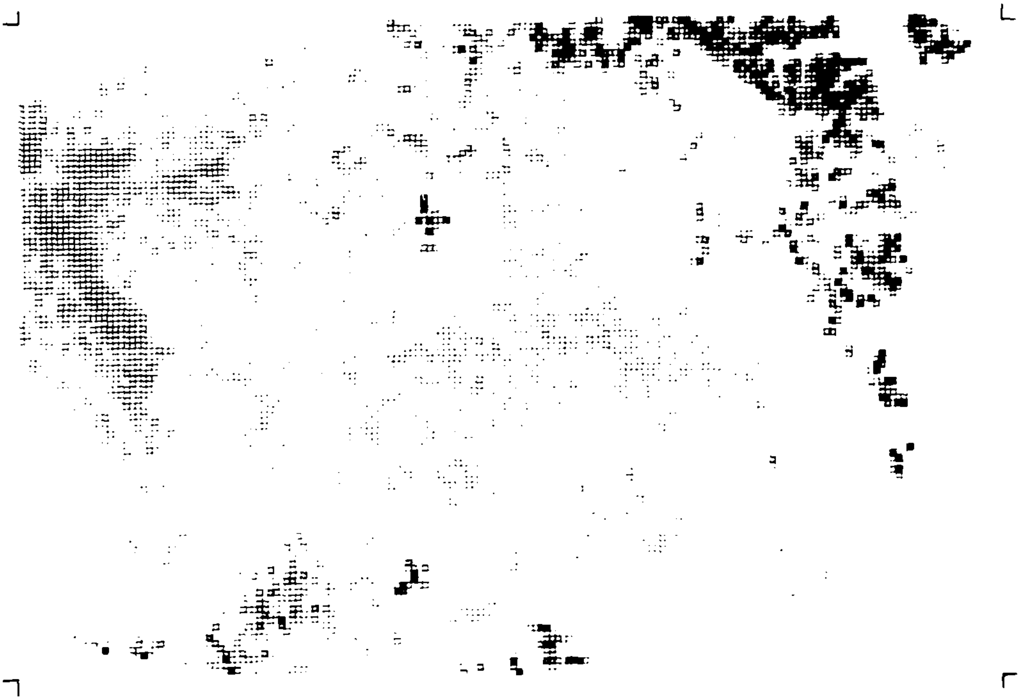

Ls4 Landsat Band 4

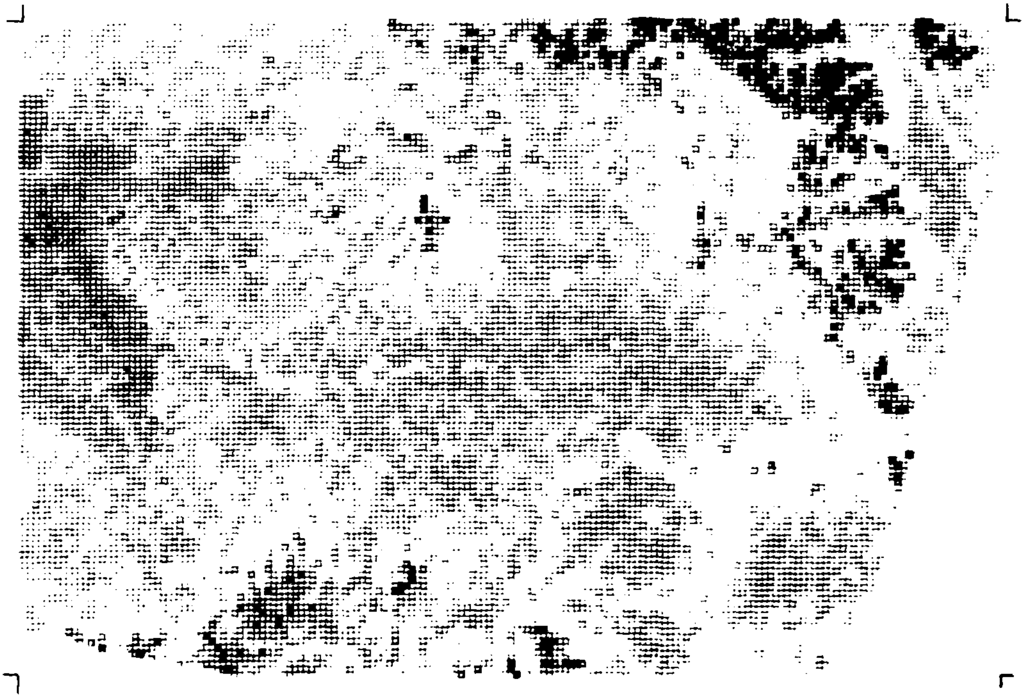

Ls5 Landsat Band 5

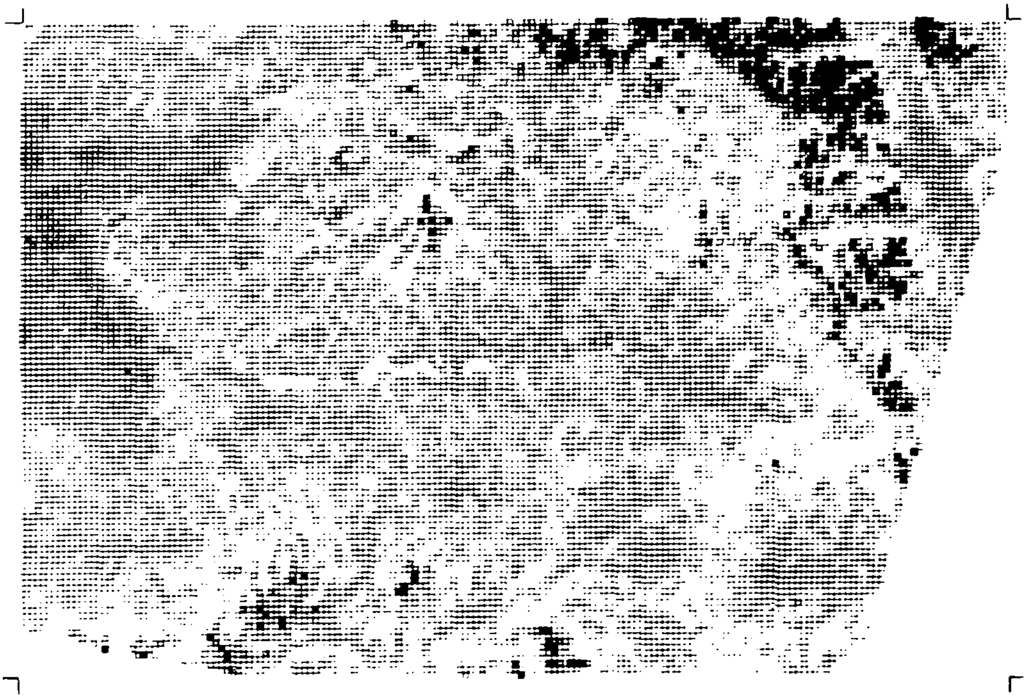

Ls6 Landsat Band 6

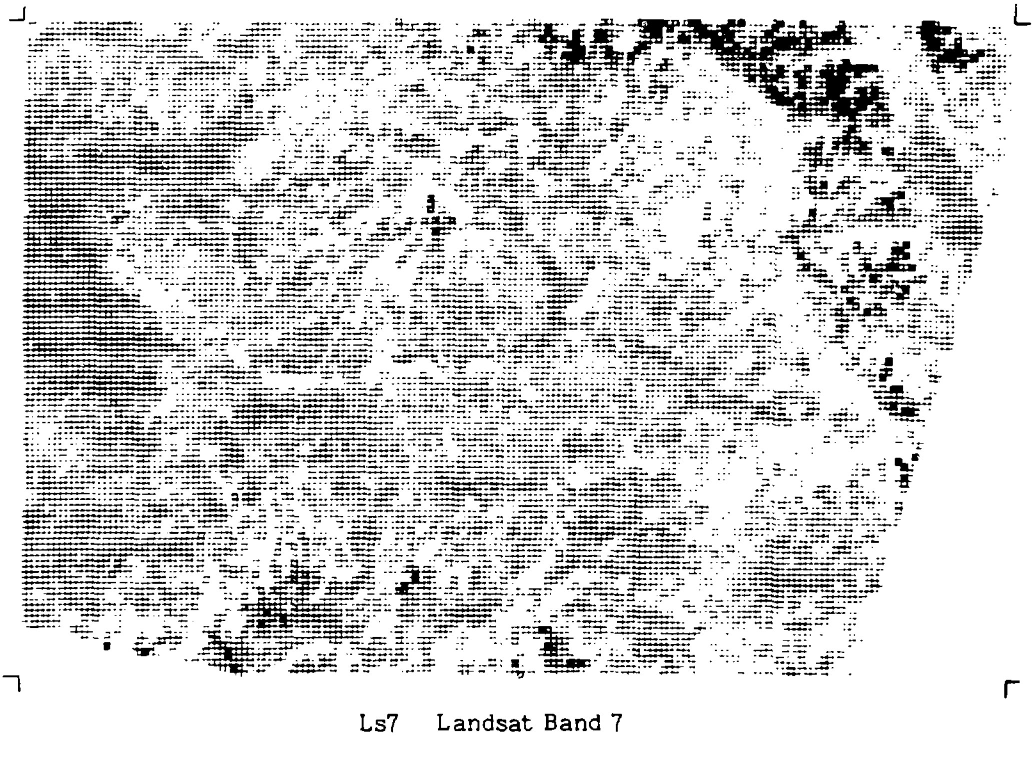

Ls7 Landsat Band 7

ALUMINUM IN SEDIMENTS, MONTROSE

STATISTICS FOR CRYSTALL.

NUMBER OF POINTS USED	2319	
NUMBER BELOW DETECTION LEVEL	1	
RANGE	4607.0	.11120E+06
MEDIAN	65545.	
LOWER QUARTILE	59840.	
UPPER QUARTILE	70370.	
90TH	74755.	
95TH	77350.	
AVERAGE	63776.	
S.D.	11307.	
MEAN + S.D.	75083.	
MEAN + 2*S.D.	86391.	
MEAN + 3*S.D.	97698.	
MEAN + 4*S.D.	.10901E+06	
MEAN + 5*S.D.	.12031E+06	

STATISTICS FOR PLATEAU

NUMBER OF POINTS USED	408	
NUMBER BELOW DETECTION LEVEL	1	
RANGE	13040.	89070.
MEDIAN	57090.	
LOWER QUARTILE	50350.	
UPPER QUARTILE	64205.	
90TH	70295.	
95TH	73025.	
AVERAGE	57022.	
S.D.	10283.	
MEAN + S.D.	67305.	
MEAN + 2*S.D.	77588.	
MEAN + 3*S.D.	87871.	
MEAN + 4*S.D.	98154.	
MEAN + 5*S.D.	.10844E+06	

STATISTICS FOR VOLCANIC

NUMBER OF POINTS USED	1213	
NUMBER BELOW DETECTION LEVEL	1	
RANGE	6600.0	94610.
MEDIAN	69275.	
LOWER QUARTILE	63800.	
UPPER QUARTILE	74065.	
90TH	78090.	
95TH	80535.	
AVERAGE	67805.	
S.D.	9885.2	
MEAN + S.D.	77691.	
MEAN + 2*S.D.	87576.	
MEAN + 3*S.D.	97461.	
MEAN + 4*S.D.	.10735E+06	
MEAN + 5*S.D.	.11723E+06	

STATISTICS FOR ALL POINTS

NUMBER OF POINTS USED	3940	
NUMBER BELOW DETECTION LEVEL	3	
RANGE	4607.0	.11120E+06
MEDIAN	66050.	
LOWER QUARTILE	59620.	
UPPER QUARTILE	71245.	
90TH	75860.	
95TH	78600.	
AVERAGE	64317.	
S.D.	11210.	
MEAN + S.D.	75527.	
MEAN + 2*S.D.	86737.	
MEAN + 3*S.D.	97947.	
MEAN + 4*S.D.	.10916E+06	
MEAN + 5*S.D.	.12037E+06	

1 ARSENIC IN SEDIMENTS, MONTROSE

STATISTICS FOR ALL POINTS

NUMBER OF POINTS USED	1177	
NUMBER BELOW DETECTION LEVEL	872	
RANGE	5.0000	330.00
MEDIAN	9.0000	
LOWER QUARTILE	6.0000	
UPPER QUARTILE	12.000	
90TH	17.000	
95TH	24.000	
AVERAGE	11.984	
S.D.	18.448	
MEAN + S.D.	30.431	
MEAN + 2*S.D.	48.879	
MEAN + 3*S.D.	67.327	
MEAN + 4*S.D.	85.774	
MEAN + 5*S.D.	104.22	

1 ARSENIC IN SEDIMENTS, MONTROSE

BARIUM IN SEDIMENTS, MONTROSE

STATISTICS FOR CRYSTALL.

NUMBER OF POINTS USED		2224
NUMBER BELOW DETECTION LEVEL		96
RANGE	152.00	19680.
MEDIAN	655.00	
LOWER QUARTILE	544.00	
UPPER QUARTILE	768.00	
90TH	896.00	
95TH	989.00	
AVERAGE	678.03	
S.D.	451.93	
MEAN + S.D.	1130.0	
MEAN + 2*S.D.	1581.9	
MEAN + 3*S.D.	2033.8	
MEAN + 4*S.D.	2485.8	
MEAN + 5*S.D.	2937.7	

STATISTICS FOR PLATEAU

NUMBER OF POINTS USED		402
NUMBER BELOW DETECTION LEVEL		7
RANGE	172.00	1224.0
MEDIAN	570.00	
LOWER QUARTILE	470.00	
UPPER QUARTILE	692.00	
90TH	801.50	
95TH	866.00	
AVERAGE	586.24	
S.D.	160.39	
MEAN + S.D.	746.63	
MEAN + 2*S.D.	907.02	
MEAN + 3*S.D.	1067.4	
MEAN + 4*S.D.	1227.8	
MEAN + 5*S.D.	1388.2	

STATISTICS FOR VOLCANIC

NUMBER OF POINTS USED		1192
NUMBER BELOW DETECTION LEVEL		22
RANGE	297.00	7210.0
MEDIAN	793.00	
LOWER QUARTILE	656.50	
UPPER QUARTILE	971.50	
90TH	1175.5	
95TH	1296.5	
AVERAGE	863.48	
S.D.	422.64	
MEAN + S.D.	1286.1	
MEAN + 2*S.D.	1708.8	
MEAN + 3*S.D.	2131.4	
MEAN + 4*S.D.	2554.1	
MEAN + 5*S.D.	2976.7	

STATISTICS FOR ALL POINTS

NUMBER OF POINTS USED		3818
NUMBER BELOW DETECTION LEVEL		125
RANGE	152.00	19680.
MEDIAN	681.00	
LOWER QUARTILE	561.00	
UPPER QUARTILE	820.00	
90TH	994.00	
95TH	1126.0	
AVERAGE	726.26	
S.D.	432.08	
MEAN + S.D.	1158.3	
MEAN + 2*S.D.	1590.4	
MEAN + 3*S.D.	2022.5	
MEAN + 4*S.D.	2454.6	
MEAN + 5*S.D.	2886.6	

CALCIUM IN SEDIMENTS, MONTROSE

STATISTICS FOR CRYSTALL.

NUMBER OF POINTS USED	2306	
NUMBER BELOW DETECTION LEVEL	14	
RANGE	603.00	.31320E+06
MEDIAN	17300.	
LOWER QUARTILE	12330.	
UPPER QUARTILE	23660.	
90TH	33010.	
95TH	40825.	
AVERAGE	21001.	
S.D.	19079.	
MEAN + S.D.	40080.	
MEAN + 2*S.D.	59158.	
MEAN + 3*S.D.	78237.	
MEAN + 4*S.D.	97316.	
MEAN + 5*S.D.	.11639E+06	

STATISTICS FOR PLATEAU

NUMBER OF POINTS USED	407	
NUMBER BELOW DETECTION LEVEL	1	
RANGE	1502.0	.30810E+06
MEDIAN	24275.	
LOWER QUARTILE	13360.	
UPPER QUARTILE	43670.	
90TH	85495.	
95TH	.10850E+06	
AVERAGE	36280.	
S.D.	35965.	
MEAN + S.D.	72246.	
MEAN + 2*S.D.	.10821E+06	
MEAN + 3*S.D.	.14418E+06	
MEAN + 4*S.D.	.18014E+06	
MEAN + 5*S.D.	.21611E+06	

STATISTICS FOR VOLCANIC

NUMBER OF POINTS USED	1192	
NUMBER BELOW DETECTION LEVEL	22	
RANGE	1955.0	.15020E+06
MEDIAN	18040.	
LOWER QUARTILE	12340.	
UPPER QUARTILE	25610.	
90TH	34970.	
95TH	40090.	
AVERAGE	20630.	
S.D.	13107.	
MEAN + S.D.	33736.	
MEAN + 2*S.D.	46843.	
MEAN + 3*S.D.	59950.	
MEAN + 4*S.D.	73057.	
MEAN + 5*S.D.	86164.	

STATISTICS FOR ALL POINTS

NUMBER OF POINTS USED	3905	
NUMBER BELOW DETECTION LEVEL	37	
RANGE	603.00	.31320E+06
MEDIAN	17895.	
LOWER QUARTILE	12365.	
UPPER QUARTILE	25215.	
90TH	35805.	
95TH	48725.	
AVERAGE	22480.	
S.D.	20592.	
MEAN + S.D.	43072.	
MEAN + 2*S.D.	63664.	
MEAN + 3*S.D.	84256.	
MEAN + 4*S.D.	.10485E+06	
MEAN + 5*S.D.	.12544E+06	

CERIUM IN SEDIMENTS, MONTROSE

STATISTICS FOR CRYSTALL.

NUMBER OF POINTS USED	2319	
NUMBER BELOW DETECTION LEVEL	2	
RANGE	12.000	4690.0
MEDIAN	123.00	
LOWER QUARTILE	81.000	
UPPER QUARTILE	178.00	
90TH	264.00	
95TH	330.50	
AVERAGE	151.89	
S.D.	151.29	
MEAN + S.D.	303.18	
MEAN + 2*S.D.	454.47	
MEAN + 3*S.D.	605.76	
MEAN + 4*S.D.	757.04	
MEAN + 5*S.D.	908.33	

STATISTICS FOR PLATEAU

NUMBER OF POINTS USED	409	
NUMBER BELOW DETECTION LEVEL	0	
RANGE	8.0000	1394.0
MEDIAN	63.500	
LOWER QUARTILE	53.000	
UPPER QUARTILE	76.000	
90TH	92.000	
95TH	102.00	
AVERAGE	71.222	
S.D.	70.357	
MEAN + S.D.	141.58	
MEAN + 2*S.D.	211.94	
MEAN + 3*S.D.	282.29	
MEAN + 4*S.D.	352.65	
MEAN + 5*S.D.	423.01	

STATISTICS FOR VOLCANIC

NUMBER OF POINTS USED	1213	
NUMBER BELOW DETECTION LEVEL	0	
RANGE	33.000	1004.0
MEDIAN	92.500	
LOWER QUARTILE	75.000	
UPPER QUARTILE	119.00	
90TH	150.50	
95TH	171.50	
AVERAGE	103.44	
S.D.	50.909	
MEAN + S.D.	154.35	
MEAN + 2*S.D.	205.25	
MEAN + 3*S.D.	256.16	
MEAN + 4*S.D.	307.07	
MEAN + 5*S.D.	357.98	

STATISTICS FOR ALL POINTS

NUMBER OF POINTS USED	3941	
NUMBER BELOW DETECTION LEVEL	2	
RANGE	8.0000	4690.0
MEDIAN	100.00	
LOWER QUARTILE	73.000	
UPPER QUARTILE	149.00	
90TH	220.00	
95TH	289.50	
AVERAGE	128.61	
S.D.	125.03	
MEAN + S.D.	253.63	
MEAN + 2*S.D.	378.66	
MEAN + 3*S.D.	503.68	
MEAN + 4*S.D.	628.71	
MEAN + 5*S.D.	753.74	

CHROMIUM IN SEDIMENTS, MONTROSE

STATISTICS FOR CRYSTALL.

NUMBER OF POINTS USED		2210	
NUMBER BELOW DETECTION LEVEL		111	
RANGE	10.000		616.00
MEDIAN	48.000		
LOWER QUARTILE	36.000		
UPPER QUARTILE	66.000		
90TH	95.000		
95TH	124.00		
AVERAGE	57.248		
S.D.	36.613		
MEAN + S.D.	93.862		
MEAN + 2*S.D.	130.47		
MEAN + 3*S.D.	167.09		
MEAN + 4*S.D.	203.70		
MEAN + 5*S.D.	240.31		

STATISTICS FOR PLATEAU

NUMBER OF POINTS USED		403	
NUMBER BELOW DETECTION LEVEL		6	
RANGE	13.000		217.00
MEDIAN	41.000		
LOWER QUARTILE	34.000		
UPPER QUARTILE	53.000		
90TH	65.000		
95TH	71.500		
AVERAGE	44.191		
S.D.	17.263		
MEAN + S.D.	61.454		
MEAN + 2*S.D.	78.718		
MEAN + 3*S.D.	95.981		
MEAN + 4*S.D.	113.24		
MEAN + 5*S.D.	130.51		

STATISTICS FOR VOLCANIC

NUMBER OF POINTS USED		1060	
NUMBER BELOW DETECTION LEVEL		153	
RANGE	10.000		224.00
MEDIAN	32.000		
LOWER QUARTILE	25.000		
UPPER QUARTILE	41.500		
90TH	56.000		
95TH	67.000		
AVERAGE	35.915		
S.D.	18.106		
MEAN + S.D.	54.023		
MEAN + 2*S.D.	72.131		
MEAN + 3*S.D.	90.238		
MEAN + 4*S.D.	108.35		
MEAN + 5*S.D.	126.45		

STATISTICS FOR ALL POINTS

NUMBER OF POINTS USED		3673	
NUMBER BELOW DETECTION LEVEL		270	
RANGE	10.000		616.00
MEDIAN	42.000		
LOWER QUARTILE	31.000		
UPPER QUARTILE	58.500		
90TH	80.000		
95TH	108.00		
AVERAGE	49.659		
S.D.	32.033		
MEAN + S.D.	81.692		
MEAN + 2*S.D.	113.72		
MEAN + 3*S.D.	145.76		
MEAN + 4*S.D.	177.79		
MEAN + 5*S.D.	209.82		

COBALT IN SEDIMENTS, MONTROSE

STATISTICS FOR CRYSTALL.

NUMBER OF POINTS USED	2299	
NUMBER BELOW DETECTION LEVEL	21	
RANGE	1.7000	53.300
MEDIAN	11.100	
LOWER QUARTILE	8.5000	
UPPER QUARTILE	14.600	
90TH	18.650	
95TH	21.600	
AVERAGE	12.033	
S.D.	5.4930	
MEAN + S.D.	17.526	
MEAN + 2*S.D.	23.019	
MEAN + 3*S.D.	28.512	
MEAN + 4*S.D.	34.005	
MEAN + 5*S.D.	39.498	

STATISTICS FOR PLATEAU

NUMBER OF POINTS USED	609	
NUMBER BELOW DETECTION LEVEL	0	
RANGE	3.7000	64.600
MEDIAN	9.0000	
LOWER QUARTILE	7.4500	
UPPER QUARTILE	12.100	
90TH	15.500	
95TH	19.800	
AVERAGE	10.687	
S.D.	6.1194	
MEAN + S.D.	16.806	
MEAN + 2*S.D.	22.926	
MEAN + 3*S.D.	29.045	
MEAN + 4*S.D.	35.164	
MEAN + 5*S.D.	41.284	

STATISTICS FOR VOLCANIC

NUMBER OF POINTS USED	1208	
NUMBER BELOW DETECTION LEVEL	5	
RANGE	1.6000	108.30
MEDIAN	11.000	
LOWER QUARTILE	8.7000	
UPPER QUARTILE	14.200	
90TH	19.050	
95TH	23.050	
AVERAGE	12.538	
S.D.	7.2141	
MEAN + S.D.	19.752	
MEAN + 2*S.D.	26.966	
MEAN + 3*S.D.	34.180	
MEAN + 4*S.D.	41.394	
MEAN + 5*S.D.	48.608	

STATISTICS FOR ALL POINTS

NUMBER OF POINTS USED	3916	
NUMBER BELOW DETECTION LEVEL	26	
RANGE	1.6000	108.30
MEDIAN	10.900	
LOWER QUARTILE	8.4000	
UPPER QUARTILE	14.200	
90TH	18.550	
95TH	21.950	
AVERAGE	12.048	
S.D.	6.1584	
MEAN + S.D.	18.207	
MEAN + 2*S.D.	24.365	
MEAN + 3*S.D.	30.524	
MEAN + 4*S.D.	36.682	
MEAN + 5*S.D.	42.840	

COPPER IN SEDIMENTS, MONTROSE

STATISTICS FOR CRYSTALL.

NUMBER OF POINTS USED	2236	
NUMBER BELOW DETECTION LEVEL	47	
RANGE	10.000	10358.
MEDIAN	32.000	
LOWER QUARTILE	24.000	
UPPER QUARTILE	45.000	
90TH	65.000	
95TH	111.00	
AVERAGE	61.965	
S.D.	281.22	
MEAN + S.D.	343.18	
MEAN + 2*S.D.	624.40	
MEAN + 3*S.D.	905.62	
MEAN + 4*S.D.	1186.8	
MEAN + 5*S.D.	1468.1	

STATISTICS FOR PLATEAU

NUMBER OF POINTS USED	405	
NUMBER BELOW DETECTION LEVEL	4	
RANGE	11.000	2456.0
MEDIAN	27.000	
LOWER QUARTILE	23.000	
UPPER QUARTILE	34.000	
90TH	47.000	
95TH	72.500	
AVERAGE	40.807	
S.D.	130.89	
MEAN + S.D.	171.70	
MEAN + 2*S.D.	302.60	
MEAN + 3*S.D.	433.49	
MEAN + 4*S.D.	564.39	
MEAN + 5*S.D.	695.28	

STATISTICS FOR VOLCANIC

NUMBER OF POINTS USED	1200	
NUMBER BELOW DETECTION LEVEL	13	
RANGE	10.000	4339.0
MEDIAN	29.000	
LOWER QUARTILE	22.000	
UPPER QUARTILE	36.000	
90TH	53.000	
95TH	94.000	
AVERAGE	63.788	
S.D.	236.43	
MEAN + S.D.	300.22	
MEAN + 2*S.D.	536.65	
MEAN + 3*S.D.	773.07	
MEAN + 4*S.D.	1009.5	
MEAN + 5*S.D.	1245.9	

STATISTICS FOR ALL POINTS

NUMBER OF POINTS USED	3841	
NUMBER BELOW DETECTION LEVEL	64	
RANGE	10.000	10358.
MEDIAN	30.000	
LOWER QUARTILE	23.000	
UPPER QUARTILE	41.000	
90TH	61.000	
95TH	99.000	
AVERAGE	60.304	
S.D.	255.60	
MEAN + S.D.	315.90	
MEAN + 2*S.D.	571.50	
MEAN + 3*S.D.	827.10	
MEAN + 4*S.D.	1082.7	
MEAN + 5*S.D.	1338.3	

DYSPROSIUM IN SEDIMENTS, MONTROSE

STATISTICS FOR CRYSTALL.

NUMBER OF POINTS USED	2308	
NUMBER BELOW DETECTION LEVEL	12	
RANGE	.70000	117.50
MEDIAN	6.9000	
LOWER QUARTILE	5.1000	
UPPER QUARTILE	10.400	
90TH	14.650	
95TH	18.900	
AVERAGE	8.5912	
S.D.	6.1537	
MEAN + S.D.	14.745	
MEAN + 2*S.D.	20.899	
MEAN + 3*S.D.	27.052	
MEAN + 4*S.D.	33.206	
MEAN + 5*S.D.	39.360	

STATISTICS FOR VOLCANIC

NUMBER OF POINTS USED	1204	
NUMBER BELOW DETECTION LEVEL	10	
RANGE	1.9000	32.700
MEDIAN	4.4000	
LOWER QUARTILE	3.8000	
UPPER QUARTILE	5.3000	
90TH	6.5000	
95TH	7.6000	
AVERAGE	4.7641	
S.D.	1.9192	
MEAN + S.D.	6.6833	
MEAN + 2*S.D.	8.6024	
MEAN + 3*S.D.	10.522	
MEAN + 4*S.D.	12.441	
MEAN + 5*S.D.	14.360	

STATISTICS FOR PLATEAU

NUMBER OF POINTS USED	408	
NUMBER BELOW DETECTION LEVEL	1	
RANGE	1.2000	75.500
MEDIAN	3.8000	
LOWER QUARTILE	3.4000	
UPPER QUARTILE	4.2000	
90TH	5.0000	
95TH	6.2500	
AVERAGE	4.1909	
S.D.	3.8406	
MEAN + S.D.	8.0315	
MEAN + 2*S.D.	11.872	
MEAN + 3*S.D.	15.713	
MEAN + 4*S.D.	19.553	
MEAN + 5*S.D.	23.394	

STATISTICS FOR ALL POINTS

NUMBER OF POINTS USED	3920	
NUMBER BELOW DETECTION LEVEL	23	
RANGE	.70000	117.50
MEDIAN	5.3000	
LOWER QUARTILE	4.1000	
UPPER QUARTILE	8.0000	
90TH	12.100	
95TH	15.900	
AVERAGE	6.9577	
S.D.	5.3666	
MEAN + S.D.	12.324	
MEAN + 2*S.D.	17.691	
MEAN + 3*S.D.	23.058	
MEAN + 4*S.D.	28.424	
MEAN + 5*S.D.	33.791	

HAFNIUM IN SEDIMENTS, MONTROSE

STATISTICS FOR CRYSTALL.

NUMBER OF POINTS USED	2315	
NUMBER BELOW DETECTION LEVEL	6	
RANGE	1.5000	330.00
MEDIAN	13.400	
LOWER QUARTILE	9.1000	
UPPER QUARTILE	21.400	
90TH	38.650	
95TH	56.900	
AVERAGE	20.231	
S.D.	23.517	
MEAN + S.D.	43.748	
MEAN + 2*S.D.	67.265	
MEAN + 3*S.D.	90.782	
MEAN + 4*S.D.	114.30	
MEAN + 5*S.D.	137.82	

STATISTICS FOR PLATEAU

NUMBER OF POINTS USED	409	
NUMBER BELOW DETECTION LEVEL	1	
RANGE	2.6000	51.000
MEDIAN	7.7000	
LOWER QUARTILE	5.7000	
UPPER QUARTILE	10.100	
90TH	13.700	
95TH	17.200	
AVERAGE	8.7892	
S.D.	5.3508	
MEAN + S.D.	14.140	
MEAN + 2*S.D.	19.491	
MEAN + 3*S.D.	24.842	
MEAN + 4*S.D.	30.192	
MEAN + 5*S.D.	35.543	

STATISTICS FOR VOLCANIC

NUMBER OF POINTS USED	1213	
NUMBER BELOW DETECTION LEVEL	0	
RANGE	3.0000	64.200
MEDIAN	9.8000	
LOWER QUARTILE	7.4000	
UPPER QUARTILE	13.200	
90TH	17.300	
95TH	20.400	
AVERAGE	11.029	
S.D.	5.7429	
MEAN + S.D.	16.772	
MEAN + 2*S.D.	22.515	
MEAN + 3*S.D.	28.257	
MEAN + 4*S.D.	34.000	
MEAN + 5*S.D.	39.743	

STATISTICS FOR ALL POINTS

NUMBER OF POINTS USED	3936	
NUMBER BELOW DETECTION LEVEL	7	
RANGE	1.5000	330.00
MEDIAN	11.100	
LOWER QUARTILE	7.9000	
UPPER QUARTILE	17.100	
90TH	28.500	
95TH	43.650	
AVERAGE	16.209	
S.D.	19.022	
MEAN + S.D.	35.231	
MEAN + 2*S.D.	54.253	
MEAN + 3*S.D.	73.275	
MEAN + 4*S.D.	92.297	
MEAN + 5*S.D.	111.32	

IRON IN SEDIMENTS, MONTROSE

STATISTICS FOR CRYSTALL.

NUMBER OF POINTS USED	2321	
NUMBER BELOW DETECTION LEVEL	0	
RANGE	2360.0	.42780E+06
MEDIAN	35350.	
LOWER QUARTILE	25840.	
UPPER QUARTILE	48835.	
90TH	66675.	
95TH	87875.	
AVERAGE	41542.	
S.D.	27088.	
MEAN + S.D.	68630.	
MEAN + 2*S.D.	95718.	
MEAN + 3*S.D.	.12281E+06	
MEAN + 4*S.D.	.14989E+06	
MEAN + 5*S.D.	.17698E+06	

STATISTICS FOR PLATEAU

NUMBER OF POINTS USED	409	
NUMBER BELOW DETECTION LEVEL	0	
RANGE	4979.0	.10220E+06
MEDIAN	17145.	
LOWER QUARTILE	14120.	
UPPER QUARTILE	23615.	
90TH	34600.	
95TH	46435.	
AVERAGE	20980.	
S.D.	12579.	
MEAN + S.D.	33560.	
MEAN + 2*S.D.	46139.	
MEAN + 3*S.D.	58718.	
MEAN + 4*S.D.	71298.	
MEAN + 5*S.D.	83877.	

STATISTICS FOR VOLCANIC

NUMBER OF POINTS USED	1213	
NUMBER BELOW DETECTION LEVEL	0	
RANGE	7709.0	.19280E+06
MEDIAN	28935.	
LOWER QUARTILE	20520.	
UPPER QUARTILE	39800.	
90TH	54215.	
95TH	67570.	
AVERAGE	33086.	
S.D.	18989.	
MEAN + S.D.	52076.	
MEAN + 2*S.D.	71065.	
MEAN + 3*S.D.	90054.	
MEAN + 4*S.D.	.10904E+06	
MEAN + 5*S.D.	.12803E+06	

STATISTICS FOR ALL POINTS

NUMBER OF POINTS USED	3943	
NUMBER BELOW DETECTION LEVEL	0	
RANGE	2360.0	.42780E+06
MEDIAN	31290.	
LOWER QUARTILE	21610.	
UPPER QUARTILE	44770.	
90TH	61345.	
95TH	77500.	
AVERAGE	36808.	
S.D.	24547.	
MEAN + S.D.	61354.	
MEAN + 2*S.D.	85901.	
MEAN + 3*S.D.	.11045E+06	
MEAN + 4*S.D.	.13499E+06	
MEAN + 5*S.D.	.15954E+06	

LEAD IN SEDIMENTS, MONTROSE

STATISTICS FOR CRYSTALL.

NUMBER OF POINTS USED	2162	
NUMBER BELOW DETECTION LEVEL	121	
RANGE	5.0000	11481.
MEDIAN	24.000	
LOWER QUARTILE	16.000	
UPPER QUARTILE	40.000	
90TH	88.500	
95TH	181.50	
AVERAGE	89.386	
S.D.	475.95	
MEAN + S.D.	565.34	
MEAN + 2*S.D.	1041.3	
MEAN + 3*S.D.	1517.2	
MEAN + 4*S.D.	1993.2	
MEAN + 5*S.D.	2469.1	

STATISTICS FOR PLATEAU

NUMBER OF POINTS USED	392	
NUMBER BELOW DETECTION LEVEL	27	
RANGE	5.0000	3955.0
MEDIAN	15.000	
LOWER QUARTILE	11.000	
UPPER QUARTILE	22.000	
90TH	69.000	
95TH	145.50	
AVERAGE	44.976	
S.D.	210.39	
MEAN + S.D.	255.37	
MEAN + 2*S.D.	465.76	
MEAN + 3*S.D.	676.15	
MEAN + 4*S.D.	886.55	
MEAN + 5*S.D.	1096.9	

STATISTICS FOR VOLCANIC

NUMBER OF POINTS USED	1067	
NUMBER BELOW DETECTION LEVEL	146	
RANGE	5.0000	5651.0
MEDIAN	16.000	
LOWER QUARTILE	11.000	
UPPER QUARTILE	23.000	
90TH	57.000	
95TH	226.00	
AVERAGE	7[illegible].685	
S.D.	344.94	
MEAN + S.D.	419.63	
MEAN + 2*S.D.	764.57	
MEAN + 3*S.D.	1109.5	
MEAN + 4*S.D.	1454.5	
MEAN + 5*S.D.	1799.4	

STATISTICS FOR ALL POINTS

NUMBER OF POINTS USED	3611	
NUMBER BELOW DETECTION LEVEL	294	
RANGE	5.0000	11481.
MEDIAN	19.000	
LOWER QUARTILE	13.000	
UPPER QUARTILE	34.000	
90TH	83.000	
95TH	179.50	
AVERAGE	80.344	
S.D.	419.05	
MEAN + S.D.	499.39	
MEAN + 2*S.D.	918.44	
MEAN + 3*S.D.	1337.5	
MEAN + 4*S.D.	1756.5	
MEAN + 5*S.D.	2175.6	

LITHIUM IN SEDIMENTS, MONTROSE

STATISTICS FOR CRYSTALL.

NUMBER OF POINTS USED		2281
NUMBER BELOW DETECTION LEVEL		3
RANGE	1.0000	152.00
MEDIAN	42.000	
LOWER QUARTILE	32.000	
UPPER QUARTILE	50.000	
90TH	67.000	
95TH	80.000	
AVERAGE	43.399	
S.D.	19.052	
MEAN + S.D.	62.451	
MEAN + 2*S.D.	81.503	
MEAN + 3*S.D.	100.56	
MEAN + 4*S.D.	119.61	
MEAN + 5*S.D.	138.66	

STATISTICS FOR PLATEAU

NUMBER OF POINTS USED		409
NUMBER BELOW DETECTION LEVEL		0
RANGE	6.0000	108.00
MEDIAN	34.000	
LOWER QUARTILE	24.000	
UPPER QUARTILE	50.000	
90TH	65.500	
95TH	76.000	
AVERAGE	38.746	
S.D.	19.770	
MEAN + S.D.	58.516	
MEAN + 2*S.D.	78.287	
MEAN + 3*S.D.	98.057	
MEAN + 4*S.D.	117.83	
MEAN + 5*S.D.	137.60	

STATISTICS FOR VOLCANIC

NUMBER OF POINTS USED		1201
NUMBER BELOW DETECTION LEVEL		12
RANGE	2.0000	575.00
MEDIAN	27.000	
LOWER QUARTILE	20.000	
UPPER QUARTILE	37.000	
90TH	45.000	
95TH	49.000	
AVERAGE	29.789	
S.D.	21.577	
MEAN + S.D.	51.367	
MEAN + 2*S.D.	72.944	
MEAN + 3*S.D.	94.522	
MEAN + 4*S.D.	116.10	
MEAN + 5*S.D.	137.68	

STATISTICS FOR ALL POINTS

NUMBER OF POINTS USED		3891
NUMBER BELOW DETECTION LEVEL		15
RANGE	1.0000	575.00
MEDIAN	37.000	
LOWER QUARTILE	25.000	
UPPER QUARTILE	47.000	
90TH	62.000	
95TH	74.000	
AVERAGE	38.709	
S.D.	20.853	
MEAN + S.D.	59.562	
MEAN + 2*S.D.	80.415	
MEAN + 3*S.D.	101.27	
MEAN + 4*S.D.	122.12	
MEAN + 5*S.D.	142.97	

MANGANESE IN SEDIMENTS, MONTROSE

STATISTICS FOR CRYSTALL.

NUMBER OF POINTS USED	2320	
NUMBER BELOW DETECTION LEVEL	0	
RANGE	107.00	14610.
MEDIAN	946.00	
LOWER QUARTILE	724.50	
UPPER QUARTILE	1225.5	
90TH	1559.0	
95TH	1950.0	
AVERAGE	1055.9	
S.D.	709.29	
MEAN + S.D.	1765.1	
MEAN + 2*S.D.	2474.4	
MEAN + 3*S.D.	3183.7	
MEAN + 4*S.D.	3893.0	
MEAN + 5*S.D.	4602.3	

STATISTICS FOR PLATEAU

NUMBER OF POINTS USED	409	
NUMBER BELOW DETECTION LEVEL	0	
RANGE	44.000	5159.0
MEDIAN	454.50	
LOWER QUARTILE	304.00	
UPPER QUARTILE	706.50	
90TH	1110.0	
95TH	1352.5	
AVERAGE	589.45	
S.D.	464.13	
MEAN + S.D.	1053.6	
MEAN + 2*S.D.	1517.7	
MEAN + 3*S.D.	1982.0	
MEAN + 4*S.D.	2446.2	
MEAN + 5*S.D.	2910.3	

STATISTICS FOR VOLCANIC

NUMBER OF POINTS USED	1214	
NUMBER BELOW DETECTION LEVEL	0	
RANGE	107.00	45610.
MEDIAN	999.00	
LOWER QUARTILE	733.00	
UPPER QUARTILE	1309.0	
90TH	1765.5	
95TH	2071.5	
AVERAGE	1205.3	
S.D.	1726.6	
MEAN + S.D.	2931.9	
MEAN + 2*S.D.	4658.5	
MEAN + 3*S.D.	6385.2	
MEAN + 4*S.D.	8111.8	
MEAN + 5*S.D.	9838.4	

STATISTICS FOR ALL POINTS

NUMBER OF POINTS USED	3943	
NUMBER BELOW DETECTION LEVEL	0	
RANGE	44.000	45610.
MEDIAN	922.00	
LOWER QUARTILE	644.00	
UPPER QUARTILE	1219.0	
90TH	1566.5	
95TH	1959.5	
AVERAGE	1053.5	
S.D.	1124.7	
MEAN + S.D.	2178.2	
MEAN + 2*S.D.	3303.0	
MEAN + 3*S.D.	4427.7	
MEAN + 4*S.D.	5552.5	
MEAN + 5*S.D.	6677.2	

POTASSIUM IN SEDIMENTS, MONTROSE

STATISTICS FOR CRYSTALL.

NUMBER OF POINTS USED	2278	
NUMBER BELOW DETECTION LEVEL	42	
RANGE	2266.0	42450.
MEDIAN	19550.	
LOWER QUARTILE	16310.	
UPPER QUARTILE	23290.	
90TH	26640.	
95TH	28765.	
AVERAGE	19846.	
S.D.	5270.3	
MEAN + S.D.	25116.	
MEAN + 2*S.D.	30386.	
MEAN + 3*S.D.	35657.	
MEAN + 4*S.D.	40927.	
MEAN + 5*S.D.	46197.	

STATISTICS FOR PLATEAU

NUMBER OF POINTS USED	404	
NUMBER BELOW DETECTION LEVEL	5	
RANGE	5494.0	30100.
MEDIAN	14900.	
LOWER QUARTILE	13245.	
UPPER QUARTILE	17030.	
90TH	18840.	
95TH	19870.	
AVERAGE	15157.	
S.D.	2983.6	
MEAN + S.D.	18140.	
MEAN + 2*S.D.	21124.	
MEAN + 3*S.D.	24107.	
MEAN + 4*S.D.	27091.	
MEAN + 5*S.D.	30075.	

STATISTICS FOR VOLCANIC

NUMBER OF POINTS USED	1183	
NUMBER BELOW DETECTION LEVEL	30	
RANGE	7595.0	35240.
MEDIAN	18535.	
LOWER QUARTILE	15670.	
UPPER QUARTILE	21950.	
90TH	25340.	
95TH	27660.	
AVERAGE	18923.	
S.D.	4845.7	
MEAN + S.D.	23768.	
MEAN + 2*S.D.	28614.	
MEAN + 3*S.D.	33460.	
MEAN + 4*S.D.	38306.	
MEAN + 5*S.D.	43151.	

STATISTICS FOR ALL POINTS

NUMBER OF POINTS USED	3865	
NUMBER BELOW DETECTION LEVEL	77	
RANGE	2266.0	42450.
MEDIAN	18620.	
LOWER QUARTILE	15475.	
UPPER QUARTILE	22290.	
90TH	25790.	
95TH	28125.	
AVERAGE	19073.	
S.D.	5142.1	
MEAN + S.D.	24215.	
MEAN + 2*S.D.	29357.	
MEAN + 3*S.D.	34500.	
MEAN + 4*S.D.	39642.	
MEAN + 5*S.D.	44784.	

SCANDIUM IN SEDIMENTS, MONTROSE

STATISTICS FOR CRYSTALL.

NUMBER OF POINTS USED	2321	
NUMBER BELOW DETECTION LEVEL	0	
RANGE	1.0000	45.100
MEDIAN	11.400	
LOWER QUARTILE	8.7000	
UPPER QUARTILE	15.000	
90TH	19.400	
95TH	23.350	
AVERAGE	12.471	
S.D.	5.3611	
MEAN + S.D.	17.832	
MEAN + 2*S.D.	23.193	
MEAN + 3*S.D.	28.554	
MEAN + 4*S.D.	33.916	
MEAN + 5*S.D.	39.277	

STATISTICS FOR PLATEAU

NUMBER OF POINTS USED	409	
NUMBER BELOW DETECTION LEVEL	0	
RANGE	1.8000	18.900
MEDIAN	7.7000	
LOWER QUARTILE	6.2000	
UPPER QUARTILE	9.0500	
90TH	11.300	
95TH	12.500	
AVERAGE	7.9499	
S.D.	2.5672	
MEAN + S.D.	10.517	
MEAN + 2*S.D.	13.084	
MEAN + 3*S.D.	15.651	
MEAN + 4*S.D.	18.219	
MEAN + 5*S.D.	20.786	

STATISTICS FOR VOLCANIC

NUMBER OF POINTS USED	1213	
NUMBER BELOW DETECTION LEVEL	0	
RANGE	3.4000	25.700
MEDIAN	9.6000	
LOWER QUARTILE	8.0000	
UPPER QUARTILE	11.900	
90TH	14.650	
95TH	16.700	
AVERAGE	10.273	
S.D.	3.4225	
MEAN + S.D.	13.695	
MEAN + 2*S.D.	17.118	
MEAN + 3*S.D.	20.540	
MEAN + 4*S.D.	23.963	
MEAN + 5*S.D.	27.385	

STATISTICS FOR ALL POINTS

NUMBER OF POINTS USED	3943	
NUMBER BELOW DETECTION LEVEL	0	
RANGE	1.0000	45.100
MEDIAN	10.200	
LOWER QUARTILE	8.0000	
UPPER QUARTILE	13.500	
90TH	17.500	
95TH	20.950	
AVERAGE	11.326	
S.D.	4.8472	
MEAN + S.D.	16.173	
MEAN + 2*S.D.	21.020	
MEAN + 3*S.D.	25.867	
MEAN + 4*S.D.	30.714	
MEAN + 5*S.D.	35.562	

```
1    SELENIUM IN SEDIMENTS, MONTROSE


STATISTICS FOR ALL POINTS

NUMBER OF POINTS USED            18
NUMBER BELOW DETECTION LEVEL 2031
     RANGE              5.0000        19.000
     MEDIAN             7.0000
     LOWER QUARTILE     5.0000
     UPPER QUARTILE     9.0000
     90TH               16.500
     95TH               16.500

     AVERAGE            8.7222
     S.D.               4.5865
     MEAN + S.D.        13.309
     MEAN + 2*S.D.      17.895
     MEAN + 3*S.D.      22.482
     MEAN + 4*S.D.      27.068
     MEAN + 5*S.D.      31.655
```
1   SELENIUM IN SEDIMENTS, MONTROSE

THORIUM IN SEDIMENTS, MONTROSE

STATISTICS FOR CRYSTALL.

NUMBER OF POINTS USED	2318	
NUMBER BELOW DETECTION LEVEL	3	
RANGE	1.6000	999.00
MEDIAN	15.500	
LOWER QUARTILE	9.8000	
UPPER QUARTILE	28.200	
90TH	46.750	
95TH	62.600	
AVERAGE	23.568	
S.D.	32.452	
MEAN + S.D.	56.021	
MEAN + 2*S.D.	88.473	
MEAN + 3*S.D.	120.93	
MEAN + 4*S.D.	153.38	
MEAN + 5*S.D.	185.83	

STATISTICS FOR VOLCANIC

NUMBER OF POINTS USED	1213	
NUMBER BELOW DETECTION LEVEL	0	
RANGE	3.0000	178.10
MEDIAN	10.800	
LOWER QUARTILE	8.6000	
UPPER QUARTILE	13.800	
90TH	17.000	
95TH	19.000	
AVERAGE	11.692	
S.D.	6.5831	
MEAN + S.D.	18.275	
MEAN + 2*S.D.	24.859	
MEAN + 3*S.D.	31.442	
MEAN + 4*S.D.	38.025	
MEAN + 5*S.D.	44.608	

STATISTICS FOR PLATEAU

NUMBER OF POINTS USED	409	
NUMBER BELOW DETECTION LEVEL	0	
RANGE	1.8000	38.000
MEDIAN	9.4000	
LOWER QUARTILE	8.3000	
UPPER QUARTILE	10.800	
90TH	12.550	
95TH	14.150	
AVERAGE	9.8154	
S.D.	3.1103	
MEAN + S.D.	12.926	
MEAN + 2*S.D.	16.036	
MEAN + 3*S.D.	19.146	
MEAN + 4*S.D.	22.257	
MEAN + 5*S.D.	25.367	

STATISTICS FOR ALL POINTS

NUMBER OF POINTS USED	3940	
NUMBER BELOW DETECTION LEVEL	3	
RANGE	1.6000	999.00
MEDIAN	12.100	
LOWER QUARTILE	9.0000	
UPPER QUARTILE	19.300	
90TH	35.100	
95TH	50.000	
AVERAGE	18.484	
S.D.	25.904	
MEAN + S.D.	44.389	
MEAN + 2*S.D.	70.293	
MEAN + 3*S.D.	96.198	
MEAN + 4*S.D.	122.10	
MEAN + 5*S.D.	148.01	

TITANIUM IN SEDIMENTS, MONTROSE

STATISTICS FOR CRYSTALL.

NUMBER OF POINTS USED	2282	
NUMBER BELOW DETECTION LEVEL	38	
RANGE	1073.0	23340.
MEDIAN	4414.0	
LOWER QUARTILE	3509.0	
UPPER QUARTILE	5767.0	
90TH	7855.5	
95TH	9771.5	
AVERAGE	4991.3	
S.D.	2341.1	
MEAN + S.D.	7332.4	
MEAN + 2*S.D.	9673.5	
MEAN + 3*S.D.	12015.	
MEAN + 4*S.D.	14356.	
MEAN + 5*S.D.	16697.	

STATISTICS FOR VOLCANIC

NUMBER OF POINTS USED	1190	
NUMBER BELOW DETECTION LEVEL	23	
RANGE	1886.0	20970.
MEDIAN	4623.0	
LOWER QUARTILE	3827.0	
UPPER QUARTILE	5879.0	
90TH	7538.0	
95TH	9639.0	
AVERAGE	5175.3	
S.D.	2168.0	
MEAN + S.D.	7343.3	
MEAN + 2*S.D.	9511.3	
MEAN + 3*S.D.	11679.	
MEAN + 4*S.D.	13847.	
MEAN + 5*S.D.	16015.	

STATISTICS FOR PLATEAU

NUMBER OF POINTS USED	404	
NUMBER BELOW DETECTION LEVEL	5	
RANGE	1761.0	10190.
MEDIAN	3606.0	
LOWER QUARTILE	3037.5	
UPPER QUARTILE	4505.0	
90TH	5731.0	
95TH	6703.5	
AVERAGE	3930.9	
S.D.	1378.9	
MEAN + S.D.	5309.8	
MEAN + 2*S.D.	6688.6	
MEAN + 3*S.D.	8067.5	
MEAN + 4*S.D.	9446.4	
MEAN + 5*S.D.	10825.	

STATISTICS FOR ALL POINTS

NUMBER OF POINTS USED	3876	
NUMBER BELOW DETECTION LEVEL	66	
RANGE	1073.0	23340.
MEDIAN	4404.0	
LOWER QUARTILE	3521.5	
UPPER QUARTILE	5666.5	
90TH	7535.5	
95TH	9356.5	
AVERAGE	4937.2	
S.D.	2234.0	
MEAN + S.D.	7171.3	
MEAN + 2*S.D.	9405.3	
MEAN + 3*S.D.	11639.	
MEAN + 4*S.D.	13873.	
MEAN + 5*S.D.	16107.	

URANIUM IN SEDIMENTS, MONTROSE

STATISTICS FOR CRYSTALL.

NUMBER OF POINTS USED	2321	
NUMBER BELOW DETECTION LEVEL	0	
RANGE	.94000	359.40
MEDIAN	7.0800	
LOWER QUARTILE	4.3000	
UPPER QUARTILE	15.190	
90TH	31.505	
95TH	48.345	
AVERAGE	14.923	
S.D.	24.511	
MEAN + S.D.	39.434	
MEAN + 2*S.D.	63.945	
MEAN + 3*S.D.	88.457	
MEAN + 4*S.D.	112.97	
MEAN + 5*S.D.	137.48	

STATISTICS FOR PLATEAU

NUMBER OF POINTS USED	409	
NUMBER BELOW DETECTION LEVEL	0	
RANGE	1.6300	8.4000
MEDIAN	3.5600	
LOWER QUARTILE	3.0950	
UPPER QUARTILE	4.1050	
90TH	4.8850	
95TH	5.3800	
AVERAGE	3.6789	
S.D.	.93301	
MEAN + S.D.	4.6119	
MEAN + 2*S.D.	5.5449	
MEAN + 3*S.D.	6.4780	
MEAN + 4*S.D.	7.4110	
MEAN + 5*S.D.	8.3440	

STATISTICS FOR VOLCANIC

NUMBER OF POINTS USED	1214	
NUMBER BELOW DETECTION LEVEL	0	
RANGE	1.0200	59.950
MEDIAN	3.7400	
LOWER QUARTILE	2.9100	
UPPER QUARTILE	5.0000	
90TH	6.8400	
95TH	8.4500	
AVERAGE	4.5048	
S.D.	3.4875	
MEAN + S.D.	7.9923	
MEAN + 2*S.D.	11.480	
MEAN + 3*S.D.	14.967	
MEAN + 4*S.D.	18.455	
MEAN + 5*S.D.	21.943	

STATISTICS FOR ALL POINTS

NUMBER OF POINTS USED	3944	
NUMBER BELOW DETECTION LEVEL	0	
RANGE	.94000	359.40
MEDIAN	4.8500	
LOWER QUARTILE	3.4800	
UPPER QUARTILE	9.2950	
90TH	21.500	
95TH	34.860	
AVERAGE	10.550	
S.D.	19.615	
MEAN + S.D.	30.165	
MEAN + 2*S.D.	49.780	
MEAN + 3*S.D.	69.394	
MEAN + 4*S.D.	89.009	
MEAN + 5*S.D.	108.62	

URANIUM IN WATER, MONTROSE

STATISTICS FOR CRYSTALL.

NUMBER OF POINTS USED	1328	
NUMBER BELOW DETECTION LEVEL	0	
RANGE	.10000E-01	197.60
MEDIAN	.62000	
LOWER QUARTILE	.28000	
UPPER QUARTILE	1.4200	
90TH	2.8500	
95TH	4.2650	
AVERAGE	2.0094	
S.D.	9.7420	
MEAN + S.D.	11.751	
MEAN + 2*S.D.	21.493	
MEAN + 3*S.D.	31.235	
MEAN + 4*S.D.	40.977	
MEAN + 5*S.D.	50.720	

STATISTICS FOR PLATEAU

NUMBER OF POINTS USED	269	
NUMBER BELOW DETECTION LEVEL	0	
RANGE	.10000E-01	209.50
MEDIAN	1.4400	
LOWER QUARTILE	.40000	
UPPER QUARTILE	3.9750	
90TH	10.655	
95TH	21.125	
AVERAGE	5.0464	
S.D.	15.812	
MEAN + S.D.	20.858	
MEAN + 2*S.D.	36.670	
MEAN + 3*S.D.	52.482	
MEAN + 4*S.D.	68.294	
MEAN + 5*S.D.	84.106	

STATISTICS FOR VOLCANIC

NUMBER OF POINTS USED	802	
NUMBER BELOW DETECTION LEVEL	0	
RANGE	.10000E-01	7.4700
MEDIAN	.23000	
LOWER QUARTILE	.10000	
UPPER QUARTILE	.51000	
90TH	.98000	
95TH	1.4500	
AVERAGE	.44569	
S.D.	.70241	
MEAN + S.D.	1.1481	
MEAN + 2*S.D.	1.8505	
MEAN + 3*S.D.	2.5529	
MEAN + 4*S.D.	3.2553	
MEAN + 5*S.D.	3.9577	

STATISTICS FOR ALL POINTS

NUMBER OF POINTS USED	2399	
NUMBER BELOW DETECTION LEVEL	0	
RANGE	.10000E-01	209.50
MEDIAN	.48000	
LOWER QUARTILE	.19000	
UPPER QUARTILE	1.2100	
90TH	2.7600	
95TH	4.8900	
AVERAGE	1.8272	
S.D.	9.0799	
MEAN + S.D.	10.907	
MEAN + 2*S.D.	19.987	
MEAN + 3*S.D.	29.067	
MEAN + 4*S.D.	38.147	
MEAN + 5*S.D.	47.227	

VANADIUM IN SEDIMENTS, MONTROSE

STATISTICS FOR CRYSTALL.

NUMBER OF POINTS USED	2306	
NUMBER BELOW DETECTION LEVEL	14	
RANGE	9.0000	826.00
MEDIAN	82.000	
LOWER QUARTILE	61.000	
UPPER QUARTILE	111.00	
90TH	157.50	
95TH	190.50	
AVERAGE	95.075	
S.D.	58.119	
MEAN + S.D.	153.19	
MEAN + 2*S.D.	211.31	
MEAN + 3*S.D.	269.43	
MEAN + 4*S.D.	327.55	
MEAN + 5*S.D.	385.67	

STATISTICS FOR PLATEAU

NUMBER OF POINTS USED	408	
NUMBER BELOW DETECTION LEVEL	1	
RANGE	22.000	365.00
MEDIAN	87.000	
LOWER QUARTILE	63.500	
UPPER QUARTILE	129.00	
90TH	166.00	
95TH	204.50	
AVERAGE	101.52	
S.D.	53.691	
MEAN + S.D.	155.21	
MEAN + 2*S.D.	208.90	
MEAN + 3*S.D.	262.59	
MEAN + 4*S.D.	316.29	
MEAN + 5*S.D.	369.98	

STATISTICS FOR VOLCANIC

NUMBER OF POINTS USED	1204	
NUMBER BELOW DETECTION LEVEL	10	
RANGE	22.000	627.00
MEDIAN	87.000	
LOWER QUARTILE	65.000	
UPPER QUARTILE	120.00	
90TH	174.50	
95TH	236.00	
AVERAGE	105.73	
S.D.	68.248	
MEAN + S.D.	173.98	
MEAN + 2*S.D.	242.23	
MEAN + 3*S.D.	310.48	
MEAN + 4*S.D.	378.72	
MEAN + 5*S.D.	446.97	

STATISTICS FOR ALL POINTS

NUMBER OF POINTS USED	3918	
NUMBER BELOW DETECTION LEVEL	25	
RANGE	9.0000	826.00
MEDIAN	84.000	
LOWER QUARTILE	63.000	
UPPER QUARTILE	116.00	
90TH	164.00	
95TH	204.00	
AVERAGE	99.021	
S.D.	61.167	
MEAN + S.D.	160.19	
MEAN + 2*S.D.	221.36	
MEAN + 3*S.D.	282.52	
MEAN + 4*S.D.	343.69	
MEAN + 5*S.D.	404.86	

ZINC IN SEDIMENTS, MONTROSE

STATISTICS FOR CRYSTALL.

NUMBER OF POINTS USED	1657	
NUMBER BELOW DETECTION LEVEL	639	
RANGE	25.000	24760.
MEDIAN	139.00	
LOWER QUARTILE	101.00	
UPPER QUARTILE	196.50	
90TH	323.00	
95TH	580.50	
AVERAGE	260.55	
S.D.	836.18	
MEAN + S.D.	1096.7	
MEAN + 2*S.D.	1932.9	
MEAN + 3*S.D.	2769.1	
MEAN + 4*S.D.	3605.3	
MEAN + 5*S.D.	4441.4	

STATISTICS FOR PLATEAU

NUMBER OF POINTS USED	292	
NUMBER BELOW DETECTION LEVEL	114	
RANGE	22.000	11830.
MEDIAN	105.00	
LOWER QUARTILE	82.000	
UPPER QUARTILE	142.00	
90TH	283.50	
95TH	376.50	
AVERAGE	186.94	
S.D.	708.41	
MEAN + S.D.	895.35	
MEAN + 2*S.D.	1603.8	
MEAN + 3*S.D.	2312.2	
MEAN + 4*S.D.	3020.6	
MEAN + 5*S.D.	3729.0	

STATISTICS FOR VOLCANIC

NUMBER OF POINTS USED	915	
NUMBER BELOW DETECTION LEVEL	285	
RANGE	29.000	18570.
MEDIAN	123.00	
LOWER QUARTILE	94.000	
UPPER QUARTILE	166.00	
90TH	292.00	
95TH	1039.5	
AVERAGE	307.57	
S.D.	964.92	
MEAN + S.D.	1272.5	
MEAN + 2*S.D.	2237.4	
MEAN + 3*S.D.	3202.3	
MEAN + 4*S.D.	4167.3	
MEAN + 5*S.D.	5132.2	

STATISTICS FOR ALL POINTS

NUMBER OF POINTS USED	2866	
NUMBER BELOW DETECTION LEVEL	1038	
RANGE	22.000	24760.
MEDIAN	129.00	
LOWER QUARTILE	96.000	
UPPER QUARTILE	181.00	
90TH	313.00	
95TH	625.50	
AVERAGE	268.07	
S.D.	868.26	
MEAN + S.D.	1136.3	
MEAN + 2*S.D.	2004.6	
MEAN + 3*S.D.	2872.8	
MEAN + 4*S.D.	3741.1	
MEAN + 5*S.D.	4609.4	

1 ZIRCONIUM IN SEDIMENTS, MONTROSE

STATISTICS FOR ALL POINTS

NUMBER OF POINTS USED	2049	
NUMBER BELOW DETECTION LEVEL	0	
RANGE	37.000	10155.
MEDIAN	366.00	
LOWER QUARTILE	248.00	
UPPER QUARTILE	542.00	
90TH	944.00	
95TH	1380.5	
AVERAGE	530.27	
S.D.	629.55	
MEAN + S.D.	1159.6	
MEAN + 2*S.D.	1789.4	
MEAN + 3*S.D.	2418.9	
MEAN + 4*S.D.	3048.5	
MEAN + 5*S.D.	3678.0	

1 ZIRCONIUM IN SEDIMENTS, MONTROSE

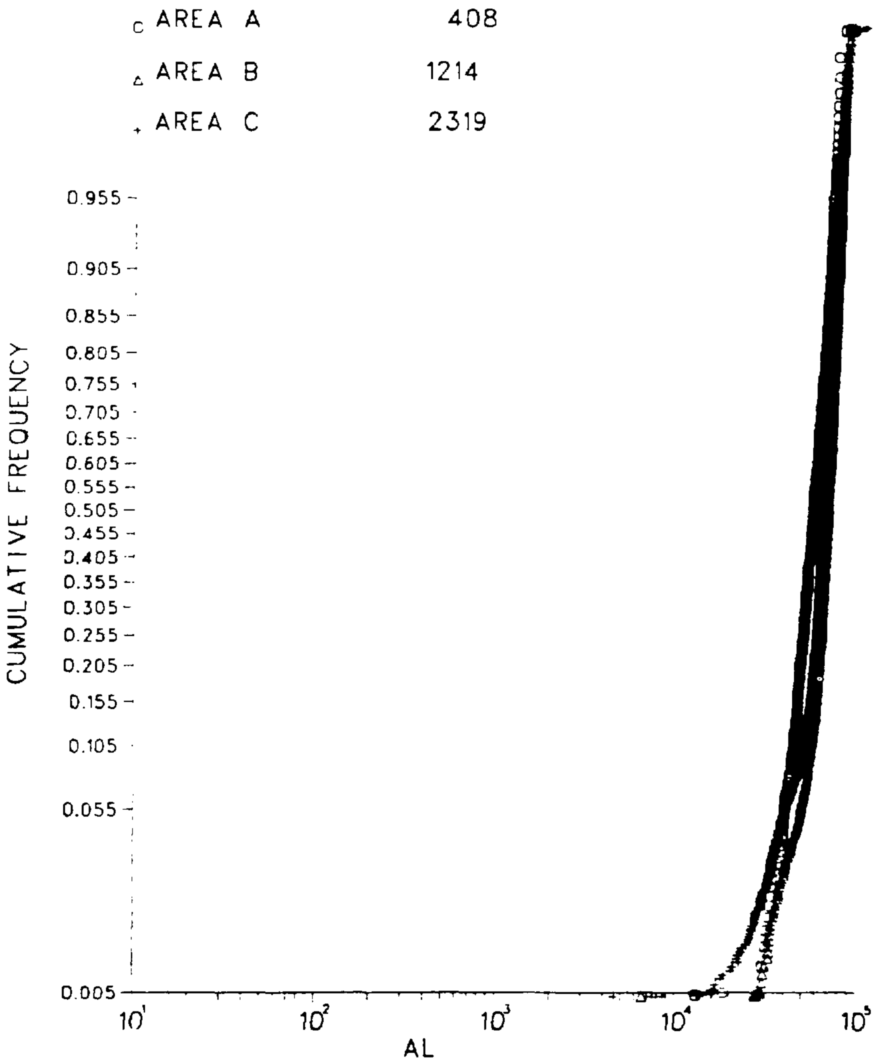

AREA A 408
AREA B 1214
AREA C 2319
CUMULATIVE FREQUENCY
0.955
0.905
0.855
0.805
0.755
0.705
0.655
0.605
0.555
0.505
0.455
0.405
0.355
0.305
0.255
0.205
0.155
0.105
0.055
0.005
10^1
10^2
10^3
10^4
10^5
AL

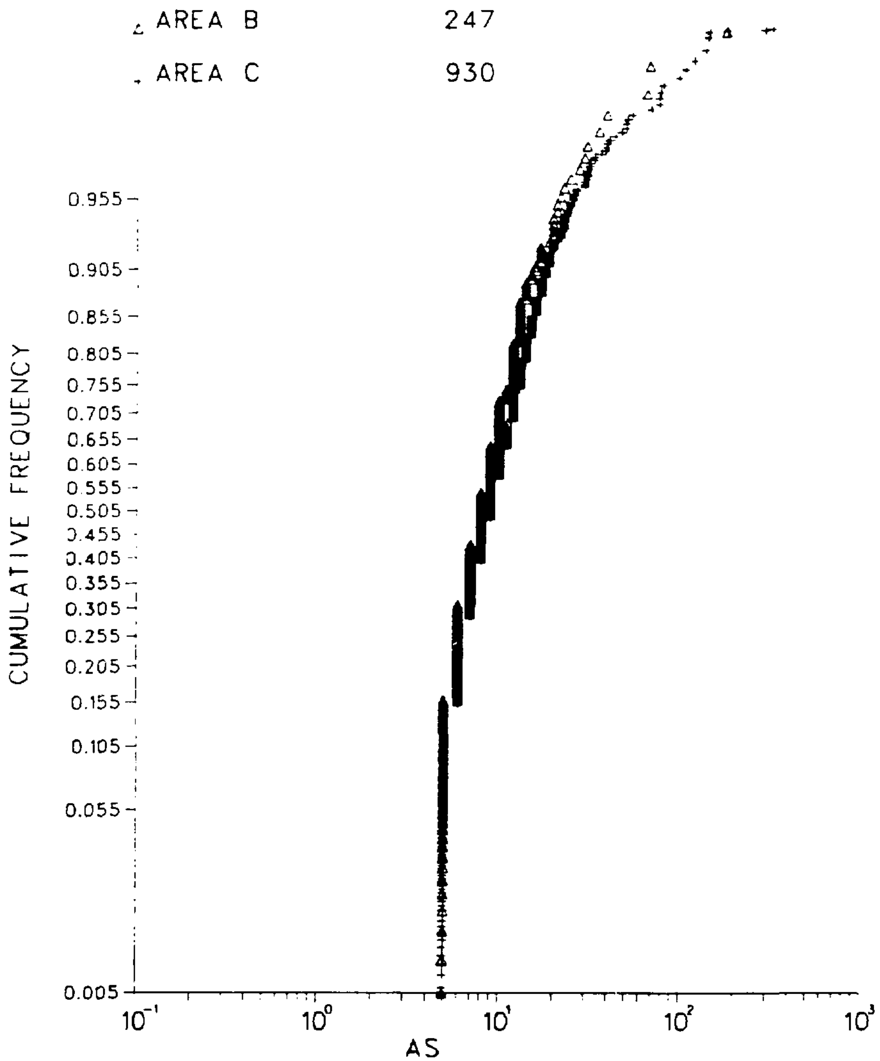

AREA B 247
AREA C 930
CUMULATIVE FREQUENCY
0.955
0.905
0.855
0.805
0.755
0.705
0.655
0.605
0.555
0.505
0.455
0.405
0.355
0.305
0.255
0.205
0.155
0.105
0.055
0.005
10^{-1}
10^{0}
10^{1}
10^{2}
10^{3}
AS

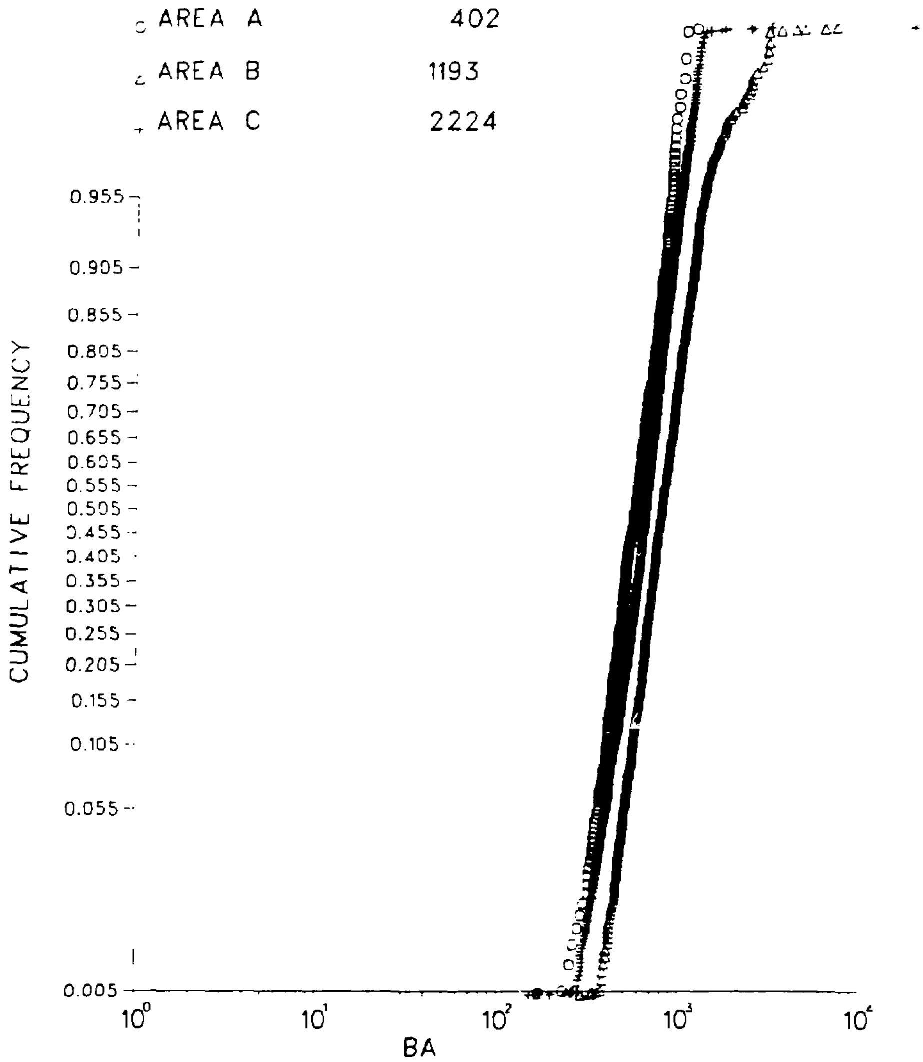
AREA A 402
AREA B 1193
AREA C 2224
CUMULATIVE FREQUENCY
0.955
0.905
0.855
0.805
0.755
0.705
0.655
0.605
0.555
0.505
0.455
0.405
0.355
0.305
0.255
0.205
0.155
0.105
0.055
0.005
10^0
10^1
10^2
10^3
10^4
BA

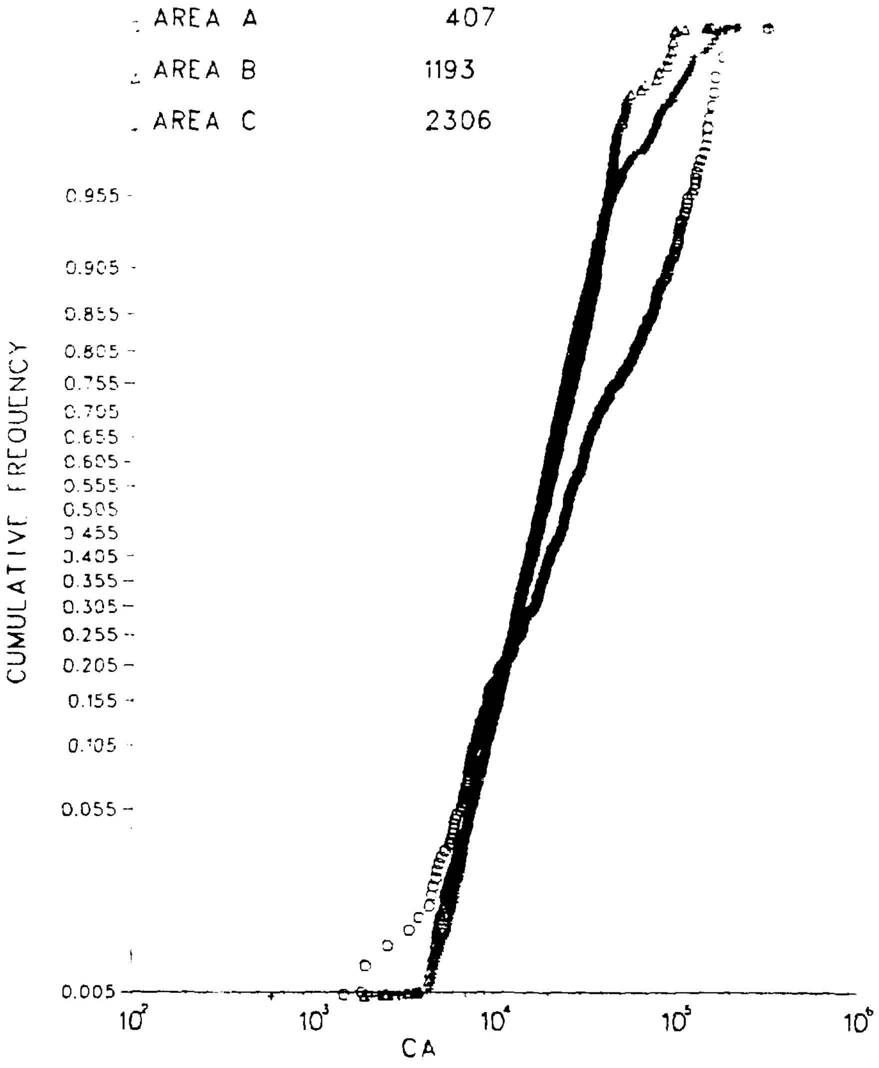
AREA A 407
AREA B 1193
AREA C 2306
CUMULATIVE FREQUENCY
0.955
0.905
0.855
0.805
0.755
0.705
0.655
0.605
0.555
0.505
0.455
0.405
0.355
0.305
0.255
0.205
0.155
0.105
0.055
0.005
10^2
10^3
10^4
10^5
10^6
CA

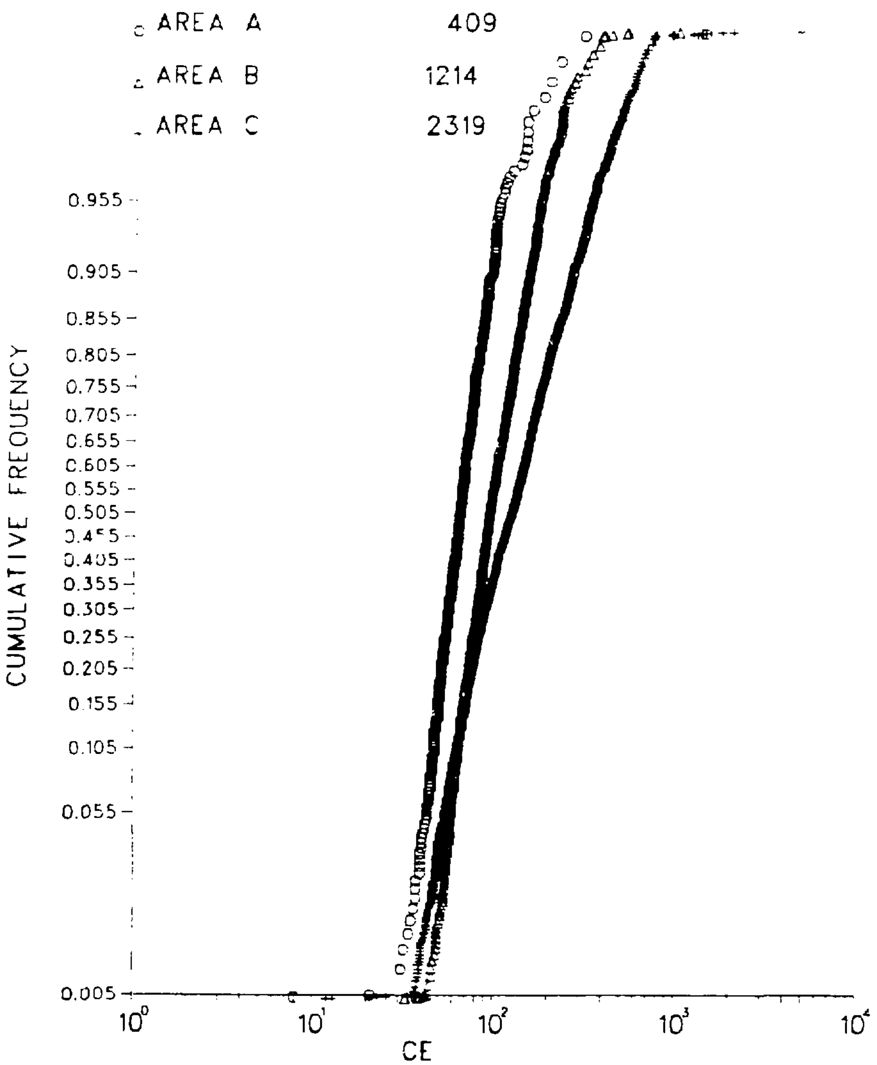

AREA A 409
AREA B 1214
AREA C 2319
CUMULATIVE FREQUENCY
0.955
0.905
0.855
0.805
0.755
0.705
0.655
0.605
0.555
0.505
0.405
0.355
0.305
0.255
0.205
0.155
0.105
0.055
0.005
10^0
10^1
10^2
10^3
10^4
CE

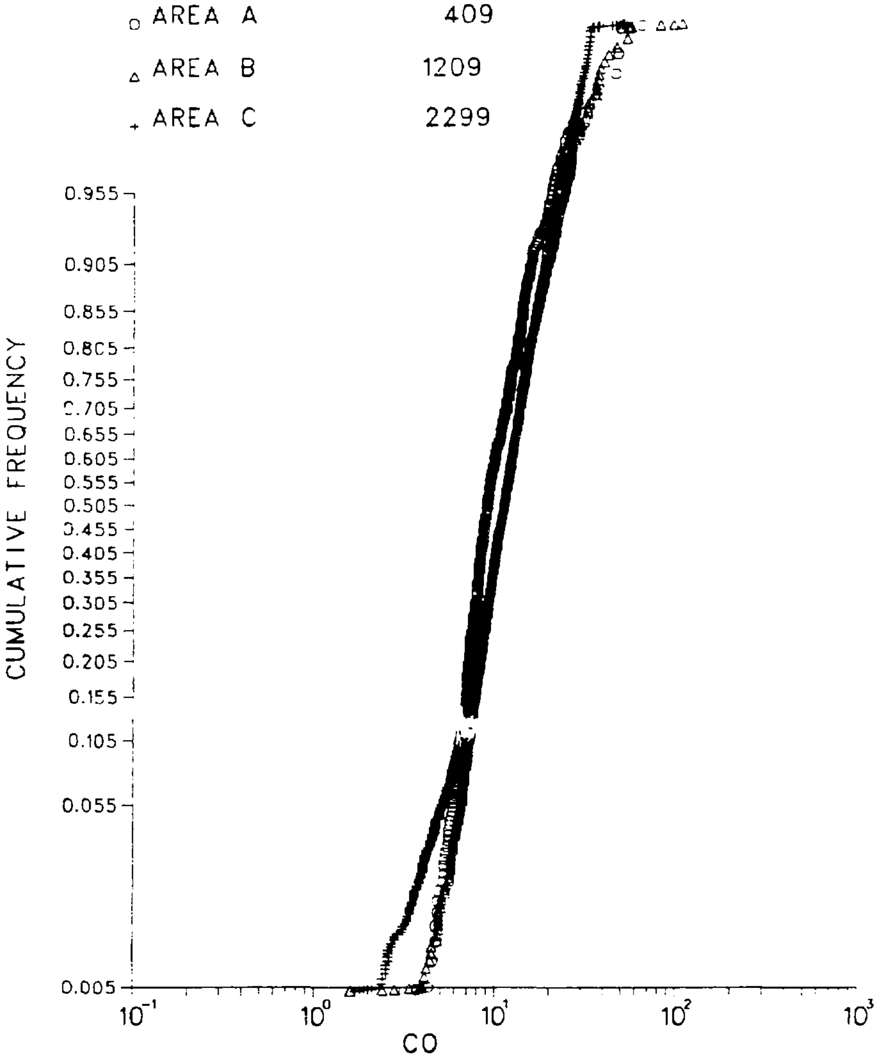

AREA A 409
AREA B 1209
AREA C 2299
CUMULATIVE FREQUENCY
0.955
0.905
0.855
0.805
0.755
0.705
0.655
0.605
0.555
0.505
0.455
0.405
0.355
0.305
0.255
0.205
0.155
0.105
0.055
0.005
10^{-1}
10^{0}
10^{1}
10^{2}
10^{3}
CO

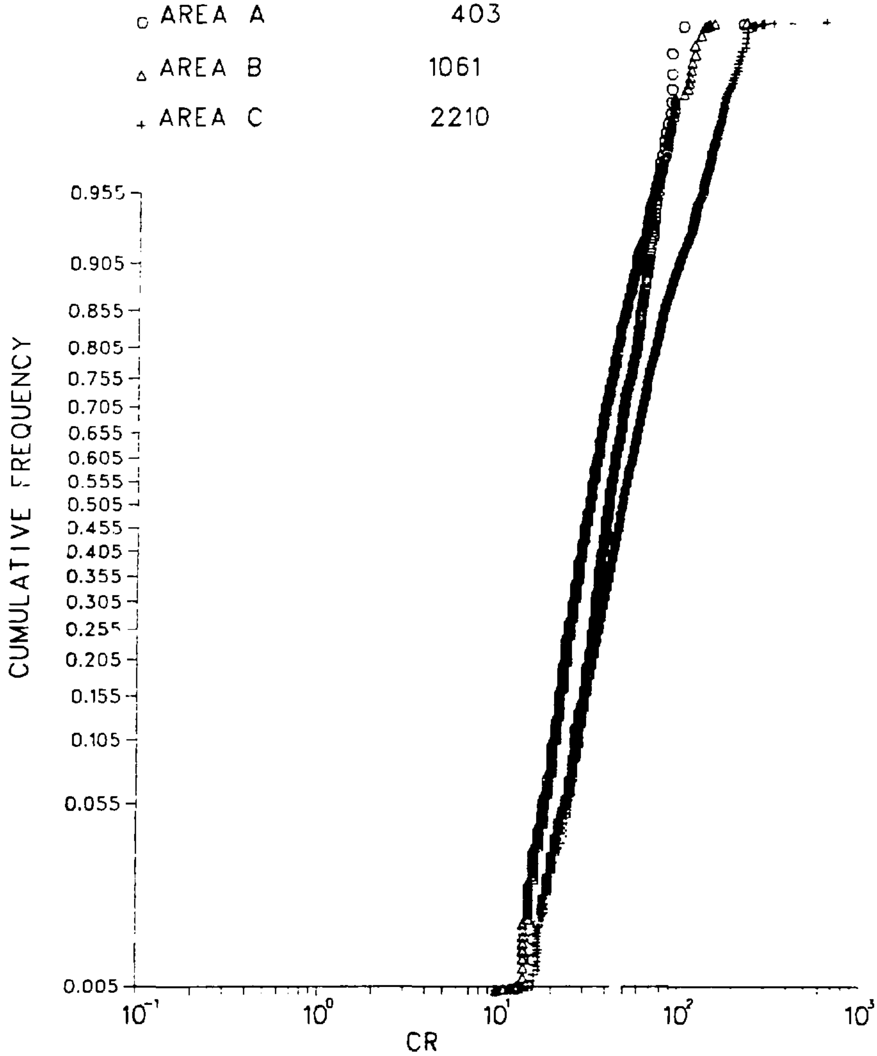

○ AREA A 403
△ AREA B 1061
+ AREA C 2210
CUMULATIVE FREQUENCY
0.955
0.905
0.855
0.805
0.755
0.705
0.655
0.605
0.555
0.505
0.455
0.405
0.355
0.305
0.255
0.205
0.155
0.105
0.055
0.005
10^{-1}
10^{0}
10^{1}
10^{2}
10^{3}
CR

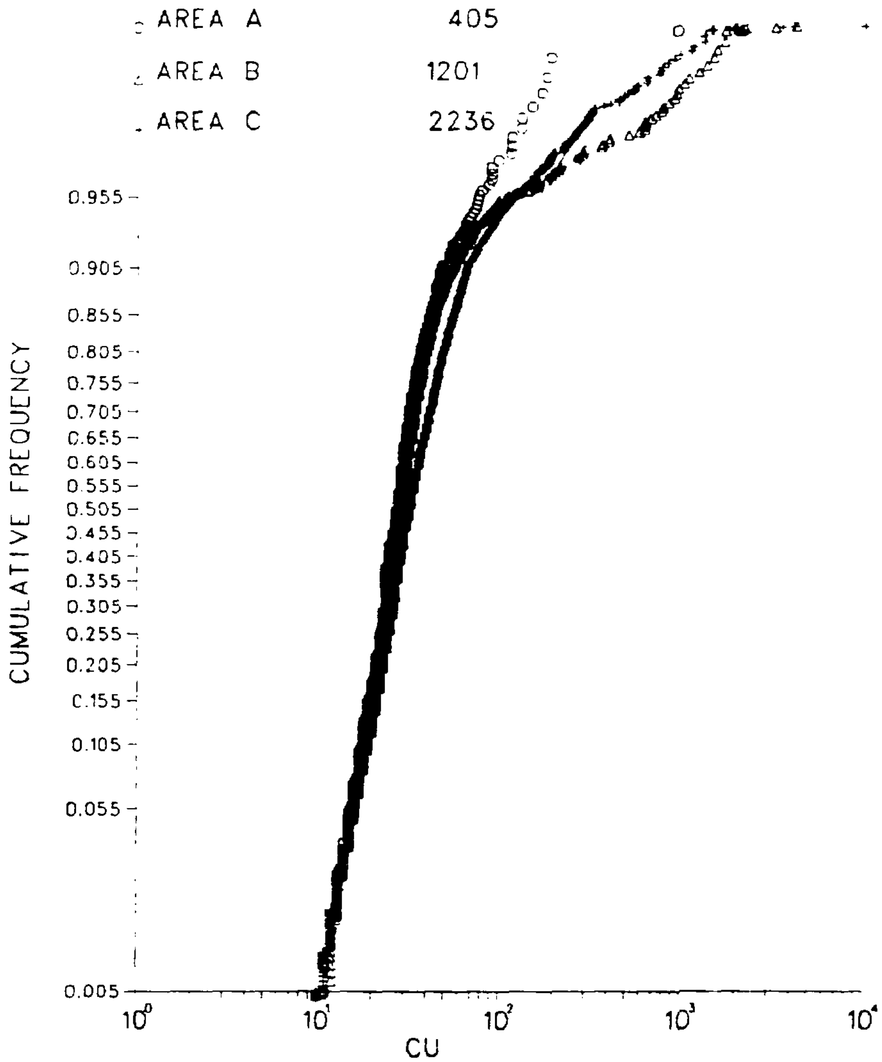
AREA A 405
AREA B 1201
AREA C 2236
CUMULATIVE FREQUENCY
0.955
0.905
0.855
0.805
0.755
0.705
0.655
0.605
0.555
0.505
0.455
0.405
0.355
0.305
0.255
0.205
0.155
0.105
0.055
0.005
10^0
10^1
10^2
10^3
10^4
CU

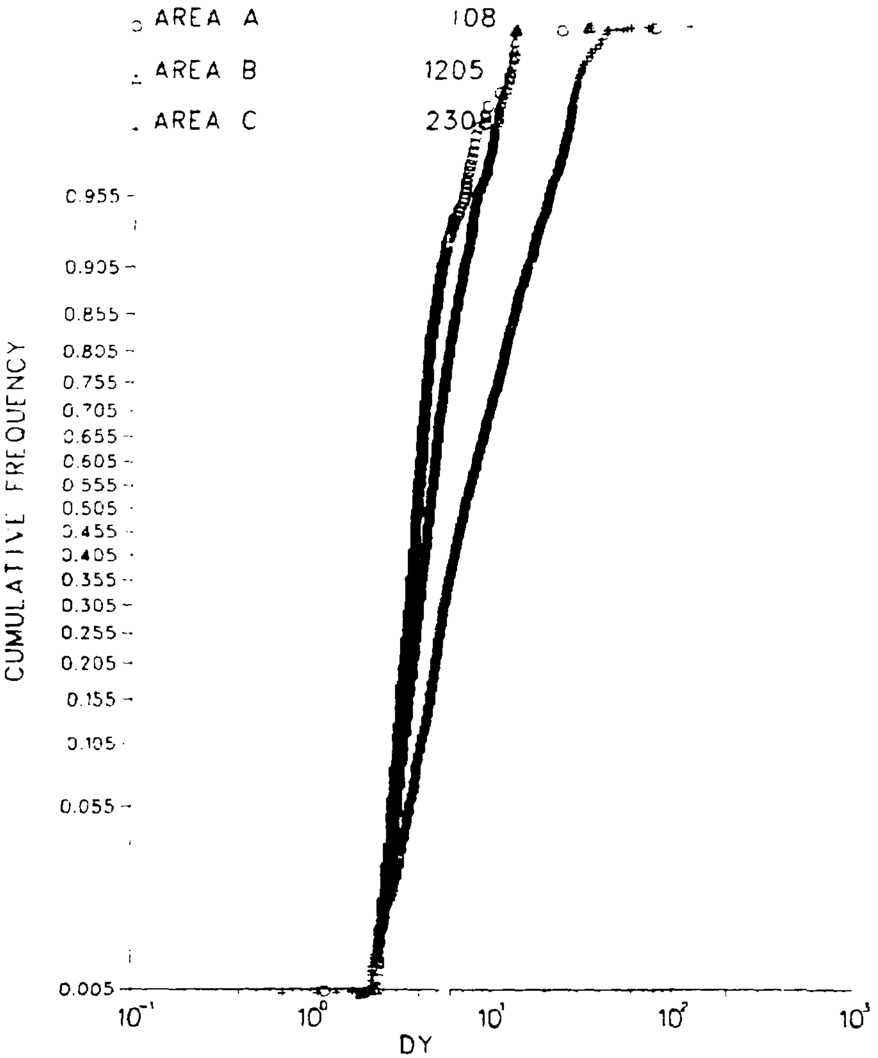
AREA A 108
AREA B 1205
AREA C 2308
CUMULATIVE FREQUENCY
0.955
0.905
0.855
0.805
0.755
0.705
0.655
0.605
0.555
0.505
0.455
0.405
0.355
0.305
0.255
0.205
0.155
0.105
0.055
0.005
10^{-1}
10^{0}
10^{1}
10^{2}
10^{3}
DY

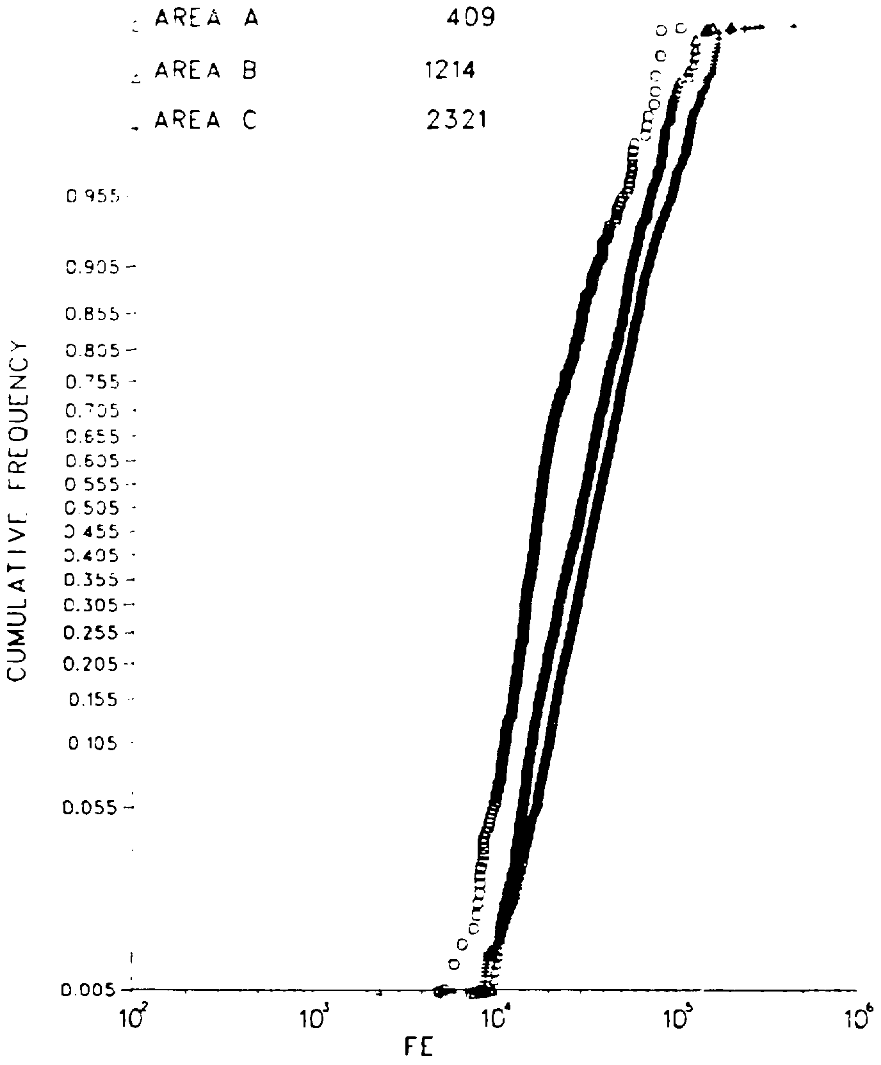

AREA A 409
AREA B 1214
AREA C 2321
CUMULATIVE FREQUENCY
0.955
0.905
0.855
0.805
0.755
0.705
0.655
0.605
0.555
0.505
0.455
0.405
0.355
0.305
0.255
0.205
0.155
0.105
0.055
0.005
10^2
10^3
10^4
10^5
10^6
FE

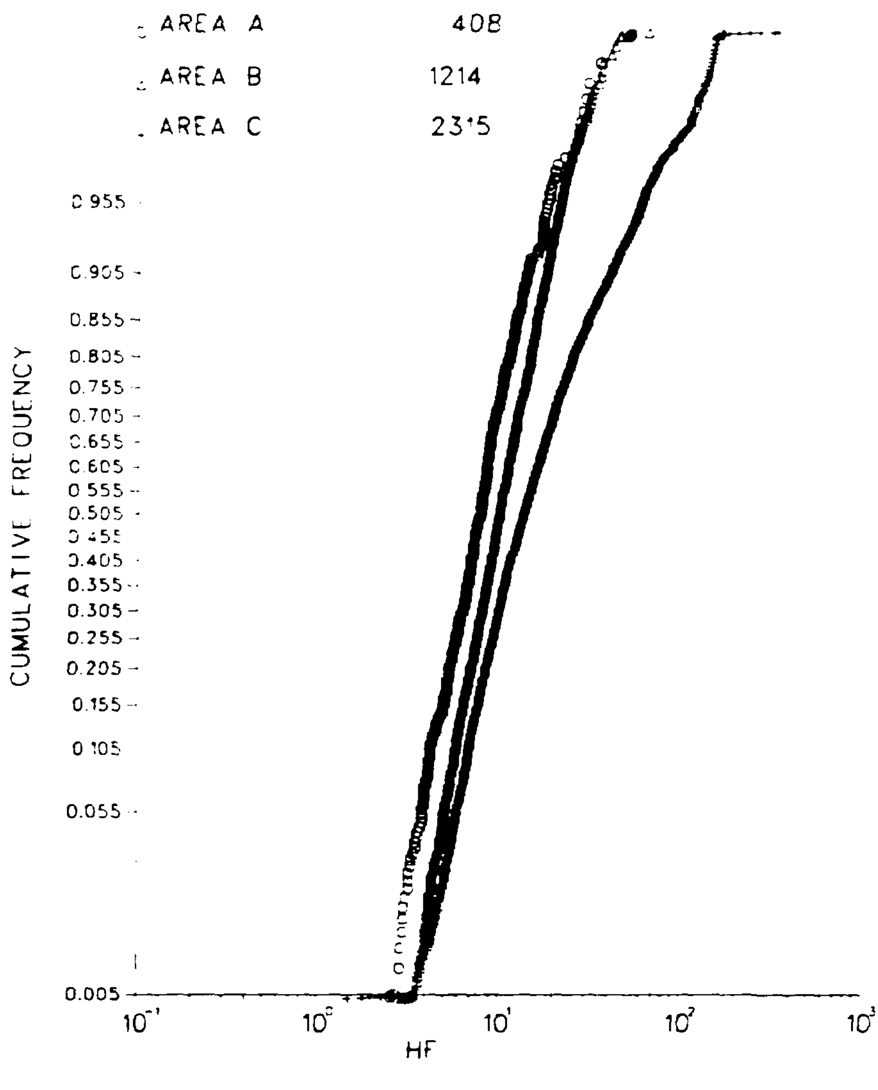

AREA A 408
AREA B 1214
AREA C 23'5
0.955
0.905
0.855
0.805
0.755
0.705
0.655
0.605
0.555
0.505
0.455
0.405
0.355
0.305
0.255
0.205
0.155
0.105
0.055
0.005
CUMULATIVE FREQUENCY
10^{-1}
10^{0}
10^{1}
10^{2}
10^{3}
HF

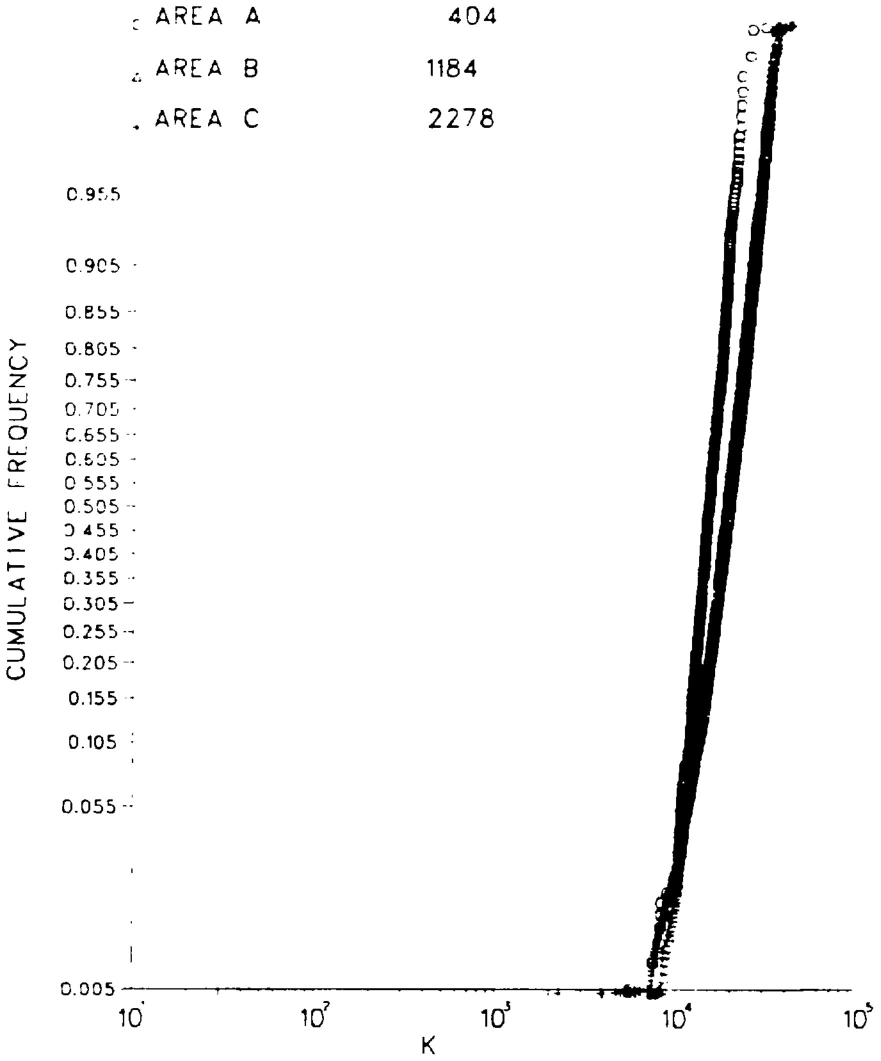

AREA A 404
AREA B 1184
AREA C 2278
CUMULATIVE FREQUENCY
0.955
0.905
0.855
0.805
0.755
0.705
0.655
0.605
0.555
0.505
0.455
0.405
0.355
0.305
0.255
0.205
0.155
0.105
0.055
0.005
K

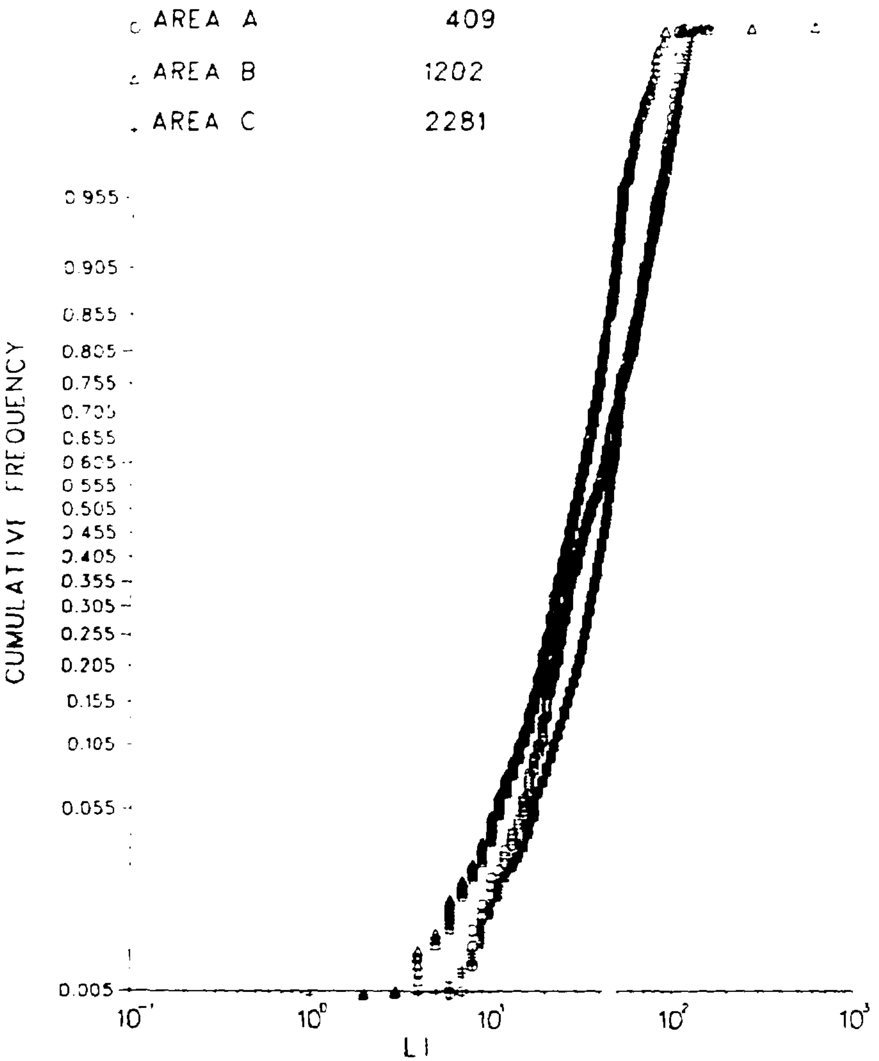

AREA A 409
AREA B 1202
AREA C 2281
CUMULATIVE FREQUENCY
0.955
0.905
0.855
0.805
0.755
0.705
0.655
0.605
0.555
0.505
0.455
0.405
0.355
0.305
0.255
0.205
0.155
0.105
0.055
0.005
10^{-1}
10^{0}
10^{1}
10^{2}
10^{3}
LI

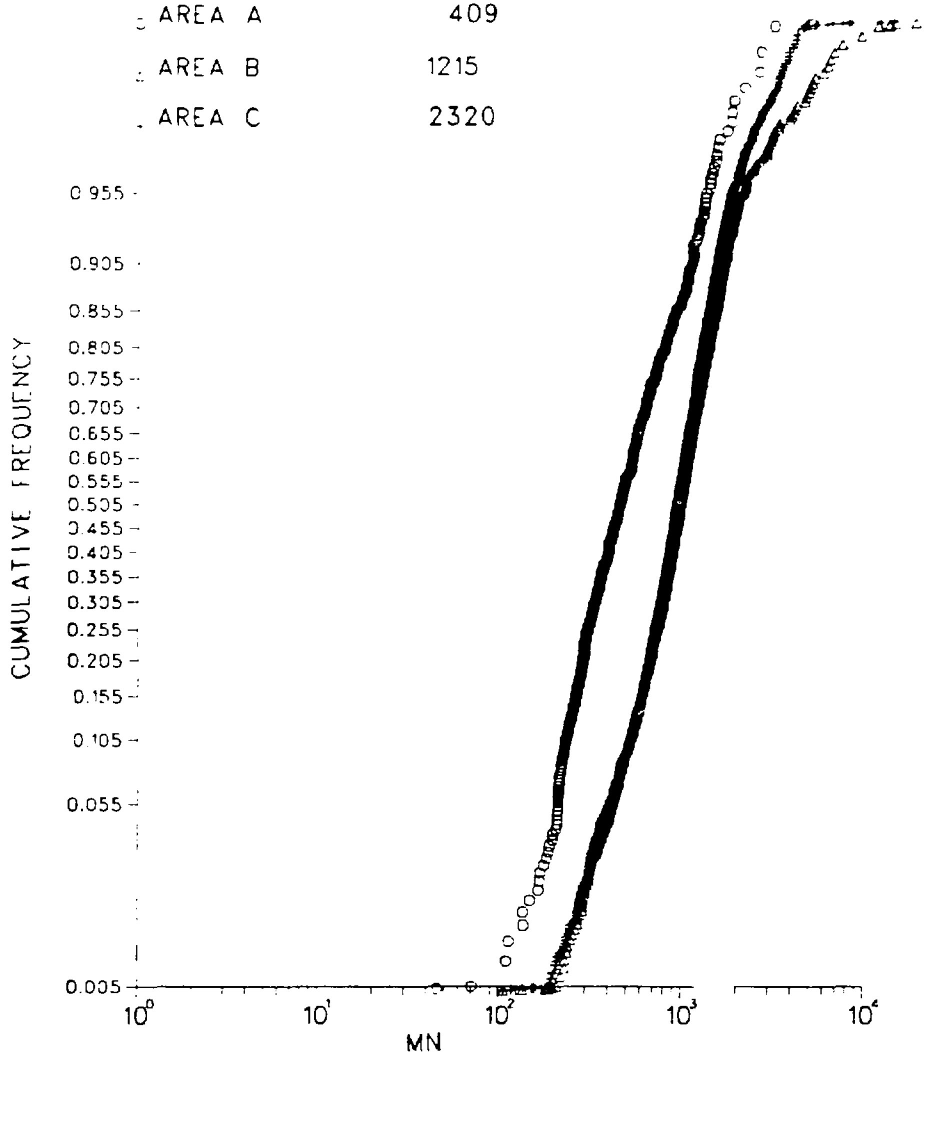

AREA A 409
AREA B 1215
AREA C 2320
CUMULATIVE FREQUENCY
0.955
0.905
0.855
0.805
0.755
0.705
0.655
0.605
0.555
0.505
0.455
0.405
0.355
0.305
0.255
0.205
0.155
0.105
0.055
0.005
10^0
10^1
10^2
10^3
10^4
MN

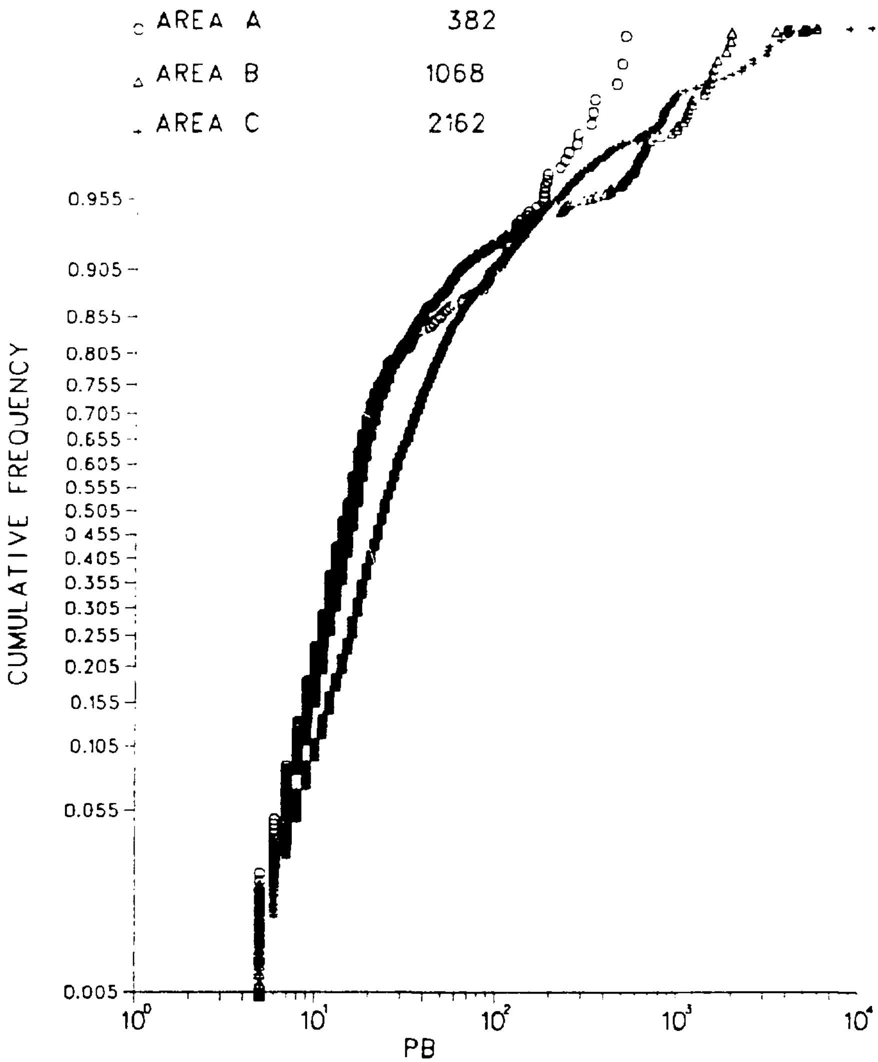

AREA A 382
AREA B 1068
AREA C 2162
CUMULATIVE FREQUENCY
0.955
0.905
0.855
0.805
0.755
0.705
0.655
0.605
0.555
0.505
0.455
0.405
0.355
0.305
0.255
0.205
0.155
0.105
0.055
0.005
10^0
10^1
10^2
10^3
10^4
PB

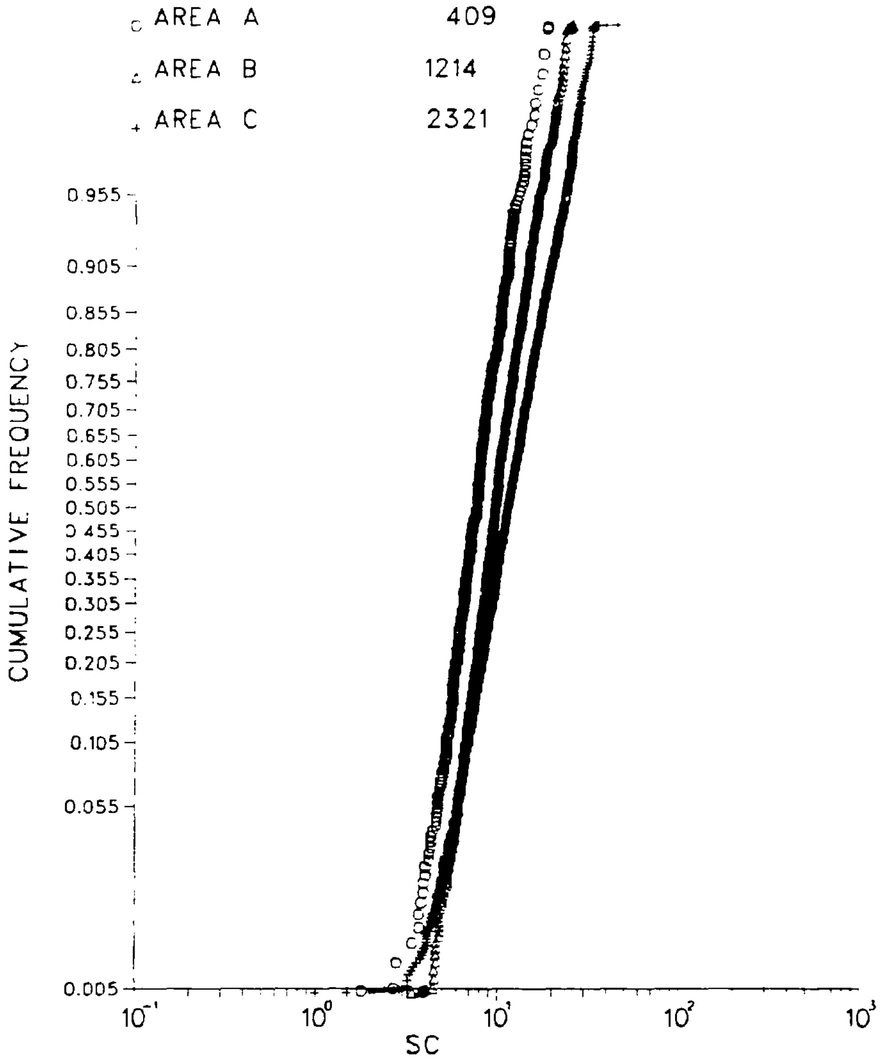

AREA A 409
AREA B 1214
AREA C 2321
CUMULATIVE FREQUENCY
0.955
0.905
0.855
0.805
0.755
0.705
0.655
0.605
0.555
0.505
0.455
0.405
0.355
0.305
0.255
0.205
0.155
0.105
0.055
0.005
10^{-1}
10^{0}
10^{1}
10^{2}
10^{3}
SC

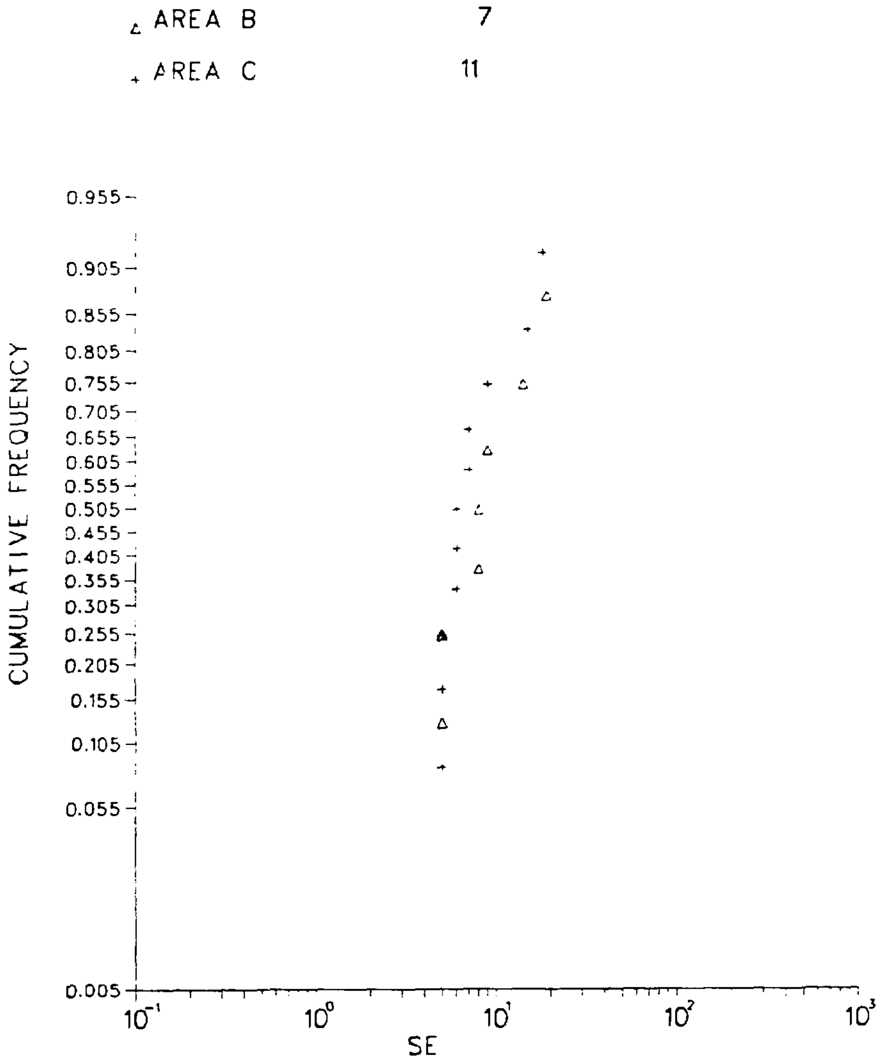
AREA B 7
AREA C 11
CUMULATIVE FREQUENCY
0.955
0.905
0.855
0.805
0.755
0.705
0.655
0.605
0.555
0.505
0.455
0.405
0.355
0.305
0.255
0.205
0.155
0.105
0.055
0.005
10^{-1}
10^{0}
10^{1}
10^{2}
10^{3}
SE

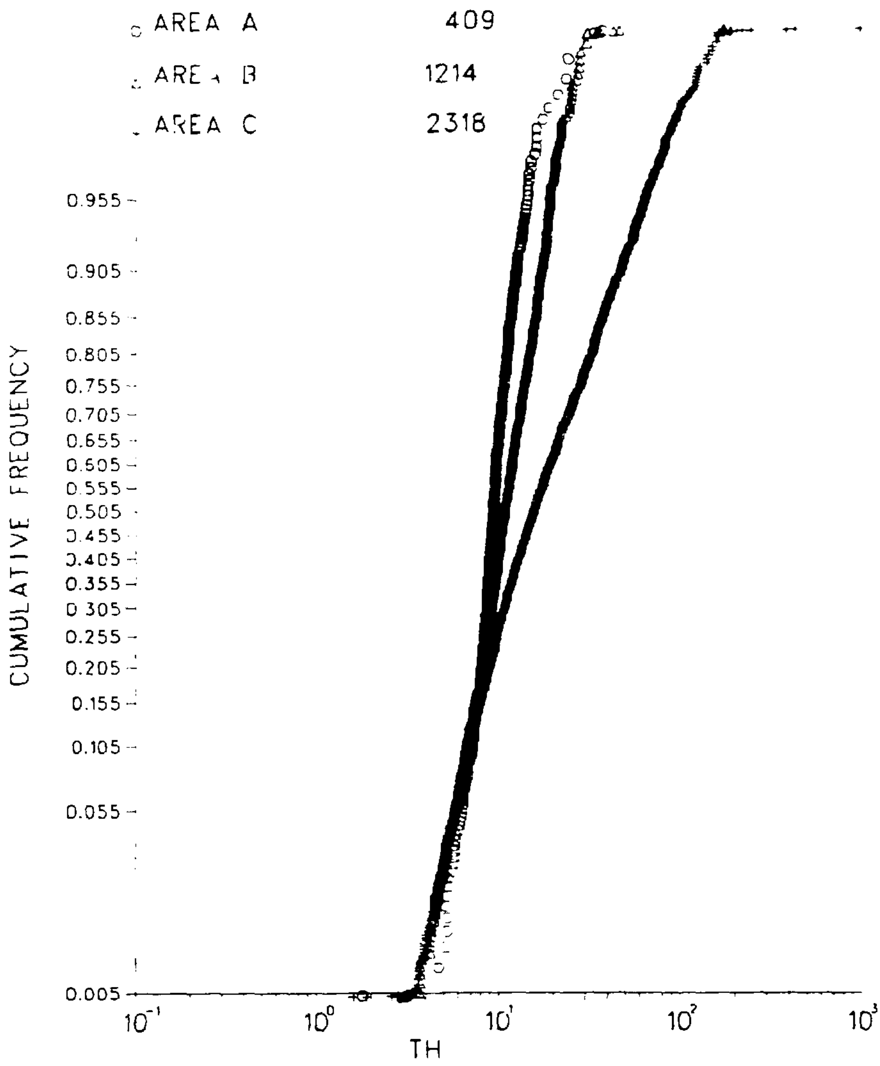
AREA A 409
AREA B 1214
AREA C 2318
CUMULATIVE FREQUENCY
0.955
0.905
0.855
0.805
0.755
0.705
0.655
0.605
0.555
0.505
0.455
0.405
0.355
0.305
0.255
0.205
0.155
0.105
0.055
0.005
10^{-1}
10^{0}
10^{1}
10^{2}
10^{3}
TH

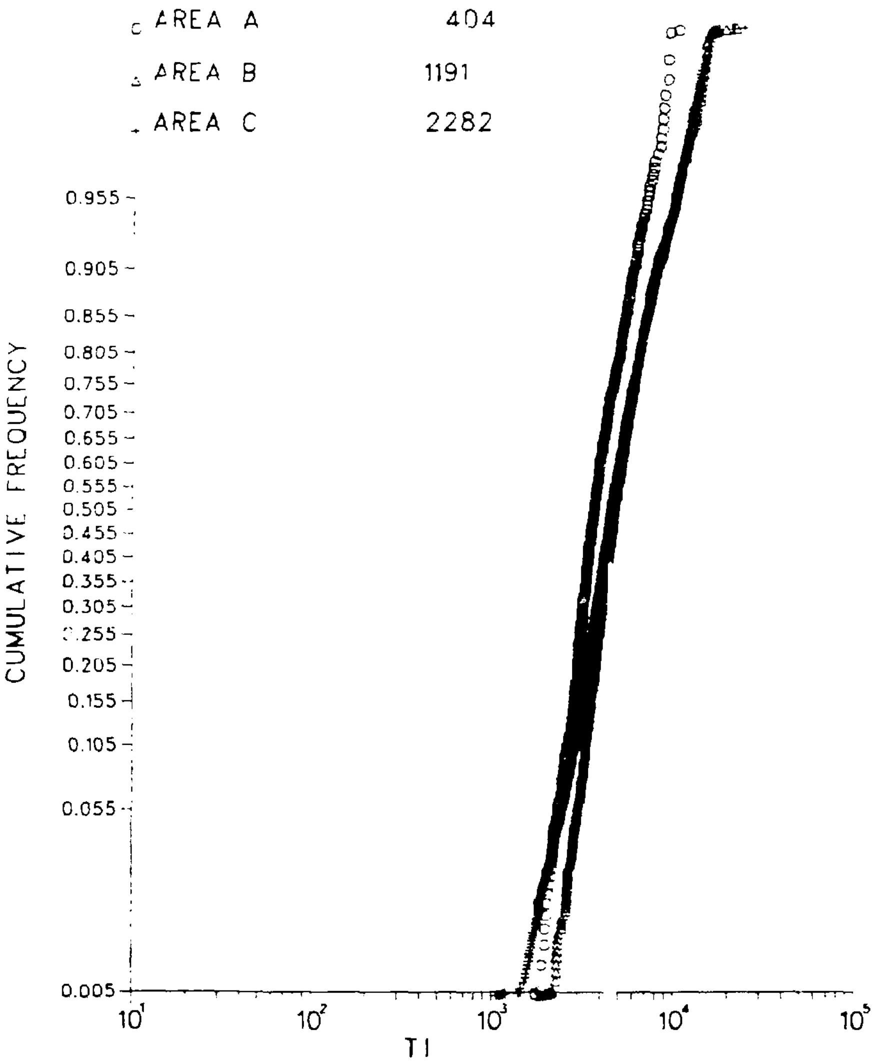
AREA A 404
AREA B 1191
AREA C 2282
CUMULATIVE FREQUENCY
0.955
0.905
0.855
0.805
0.755
0.705
0.655
0.605
0.555
0.505
0.455
0.405
0.355
0.305
0.255
0.205
0.155
0.105
0.055
0.005
10^1
10^2
10^3
10^4
10^5
TI

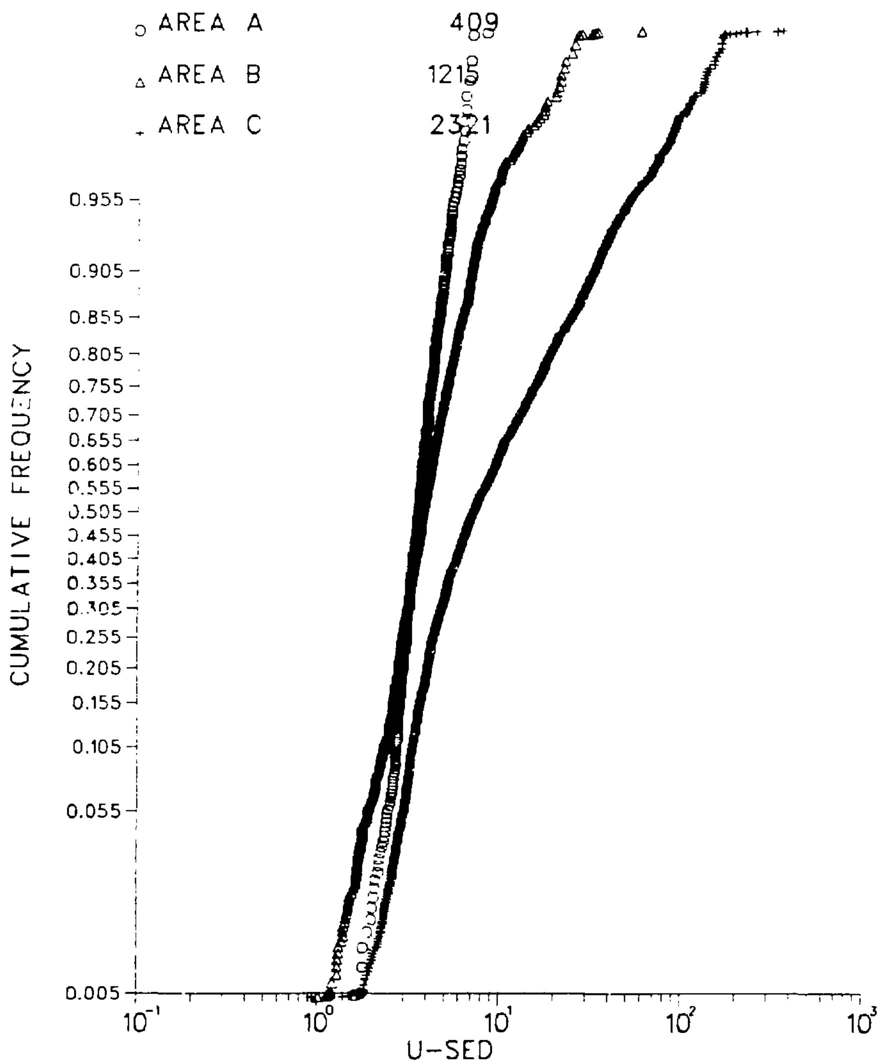
AREA A 409
AREA B 1215
AREA C 2321
CUMULATIVE FREQUENCY
0.955
0.905
0.855
0.805
0.755
0.705
0.655
0.605
0.555
0.505
0.455
0.405
0.355
0.305
0.255
0.205
0.155
0.105
0.055
0.005
10^{-1}
10^{0}
10^{1}
10^{2}
10^{3}
U-SED

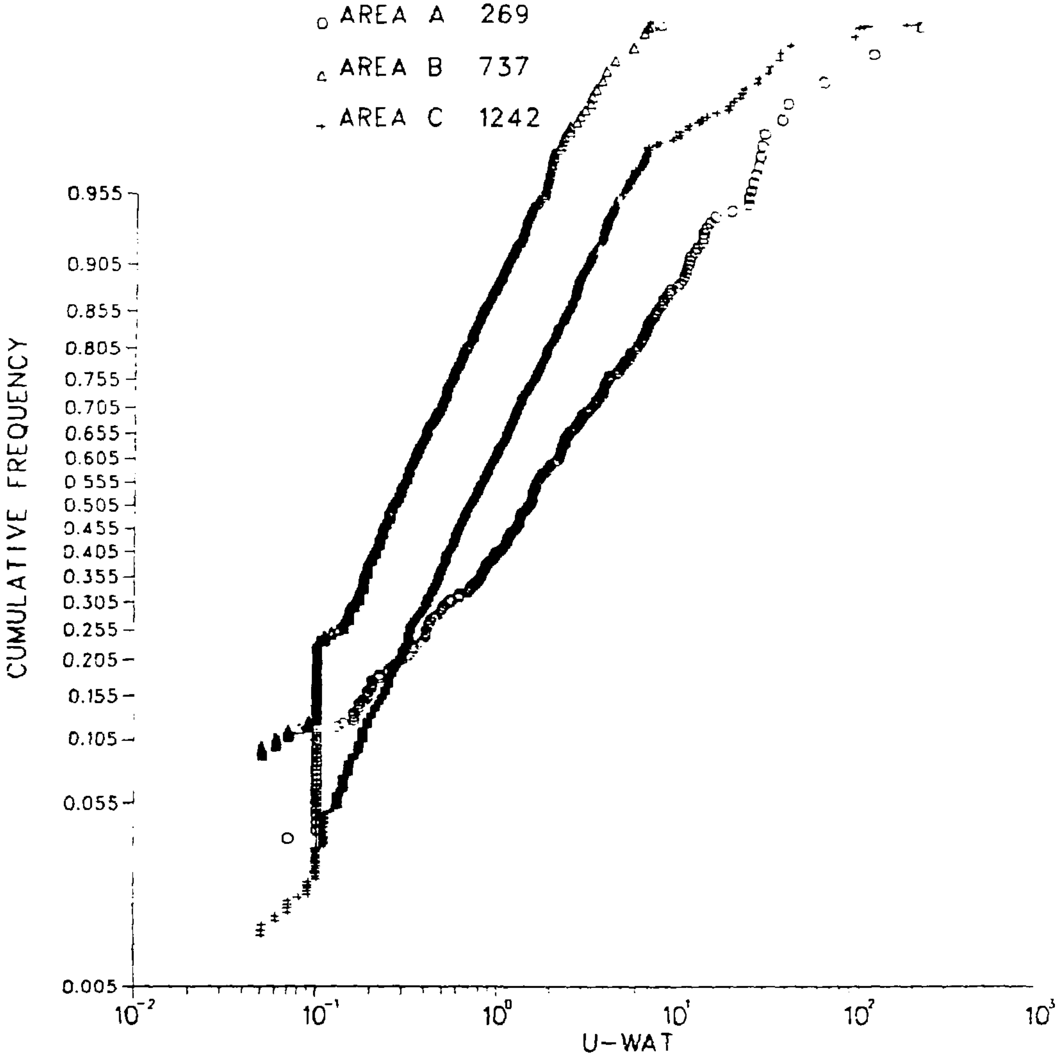

AREA A 269
AREA B 737
AREA C 1242
CUMULATIVE FREQUENCY
0.955
0.905
0.855
0.805
0.755
0.705
0.655
0.605
0.555
0.505
0.455
0.405
0.355
0.305
0.255
0.205
0.155
0.105
0.055
0.005
10^{-2}
10^{-1}
10^{0}
10^{1}
10^{2}
10^{3}
U-WAT

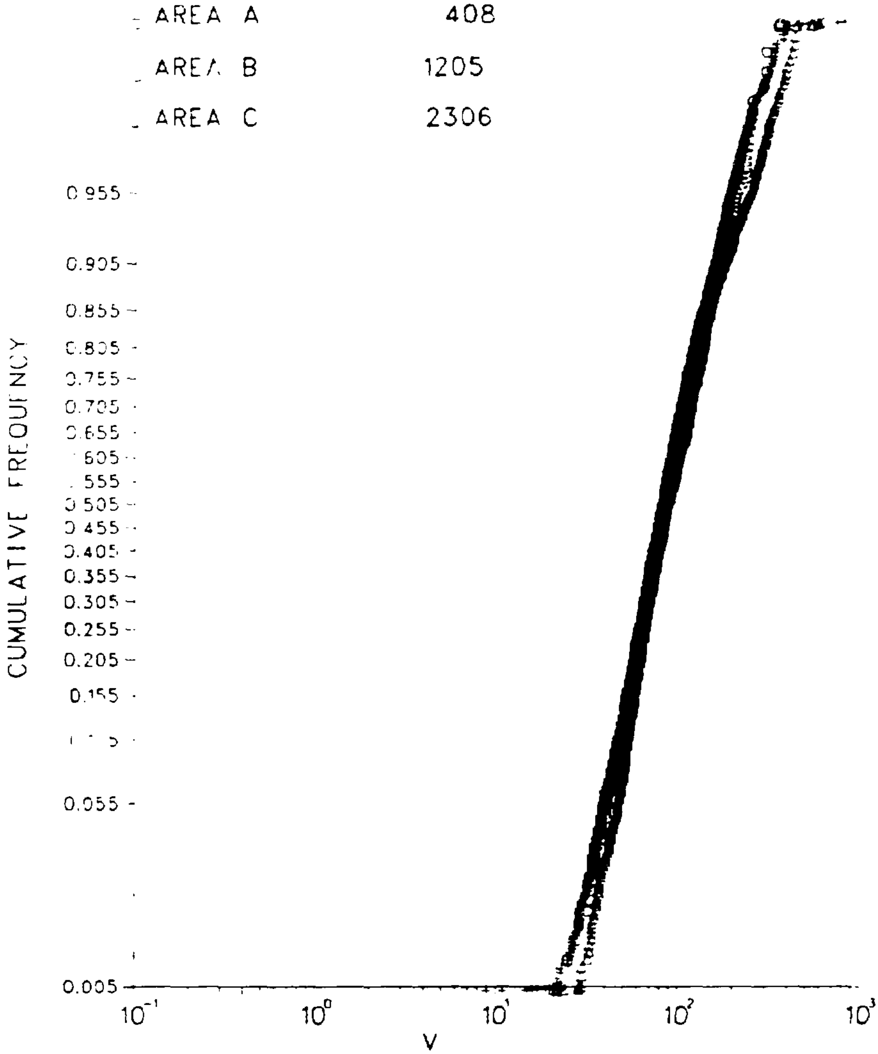

AREA A 408
AREA B 1205
AREA C 2306
CUMULATIVE FREQUENCY
0.955
0.905
0.855
0.805
0.755
0.705
0.655
0.505
0.455
0.405
0.355
0.305
0.255
0.205
0.055
0.005
10^{-1}
10^{0}
10^{1}
10^{2}
10^{3}
V

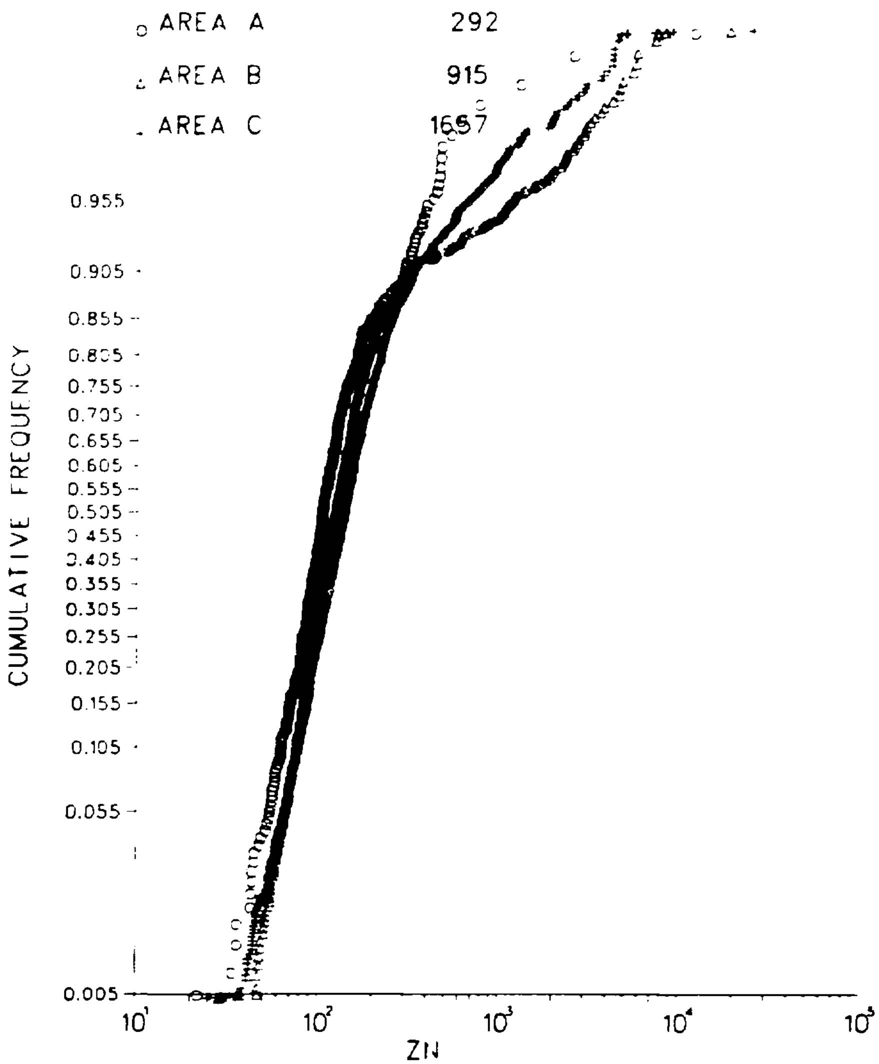
AREA A 292
AREA B 915
AREA C 1657
CUMULATIVE FREQUENCY
0.955
0.905
0.855
0.805
0.755
0.705
0.655
0.605
0.555
0.505
0.455
0.405
0.355
0.305
0.255
0.205
0.155
0.105
0.055
0.005
10^1
10^2
10^3
10^4
10^5
ZN

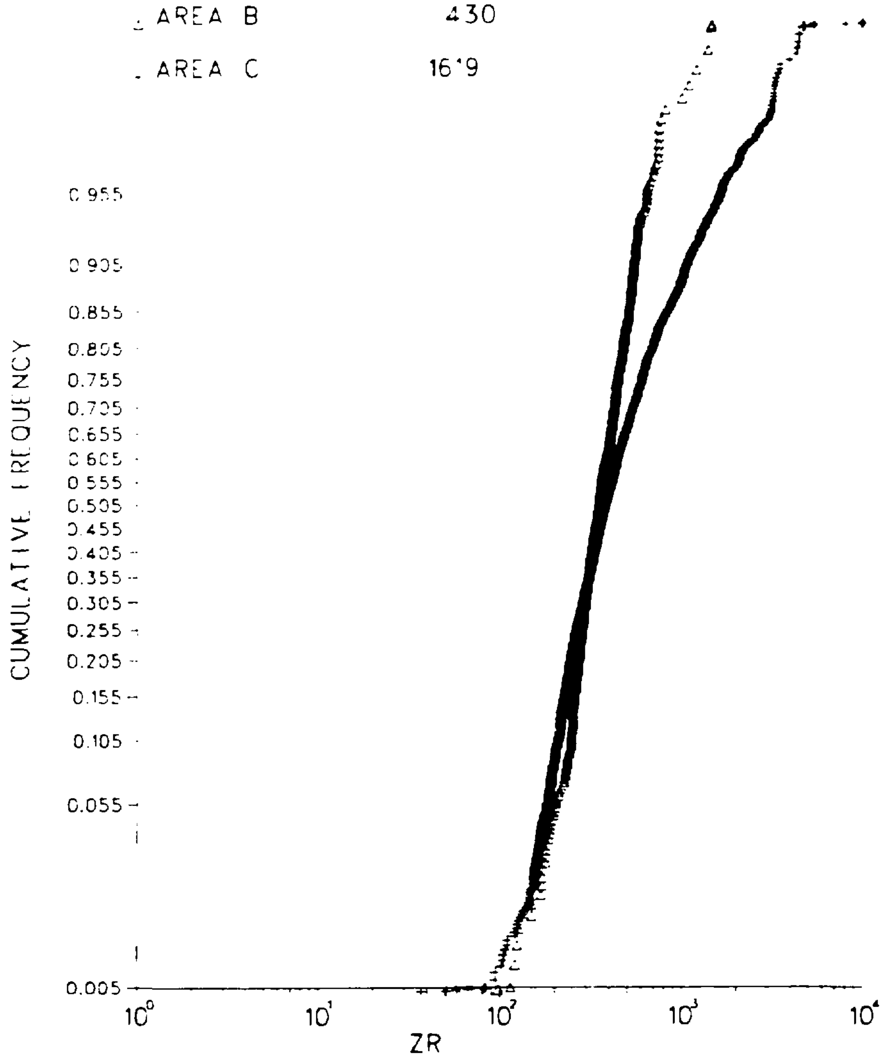

AREA B 430
AREA C 1619
0.955
0.905
0.855
0.805
0.755
0.705
0.655
0.605
0.555
0.505
0.455
0.405
0.355
0.305
0.255
0.205
0.155
0.105
0.055
0.005
CUMULATIVE FREQUENCY
10^0
10^1
10^2
10^3
10^4
ZR

COMPARISON FOR DEPOSIT TYPE 1
USING LOG NORMAL ASSUMPTION FOR STARRED VARIABLES

	DIFFERENCE	PROBABILITY	RATIO	PROBABILITY	D.F.
*U/TH	7.1012	.0000	.1557	.0000	49
*U-S	5.7369	.0000	.3141	.0000	49
K	5.1173	.0000	.5503	.0044	49
*SC	4.2661	.0001	.7436	.0932	49
AL	4.2628	.0001	.5454	.0040	49
BA	4.0517	.0002	1.3952	.9649	49
*LI	4.0274	.0002	.7009	.0557	49
*CE	3.9395	.0003	.7647	.1146	49
*FE	3.8277	.0004	.5493	.0044	49
*HF	3.7656	.0004	.5613	.0056	49
*ZN	3.5132	.0009	.4352	.0009	49
*TH	3.1339	.0029	.6257	.0136	49
*DY	3.0996	.0033	.3650	.2634	49
MN	2.6191	.0117	2.3100	1.0000	49
*CO	2.5324	.0146	.8010	.1609	49
*PB	2.5010	.0153	.6651	.0343	49
*TI	2.3491	.0234	.8599	.2542	49
*E-TH	1.9992	.0531	1.3026	.9262	50
*E-U	1.9435	.0576	1.1719	.8096	50
*U-W	1.6839	.0980	.3901	.0001	47
%K	1.6626	.1026	1.3256	.9337	50
*CU	1.5635	.1232	.3932	.0001	49
*CR	1.4451	.1543	.9673	.4617	49
MAGNETICS	1.2977	.2003	1.9285	.9999	50
*ZR	1.2530	.2214	.6726	.1064	26
*V	.6165	.5404	.5455	.0040	49
*CA	.0372	.9702	.4395	.0008	49
*AS	-.0396	.9687	1.3594	.9951	26

COMPARISON FOR DEPOSIT TYPE 2
USING LOG NORMAL ASSUMPTION FOR STARRED VARIABLES

	DIFFERENCE	PROBABILITY	RATIO	PROBABILITY	D.F.
*U/TH	5.4631	.0000	.3545	.0029	21
*U-S	5.0962	.0000	.2670	.0003	21
*U-W	3.6689	.0015	.9591	.4399	20
*ZR	-3.5306	.0022	.1168	.0000	19
*TI	-3.3214	.0032	.7546	.2218	21
*CR	2.8971	.0056	.8574	.3514	21
*V	-2.8395	.0093	.7100	.1726	21
AL	-2.8037	.0106	1.6590	.9706	21
*PB	2.5664	.0180	.3306	.0043	21
*LI	2.3993	.0258	.5765	.0633	21
*HF	2.3534	.0284	.1410	.0000	21
*DY	2.2554	.0349	.3435	.0026	21
*CO	-2.1513	.0432	1.0640	.6201	21
*E-U	1.9680	.0624	1.4674	.9232	21
*ZN	1.9536	.0642	.5012	.0288	21
*E-TH	-1.3486	.1913	1.0541	.6083	21
*CE	1.1910	.2469	.3525	.0028	21
BA	-.9613	.3473	1.2617	.8118	21
*TH	.8361	.4125	.3377	.0020	21
*SC	-.8333	.4140	.8931	.3992	21
K	.5692	.5753	1.8593	.9903	21
%K	-.5510	.5874	1.4335	.9101	21
MAGNETICS	-.4973	.6233	1.0435	.5955	21
*AS	.3886	.7019	2.3143	.9990	19
*CU	.3427	.7353	.1458	.0000	21
*FE	.1659	.8693	.5902	.0716	21
*CA	.1530	.8799	1.5297	.9431	21
MN	-.0543	.9568	1.3124	.8469	21

COMPARISON FOR DEPOSIT TYPE 3
USING LOG NORMAL ASSUMPTION FOR STARRED VARIABLES

	DIFFERENCE	PROBABILITY	RATIO	PROBABILITY	D.F.
K	-7.9937	.0002	.0787	.0018	6
%K	-7.5052	.0003	.1672	.0145	6
*U/TH	5.2049	.0020	.0258	.0001	6
*HF	-4.3737	.0047	.0358	.0002	6
*LI	4.3369	.0049	.2860	.0561	6
*E-U	3.9296	.0077	.9090	.5130	6
*CA	3.0792	.0217	.9190	.5203	6
AL	-3.0715	.0219	.4446	.1507	6
*TI	-2.8236	.0300	.7166	.3638	6
MAGNETICS	2.3932	.0534	.1825	.0183	6
*ZN	2.2910	.0619	.3397	.1139	6
*U-S	2.2833	.0621	.0137	.0000	6
*TH	-2.0815	.0376	.0111	.0000	6
*U-W	2.1418	.0351	1.3843	.7735	5
*CR	2.0534	.0352	.2137	.0274	6
BA	-1.7306	.1253	1.3831	.7830	6
*SC	-1.7295	.1345	.6023	.2712	6
MN	-1.4513	.1969	1.7328	.8911	6
*FE	-1.0374	.3136	1.1593	.6750	6
*CO	1.0033	.3522	1.3256	.7585	6
*PB	.8704	.4175	.6323	.2955	6
*V	.6254	.5547	.5086	.1976	6
*E-TH	.6035	.5683	.2454	.0387	6
*DY	.4738	.6524	.7527	.3928	6
*CE	-.4550	.6651	.6412	.3026	6
*CU	.4295	.6826	.4169	.1317	6

COMPARISON FOR DEPOSIT TYPE 4
USING LOG NORMAL ASSUMPTION FOR STARRED VARIABLES

	DIFFERENCE	PROBABILITY	RATIO	PROBABILITY	D.F.
%K	-5.9442	.0040	.1713	.0468	4
*U-S	3.0479	.0381	.2697	.1024	4
*ZN	2.9992	.0400	.2773	.1072	4
*PB	2.7813	.0498	.5780	.3214	4
*TH	2.3424	.0792	.2152	.0699	4
*CA	2.3371	.0796	.0293	.0016	4
*U/TH	2.2336	.0892	.3065	.1275	4
*FE	2.2217	.0904	.3507	.1563	4
*CR	2.1315	.1000	.4558	.2317	4
*DY	1.7933	.1474	.8914	.5321	4
*CE	1.6473	.1748	.4393	.2197	4
*LI	1.6103	.1826	.7404	.4357	4
*SC	1.4191	.2289	.2091	.0665	4
AL	1.2674	.2738	.4502	.2277	4
K	1.2235	.2883	.5311	.2871	4
*CU	1.2132	.2918	.7538	.4447	4
*U-W	1.2014	.2958	.4312	.2138	4
*HF	1.1570	.3117	.3390	.1833	4
MAGNETICS	-.9478	.3969	.3371	.1469	4
MN	.8760	.4305	.7118	.4163	[illegible]
*E-U	-.8218	.4573	.5528	.3030	4
*AS	-.7327	.5168	1.6033	.8138	3
*ZR	-.6959	.5365	.3638	.2209	3
*E-TH	-.3932	.7142	2.0979	.9218	4
*CO	.2127	.8420	.8449	.5036	4
*V	.1797	.8661	.9485	.5654	4
*TI	-.0672	.9497	.4145	.2017	4
BA	.0236	.9823	.4524	.2293	4

COMPARISON FOR DEPOSITS OF ALL TYPES
USING LOG NORMAL ASSUMPTION FOR STARRED VARIABLES

	DIFFERENCE	PROBABILITY	RATIO	PROBABILITY	D.F.
*U/TH	9.5337	-.0000	.2157	.0000	35
*U-S	9.2379	-.0000	.2827	.0000	35
*LI	5.2175	.0000	.6940	.0142	35
*ZN	5.0119	.0000	.4658	.0000	35
*U-W	4.4543	.0000	.6882	.0145	31
*PB	4.1434	.0001	.5337	.0003	85
*DY	4.1377	.0001	.7023	.0169	35
*HF	4.0224	.0001	.4232	.0000	85
*CE	3.9306	.0001	.6404	.0040	35
*TH	3.4781	.0008	.4315	.0000	35
*CR	3.4170	.0010	.8505	.1646	35
/ *E-U	3.1028	.0026	1.3289	.9776	[illegible]
K	2.8610	.0053	.9334	.4901	35
*FE	2.6563	.0094	.6562	.0060	85
*SC	2.2146	.0295	.8659	.1935	35
BA	2.0707	.0414	1.5148	.9935	85
*CU	1.9519	.0542	.3462	.0000	85
MN	1.7911	.0768	1.9974	1.0000	35
*CA	1.0430	.2999	.8522	.1675	35
*V	-.9835	.3257	.6436	.0049	35
MAGNETICS	.9441	.3478	1.4610	.9966	36
*CD	.8932	.3743	.9979	.5150	35
*E-TH	.6941	.4895	1.2354	.9315	36
*TI	-.6338	.5279	.9899	.4941	35
%K	-.3976	.6919	1.4033	.9920	36
*ZR	-.2144	.8311	.4728	.0096	50
AL	.0616	.9510	1.1290	.8045	35
*AS	.0231	.9777	1.9728	1.0000	50

APPENDIX F

CORRELATION COEFFICIENTS RAW DATA, MONTROSE QUADRANGLE, COLORADO

(Pages 162 through 169)

(Correlation coefficients >0.50 are graphically plotted for the entire quadrangle and for the plateau, volcanic, and crystalline physiographic/geochemical provinces. The raw data for data set are also included.)

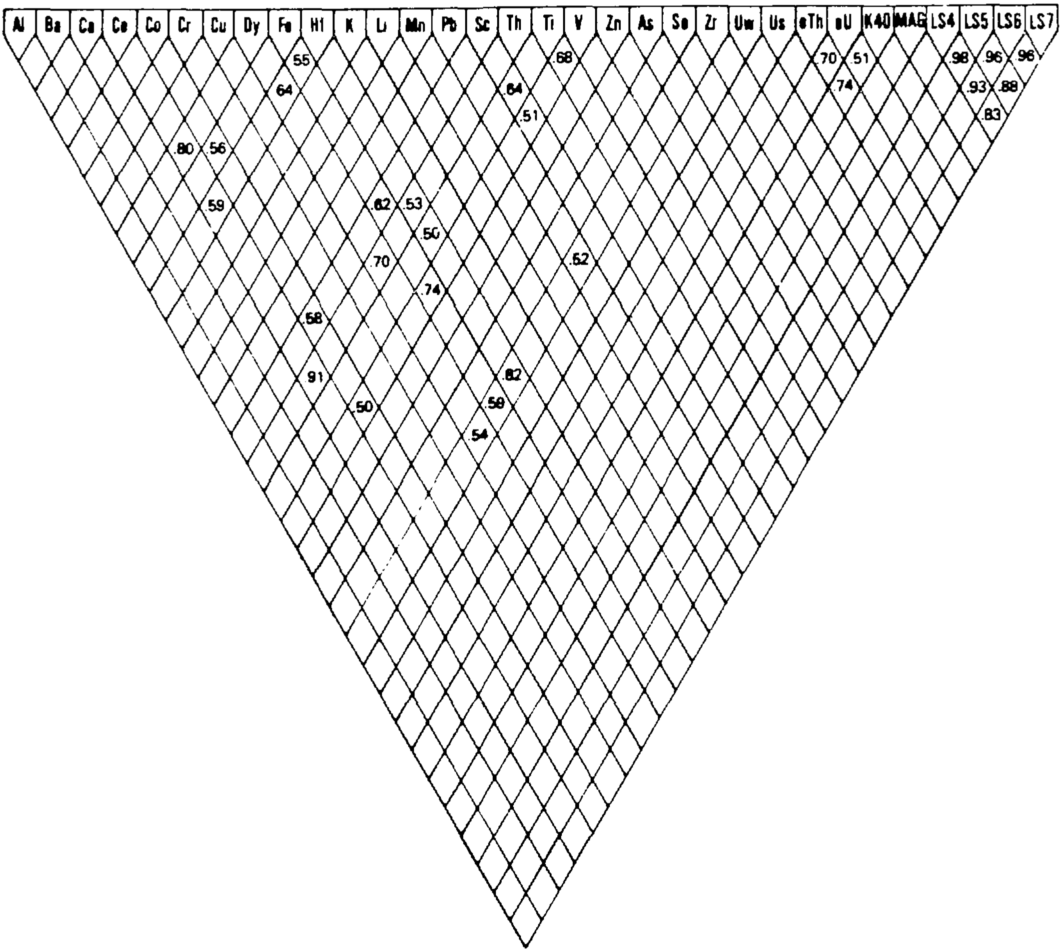

Fig. 1. *Correlation coefficients >0.50 for the entire quadrangle.*

	AL	BA	CA	CE	CO	CR	CU	DY	FE	HF
AL	1.00000	.21774	-.20314	.06679	.13157	-.06022	-.05825	.10541	.03029	-.03190
BA	.21774	1.00000	-.06737	-.01185	-.06773	-.07232	.01466	-.01637	-.00811	-.03760
CA	-.20314	-.06737	1.00000	-.06686	.04944	.04344	-.07867	-.06428	-.01972	-.03469
CE	.06679	-.01185	-.06686	1.00000	.11640	.19458	.00678	.79749	.37475	.59103
CO	.13157	-.02773	.04944	.11640	1.00000	.37772	.17865	.06129	.55994	.11997
CR	-.06022	-.07237	.04344	.19458	.37772	1.00000	-.05918	.26569	.43627	.70550
CU	-.05825	.01466	-.07867	.00678	.17865	-.05918	1.00000	-.00394	.05263	-.02929
DY	.10541	-.01837	-.06428	.79749	.06129	.26569	-.00394	1.00000	.36661	.63619
FE	.03029	-.00811	-.01972	.37475	.55994	.43627	.05265	.36661	1.00000	.56625
HF	-.03190	-.03760	-.03080	.59103	.11997	.70553	-.02929	.63619	.56625	1.00000
K	.46438	.25595	-.20245	.12595	-.21647	-.04274	-.05477	.22831	-.06093	.06978
LI	.12288	-.00514	.11383	.09670	.03712	.17736	.00827	.17163	.07623	.09347
MN	-.02145	-.22387	-.12714	.10931	.44615	-.00620	.75466	-.09700	.20408	.04362
PB	-.06606	.25621	-.06808	.01770	.04477	-.07548	.46590	-.03571	.03763	-.00527
SC	.24056	-.04541	.05564	.24462	.58079	.48337	-.02737	.27545	.62152	.35604
TH	.07466	-.05196	-.06886	.91334	.02831	.13206	-.00394	.68729	.34602	.13236
TI	.23967	.11662	.05972	.31236	.34451	.30785	-.09855	.37120	.57012	.49466
V	.11098	.02551	.18000	.16721	.40577	.32635	-.06654	.15222	.72859	.31313
ZN	-.13366	-.01534	-.00052	.04827	.21490	-.09573	.46049	-.10252	.07454	-.00445
AS	-.10815	.92891	.03207	.16634	.05872	.15208	.03434	.18219	.33234	.25035
SE	-.10638	-.05597	.17669	-.15744	-.07732	-.17167	-.03602	-.25016	-.24609	-.16920
ZR	-.00454	.00649	-.04102	.43637	.14348	.21971	-.00719	.53781	.50763	.67314
UW	-.17833	-.04080	.13547	-.02470	-.06477	.01093	-.01374	-.01702	-.04428	-.01835
US	-.01685	-.03945	-.10082	.22231	-.08343	.06879	.07506	.31534	.09215	.14751
ETH	.09477	.07145	-.10122	.29744	.05032	-.13366	.10019	.21210	.20272	.28056
EU	.01815	.03902	.04177	.15177	-.00943	-.14029	.08142	.08231	.02447	.08744
K40	.19497	.12635	-.17504	.32409	.02054	-.13576	.06454	.24632	.19688	.32710
MAG	-.10158	-.04650	.13482	.07737	.04562	.07426	-.00952	.10398	.08514	.22539
LS4	-.01755	-.06736	.08731	-.01357	-.00534	.02334	-.04876	.00684	-.02195	.01737
LS5	-.02683	-.06010	.10500	-.01765	-.00693	.01556	-.05110	-.00222	-.03346	.01462
LS6	-.02615	-.06948	.21560	-.00556	-.00117	.02960	-.04100	.01316	-.02599	.02318
LS7	-.03220	-.07013	.11540	-.01546	-.00860	.03021	-.03889	.00749	-.03973	.01570

Table 1. ***Correlation coefficients raw data for the entire quadrangle.***

Table 1 continued.

	K	LI	MN	PB	SC	TH	TI	V	ZN	AS
AL	[illegible]	[illegible]	-.02145	[illegible]	.24644	.07641	.23987	.11008	-.13366	-.10815
BA	[illegible]	[illegible]	-.33387	[illegible]	-.04541	-.08155	.21662	.62131	-.01438	.05651
CA	-.33248	.11383	-.12216	-.06468	.05566	-.06664	.05572	.18000	-.09657	.03707
CE	[illegible]	.03670	.10535	.01770	.24607	.51334	.31238	.16721	.04523	.13634
CO	-.22107	.33717	.44535	.04477	.54073	.07831	.38401	.50677	.21490	.08577
CR	[illegible]	.33334	-.00130	-.07046	.46332	.13204	.30765	.32635	-.09973	.15206
CU	-.21472	.00833	.25404	.40590	-.02733	-.00344	-.09896	-.06644	.44049	.03434
DY	.72831	.17163	-.09700	-.03071	.77146	.69770	.37120	.15722	-.10297	.16269
FE	-.06063	.07473	.70409	.03743	.62152	.34602	.57617	.73659	.07554	.33234
HF	.06576	.03367	.06382	-.00622	.35904	.53236	.49468	.31313	-.00445	.25035
K	1.00000	.33314	-.34337	-.07013	-.05318	.13678	.10549	-.09394	-.16410	-.01565
LI	[illegible]	1.00000	-.01149	.01056	.17566	.07326	.01835	-.05145	-.00379	.03366
MN	-.34337	-.01149	1.00000	.17337	.13019	.03547	-.09098	-.03931	.48716	.03141
PB	-.07013	.01056	.17337	1.00000	-.04743	.01657	-.11464	-.06083	.52335	.08643
SC	-.05318	.17566	.13019	-.04743	1.00000	.13428	.63508	.51285	-.04714	.12424
TH	.13678	.07326	.03547	.01657	.13428	1.00000	.21288	.19575	.01998	.16183
TI	.10549	.01835	-.09098	-.11464	.63508	.21288	1.00000	.68114	-.16443	.09930
V	-.09394	-.05145	-.03931	-.06083	.51285	.19575	.68114	1.00000	-.10917	.16796
ZN	-.16410	-.00379	.48716	.52335	-.04714	.01998	-.16443	-.10917	1.00000	.06301
AS	-.01565	.03366	.03141	.08643	.12424	.16183	.09930	.16796	.06301	1.00000
SE	-.27376	-.10868	-.10531	-.01787	-.25076	-.10753	.02346	.06828	-.00052	-.12960
ZR	.13617	.17845	.06802	-.00198	.39865	.36999	.35864	.25890	.00645	.32967
UW	[illegible]	.01083	-.03877	-.00487	-.07567	-.01198	-.05403	-.01025	-.01326	.00756
US	.05970	.11311	.03170	.02433	-.01460	.22714	-.06508	-.04673	.01550	.01366
ETH	.26049	.07707	.11317	.12692	.06676	.33658	.10807	.69307	.14105	.00747
EU	.15887	.06717	.06142	.11436	-.09644	.20686	-.02709	.06332	.09728	-.03166
K40	.31866	.33373	.13660	.08715	.05631	.30126	.13595	.03777	.10762	.00530
MAG	[illegible]	.09676	-.06720	-.04012	.12763	.05296	.17101	.11097	-.07924	.05567
LS4	[illegible]	.10655	-.04059	-.04086	-.00217	.00801	.00447	.01390	-.05362	-.03654
LS5	-.01661	.10092	-.07448	-.04677	-.00465	.00305	.01132	.02567	-.05667	-.03561
LS6	-.06445	.11336	-.09042	-.03767	-.00128	.01679	.02461	.04134	-.05825	-.04874
LS7	[illegible]	.10106	-.10137	-.03709	-.01119	.01149	.02432	.04541	-.05578	-.05534

	SE	ZR	UW	US	ETH	EU	K40	MAG	LS4	LS5
AL	[illegible]	[illegible]	[illegible]	-.01786	.09477	.01619	.19467	-.10158	-.01755	-.02483
BA	[illegible]	.03049	-.04080	-.05565	.07149	.00902	.12635	-.04650	-.06736	-.08010
CA	[illegible]	-.34192	.13947	-.10087	-.10173	.04127	-.17504	.13482	.08731	.10500
CE	[illegible]	.43537	-.03470	.22231	.29744	.15177	.32469	.07037	-.01352	-.01784
CO	[illegible]	.14344	-.05477	-.09343	.05032	-.00549	.07054	.04672	-.00934	-.00643
CR	[illegible]	.31071	.01003	.06875	-.17306	-.14026	-.13376	.07426	.02334	.01950
CU	[illegible]	-.00710	-.03374	.07806	.10015	.06142	.08454	-.00502	-.04826	[illegible]
DY	[illegible]	.13731	-.03707	.31934	.31280	.09221	.28832	.10369	.00666	-.00222
FE	[illegible]	.49700	-.04424	.09931	.20247	.02447	.19486	.06516	-.02195	-.03348
HF	[illegible]	.82776	-.07638	.10751	.28044	.08744	.37710	.22539	.01237	.01462
K	-.27376	[illegible]	[illegible]	.05970	.26049	.15887	.31866	-.06890	-.00585	-.02451
LI	-.10868	.17845	.01083	.11311	.07707	.04213	.03770	.06694	.10455	.10037
MN	-.10531	.06802	-.03877	.03170	.11317	.04142	.13660	-.06720	-.06059	-.07440
PB	-.01787	-.00198	-.00487	.02433	.12692	.11418	.08715	-.04012	-.04086	-.04673
SC	-.25076	.39865	-.07567	-.01460	.06676	-.09644	.05631	.12763	-.00217	-.00465
TH	-.10753	.36999	-.01198	.22714	.33658	.20686	.30126	.05166	.00801	.00305
TI	.02346	.35864	-.05403	-.06508	.10807	-.02709	.13595	.17101	.00447	.01132
V	.06828	.25890	-.01025	-.04673	.69307	.06332	.03777	.11097	.01390	.02567
ZN	-.00052	.00645	-.01326	.01550	.14105	.09728	.10762	-.07924	-.05362	-.05667
AS	-.12960	.32967	.00756	.01366	.00747	-.03166	.00530	.05567	-.03654	-.03561
SE	1.00000	-.44178	.03077	-.04147	-.31030	.04181	-.17761	.11882	.06416	.10843
ZR	-.44178	1.00000	-.01115	.10342	.23274	.04556	.28221	.10100	-.01325	-.01938
UW	.03077	-.01115	1.00000	.03761	-.02467	.00793	-.06501	.00279	.03339	.03636
US	-.04147	.10342	.03761	1.00000	.04000	.07044	.13275	-.05044	.04961	.01329
ETH	[illegible]	.23276	-.02467	.04000	1.00000	.70042	.74013	.13167	-.01353	-.00355
EU	.04181	.04556	.07263	.07044	.70042	1.00000	.50442	.15954	.05367	.00712
K40	-.17761	.28221	-.06501	.13275	.74013	.50442	1.00000	.03162	-.08649	-.08279
MAG	.11882	.10100	.00279	-.05044	.13167	.15954	.03162	1.00000	.14815	.17056
LS4	.06416	-.01325	.03339	.04961	-.01353	.05367	-.08649	.14815	1.00000	.97707
LS5	.10843	-.01938	.03636	.01329	-.00349	.08710	-.08279	.17059	.97707	1.00000
LS6	.10923	-.01567	.04402	.02766	-.01838	.08201	-.10645	.17467	.92592	.95541
LS7	.12613	-.03028	.04652	.01876	-.03930	.05223	-.13271	.15835	.83086	.87757

	LS6	LS7
AL	-.02815	[illegible]
BA	-.06546	-.07013
CA	.11160	.11540
CE	-.03990	-.01564
CO	-.06117	[illegible]
CR	.02940	.03021
CU	-.04100	[illegible]
DY	.01314	.09740
FE	-.02599	[illegible]
HF	.02318	.01570
K	-.00445	-.01134
LI	.11306	.10106
MN	-.09042	-.10137
PB	-.03767	-.03709
SC	-.00128	-.01119
TH	.01679	.01149
TI	.02461	.02432
V	.04134	.04541
ZN	-.05825	-.05578
AS	-.04874	-.05534
SE	.10923	.12613
ZR	-.01567	-.03028
UW	.04402	.04652
US	.02766	.01876
ETH	-.01838	-.03930
EU	.08201	.05223
K40	-.10645	-.13271
MAG	.17467	.15835
LS4	.92592	.83086
LS5	.95541	.87757
LS6	1.00000	[illegible]
LS7	[illegible]	1.00000

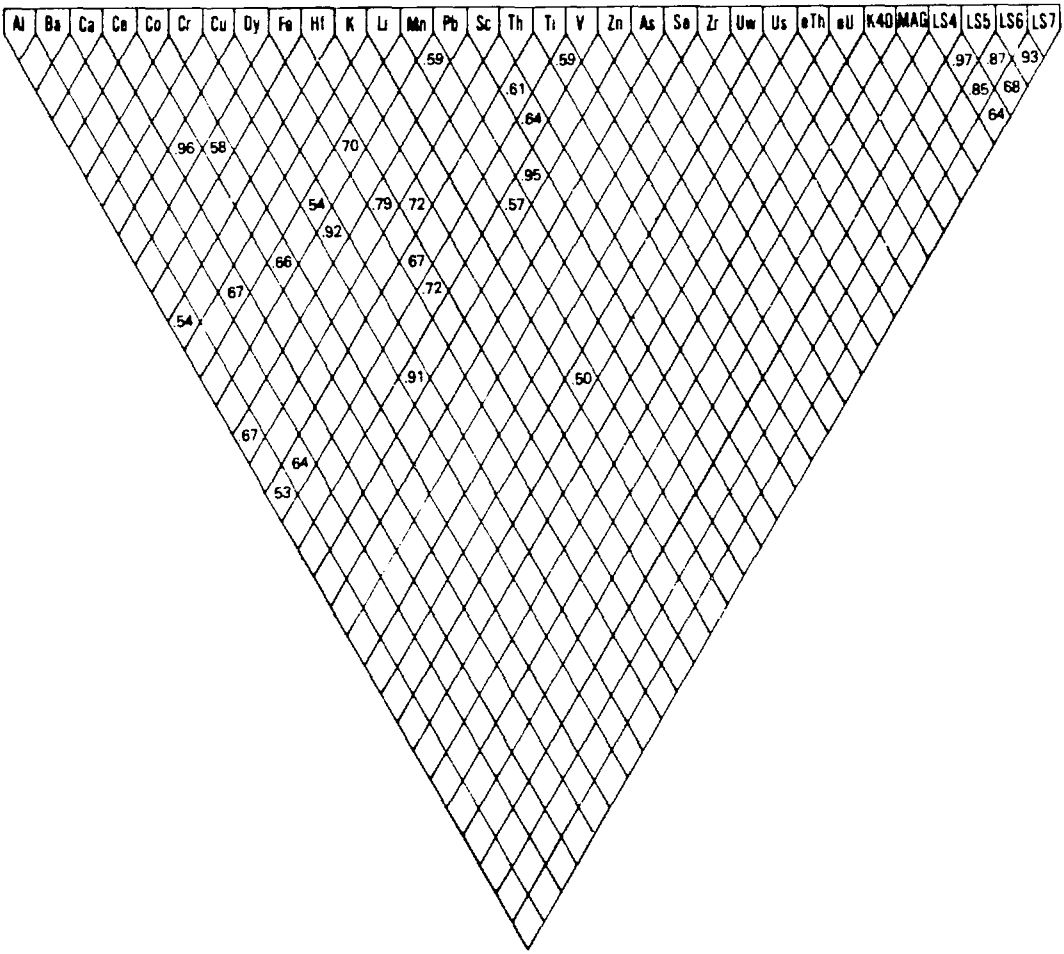

Fig. 2. *Correlation coefficients >0.50 for the plateau province.*

	AL	BA	CA	CE	CO	CR	CU	DY	FE	HF
AL	1.00000	.45547	-.20427	.06681	.22903	.14357	-.19252	.05099	.38008	-.17991
BA	.45547	1.00000	-.22711	-.14065	-.09402	.09496	-.19628	-.20834	.33397	.11766
CA	-.20427	-.22711	1.00000	-.07264	.05175	.07760	-.08080	-.02506	-.06781	-.30163
CE	.06681	-.14065	-.07264	1.00000	.37760	.20561	-.00091	.95610	.70209	.24622
CO	.22903	-.09403	.05175	.37760	1.00000	-.00906	.33875	.36111	.57913	-.05316
CR	.14357	.09406	.02760	.20961	-.00906	1.00000	-.11214	.14623	.06122	.21513
CU	-.19252	-.19628	-.08080	-.00091	.33875	-.11214	1.00000	-.07339	.29084	-.06922
DY	.05099	-.20834	-.02506	.95610	.38111	.14623	-.07339	1.00000	.07836	.17706
FE	.38008	.33397	-.06781	.20209	.57913	.06172	.29084	.07836	1.00000	-.02389
HF	-.17991	.11766	-.30163	.24622	-.05316	.21513	-.06822	.17766	-.62389	1.00000
K	.53975	.43847	-.25791	-.02791	-.26870	.19734	-.33334	-.01232	-.16272	.10259
LI	-.07840	-.28738	.68771	-.04338	.01878	.09047	.03048	.00953	-.11278	-.40989
MN	.08322	.05749	-.06953	.21231	.66376	-.17577	.53600	.11908	.70508	.07383
PB	-.25151	-.21714	-.08265	-.01550	.32666	-.08226	.91987	-.10192	.29456	-.05438
SC	.67215	.39902	-.06670	.14090	.47436	.23838	.05704	.02872	.78745	-.08978
TH	.20320	.19590	-.22348	.24736	.03163	.34248	-.06745	.14751	.08983	.71899
TI	.53158	.64417	-.28403	.05076	.17804	.21377	-.16349	-.02349	.66974	.24959
V	.44622	.39513	.29772	-.02907	.31976	.16487	-.06931	-.07093	.72305	-.25554
ZN	-.24421	-.25718	-.05906	.09726	.38273	-.05586	.90590	.02717	.27928	-.03378
AS	99.00000	99.00000	99.00000	99.00000	99.00000	99.00000	99.00000	99.00000	99.00000	99.00000
SE	99.00000	99.00000	99.00000	99.00000	99.00000	99.00000	99.00000	99.00000	99.00000	99.00000
ZR	99.00000	99.00000	99.00000	99.00000	99.00000	99.00000	99.00000	99.00000	99.00000	99.00000
UW	-.05598	.00968	.13306	-.03235	-.02619	.01832	-.01760	-.01179	-.03981	-.06530
US	.09836	-.21225	.45674	.21301	.15701	.23224	-.06952	.24784	.00507	.08651
ETH	.03776	-.07867	.08443	.04108	-.08769	.10381	-.15581	.10074	-.20615	-.09474
EU	-.12766	-.21440	.43307	.02957	-.08560	.15205	-.09118	.10173	-.22358	-.21657
K40	.33546	.24541	-.00701	.00383	.07550	.12458	.07215	-.02651	.21970	-.10103
MAG	-.04163	-.14473	.06556	-.07445	-.19001	.00119	-.11837	-.02834	-.21476	-.08547
LS4	-.12013	-.21573	.28830	-.06836	-.15988	.04753	-.05262	-.02640	-.18351	-.22982
LS5	-.13519	-.21464	.25818	-.07203	-.18369	.02867	-.01281	-.03116	-.18433	-.21593
LS6	-.11661	-.18922	.24652	-.04893	-.13774	.03728	-.01188	-.02649	-.12839	-.17356
LS7	-.06476	-.16310	.18625	-.00960	-.11178	.03614	-.00583	-.00360	-.08155	-.11055

Table 2. *Correlation coefficients raw data for the plateau province*

Table 2 continued.

	K	LI	MN	PB	SC	TH	TI	V	ZN	AS
AL	.53975	-.07960	.08327	-.25151	.67219	.20320	.53158	.44822	-.24471	99.00000
BA	.43447	-.28738	.05740	-.21716	.38907	.15950	.64417	.30513	-.25718	99.00000
CA	-.25791	.68771	-.08953	-.08265	-.06670	-.22348	-.28603	.29772	-.05906	99.00000
CE	-.02791	-.04338	.23231	-.01550	.14090	.24736	.05076	-.02907	.09728	99.00000
CO	-.26870	.01879	.46376	.32666	.47636	.03163	.17804	.31976	.38273	99.00000
CR	.15234	.09067	-.12477	-.08226	.23838	.34748	.21377	.16487	-.05446	99.00000
CU	-.13334	.03049	.53600	.91987	.05704	-.06245	-.16349	-.06931	.40590	99.00000
DY	-.01232	.09953	.11908	-.10192	.02672	.14751	-.02349	-.07093	.02717	99.00000
FE	-.11272	-.11979	.70108	.29856	.78745	.08983	.66974	.72305	.27928	99.00000
HF	.10299	-.40980	.07383	-.05438	-.08978	.71899	.24959	-.25554	-.03378	99.00000
K	1.00000	-.15106	-.40616	-.44344	.11170	.27315	.30545	-.01170	-.42995	99.00000
LI	-.15106	1.00000	-.14291	.02990	-.03770	-.12687	-.36908	.19282	.04169	99.00000
MN	-.40616	-.14291	1.00000	.59058	.45848	.01444	.26707	.28617	.57098	99.00000
PB	-.44344	.02990	.59058	1.00000	.05680	-.06523	-.16551	-.09682	.95005	99.00000
SC	.11170	-.03770	.45848	.05680	1.00000	.19139	.61297	.63979	.03880	99.00000
TH	.27315	-.12887	.01444	-.06523	.19139	1.00000	.25356	-.01188	-.05026	99.00000
TI	.30545	-.36908	.26207	-.16551	.61297	.25356	1.00000	.59179	-.17445	99.00000
V	-.01170	.19282	.28617	-.05682	.63979	-.01188	.59179	1.00000	-.07517	99.00000
ZN	-.42995	.04169	.57098	.95005	.03880	-.05026	-.17445	-.07517	1.00000	99.00000
AS	99.00000	99.00000	99.00000	99.00000	99.00000	99.00000	99.00000	99.00000	99.00000	99.00000
SE	99.00000	99.00000	99.00000	99.00000	99.00000	99.00000	99.00000	99.00000	99.00000	99.00000
ZR	99.00000	99.00000	99.00000	99.00000	99.00000	99.00000	99.00000	99.00000	99.00000	99.00000
UW	-.02986	.10731	-.04786	-.01736	-.06130	-.07097	-.03186	.07908	-.01691	99.00000
US	-.00470	.59701	-.09052	-.09796	.07650	.36754	-.11068	.30740	-.05823	99.00000
ETH	.12175	.11974	-.26907	-.15322	-.13866	.09165	-.14530	-.06433	-.11287	99.00000
EU	-.05873	.38813	-.27735	-.09681	-.18669	-.08196	-.33148	.03179	-.07700	99.00000
K40	.21349	-.06747	.08798	.04506	.29497	.04938	.22613	.28106	.05707	99.00000
MAG	-.01506	.17908	-.19079	-.12651	-.17276	-.11468	-.18922	-.09055	-.13334	99.00000
LS4	-.06038	.38136	-.27571	-.06254	-.14397	-.05950	-.26044	.03752	-.06478	99.00000
LS5	-.09175	.34231	-.27467	-.06257	-.14817	-.07092	-.24969	.07335	-.06619	99.00000
LS6	-.06345	.31207	-.21528	-.02001	-.11083	-.05460	-.21749	.05229	-.03464	99.00000
LS7	-.04206	.21389	-.19188	.00800	-.06859	-.02903	-.15015	.05654	-.01325	99.00000

	SE	ZR	UW	US	ETH	EU	K40	MAG	LS4	LS5
AL	99.00000	99.00000	-.08908	.09836	.03776	-.12766	.33546	-.09163	-.12013	-.13519
BA	99.00000	99.00000	.00968	-.21275	-.07867	-.21640	.24541	-.14823	-.21570	-.21464
CA	99.00000	99.00000	.13306	.45874	.06443	.43307	-.00701	.06555	.28830	.25618
CE	99.00000	99.00000	-.03235	.71301	.04108	.07997	.00383	-.07445	-.06836	-.07203
CO	99.00000	99.00000	-.02419	.15701	-.04769	-.08560	.07530	-.19001	-.15986	-.16365
CR	99.00000	99.00000	.01877	.23724	.10381	.15205	.12458	.00119	.04753	.02667
CU	99.00000	99.00000	-.01780	-.06587	-.35581	-.09110	.07715	-.11837	-.05767	-.05281
DY	99.00000	99.00000	-.01179	.24784	.10074	.10173	-.02051	-.02834	-.02640	-.03116
FE	99.00000	99.00000	-.03981	.00107	-.20615	-.22358	.21970	-.21476	-.18351	-.18433
HF	99.00000	99.00000	-.06530	.08651	-.09476	-.21657	-.10103	-.08547	-.22982	-.21593
K	99.00000	99.00000	-.02986	-.00470	.12175	-.05873	.21349	-.01506	-.08038	-.09175
LI	99.00000	99.00000	.10731	.59701	.11924	.38513	-.06747	.17908	.38136	.34231
MN	99.00000	99.00000	-.04784	-.09052	-.26907	-.27735	.08798	-.19079	-.27571	-.27467
PB	99.00000	99.00000	-.01736	-.09796	-.15322	-.09681	.04506	-.12651	-.06254	-.06257
SC	[illegible]	[illegible]	-.06130	.07650	-.13866	-.18669	.29497	-.17276	-.14397	-.14817
TH	[illegible]	99.00000	-.07097	.36754	.09165	-.08196	.04938	-.11468	-.05950	-.07092
TI	99.00000	99.00000	-.03186	-.11068	-.14530	-.33148	.22613	-.18922	-.26044	-.24969
V	99.00000	99.00000	.07908	.30740	-.06433	.03179	.28106	-.09055	.03752	.07335
ZN	99.00000	99.00000	-.01691	-.05823	-.11287	-.07700	.05707	-.13334	-.06478	-.06619
AS	99.00000	99.00000	99.00000	99.00000	99.00000	99.00000	99.00000	99.00000	99.00000	99.00000
SE	99.00000	99.00000	99.00000	99.00000	99.00000	99.00000	99.00000	99.00000	99.00000	99.00000
ZR	99.00000	99.00000	99.00000	99.00000	99.00000	99.00000	99.00000	99.00000	99.00000	99.00000
UW	99.00000	99.00000	1.00000	.17309	.11467	.12774	.07332	.02743	.12075	.11174
US	99.00000	99.00000	.17309	1.00000	.14170	.32637	.06964	.08445	.25226	.22912
ETH	99.00000	99.00000	.11467	.14170	1.00000	.44680	.45424	.03054	.16341	.14458
EU	99.00000	99.00000	.12774	.32637	.44680	1.00000	.13880	.12296	.47800	.41039
K40	99.00000	99.00000	.07332	.06964	.45424	.13880	1.00000	-.06888	-.18482	-.21147
MAG	99.00000	99.00000	.02743	.08445	.03054	.12296	-.06888	1.00000	.05887	.05487
LS4	99.00000	99.00000	.12075	.25226	.16341	.47800	-.18482	.05887	1.00000	.97266
LS5	99.00000	99.00000	.11174	.22912	.14458	.41039	-.21147	.05487	.97266	1.00000
LS6	99.00000	99.00000	.04123	.22360	.05237	.34695	-.20513	.03669	.85043	.87206
LS7	99.00000	99.00000	.04231	.18267	.03126	.21347	-.16574	-.03476	.64021	.67669

	LS6	LS7
AL	-.11861	-.29476
BA	-.18502	-.16410
CA	.24617	.18625
CE	-.04853	-.09049
CO	-.13774	-.11176
CR	.05228	.07414
CU	-.01888	-.00547
DY	-.02449	-.00140
FE	-.17630	-.09155
HF	-.17356	-.11044
K	-.06345	-.04206
LI	.31207	.21389
MN	-.21528	-.19188
PB	-.02001	.00800
SC	-.11083	-.06859
TH	-.05460	-.02903
TI	-.21749	-.15015
V	.05229	.05654
ZN	-.03464	-.01325
AS	99.00000	99.00000
SE	99.00000	99.00000
ZR	99.00000	99.00000
UW	.04120	.04231
US	.22360	.18267
ETH	.05237	.03126
EU	.34695	.21347
K40	-.20513	-.16574
MAG	.03669	-.03476
LS4	.85043	.64021
LS5	.87206	.67669
LS6	1.00000	.82844
LS7	.82844	1.00000

NOTE: 99.00000 indicates no data

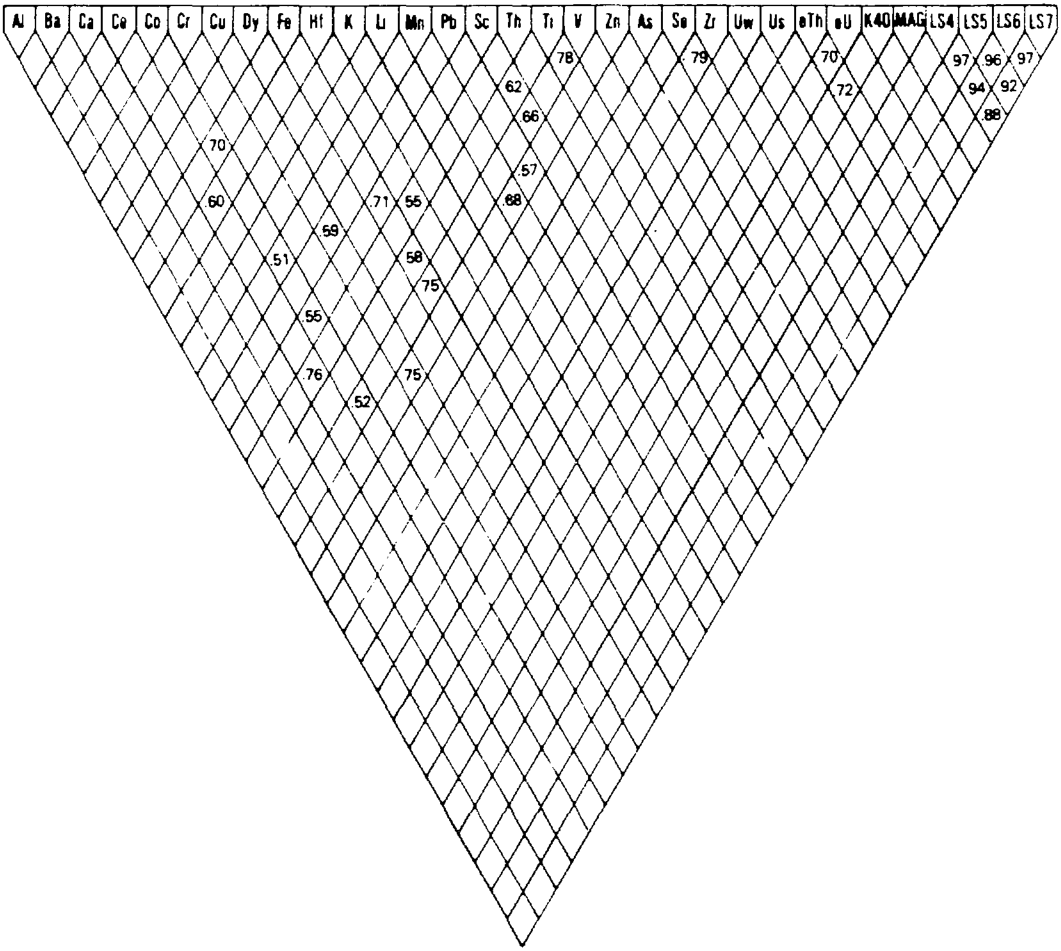

Fig. 3. Correlation coefficients >0.50 for the volcanic province.

	AL	BA	CA	CE	CO	CR	CU	DY	FE	HF
AL	1.00000	.14717	.11964	.13467	.12204	.00111	-.10437	.21249	.06161	.04831
BA	.14717	1.00000	.02147	.12722	-.13922	.05085	.13617	.22217	.19460	.15559
CA	.11964	.02147	1.00000	-.05948	.12265	.05892	-.20367	.05324	.17113	-.12531
CE	.13467	.12722	-.05948	1.00000	.23677	.31306	.21048	.49766	.26300	.06470
CO	.12204	-.13922	.22766	.23677	1.00000	.26069	.27206	-.10664	.69669	.07799
CR	.00111	.05085	.05892	.31306	.26069	1.00000	-.06826	.32313	.28080	.31660
CU	-.10437	.13617	-.20367	.21048	.27206	-.06826	1.00000	-.18669	.20525	.05519
DY	.21249	.22217	.05324	.49766	-.10664	.32313	-.18669	1.00000	.11673	.40135
FE	.06161	.19460	.17113	.26300	.69669	.28060	.20525	.11673	1.00000	.26913
HF	.04831	.15553	-.12534	.06470	.07799	.31689	.05519	.40135	.26913	1.00000
K	.42691	.47767	-.06948	.13565	-.27614	.07610	-.16613	.34434	-.12754	.19567
LI	.12675	.13685	.03860	.18383	-.02670	.10510	.02467	.13694	.00987	.15098
MN	-.04975	-.40834	-.14615	.27741	.01234	-.06436	.44001	-.45478	.19989	.02973
PB	-.06676	.26010	-.16616	.11790	.01664	-.07387	.59330	-.05461	.15156	.03554
SC	.38150	.04336	.26932	.21436	.14188	.29798	.00467	.22740	.71083	.12170
TH	.20023	.17503	-.19900	.76204	.01564	.26224	.11468	.45537	.08990	.55127
TI	.27004	.18068	.37676	.19067	.30226	.27641	-.10966	.29409	.58223	.25076
V	.19956	.11437	.35163	.01901	.51976	.36053	-.09149	.11646	.75427	.09752
ZN	-.12029	.08864	-.22675	.22691	.35467	-.09536	.74605	-.33282	.21724	.05037
AS	-.07835	.47130	-.07587	.66014	.06238	.03974	.33169	.15730	.31032	.13195
SE	-.04567	-.16775	.14656	-.31433	-.05571	-.18460	-.03575	-.24729	-.24799	-.23087
ZR	.01032	.24065	-.17620	.30738	.09204	.21775	.17132	.26553	.30714	.40866
UW	-.12938	.00374	.01865	-.04548	-.06604	-.06922	.04316	-.06384	-.08575	-.04166
US	.02241	.06959	-.20200	.35963	.01662	.05170	.14177	.28250	-.02648	.25668
ETH	.00957	.18556	-.28763	.25690	-.03067	-.03064	.20366	.02327	.03131	.14767
EU	.01621	.07307	-.25648	.11600	-.03106	-.07772	.12037	.01460	-.06206	.08466
K40	.00804	.15496	-.26137	.26256	-.05306	-.02645	.13947	.01605	-.03416	.19643
MAG	-.09279	-.10677	.00110	-.19229	-.09365	-.01570	-.07430	-.08165	-.10109	-.08330
LS4	.12034	-.04154	.12971	-.15151	-.03406	-.06122	-.13583	-.01621	-.05588	-.03446
LS5	.11896	-.03907	.13651	-.15161	-.03567	-.04769	-.13349	-.02762	-.05549	-.02737
LS6	.13747	-.04768	.15076	-.18139	-.02611	-.06293	-.15098	-.04184	-.05496	-.04796
LS7	.13257	-.06154	.14561	-.18605	-.02554	-.06624	-.15171	-.04072	-.06118	-.05423

Table 3. Correlation coefficients raw data for the volcanic province.

Table 3 continued.

	K	LI	MN	PB	SC	TH	TI	V	ZN	AS
AL	[illegible]	[illegible]	[illegible]	[illegible]	.31109	.10127	.27004	.29976	-.12079	[illegible]
BA	[illegible]	[illegible]	-.40628	[illegible]	.04386	.17743	.16108	.11437	.06015	.42130
CA	[illegible]	.13846	-.18615	-.14831	.36130	-.15570	.37176	.35113	-.22675	[illegible]
CE	[illegible]	.18313	.27761	.11700	.21634	.74705	.19092	.04901	.22691	.09016
CO	[illegible]	-.09870	.01776	.55554	.54186	.01544	.36776	.51976	.35407	.06036
CR	[illegible]	.10510	-.06474	-.07787	.29705	.26224	.27661	.30013	-.08536	[illegible]
CU	[illegible]	.07687	.44001	.59350	.00467	.11454	-.10900	-.09159	.74605	[illegible]
DY	[illegible]	.17704	-.45479	-.01461	.22740	.45037	.20409	.11468	-.33287	[illegible]
FE	[illegible]	.08087	.10088	.15114	.71063	.08590	.86223	.75427	.21774	.31092
HF	[illegible]	[illegible]	.02073	.03554	.12170	.59127	.25076	.09752	.05035	.13195
K	1.00000	.22861	-.41711	-.06757	-.07230	.24719	.17889	-.06610	-.2142.	.00410
LI	[illegible]	1.00000	.07768	.02414	.05651	.12037	-.05482	-.07569	.01145	.05906
MN	-.41711	.07768	1.00000	.15367	.10571	.08504	-.19390	-.10913	.68195	.02591
PB	[illegible]	.07416	.10347	1.00000	.00774	2207	-.10243	-.00908	.56722	.20926
SC	[illegible]	.05651	.10571	.00774	1.00000	02313	.62124	.66776	-.00867	.04015
TH	[illegible]	.13077	.08804	.12207	.02313	1.00000	.11756	-.02474	.10954	.07043
TI	[illegible]	-.05477	-.10900	-.10263	.62124	.11756	1.00000	.78362	-.17705	.00675
V	[illegible]	-.07540	-.10513	-.00908	.64774	-.02474	.78362	1.00000	-.12451	.03633
ZN	[illegible]	.01145	.68105	.56722	-.00867	.10956	-.17705	-.12451	1.00000	.32046
AS	[illegible]	.05800	.02501	.20926	.04015	.07043	.00675	.03933	.32046	1.00000
SE	[illegible]	-.27054	-.05555	-.04555	-.12895	-.21472	.09604	.06476	-.00209	-.06342
ZR	[illegible]	.17005	.13098	.07559	.14388	.26642	-.02170	-.01950	.14940	.29362
UW	[illegible]	.08471	-.02904	.02653	-.13246	-.07142	-.09227	-.06931	.04378	.05314
US	[illegible]	.11974	.10087	.14154	-.07770	.42057	-.07855	-.11029	.14565	.03685
ETH	.20440	.16776	.14288	.20858	-.10331	.29108	-.13633	-.14115	.20333	.09176
EU	[illegible]	.03871	.09727	.14815	-.13744	.21454	-.08984	-.09168	.17399	.07944
K40	.22229	.17454	.13737	.14566	-.14577	.21201	-.19542	-.21317	.14915	.09035
MAG	[illegible]	-.03115	-.09020	-.05844	-.16108	-.12448	-.13077	-.07533	-.09765	-.03456
LS4	[illegible]	-.00011	-.13717	-.00005	-.01048	-.10407	.08062	.09222	-.15967	-.11034
LS5	[illegible]	.01577	-.13471	-.00577	-.00203	-.11674	.07485	.08977	-.16000	[illegible]
LS6	[illegible]	.00315	-.14982	-.11106	-.00256	-.14378	.10806	.11655	-.17958	-.11772
LS7	[illegible]	-.07588	-.15406	-.11466	-.00648	-.14292	.11874	.12391	-.18230	[illegible]

	SE	ZR	UW	US	ETH	EU	K40	MAG	LS4	LS5
AL	[illegible]	[illegible]	-.12936	.02741	.00992	.01921	.00864	-.09279	.12034	.11694
BA	[illegible]	.26744	.00374	.06959	[illegible]	.02392	.15694	-.10473	-.04154	-.03907
CA	[illegible]	-.17836	.01805	-.10200	-.24763	-.20480	-.26117	.00110	.1757	[illegible]
CE	[illegible]	[illegible]	-.04548	[illegible]	[illegible]	.11600	.26756	-.19229	-.15151	[illegible]
CO	[illegible]	.30704	-.04164	.01482	-.03087	-.03104	-.05904	-.09345	-.03905	[illegible]
CR	[illegible]	[illegible]	-.04577	.01130	-.03054	-.07772	-.02645	-.01576	-.06122	[illegible]
CU	[illegible]	.17177	.06314	.14277	.30244	.12077	.17947	-.07530	-.13563	[illegible]
DY	[illegible]	[illegible]	-.01344	.29410	.02227	.01468	.01605	-.07168	-.01621	-.02767
FE	[illegible]	.34774	-.04728	-.07444	.07171	-.08271	-.02414	-.17104	-.05588	[illegible]
HF	[illegible]	.34564	-.04106	.21008	.14767	.01448	.19843	-.06330	-.03446	[illegible]
K	[illegible]	[illegible]	-.00010	.17712	.20440	.02187	.22809	-.05175	.05638	.00716
LI	[illegible]	[illegible]	.01475	.11164	.14776	.03471	.17456	-.03111	-.00111	.01535
MN	[illegible]	[illegible]	[illegible]	[illegible]	[illegible]	.06727	.13737	-.05028	-.13717	-.13421
PB	[illegible]	[illegible]	.02653	.14154	.20858	.14815	.14566	-.05645	-.09405	-.00877
SC	[illegible]	.14388	-.13246	-.07735	-.10331	-.13744	-.16972	-.16108	-.01048	[illegible]
TH	[illegible]	.26642	-.07142	.42057	.29108	.21454	.21201	-.12448	-.10407	-.11474
TI	[illegible]	-.02170	-.09227	-.07855	-.13633	-.08984	-.19542	-.13077	.08062	.07685
V	[illegible]	-.01950	-.06931	-.11029	-.14115	-.09168	-.21317	-.07533	.09222	.08977
ZN	[illegible]	.14940	.04378	.14565	.20333	.17399	.15915	-.09765	-.15967	-.16000
AS	-.06342	.29362	.05314	.03685	.09178	.02944	.09039	-.03456	-.11034	[illegible]
SE	1.00000	-.28220	.12123	-.20700	-.37148	-.07974	-.30304	.15230	.18116	.16287
ZR	-.28220	1.00000	-.04737	.23977	.36408	.07576	.32605	-.14782	-.18328	-.14076
UW	.12123	-.04737	1.00000	.02652	-.00353	-.01362	-.03153	.05227	-.01065	-.00683
US	-.20701	.23977	.02652	1.00000	.36635	.26650	.28447	-.08351	-.05417	-.06253
ETH	-.37148	.36403	-.00353	.36635	1.00000	.70394	.72032	-.04702	-.13351	-.12072
EU	-.07974	.07866	-.01362	.26650	.70394	1.00000	.46548	.06072	-.00817	-.00405
K40	-.30304	.32605	-.03153	.28447	.72032	.46548	1.00000	-.02137	-.13645	-.11936
MAG	.15730	-.14982	.01227	-.08351	-.04702	.06072	-.02137	1.00000	.16173	.19769
LS4	.18116	-.18328	-.01065	-.05417	-.13351	-.00817	-.13645	.16173	1.00000	.97414
LS5	.16257	-.18076	-.00683	-.08253	-.12072	-.00405	-.11936	.19769	.97414	1.00000
LS6	.22454	-.22462	-.00903	-.10641	-.17012	-.02493	-.17417	.17647	.93651	.96705
LS7	.25192	-.25276	-.00216	-.10956	-.15421	-.01547	-.20621	.15400	.87674	.91777

	LS6	LS7
AL	.13747	.11257
BA	-.04759	-.06156
CA	.15076	.14601
CE	-.16119	-.18805
CO	-.02611	-.02654
CR	-.06793	-.04474
CU	-.15096	-.15171
DY	-.04164	-.04072
FE	-.05496	-.06118
HF	-.04796	-.05423
K	.05178	.03935
LI	.00315	-.00588
MN	-.14987	-.15406
PB	-.11106	-.11465
SC	-.00256	-.00648
TH	-.14378	-.14292
TI	.10606	.11874
V	.11655	.12391
ZN	-.17958	-.18233
AS	-.11772	-.12773
SE	.22454	.25102
ZR	-.22462	-.25276
UW	-.00903	-.00216
US	-.10641	-.10956
ETH	-.17012	-.15421
EU	-.02493	-.01547
K40	-.17417	-.20621
MAG	.17647	.15400
LS4	.93651	.87674
LS5	.96705	.91777
LS6	1.00000	.95371
LS7	.95371	1.00000

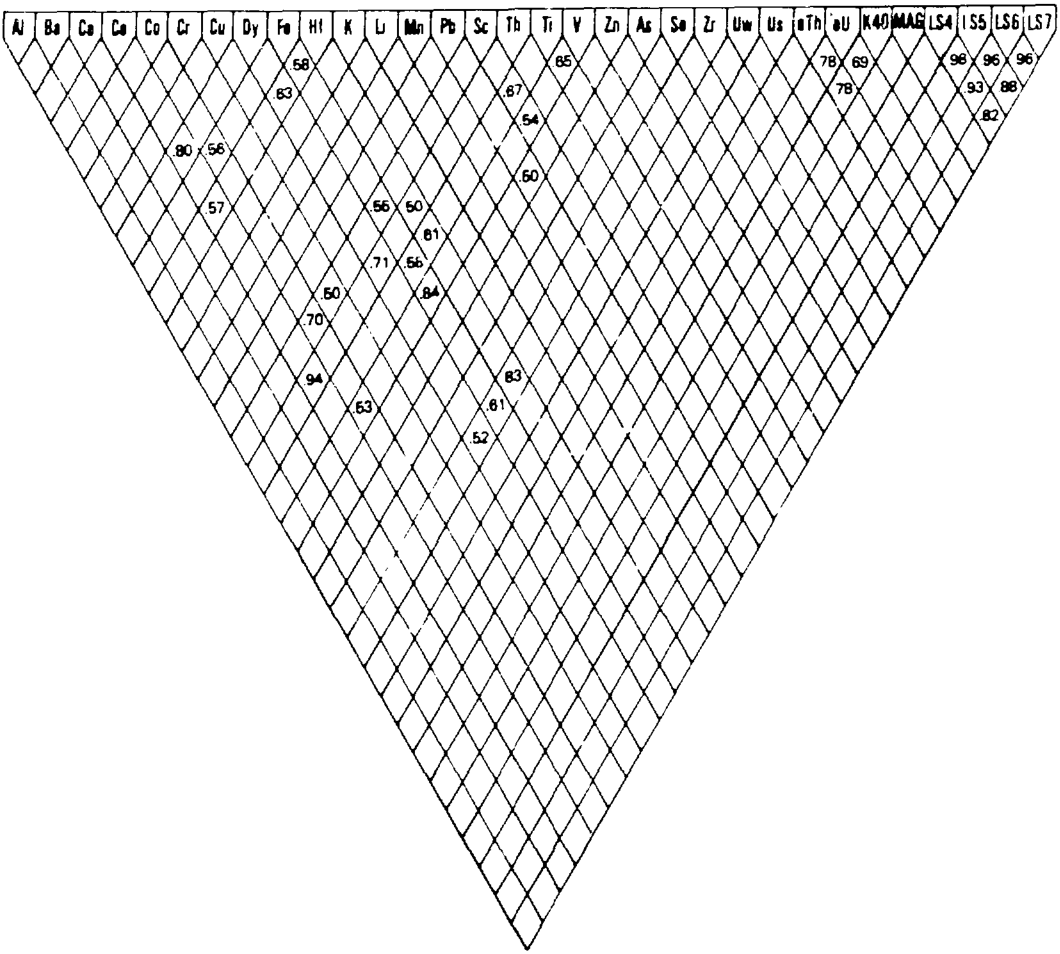

Fig. 4. Correlation coefficients >0.50 for the crystalline province.

	AL	BA	CA	CE	CO	CR	CU	DY	FE	HF
AL	1.00000	.19184	-.29261	.06212	.06784	-.05701	-.03768	.12169	-.05062	-.04671
BA	.19184	1.00000	-.05654	-.01071	-.07467	-.05197	-.03855	-.02332	-.08346	-.03735
CA	-.29261	-.05654	1.00000	-.06144	.01676	.04950	-.04538	-.05604	.00848	.01737
CE	.06212	-.01071	-.06144	1.00000	.06606	.12839	-.02549	.80302	.35863	.17393
CO	.06784	-.07467	.01676	.06606	1.00000	.48481	.11513	.08320	.51779	.17007
CR	-.05701	-.05197	.04950	.12836	.48481	1.00000	-.05809	.17790	.46343	.13591
CU	-.03768	-.03855	-.04538	-.02549	.11513	-.05809	1.00000	-.05612	-.00811	-.04440
DY	.12169	-.02332	-.05604	.80302	.08320	.17390	-.05612	1.00000	.35925	.63455
FE	-.05062	-.08349	.00848	.35863	.51779	.46343	-.00811	.35925	1.00000	.57827
HF	-.04671	-.03735	.01737	.17393	.17007	.13591	-.04440	.63455	.57827	1.00000
K	.45040	.16433	-.22466	.09264	-.19472	-.18530	.00654	.17753	-.11940	.00516
LI	.23736	.02674	-.02757	.03877	.11292	.09655	.00188	.10621	.05473	.04262
MN	-.09343	-.10994	-.08726	.08431	.36729	.07757	.11232	-.02756	.22943	.07067
PB	-.09388	.27405	-.04056	-.00241	.01726	-.09583	.32983	-.04666	-.01200	-.01835
SC	.17124	-.07709	.09130	.16688	.65564	.50071	-.04890	.33408	.54676	.39595
TH	.02339	-.04890	-.07654	.63514	.03806	.05079	-.01718	.71118	.34813	.50113
TI	.16334	.03977	.07678	.36851	.42658	.36268	-.09784	.46019	.57969	.60793
V	-.00139	-.06647	.09658	.26927	.53714	.43339	-.05563	.25830	.84773	.47576
ZN	-.15008	-.07586	-.06282	.01291	.07184	-.10641	.29066	-.07630	.00544	-.02892
AS	-.14384	-.04135	.08883	.14443	.10077	.19267	-.03746	.17479	.32758	.24571
SE	-.12160	-.05417	.06657	-.02116	-.06668	-.05373	-.03263	-.10632	-.17982	-.05769
ZR	-.02091	-.01330	.01376	.40292	.15196	.15937	-.03073	.51634	.60816	.62537
UW	-.15204	-.03813	.12733	-.01620	-.07216	-.00744	-.01529	-.07127	-.03691	-.01697
US	-.02005	-.03560	-.11099	.17141	-.13116	-.01451	.02015	.25671	.03543	.03802
ETH	.10808	.03547	-.04899	.30358	.05123	-.14665	.07009	.23586	.27908	.29556
EU	.07024	.02136	-.01768	.21745	.02750	-.17600	.06735	.15604	.11849	.14564
K40	.16224	.05521	-.07645	.34757	.02496	-.16926	.06382	.36776	.19600	.37916
MAG	-.01960	.04104	.12587	.16837	.20649	.06635	-.05683	.19514	.26155	.34097
LS4	-.00682	-.02716	-.01614	.01036	.05010	-.00647	-.01012	-.00782	.01391	.01542
LS5	-.00909	-.01358	.00053	.01721	.05929	-.00373	-.01290	-.00130	.01231	.02973
LS6	-.01441	-.01336	.00536	.03061	.06065	.00227	.01300	.01402	.02066	.03837
LS7	-.02697	-.00779	.01137	.02541	.05609	.01051	.01995	.01285	.00775	.03437

Table 4. Correlation coefficients raw data for the Crystalline province.

Table 4 continued.

	K	LI	MN	PB	SC	TH	TI	V	ZN	AS
AL	[illegible]	[illegible]	[illegible]	[illegible]	[illegible]	[illegible]	[illegible]	[illegible]	[illegible]	[illegible]
BA	[illegible]	[illegible]	[illegible]	[illegible]	[illegible]	[illegible]	[illegible]	[illegible]	[illegible]	[illegible]
CA	[illegible]	[illegible]	[illegible]	[illegible]	[illegible]	[illegible]	[illegible]	[illegible]	[illegible]	[illegible]
CE	[illegible]	[illegible]	[illegible]	[illegible]	[illegible]	[illegible]	[illegible]	[illegible]	[illegible]	[illegible]
CO	[illegible]	[illegible]	[illegible]	[illegible]	[illegible]	[illegible]	[illegible]	[illegible]	[illegible]	[illegible]
CR	[illegible]	[illegible]	[illegible]	[illegible]	[illegible]	[illegible]	[illegible]	[illegible]	[illegible]	[illegible]
CU	[illegible]	[illegible]	[illegible]	[illegible]	[illegible]	[illegible]	[illegible]	[illegible]	[illegible]	[illegible]
DY	[illegible]	[illegible]	[illegible]	[illegible]	[illegible]	[illegible]	[illegible]	[illegible]	[illegible]	[illegible]
FE	[illegible]	[illegible]	[illegible]	[illegible]	[illegible]	[illegible]	[illegible]	[illegible]	[illegible]	[illegible]
HF	[illegible]	[illegible]	[illegible]	[illegible]	[illegible]	[illegible]	[illegible]	[illegible]	[illegible]	[illegible]
K	[illegible]	[illegible]	[illegible]	[illegible]	[illegible]	[illegible]	[illegible]	[illegible]	[illegible]	[illegible]
LI	[illegible]	[illegible]	[illegible]	[illegible]	[illegible]	[illegible]	[illegible]	[illegible]	[illegible]	[illegible]
MN	[illegible]	[illegible]	[illegible]	.15812	.14479	[illegible]	-.15733	[illegible]	.27644	.04628
PB	[illegible]	[illegible]	[illegible]	1.00000	[illegible]	[illegible]	[illegible]	-.08492	.50237	[illegible]
SC	[illegible]	[illegible]	[illegible]	[illegible]	1.00000	[illegible]	[illegible]	.54099	-.06725	[illegible]
TH	[illegible]	[illegible]	[illegible]	[illegible]	[illegible]	1.00000	[illegible]	[illegible]	.01933	[illegible]
TI	[illegible]	[illegible]	[illegible]	[illegible]	[illegible]	[illegible]	1.00000	.64828	[illegible]	[illegible]
V	[illegible]	[illegible]	[illegible]	[illegible]	[illegible]	[illegible]	[illegible]	1.00000	[illegible]	[illegible]
ZN	[illegible]	[illegible]	[illegible]	[illegible]	[illegible]	[illegible]	[illegible]	-.10837	1.00000	[illegible]
AS	[illegible]	[illegible]	[illegible]	[illegible]	[illegible]	[illegible]	.12361	.24765	[illegible]	1.00000
SE	[illegible]	[illegible]	[illegible]	[illegible]	[illegible]	[illegible]	[illegible]	[illegible]	[illegible]	[illegible]
ZR	[illegible]	[illegible]	[illegible]	[illegible]	[illegible]	[illegible]	[illegible]	[illegible]	[illegible]	[illegible]
UW	[illegible]	[illegible]	[illegible]	[illegible]	[illegible]	[illegible]	[illegible]	[illegible]	[illegible]	[illegible]
US	[illegible]	[illegible]	[illegible]	[illegible]	[illegible]	[illegible]	[illegible]	[illegible]	[illegible]	[illegible]
ETH	[illegible]	[illegible]	[illegible]	[illegible]	[illegible]	[illegible]	[illegible]	[illegible]	[illegible]	[illegible]
EU	[illegible]	[illegible]	[illegible]	[illegible]	[illegible]	[illegible]	[illegible]	[illegible]	[illegible]	[illegible]
K40	[illegible]	[illegible]	[illegible]	[illegible]	[illegible]	[illegible]	[illegible]	[illegible]	[illegible]	[illegible]
MAG	[illegible]	[illegible]	[illegible]	[illegible]	[illegible]	[illegible]	[illegible]	[illegible]	[illegible]	[illegible]
LS4	[illegible]	[illegible]	[illegible]	[illegible]	[illegible]	[illegible]	[illegible]	[illegible]	[illegible]	[illegible]
LS5	[illegible]	[illegible]	[illegible]	[illegible]	[illegible]	[illegible]	[illegible]	[illegible]	[illegible]	[illegible]
LS6	[illegible]	[illegible]	[illegible]	[illegible]	[illegible]	[illegible]	[illegible]	[illegible]	[illegible]	[illegible]
LS7	[illegible]	[illegible]	[illegible]	[illegible]	[illegible]	[illegible]	[illegible]	[illegible]	[illegible]	[illegible]

	SE	ZR	UW	US	ETH	EU	K40	MAG	LS4	LS5
AL	[illegible]	[illegible]	[illegible]	[illegible]	[illegible]	[illegible]	[illegible]	[illegible]	[illegible]	[illegible]
BA	[illegible]	[illegible]	[illegible]	[illegible]	[illegible]	[illegible]	[illegible]	[illegible]	[illegible]	[illegible]
CA	[illegible]	[illegible]	[illegible]	[illegible]	[illegible]	[illegible]	[illegible]	[illegible]	[illegible]	[illegible]
CE	[illegible]	[illegible]	[illegible]	[illegible]	[illegible]	[illegible]	[illegible]	[illegible]	[illegible]	[illegible]
CO	[illegible]	[illegible]	[illegible]	[illegible]	[illegible]	[illegible]	[illegible]	[illegible]	[illegible]	[illegible]
CR	[illegible]	[illegible]	[illegible]	[illegible]	[illegible]	[illegible]	[illegible]	[illegible]	[illegible]	[illegible]
CU	[illegible]	[illegible]	[illegible]	[illegible]	[illegible]	[illegible]	[illegible]	[illegible]	[illegible]	[illegible]
DY	[illegible]	[illegible]	[illegible]	[illegible]	[illegible]	[illegible]	[illegible]	[illegible]	[illegible]	[illegible]
FE	[illegible]	[illegible]	[illegible]	[illegible]	[illegible]	[illegible]	[illegible]	[illegible]	[illegible]	[illegible]
HF	[illegible]	[illegible]	[illegible]	[illegible]	[illegible]	[illegible]	[illegible]	[illegible]	[illegible]	[illegible]
K	[illegible]	[illegible]	[illegible]	[illegible]	[illegible]	[illegible]	[illegible]	[illegible]	[illegible]	[illegible]
LI	[illegible]	[illegible]	[illegible]	[illegible]	[illegible]	[illegible]	[illegible]	[illegible]	[illegible]	[illegible]
MN	[illegible]	[illegible]	[illegible]	[illegible]	[illegible]	[illegible]	[illegible]	[illegible]	[illegible]	[illegible]
PB	[illegible]	[illegible]	[illegible]	[illegible]	[illegible]	[illegible]	[illegible]	[illegible]	[illegible]	[illegible]
SC	[illegible]	[illegible]	[illegible]	[illegible]	[illegible]	[illegible]	[illegible]	[illegible]	[illegible]	[illegible]
TH	[illegible]	[illegible]	[illegible]	[illegible]	[illegible]	[illegible]	[illegible]	[illegible]	[illegible]	[illegible]
TI	[illegible]	[illegible]	[illegible]	[illegible]	[illegible]	[illegible]	[illegible]	[illegible]	[illegible]	[illegible]
V	[illegible]	[illegible]	[illegible]	[illegible]	[illegible]	[illegible]	[illegible]	[illegible]	[illegible]	[illegible]
ZN	[illegible]	[illegible]	[illegible]	[illegible]	[illegible]	[illegible]	[illegible]	[illegible]	[illegible]	[illegible]
AS	[illegible]	[illegible]	[illegible]	[illegible]	[illegible]	[illegible]	[illegible]	[illegible]	[illegible]	[illegible]
SE	[illegible]	[illegible]	[illegible]	[illegible]	[illegible]	[illegible]	[illegible]	[illegible]	[illegible]	[illegible]
ZR	[illegible]	[illegible]	[illegible]	[illegible]	[illegible]	[illegible]	[illegible]	[illegible]	[illegible]	[illegible]
UW	[illegible]	[illegible]	[illegible]	[illegible]	[illegible]	[illegible]	[illegible]	[illegible]	[illegible]	[illegible]
US	[illegible]	[illegible]	[illegible]	[illegible]	[illegible]	[illegible]	[illegible]	[illegible]	[illegible]	[illegible]
ETH	[illegible]	[illegible]	[illegible]	[illegible]	[illegible]	[illegible]	[illegible]	[illegible]	[illegible]	[illegible]
EU	[illegible]	[illegible]	[illegible]	[illegible]	[illegible]	1.00000	[illegible]	[illegible]	[illegible]	[illegible]
K40	[illegible]	[illegible]	[illegible]	[illegible]	[illegible]	[illegible]	1.00000	[illegible]	[illegible]	[illegible]
MAG	[illegible]	[illegible]	[illegible]	[illegible]	[illegible]	[illegible]	[illegible]	1.00000	[illegible]	[illegible]
LS4	[illegible]	[illegible]	[illegible]	[illegible]	[illegible]	[illegible]	[illegible]	[illegible]	1.00000	[illegible]
LS5	[illegible]	[illegible]	[illegible]	[illegible]	[illegible]	[illegible]	[illegible]	[illegible]	[illegible]	1.00000
LS6	[illegible]	[illegible]	[illegible]	[illegible]	[illegible]	[illegible]	[illegible]	[illegible]	[illegible]	[illegible]
LS7	[illegible]	[illegible]	[illegible]	[illegible]	[illegible]	[illegible]	[illegible]	[illegible]	[illegible]	[illegible]

	LS6	LS7
AL	[illegible]	[illegible]
BA	[illegible]	[illegible]
CA	[illegible]	[illegible]
CE	[illegible]	[illegible]
CO	[illegible]	[illegible]
CR	[illegible]	[illegible]
CU	[illegible]	[illegible]
DY	[illegible]	[illegible]
FE	[illegible]	[illegible]
HF	[illegible]	[illegible]
K	[illegible]	[illegible]
LI	[illegible]	[illegible]
MN	[illegible]	[illegible]
PB	[illegible]	[illegible]
SC	[illegible]	[illegible]
TH	[illegible]	[illegible]
TI	[illegible]	[illegible]
V	[illegible]	[illegible]
ZN	[illegible]	[illegible]
AS	[illegible]	[illegible]
SE	[illegible]	[illegible]
ZR	[illegible]	[illegible]
UW	[illegible]	[illegible]
US	[illegible]	[illegible]
ETH	[illegible]	[illegible]
EU	[illegible]	[illegible]
K40	[illegible]	[illegible]
MAG	[illegible]	[illegible]
LS4	[illegible]	[illegible]
LS5	[illegible]	[illegible]
LS6	[illegible]	[illegible]
LS7	[illegible]	1.00000

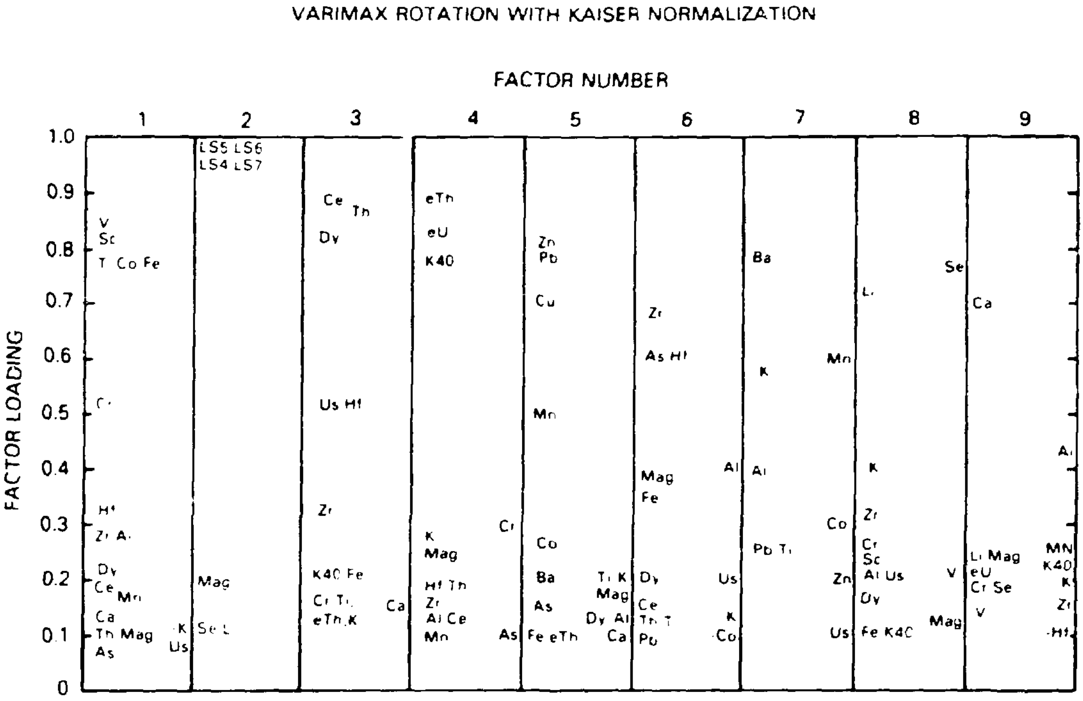

Fig. 1 *Graphical representation of factor score data for the Montrose quadrangle, Colorado.*

Table 1. Factor scores raw data for the Montrose quadrangle, Colorado.

	FACTOR 1	FACTOR 2	FACTOR 3	FACTOR 4	FACTOR 5	FACTOR 6	FACTOR 7	FACTOR 8	FACTOR 9
AL	.33075	-.33874	.01478	.14563	-.17747	-.43247	.39373	.21649	-.42116
BA	.02497	-.06157	-.33936	.07309	.20291	.06402	.77413	-.02889	-.07437
CA	.13305	.09145	-.15256	-.71109	-.10755	.06973	-.02734	-.03261	.05772
CE	.19749	-.31177	.86314	.15474	.03593	.14699	-.66651	-.02262	-.07146
CO	.77293	-.09177	-.09318	.71783	.24397	-.0[illegible]26	-.28651	.04537	-.06137
CR	[illegible]	.01770	.19523	-.73379	-.36540	.07653	-.09278	.26638	.19366
CU	.03565	-.07165	-.00247	.35711	.70854	-.03503	-.01373	.03442	-.00787
DY	.21395	.30678	.87133	.77787	-.11977	.21718	.09750	.15219	-.03774
FE	.75446	-.07777	.27658	.07887	.17775	.35100	-.07577	.10314	-.01597
HF	.11774	.32746	.51371	.19503	-.09319	.60337	-.01530	.03498	-.11150
K	-.10161	.90197	.16118	.77261	-.19773	-.13776	.57966	.39956	-.23105
LI	[illegible]	.17014	.07245	.74448	.00980	-.02974	.65914	.72625	.24342
MN	.17327	-.07127	-.02333	.31333	.47573	-.36159	-.62541	.06524	-.25449
PB	-.08401	-.01673	.00770	.74159	.79177	.14853	.24393	-.03943	.07001
SC	.81421	-.03422	.00772	-.37836	-.05391	.39849	-.05062	.73598	-.07020
TH	.33055	.37855	.34876	.19129	-.91465	.14485	.60647	-.03423	-.82455
TI	.77422	.31898	.17233	.54539	-.96182	.13490	.74581	-.13161	-.64466
V	.42617	.77777	.04378	.34566	-.17584	.89086	.49839	-.21312	.14029
ZN	-.02771	-.33773	-.70788	.79346	.90554	.03337	-.19924	-.01753	-.07175
AS	.15910	-.05777	.04945	-.11063	.14334	.60304	.08447	.07379	.63251
SE	-.05345	.17166	-.37155	-.73444	-.73189	-.24130	.01063	-.75450	.26498
ZR	.29353	-.01821	.33349	.14633	-.34044	.68591	-.01875	.31255	-.15355
UM	-.06451	.30779	.07525	.00970	.33441	-.04346	-.06773	.06699	.57143
US	-.10951	.77777	.51542	-.77570	.35537	-.18955	-.10595	.22686	.69945
ETH	.05774	-.21924	.16708	.89777	.10191	.05553	.02692	.07792	-.06493
EU	-.04524	.04195	.06330	.93589	.39005	-.45504	-.06231	-.03369	.71078
K40	.04125	-.10375	.91079	.78459	.06812	.35372	.07458	.10571	-.22267
MAG	.11049	.13433	-.37489	.76777	-.19503	.37547	-.05132	-.12079	.22053
LS4	-.03741	.95349	.00878	-.00579	-.32044	-.00255	-.02765	.07621	.00459
LS5	-.03745	.97947	-.30736	.01945	-.02771	.00854	-.01393	.00137	.02065
LS6	.00762	.98734	.91147	-.07556	-.32394	-.00149	-.00204	.00435	.04398
LS7	.00585	.94395	.01336	-.02893	-.32700	-.01255	.00602	-.01660	.05720

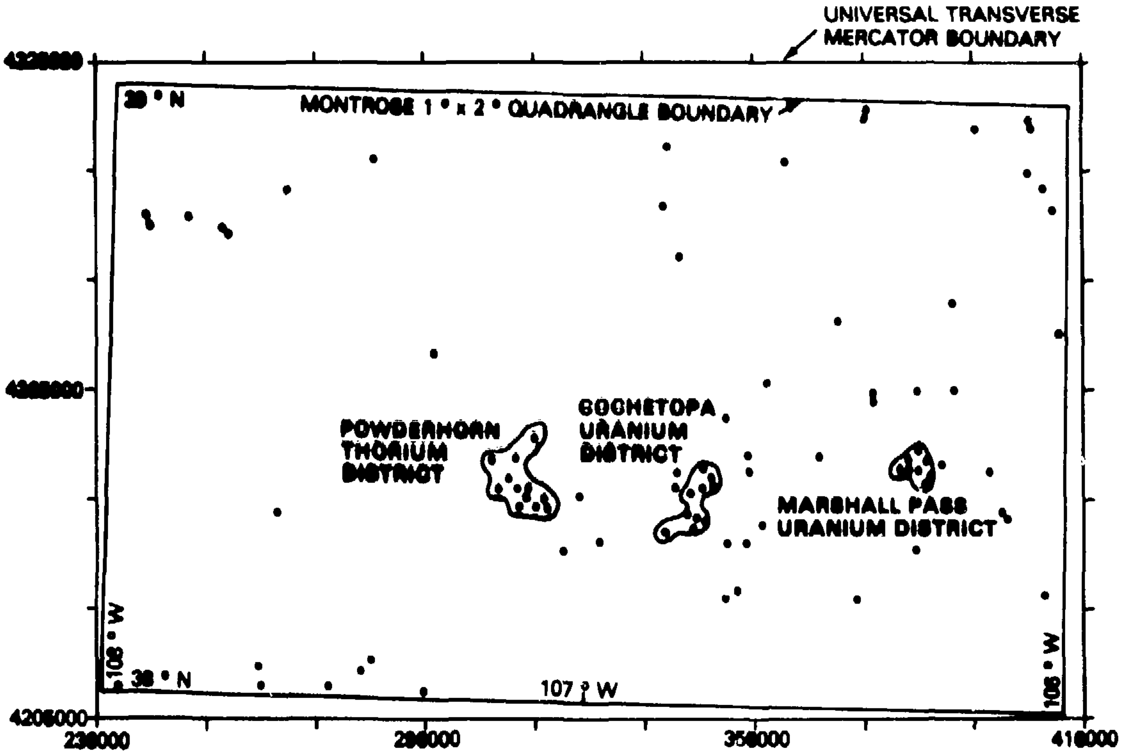

• KNOWN URANIUM OCCURRENCES; DESCRIBED IN TABLE I

PLATE I. URANIUM OCCURRENCES OVERLAY FOR THE MONTROSE 1°x 2° QUADRANGLE, COLORADO.